Investigation into the role of annexin 1 in the microcirculation of annexin 1 knockout mice

Chatterjee, Bristi Emma

INVESTIGATION INTO THE ROLE OF ANNEXIN 1 IN THE MICROCIRCULATION OF ANNEXIN 1 KNOCKOUT MICE

BRISTI EMMA CHATTERJEE

A thesis submitted to the
University of London (Faculty of Science)
for the degree of Doctor of Philosophy

Centre for Biochemical Pharmacology and Experimental Pathology
William Harvey Research Institute
Charterhouse Square
London
EC1M 6BQ

Abstract

Glucocorticoids are used therapeutically for their anti-inflammatory and immunosuppressive actions. One of the ways they produce their potent effects is *via* regulation of the anti-inflammatory protein Annexin 1 (ANX-A1; 37 kDa protein). Whereas there is sufficient information on the pharmacological properties of ANX-A1 and its bioactive peptides, as they have been studied in several models of experimental inflammation, much less is known about the functions of the endogenous protein. In this thesis I have had access to the recently generated ANX-A1 knockout (ANX-A1$^{-/-}$) mice with the scope of elucidating the role of the endogenous mediator on the process of leukocyte (mainly neutrophil) recruitment.

Two main models were used to assess leukocyte recruitment: a) a flow cytometry protocol was implemented to quantify the extent and the nature of the cellular influx into the inflamed peritoneal cavity and b) intravital microscopy of the inflamed cremaster muscle was used to identify which step of leukocyte recruitment was potentially altered.

Overall, ANX-A1$^{-/-}$ mice were found to have a heightened sensitivity to inflammation. In the peritonitis model, ANX-A1$^{-/-}$ mice displayed a higher degree of neutrophil recruitment into the peritoneal cavity, however this occurred in a stimulus specific manner. The functional role of the protein in this model was confirmed by using transgenic mice that over-express ANX-A1. These mice were shown to have the opposite response to the ANX-A1$^{-/-}$ mice, since they had a reduced influx of neutrophils into the peritoneal cavity in response to zymosan. Intravital microscopy studies

pinpointed the emigration phase of leukocyte recruitment to be significantly altered in ANX-A1$^{-/-}$ mice, and this defect was seen with application of different inflammatory agents.

In conclusion, this thesis has demonstrated, for the first time, that there are altered leukocyte-endothelium interactions in ANX-A1$^{-/-}$ mice, and these results indicate a pivotal role for endogenous ANX-A1 in the process of neutrophil recruitment that is fundamental to the host inflammatory response.

List of Contents

List of Figures and Tables

FIGURES

TABLES

Abbreviations

Ab	Antibody
APS	Ammonium persulphate
ANOVA	Analysis of variance
ANX-A1	Annexin A1
ANX-A1$^{-/-}$	Annexin A1 knockout mice
ANX-A1$^{+/+}$	Annexin A1 wild type mice
ANX-A1^{TG}	Transgenic ANX-A1 over-expressing mice
ANX-A1^{LM}	Negative littermate control mice (for over-expressing mice)
BBS	Bicarbonate buffered saline
BSA	Bovine serum albumin
Ca^{2+}	Calcium
$CaCl_2$	Calcium chloride
CAM	Cell adhesion molecule
CO_2	Carbon dioxide
COX	Cyclooxygenase
$cPLA_2$	Cyclic Phosophoslipase A2
DEX	Dexamethasone
DTT	Dithioretol
ECL	Enhanced chemiluminescence
EDTA	Ethylenediaminetetra-acetic acid
ELISA	Enzyme-linked immunosorbent assay
FACS	Flourescence activated cell sorting
FITC	Flourescein isothiocyanate
fMLP	Formyl-Met-Leu-Phe
FPR	Formyl peptide receptor
FPR$^{-/-}$	FPR knockout mice

FPRL1	Formyl peptide receptor like 1
g	Gram
g	Gravity acceleration
GC	Glucocorticoid
H_2O	Water
H_2SO_4	Sulphuric acid
hr	Hour
hrANX-A1	Human recombinant ANX-A1
HUVEC	Human umbilical vein endothelial cells
ICAM	Intercellular adhesion molecule
Ig	Immunoglobulin
IL-1β	Interleukin 1β
IL-8	Interleukin 8
i.c.v.	Intracerebroventricular
i.p.	Intraperitoneal
i.pl.	Intraplantar
i.s.	Intrascrotal
i.v.	Intravenous
i.v.m.	Intravital microscopy
I/R	Ischaemia-reperfusion
JAM	Junctional adhesion molecule
KC	Keratinocyte-derived cytokine
KCl	Potassium chloride
KDa	Kilodalton
l	Litre
LPS	Lipopolyssacharide
LTB_4	Leukotriene B4

mA	Milliamps
mAb	Monoclonal antibody
mg	Milligram
$MgSO_4$	Magnesium sulphate
min	Minute
ml	Millilitre
µg	Microlitre
NaCl	Sodium chloride
Na_2HPO_4	Di-sodium hydrogen orthophosphate dihydrate
NaH_2PO_4	Sodium di-hydrogen orthophosphate dihydrate
$NaHCO_3$	Sodium bicarbonate
nm	Nanometer
NaN_3	Sodium azide
PAF	Platelet activating factor
PBS	Phosphate buffered saline
PE	Phycoerythrin
PECAM	Platelet endothelial cell adhesion molecule
PLA_2	Phosholipase A_2
PMN	Polymorphonuclear cells
PSGL-1	P-selectin glycoprotein ligand 1
s.c.	Subcutaneous
SDS	Sodium dodecyl sulphate
SEM	Standard error of the mean
sLe^a	Sialyl-Lewis a
sLe^x	Sialyl-Lewis x
TBS-T	Tris buffered saline contained Tween 20
TNF-α	Tumour necrosis factor α
VCAM	Vascular cell adhesion molecule

V_{RBC}	Red blood cell velocity
V_{WBC}	White blood cell velocity
WBC	White blood cell
WSR	Wall shear rate
ZAS	Zymosan activated serum

Acknowledgements

I would like to thank my two supervisors, Professor Mauro Perretti and Professor Rod Flower for all the support and guidance they have given me during my PhD. I am extremely grateful as they are both amazing scientists and to have them as supervisors has been such an inspiration to me.

I would also like to thank Dr. Neil Granger and Dr. Karen Stokes for the opportunity to work in their laboratory in Shreveport (Louisiana State University) and for teaching me the technique of intravital microscopy in the mouse cremaster muscle. They were very helpful and the whole group made me feel extremely welcome when I was so far from home. I wish to thank Dr. Sussan Nourshargh and Dr. Rebecca Young (Imperial College London) for their assistance in learning the technique to examine phagocytosis in the cremaster muscle preparation.

I would really like to thank everyone in the Department of Biochemical Pharmacology because had it not been for such a great team I would never have even got through the three years of studying, let alone enjoyed them so much! I would especially like to thank Dr. Felicity Gavins and Dr. Dianne Cooper for their help with the in vivo work and intravital microscopy and also Mr. Simon Yona and Miss Connie Lam (soon to be Dr. Yona and Dr. Lam!); Simon for his help with the peritonitis model and the flow cytometer and Connie for her support and encouragement throughout my PhD.

I have made some very special friendships during my time here, you all know who you are, thank you for all the good times and also for helping me along with the hard times!

I must thank the Medical Research Council and the William Harvey Research Foundation who have funded this studentship and without them this work would not have been possible.

Finally, I would also like to thank my fiancé Darren and my family for putting up with me the last three years; I know how awful I can be when I am stressed out! Thanks for the encouragement and support you have given me and for reminding me that I could and would be able to get there in the end.

This thesis is dedicated in loving memory of
my Indian Nanny and Granddad

Every experiment proves something.

If it doesn't prove what you wanted it to prove, it proves something else.

Anon

Introduction

1. Introduction

1.1. Inflammation

The environment we live in contains a wide range of agents that can cause injury and infection to the cells of our body. A variety of microbes including viruses, bacteria, fungi, protozoa and parasites as well as physical agents such as burns, radiation, trauma or chemicals can cause injury to cells. Our immune system is a defence mechanism that has developed to protect us from these pathogens and injuries. The inflammatory process is a series of reactions that bring the cells and molecules of the immune system from throughout the body to the site of infection or damage. Inflammation appears as four cardinal signs; *Rubor et tumor cum calore et dolor*: redness and swelling with heat and pain. Cornelius Celsus first described these in the first century A.D. Later, a fifth cardinal sign, *functio laesa* or loss of function was added by Galen (129-200 AD).

The inflammatory response begins with the detection of tissue injury or a potential cause of injury (e.g. a microbe). Local tissues and cells release chemical signals (inflammatory mediators) that bring about a rapid adaptation of the microvasculature. Signals can be generated in interstitial fluid from the complement system (C3a and C5a) or from pre-formed stores in tissue cells (histamine from mast cells or neuropeptides from nerve cells) or they can be synthesised *de novo* by cells in response to the stimulus e.g. prostaglandins, leukotrienes, platelet activating factor and cytokines. Redness and swelling are the first of the cardinal signs that are manifested during inflammation due to vasodilation of blood vessels resulting in an increased blood supply to the affected area. The major function of vasodilation is to increase the

downstream supply of leukocytes and plasma protein. The next stage is an increase in vascular permeability. This occurs because of the contraction of endothelial cells, interruption of the inter-cellular junctions as well as direct and indirect injury to endothelium caused by adherent leukocytes. This allows plasma protein and leukocytes (white blood cells, WBC) to leave the vessels and enter the surrounding tissues. The extravasated fluid overloads the lymphatic clearance system and this is seen as swelling (oedema), another of the cardinal signs. There are numerous reasons for this movement of fluids and cells into the tissue; the fluid can play a role in diluting toxic factors produced at the site of damage and it allows access for important serum proteins including components of the complement system and antibodies which promote antimicrobial activity. The changes also allow for the next stage of the inflammatory process, the migration of leukocytes to the site of inflammation. The accumulation of leukocytes in inflamed tissue occurs within the microvasculature and is mainly limited to post-capillary venules (Muller, 2003).

Inflammation can be divided into either acute or chronic. Acute inflammation is usually rapid in onset, of short duration and the main cell type involved is the neutrophil (polymorphonuclear cell, PMN). It can be characterised by the exudation of fluid and plasma proteins which act to eliminate the inflammatory stimulus. This is then followed by recovery including tissue regeneration and repair. In some cases acute inflammation is not resolved and this leads to chronic inflammation. Sometimes, due to the nature of the irritant the inflammation can be chronic from the onset. Chronic inflammation lasts longer and the main cells involved are lymphocytes and macrophages. In contrast to acute inflammation the inflammation and repair occur together and this is often seen as proliferation of blood vessels and fibrosis.

1.1.1. Inflammatory Cell Recruitment

The classical three-step paradigm (Springer, 1994) of inflammatory cell recruitment are the steps of cell rolling, adhesion and emigration. Once the cells have traversed the endothelium they must penetrate the basement membrane and finally migrate through the sub-endothelial matrix and the interstitial space towards the site of inflammation. Complex interactions between the circulating blood cells and the endothelium are critical in this process and mediate each of the different stages of the recruitment process. Cell adhesion molecules (CAM's) expressed on both circulating cells and endothelium are involved in this process and include the selectins, integrins and members of the immunoglobulin superfamily, all of which will be explained in detail in the following sections. Figure 1.1. is a simple summary showing the events that occur during leukocyte recruitment which will also be described in detail in the following sections.

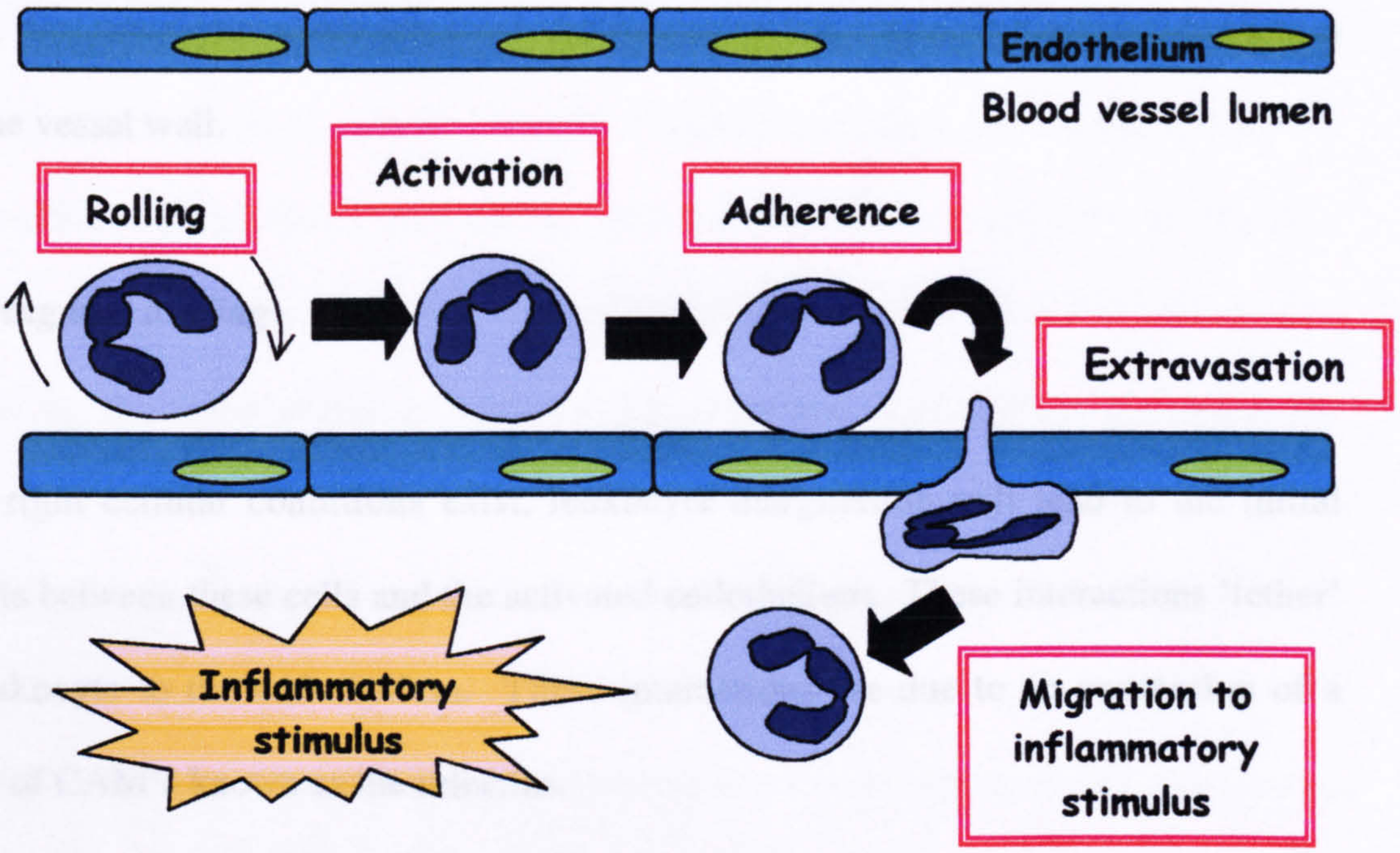

Figure 1.1. Leukocyte Recruitment. An inflammatory stimulus causes cells to roll, become activated, adhere and emigrate out of post-capillary venules where they can migrate towards the source of inflammation.

Margination

The increase in permeability of blood vessels leads to slowing of the circulation. As fluid moves out of the blood vessel to the extravascular space it leaves the blood in the vessel more concentrated and so it moves more slowly. This is described as stasis. The haemodynamic forces occurring when leukocytes exit small capillaries leading into larger post-capillary venules causes leukocytes to move to a position closer to the endothelial surface. This process is known as margination. This is recognised to be due to the interaction of leukocytes with the erythrocytes (red blood cells, RBC) travelling in a central column in normal blood flow (Nobis *et al.*, 1985; Schmid-Schonbein *et al.*,

1980). So, the erythrocytes push the leukocytes to the outside favouring interaction with the vessel wall.

Tethering and Rolling

If the right cellular conditions exist, leukocyte margination will lead to the initial contacts between these cells and the activated endothelium. These interactions 'tether' the leukocyte to the endothelium. These interactions are due to an expression of a family of CAM's known as the selectins.

Selectins are a family of three related lectin-like carbohydrate-binding molecules that are known to mediate leukocyte tethering and rolling on endothelium. A selectin molecule consists of an NH_2-terminal sugar-binding domain, an epidermal growth factor like region, a variable number of consensus repeats, a membrane spanning region and a short cytoplasmic tail. L-selectin is expressed by leukocytes, E-selectin is expressed by endothelial cells and P-selectin is expressed by endothelial cells and platelets (Rosen, 1993).

Selectin mediated cell capture initiates the interaction between leukocytes and endothelium and leads to rolling (Ley & Tedder, 1995). P-selectin is located in the membrane of Weibel-Palade bodies found in endothelial cells, and also in platelet α-granule membranes. On activation with pro-inflammatory mediators such as histamine, these organelles are rapidly translocated so they fuse with the plasma membrane and P-selectin is displayed on the surface of the cell (Geng *et al.*, 1990). For example, early leukocyte rolling (0-60 min) in the cremaster is dependent on P-selectin. This has been

demonstrated using antibodies that block P-selectin (Nolte *et al.*, 1994) and P-selectin knockout mice (Ley *et al.*, 1995). Histamine release from mast cells is responsible for the 'baseline rolling' that is seen during intravital microscopy experiments. Surgery induces trauma that causes degranulation of mast cells and this leads to expression of P-selectin by the endothelium. Consequently, treatment with a mast cell stabilizer markedly reduces trauma-induced cell rolling (Kubes & Kanwar, 1994). Besides histamine, P-selectin expression on endothelium can be activated by a number of other mediators such as thrombin (Sugama *et al.*, 1992) and oxygen radicals (Patel *et al.*, 1991). As well as rapid translocation of P-selectin to the cell surface from intracellular stores expression of this CAM can also be transcriptionally up-regulated by cytokines such as TNF-α (Weller *et al.*, 1992) such that a more sustained P-selectin expression occurs. Once P-selectin has been displayed on the endothelial cell surface, it is internalised to storage granules where it can be reused (Hattori *et al.*, 1989; Subramaniam *et al.*, 1993).

E-selectin is also important in the leukocyte-rolling phenomenon. This has been established by the use of E-selectin blocking antibodies which could prevent interleukin 1β (IL-1β) -induced rolling after 4 hr in rabbit mesenteric venules (Olofsson *et al.*, 1994). E-selectin is found on activated endothelial cells, mainly of the post-capillary venules. Whereas P-selectin is preformed and translocated to the cell surface on activation, E-selectin requires *de novo* synthesis of mRNA and protein and this can be induced by cytokines and other stimuli. IL-1β and tumour necrosis factor α (TNF-α) are capable of mediating this stimulation such that E-selectin is expressed 4-6 hr after treatment (Bevilacqua *et al.*, 1987). E-selectin is eventually internalised and transported to lysosomes for degradation (Subramaniam *et al.*, 1993).

L-selectin is constitutively expressed by most leukocytes and also participates in the adhesion of leukocytes to vascular endothelium as shown by the use of L-selectin blocking antibodies (Ley *et al.*, 1991; von Andrian *et al.*, 1991). Through the use of L-selectin knockout mice it has been shown that L-selectin rolling is mainly important at the later time-points (60-120 min) of surgery-induced rolling in the cremaster muscle where it acts in concert with P-selectin to produce rolling (Ley *et al.*, 1995). L-selectin rolling is important in cytokine (TNF-α) induced rolling, a condition in which P-selectin has been shown to have no role (Ley *et al.*, 1995). Once cells are activated L-selectin can be shed from the cell surface, for example, after activation with chemokines (Kishimoto *et al.*, 1989). A metalloproteinase (L-selectin sheddase) is responsible for this shedding although the actual molecule involved has not yet been identified (Preece *et al.*, 1996). The sheddase cleaves L-selectin at a membrane-proximal site releasing a large soluble extracellular fragment and also a small transmembrane peptide fragment (Kahn *et al.*, 1994).

The ligands for selectins are composed of a carrier molecule (glycoprotein or glycolipid) modified by specific glycosylation enzymes with certain oligosaccharides. It is the oligosaccharides that are the ligands for the selectins. All three selectins bind to the tetrasaccharide sialyl Lewis x (sLe^x), its isomer sialyl Lewis a (sLe^a) and other related oligosaccharides when assembled and presented on carrier molecules (McEver & Cummings, 1997; Vestweber & Blanks, 1999). An important molecule which presents selectin ligands is P-selectin glycoprotein ligand 1 (PSGL-1) (Moore *et al.*, 1992). PSGL-1 is found on both leukocytes (Moore *et al.*, 1995) and platelets (Frenette *et al.*, 2000). PSGL-1 has been shown to mediate rolling *in vivo* (Norman *et al.*, 1995) as the use of blocking monoclonal antibody (mAb) against PSGL-1 can significantly

reduce the rolling of human neutrophils in the rat mesentery. PSGL-1 is also a ligand for E-selectin and L-selectin (Asa *et al.*, 1995; Spertini *et al.*, 1996). E-selectin ligand 1 is a another major ligand for E selectin that has been found on mouse myeloid cells and mediates the binding of these cells to E-selectin (Steegmaier *et al.*, 1995).

The bonds formed between selectins and their ligands are not of sufficient strength to support firm adhesion of leukocytes. This is due to the both to the nature of the bonds and the force of the blood flow acting on them (Granger & Kubes, 1994). As a result, the bonds are continuously broken and reformed leading to rolling of leukocytes along the endothelium. Once a leukocyte begins rolling it is able to sample the local environment and, if the appropriate signals (i.e. chemokines, CAM expression) are present, then the cell may roll more slowly and eventually firmly adhere. If the local environment does not exhibit the appropriate signals, rolling cells can detach and return to the main blood flow (Lim *et al.*, 1998; Mancuso *et al.*, 1995; Umeno *et al.*, 1990)

Activation

During the rolling phenomenon leukocytes are brought into close contact with the endothelium. As the rolling leukocytes are in closer contact with the endothelium they can 'sample' the molecules displayed to them. Activated endothelial cells at the site of an inflammatory insult can produce chemoattractants which are either secreted into the blood vessel or held on the endothelial surface in the blood vessel lumen. If suitable chemoattractants are displayed then this can lead to activation of the leukocyte.

Leukocyte chemoattractants: A chemoattractant is any chemical that attracts cells to move towards it. It will usually be a soluble molecule that can diffuse from its source where its concentration will be at its highest. A cell can then follow the gradient from lowest concentration to highest, to seek out the source of the chemoattractant. For directional migration to occur, cells must be able to sense the concentration difference, often as little as 1%, between the leading and trailing edge of the cell. A variety of chemoattractants exist and some of these will be described in more detail in the following section

Platelet-activating factor (PAF) is a lipid mediator generated by stimulated cells (e.g. neutrophils, monocytes and endothelial cells) by the enzyme phospholipase A_2 (PLA_2). PLA_2 mobilizes phospholipids in cell membranes and converts them to arachidonic acid and a PAF precursor, lyso-PAF. The latter is then acetylated to PAF by acetyl-transferases (Rang *et al.*, 2003). PAF can be produced by endothelial cells in response to agonists such as thrombin (Zimmerman *et al.*, 1990) and IL-1β (Nourshargh *et al.*, 1995) and then retained on the cell surface where it can induce responses in target cells by binding to specific receptors (Hwang, 1988). It has been shown to be a chemoattractant for neutrophils, monocytes and eosinophils.

Leukotriene B_4 (LTB_4) is an arachidonic acid metabolite formed by the lipoxygenase pathway during activation of a variety of cells at the site of inflammation (including mast cells, basophils and macrophages) and is a chemotactic agent for neutrophils, monocytes, eosinophils and lymphocytes.

C5a originates during complement activation at the site of inflammation. Proteolysis of the C5 complement protein gives rise to a small peptide fragment, C5a, which is chemotactic for neutrophils, monocytes and macrophages and can cause basophils and mast cells to degranulate.

Formyl-Met-Leu-Phe (fMLP) is an N terminal formylated peptide that originates from prokaryotes. Prokaryotes (e.g. bacteria) initiate all protein translation with this formylated methionine and so this is considered to be a signal of bacterial presence. fMLP is a potent chemoattractant for neutrophils, monocytes and eosinophils (Marasco *et al.*, 1984) due to binding to its receptor.

Chemokines are a group of at least 40 chemotactic cytokines. They are small, homologous, 8 to 10 kDa polypeptides that have specificity for leukocyte subsets. Chemokines are arranged into four families with α- (CXC) and β- (CC) chemokines being the largest families and the basis of division being the relative position of the cysteine residues. Both α and β chemokines have 4 cysteine residues in their amino acid sequence. In α-chemokines the first two cysteine residues are separated by another amino acid (cysteine-X amino acid-cysteine). In β-chemokines the first two cysteine residues are adjacent. The α chemokines tend to act on neutrophils whereas the β chemokines tend to act on monocytes and other WBC (Adams & Lloyd, 1997; Luster, 1998). Chemokines can be released at inflammatory sites along with pro-inflammatory cytokines. They can be held in a gradient, most concentrated at the source by binding in the tissue to matrix heparan sulphate proteoglycans. Pro-inflammatory cytokines, such as IL-1 and TNF, as well as lipopolysaccharide (LPS) and viral infection stimulate the release of chemokines by the endothelial cells into the blood vessel lumen adjacent to the inflammatory site (Baggiolini *et al.*, 1994).

Chemoattractants such as chemokines induce cell activation and migration by binding to specific G-protein coupled cell-surface receptors on target cells (Premack & Schall, 1996). The binding of chemoattractant receptors can trigger the leukocyte to begin a signalling cascade to activate integrins on the leukocyte. This signalling is *via* the cytoplasmic tail of the integrin and so is known as 'inside out' signalling. This is thought to provide the signals that convert non-functional integrin molecules into functional, binding molecules switching the selectin-mediated rolling to the stronger adhesion mediated by integrins (Luster, 1998). The increased avidity of the cell integrins will in turn increase binding (Johnston & Butcher, 2002).

The specificity of chemoattractants is regulated by the cellular distribution of their receptors on leukocytes. The receptors for certain chemoattractants, for example, fMLP and PAF receptors are found on both neutrophils and monocytes. However, the chemokine receptors, CXC chemokine receptors (CXCR1-CXCR4) and CC chemokine receptors (CCR1-CCR8) are differentially distributed. For example, CXCR1 is found predominantly on neutrophils whereas CCR2 is not found on neutrophils but mainly on monocytes and basophils (Luster, 1998). Therefore, the cell type specifically recruited depends on the chemokines displayed by endothelial cells and the corresponding receptors being expressed on the circulating cells.

Firm adhesion

Leukocyte rolling frequently leads to the arrest of cells as they become firmly attached to the endothelium. This high-affinity event is also known as firm adhesion or adherence. A variety of chemoattractants can cause the induction of adhesion in post-

capillary venules (Panes *et al.*, 1999). Many agents and conditions that can cause firm adherence can also cause rolling of leukocytes. This has lead to the view that cell rolling is a prerequisite for firm adherence.

Integrins are heterodimeric transmembrane glycoproteins. Each integrin is made up of a non-covalently linked α and β subunit. To date, 18 α and 8 β subunits have been identified in man (van der Flier & Sonnenberg, 2001). These can link in different combinations and are grouped according to the β subunit. The α subunit contains an extracellular region folded into four divalent-cation-binding domains, a transmembrane region and a cytoplasmic tail. The β subunit has an extracellular region containing cysteine-rich domains, a transmembrane region and a cytoplasmic tail. The subunits are synthesized as precursors and glycosylated cotranslationally with N-linked, high-mannose carbohydrate groups. After the α and β subunits have associated they are transported to the cell surface or to intracellular secretory vesicles.

The β_2-integrins (CD11/CD18) are primarily involved in the process of leukocyte firm adhesion to post-capillary endothelium. The family consists of one of four α subunits (CD11a, CD11b, CD11c or CD11d) associated with a common β subunit (CD18). CD11a/CD18 ($\alpha_L\beta_2$, leukocyte function associated antigen-1, LFA-1) is expressed on virtually all immune cells, whereas CD11b/CD18 ($\alpha_M\beta_2$, Mac-1) is expressed mainly on monocytes, macrophages and granulocytes. Intracellular storage pools of CD11b and CD11c are found in neutrophils and monocytes however CD11a is not stored intracellulary (Arnaout, 1990). Studies using CD18-specific antibodies (which will block both CD11a/CD18 and CD11b/CD18) have shown that the β_2 integrins are involved in the recruitment of leukocytes, at the adhesion stage, as use of these

antibodies reduces the number of adherent leukocytes in post-capillary venules induced by PAF (Argenbright *et al.*, 1991; Kubes *et al.*, 1990; Zimmerman *et al.*, 1994). CD18 mutant mice (>80% reduction in CD18 expression on granulocytes) show an impaired inflammatory response with a decreased number of neutrophils emigrating into the thioglycollate inflamed peritoneal cavity (Wilson *et al.*, 1993).

As described above, stimulation of chemoattractant receptors on the rolling leukocytes leads to non-functional β_2-integrins becoming fully active binding molecules as well as increasing surface expression of integrins by mobilizing preformed stores (Arnaout, 1990). These integrins are now able to bind to their ligands, members of the endothelial immunoglobulin (Ig) superfamily, on the endothelium.

Immunoglobulin superfamily members as integrin ligands: Intercellular adhesion molecule 1 (ICAM-1) has been implicated as a ligand for both CD11a (Marlin & Springer, 1987) and CD11b (although the α subunits bind to different domains) (Diamond *et al.*, 1991). ICAM-1 has five extracellular Ig-like domains. CD11a has a binding site in the NH_2-terminal of the first domain whereas CD11b binding is localized to the third Ig-like domain. ICAM-1 is expressed on both leukocytes and endothelial cells. It is found constitutively on the surface of endothelial cells in a functionally active form but can also be up-regulated by exposure of the endothelium to various cytokines or endotoxin (Dustin *et al.*, 1986). ICAM-2 has two extracellular Ig-like domains. The domains are similar to the first domain of ICAM-1 which can therefore bind CD11a, but not CD11b. ICAM-2 is also constitutively expressed on endothelial cells however it is not up-regulated by cytokines (Staunton *et al.*, 1989). *De novo* protein synthesis is required for cytokine-induced ICAM-1 up-regulation so

the adhesive potential of endothelium increases over a period of hours. Monocytes, eosinophils and lymphocytes express $\alpha_4\beta_1$, and can also bind to vascular cell adhesion molecule-1 (VCAM-1) (Elices *et al.*, 1990). VCAM-1 has low basal expression on endothelial cells and could also be up-regulated by inflammatory cytokines (Osborn *et al.*, 1989).

In addition to being involved in firm adhesion, integrins have also been shown to play a part in leukocyte rolling in certain conditions. For instance, use of knockout mice has demonstrated that CD11a/CD18 can sustain cell rolling in mesenteric vessels after application of an inflammatory stimulus. These knockout mice show an increased rolling velocity and in turn a decreased cell adhesion and emigration in response to thioglycollate. The same study showed that $\alpha_4\beta_1$ (very late antigen-4, VLA-4) can take over the role played by β_2 integrins in sustaining cell rolling (Henderson *et al.*, 2001).

Emigration/ transmigration/ leukocyte extravasation/ diapedesis

After a leukocyte has been stationary for a period of time it may leave the post-capillary venule. The cell extends pseudopodia between apposing endothelial cells and pulls itself through to the basement membrane which it must also cross in order to migrate through the adjacent interstitial tissues. This is a complex event that depends on many cellular processes including adhesion molecule expression and activation, cytoskeletal reorganisation, and alterations in membrane fluidity. It is thought that a favourable chemoattractant gradient must exist across the vessel wall for adherent leukocytes to emigrate.

Different molecules are also important in leukocyte transmigration. Platelet endothelial cell adhesion molecule (PECAM-1, CD31) and CD99 are required for transmigration. PECAM-1 is a member of the endothelial Ig-superfamily and consists of six extracellular Ig-like domains. It is widely distributed and found on endothelial cells, leukocytes and platelets. It is constitutively expressed on endothelial cells and is found evenly along the cell borders where it is constitutively recycled (from specific vesicles) (Mamdouh *et al.*, 2003). CD99 is a molecule expressed on the surface of most leukocytes and is found concentrated at the borders of cultured endothelial cells (Schenkel *et al.*, 2002). Both PECAM-1 and CD99 are capable of homophilic interactions, i.e. leukocyte PECAM-1 binds to endothelial PECAM-1. The same applies to CD99. The use of both neutralizing antibodies (Bogen *et al.*, 1994; Muller *et al.*, 1993; Vaporciyan *et al.*, 1993) and knockout mice (Dangerfield *et al.*, 2002; Thompson *et al.*, 2001) has demonstrated the role of PECAM-1 in cell transmigration. However, neither of these strategies could totally abolish cell migration in these models. Similarly, blockade of CD99 on either monocytes or endothelial cell cultures also significantly reduced transmigration without completely abolishing it. However, blockade of both CD99 and PECAM-1 has been shown to completely abolish transmigration (Schenkel *et al.*, 2002). *In vitro* experiments, using human monocytes and human umbilical vein endothelial cells (HUVEC) have shown that PECAM-1 recycling is targeted to surround emigrating cells (Mamdouh *et al.*, 2003). This may be to provide extra endothelial PECAM-1 for interaction with leukocyte PECAM-1. Whether or not this occurs with the neutrophil is as yet unknown. Junctional adhesion molecule 1 (JAM-1) is another member of the endothelial Ig superfamily of proteins found at the junctions of endothelial cells. It has been shown, using *in vitro* studies, to

contribute to the transmigration of neutrophils and monocytes *via* interactions with CD11a/CD18 (Ostermann *et al.*, 2002).

After cells have crossed the endothelium, they must pass through the basement membrane and the extracellular matrix of the interstitial tissues to the source of the inflammation (e.g. to the bacteria or infected/dead cells). Leukocytes must interact with proteins of the extracellular matrix such as collagen, laminin and fibronectin as well as the tissue cells *via* high affinity interactions with β_1-integrins (Hemler, 1990). β_1-integrins (or very late antigens, VLA's) are only found at very low levels on blood neutrophils and are rapidly up regulated after emigration of the cell from the vasculature. They are involved in cell movement along the chemotactic gradient in the extravascular tissue (Werr *et al.*, 1998).

Figure 1.2. is a summary showing the events that occur in leukocyte recruitment.

Figure 1.3 is a summary of the adhesion molecules involved in the complex process of cell recruitment.

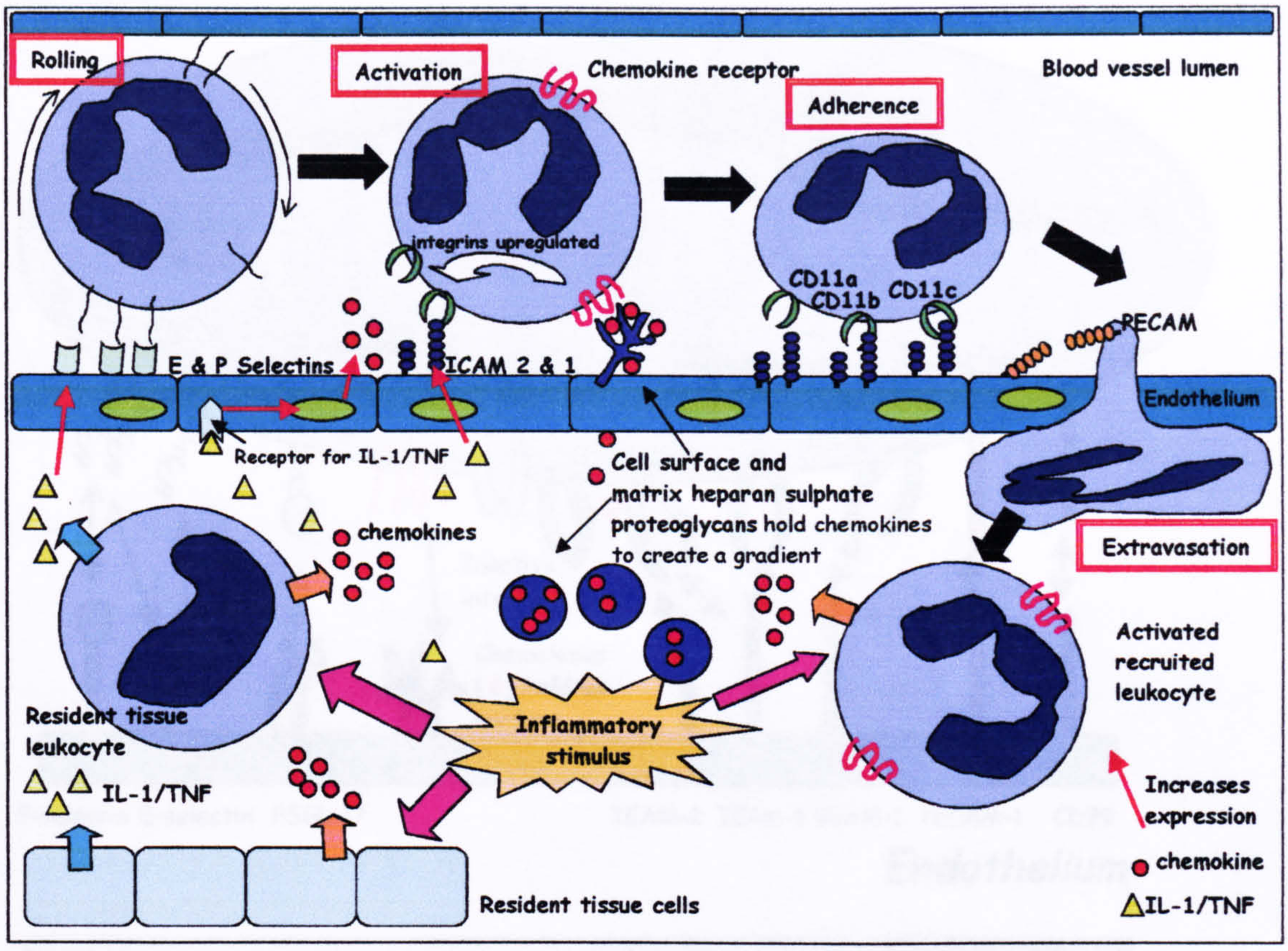

Figure 1.2. Summary of Leukocyte Recruitment. When an inflammatory stimulus or infection occurs, resident tissue cells and tissue leukocytes at the site secret chemokines and pro-inflammatory cytokines. The cytokines IL-1/TNF increase expression of selectins and ICAM-1 on the surface of endothelial cells. Circulating leukocytes begin to roll due to the interaction of oligosaccharides on their surface with the newly expressed selectins. Chemokines are released by the interaction of IL-1/TNF with receptors on endothelial cells. Chemokines are 'displayed' on the surface of the endothelium by cell surface heparan sulphate proteoglycans. Rolling cells can now 'sample' the chemokines via receptors on their surface. This leads to the up regulation of integrins on the rolling cell and the cell becomes activated. The activated cell can become firmly adherent by binding of leukocyte integrins to endothelial cell surface ICAM-1 molecules. Changes occur within the leukocyte allowing it to migrate into the surrounding tissue. Chemokine gradients build up in the tissue by the binding of chemokines to matrix heparan sulphate proteoglycans and these gradients lead recruited cells to the site of the inflammatory stimulus where they can go about removing it. Within the tissue recruited cells can also contribute to cell recruitment by the further release of chemokines making the gradient even stronger. Adapted from Luster, 1998.

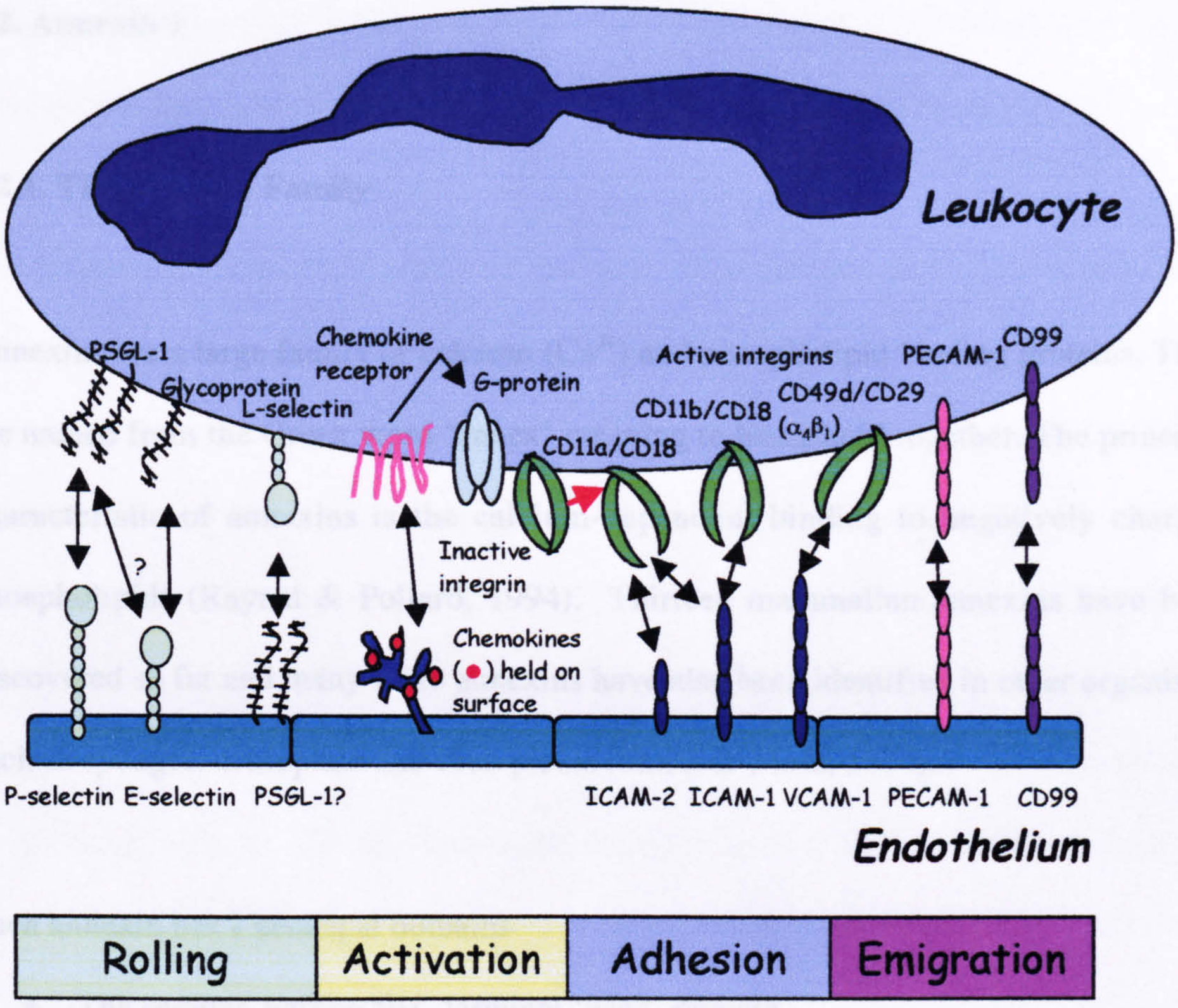

Figure 1.3. Summary of adhesion molecules involved in leukocyte recruitment.
Diagram adapted from Ulbrich *et al.*, 2003.

1.2. Annexin 1

1.2.1. The Annexin Family

Annexins are a large family of calcium (Ca^{2+}) and phospholipid binding proteins. They are named from the Greek word 'annex' meaning to bring/hold together. The principal characteristic of annexins is the calcium-dependent binding to negatively charged phospholipids (Raynal & Pollard, 1994). Thirteen mammalian annexins have been discovered so far and many more annexins have also been identified in other organisms such as sponges, drosophila and even plants (Smith & Moss, 1994).

Each annexin has 2 principal domains

- The smaller, unique NH_2-terminal 'head' domain
- The larger, conserved COOH-terminal protein core

The conserved C-terminal region is termed the annexin core and consists of 4 (or 8 in annexin VI) repeating units, the "annexin repeat", each comprising of about 70 amino acids residues. Each of the repeats corresponds to a domain found in the three-dimensional structure of the molecule. The homologous repeats/domains consist of 5 α-helices connected by short loops. There is a strong homology between each of the four repeats found in an individual annexin (25-35%) and also between corresponding repeats of the different annexins (40-60%). The helices form a slightly curved disc shape with concave and convex sides (see figure 1.4.). The convex side contains the Ca^{2+} binding sites. Specific Ca^{2+} binding sites have been identified between the first and second α-helices and between the fourth and fifth helices. The concave side points

away from the membrane and so appears to be accessible for interactions with the N-terminal domain and/or cytoplasmic binding partners (Nevid & Horseman, 1996).

The N-terminal domain is less homologous than the conserved C-terminal region. The N-terminal region varies in sequence and length (from 11 to more than 100 residues). Each annexin has a unique N-terminal domain and it is thought that each one of these alternative forms determines the specificity of biological action for each annexin. The N-terminal contains binding sites for S100 proteins (as in the case of ANX-A1, ANX-A2 and ANX-A11) and phosphorylation sites for serine/threonine and tyrosine-specific kinases (for example in ANX-A1) (Rosengarth *et al.*, 2001). Crystal structure analysis of ANX-A5 indicates that the N-terminal region is located on the concave side of the core domain (Huber *et al.*, 1992).

1.2.2. Annexin 1: Structure and Distribution

Annexin 1 (ANX-A1), also known as lipocortin-1, is a 37kDa member of the annexin family. The N-terminal domain of ANX-A1 contains 41 amino acids residues (Rosengarth *et al.*, 2001) with the complete protein consisting of 346 amino acids. Figure 1.4. shows the three-dimensional structure of ANX-A1. ANX-A1 is found in large amounts in human neutrophils, accounting for approximately 2-4% of the total cytosolic protein (Francis *et al.*, 1992). This protein is also expressed by other cells including monocytes and some subsets of lymphocytes though in smaller amounts (Morand *et al.*, 1995).

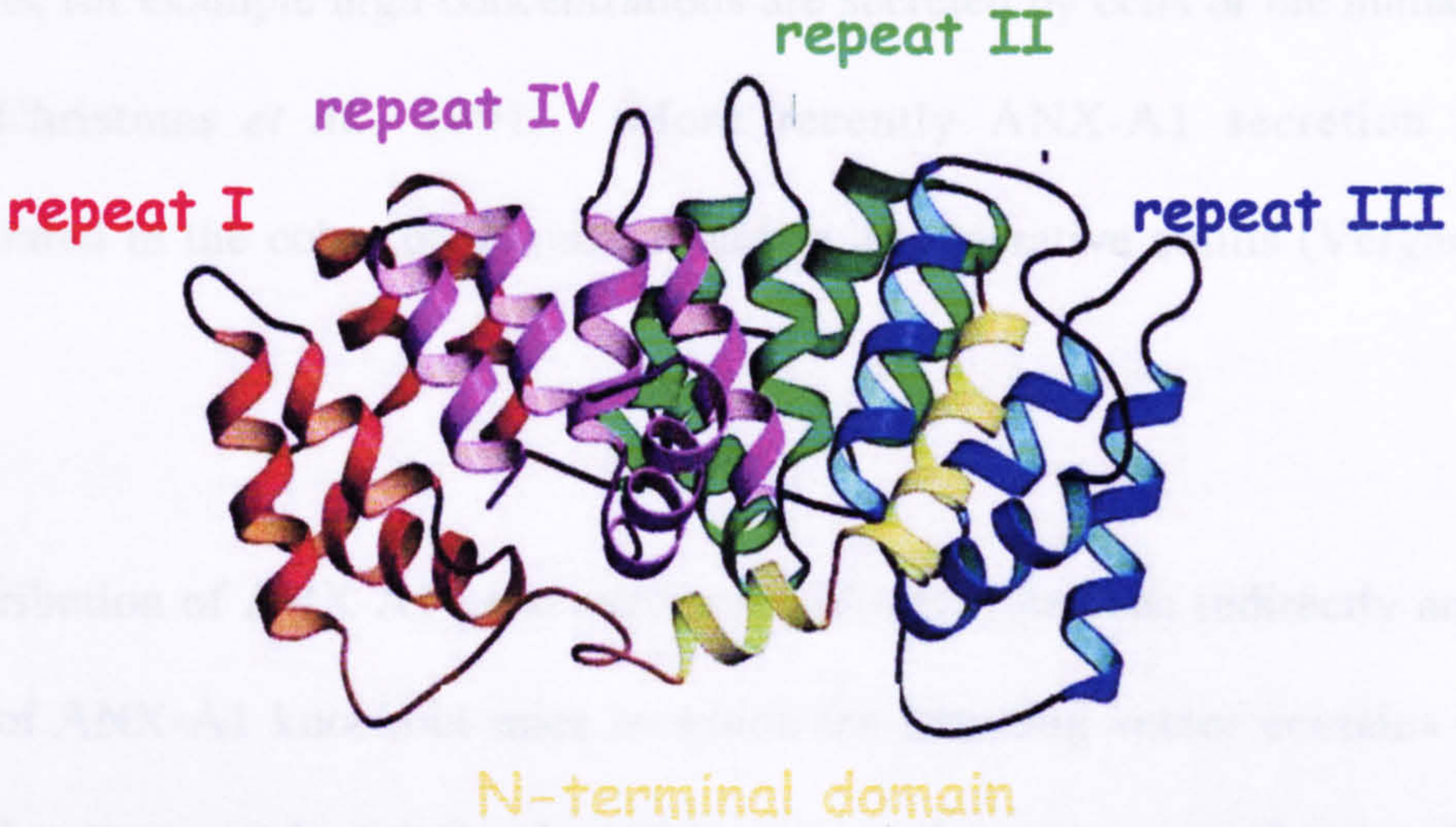

Figure 1.4. Three-dimensional structure of Annexin 1. The protein core consists of four repeats each made up of five α-helices: repeat 1 is depicted in red, repeat II in green, repeat III in blue and repeat IV in purple. The N-terminal domain of 41 amino acids is depicted in yellow. Diagram adapted from Rosengarth *et al.*, 2001.

Although ANX-A1 has been shown to be abundant in the cytoplasm of several cell types its exact location is unclear. In a kidney cell line ANX-A1 has been shown to localise around endosomal membranes, especially those of early endosomes, in a Ca^{2+} dependent manner (Seemann *et al.*, 1996). Differentiated U937 cells (cell line with a macrophage phenotype) have been shown to contain ANX-A1 protein distributed throughout the cell although mostly localised to the cytoplasm. The protein did not seem associated with any particular organelle in these cells. However, when the cells had ingested non-pathogenic bacteria (*E. coli*) or yeast, ANX-A1 localised around the phagosome (Harricane *et al.*, 1996). In human neutrophils, at high Ca^{2+} concentrations, ANX-A1 has been found associated with azurophilic granules, specific granules and secretory vesicles as well as free in the cytoplasm (Sjolin *et al.*, 1994).

Another interesting point is that ANX-A1 does not contain a signal sequence for secretion *via* the classical secretory pathway. However it can be selectively released

from cells, for example high concentrations are secreted by cells of the human prostate gland (Christmas *et al.*, 1991). More recently ANX-A1 secretion has been demonstrated in the colon of human patients with ulcerative colitis (Vergnolle *et al.*, 2004).

The distribution of ANX-A1 gene expression in mice has been indirectly analysed by the use of ANX-A1 knockout mice in which the targeting vector contains the Lac-Z gene. They were used, with β-galactosidase as a substrate, to reveal sites of ANX-A1 gene expression. ANX-A1 is differentially expressed in organs of the mouse. It is strongly expressed in the stomach, lung, spleen, ovary and uterus and expressed at intermediate levels in the kidney, thymus and heart. It was found at lower levels in thyroid, pancreas and testes and no ANX-A1 gene expression was found in the brain cortex, liver and adrenal gland (Hannon *et al.*, 2002).

1.2.3. Glucocorticoids and Annexin 1: Anti-Inflammatory Actions

The steroid hormones (progestagens, glucocorticoids, mineralocorticoids, androgens and oestrogens) are derived from cholesterol and figure 1.5. is a brief summary diagram of the actions of these hormones. Glucocorticoids (GC), which are produced by the adrenal gland *via* actions of the hypothalamo-pituitary-adrenocortical (HPA) axis, have since 1949 been used for their anti-inflammatory actions. Figure 1.6 (a) is a diagram to show the synthesis and release of GC. Figure 1.6 (b) shows how GC can affect target cells and modulate protein synthesis. Endogenous GC is carried in the plasma bound to corticosteroid binding protein (CBP) or albumin (which also carries exogenous GC). The GC diffuses into target cells where it can bind to a GC receptor (GR) which is

found in the cytoplasm in a complex with two molecules of heat shock protein, hsp90. The hsp90 molecules prevent the GR moving into the nucleus until the GR binds GC, which then causes hsp90 to dissociate leading to the exposure of nuclear localisation signals. Once this occurs the GC-GR complex is activated and it then forms a dimer which translocates to the cell nucleus. In the nucleus the complex binds to a GC recognition sequence (GC response element, GCR) located in the 5'-upstream promoter region of glucocorticoid-responsive genes. Once the complex has bound to a GRE, the GC produces its effects by altering the rate of transcription to induce or repress the gene. GR can also interact directly with transcription factors such as AP-1 (activating protein-1) and NF-κB (nuclear factor κB) as well as having other important cytoplasmic interactions. As the GR interacts with the transcription factors this prevents both the transcription factor and the GR interacting with DNA reducing the response to them (Barnes, 1998).

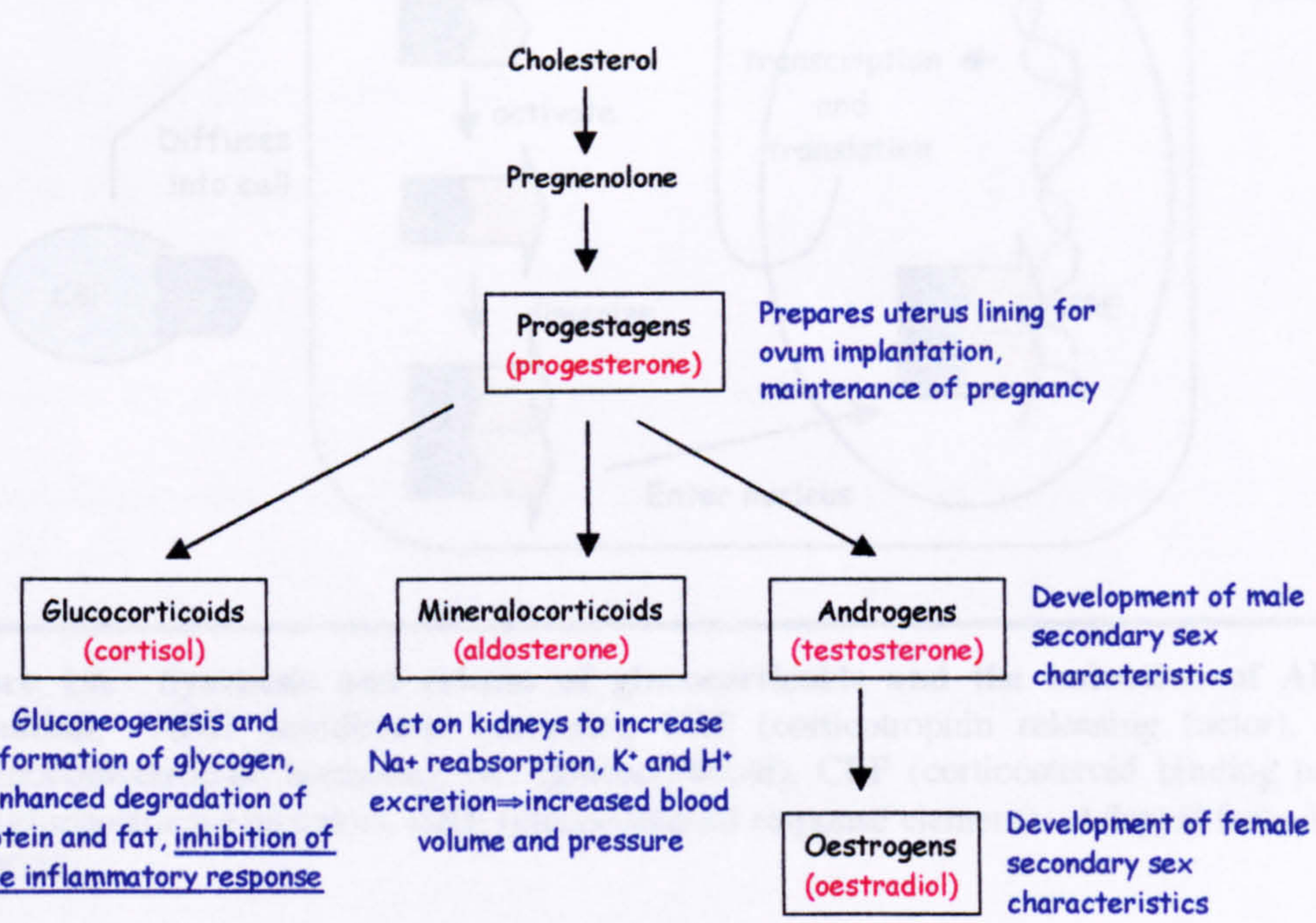

Figure 1.5. Steroid hormones and their actions. The five major classes of steroid hormones are shown in boxes with examples given in red. All are derived from cholesterol. A brief summary of action is given in blue for each steroid. Adapted from Berg *et al.*, 2002.

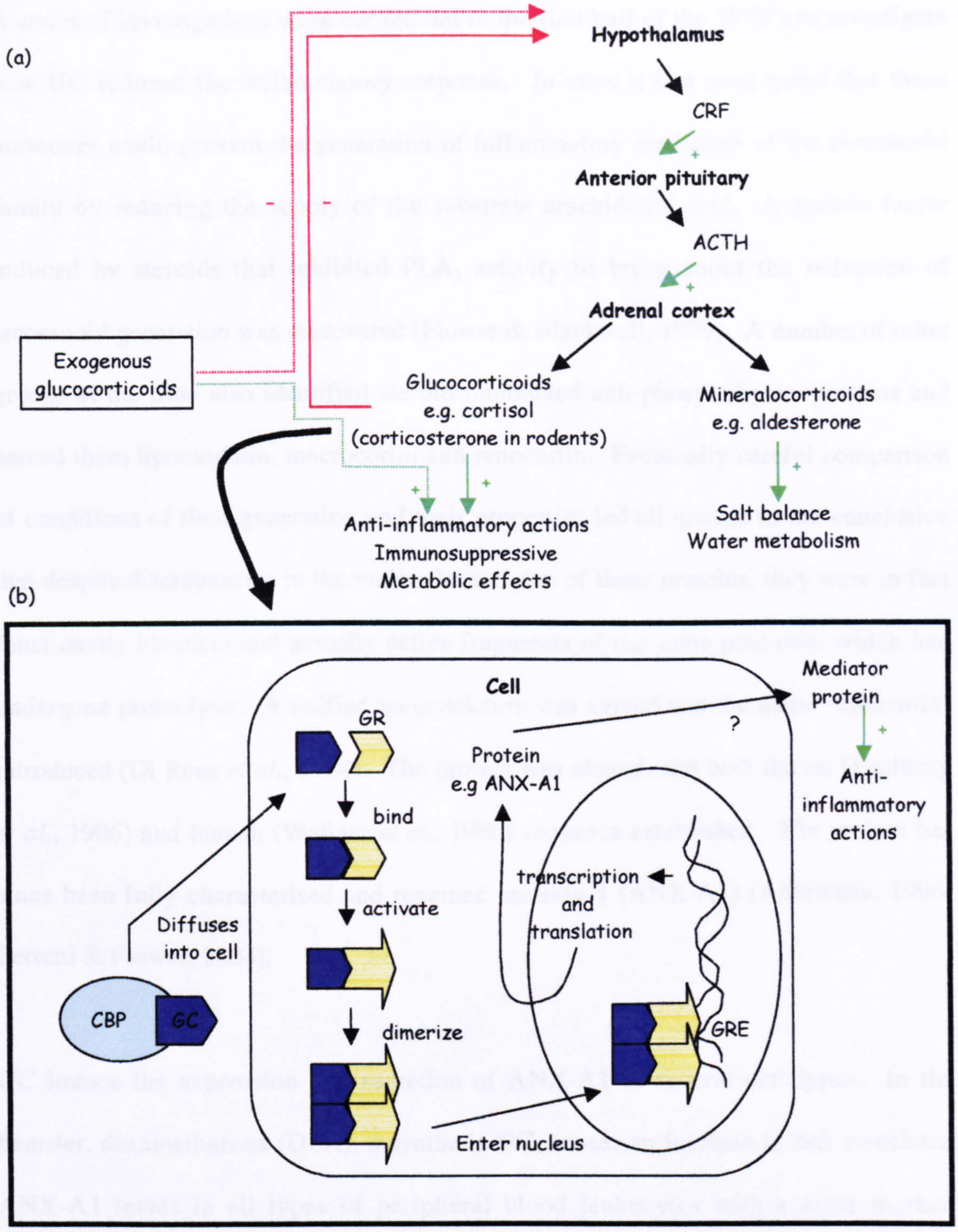

Figure 1.6. Synthesis and release of glucocorticoids and the induction of ANX-A1 formation. ADH (antidiruetic hormone), CRF (corticotrophin releasing factor), ACTH (adrenocorticotrophic hormone), GC (glucocorticoid), CBP (corticosteroid binding protein), GR (glucocorticoid receptor), GRE (glucocorticoid response element). Adapted from Rang *et al.*, 2003.

A series of investigations were carried out in the first half of the 1970's to investigate how GC reduced the inflammatory response. *In vitro* it had been noted that these hormones could prevent the generation of inflammatory mediators of the eicosanoid family by reducing the supply of the substrate arachidonic acid. A protein factor induced by steroids that inhibited PLA_2 activity to bring about the reduction of eicosanoid generation was discovered (Flower & Blackwell, 1979). A number of other groups at the time also identified steroid-modulated anti-phospholipase proteins and named them lipomodulin, macrocortin and renocortin. Eventually careful comparison of conditions of their generation and their properties led all groups to the conclusion that despite discrepancies in the molecular weights of these proteins, they were in fact functionally identical and actually active fragments of the same precursor which had undergone proteolysis. A unified nomenclature was agreed and the name 'lipocortin' introduced (Di Rosa *et al.*, 1984). The protein was cloned, and both the rat (Pepinsky *et al.*, 1986) and human (Wallner *et al.*, 1986) sequence established. The protein has since been fully characterised and renamed annexin 1 (ANX-A1) (Ahluwalia, 1996; Perretti & Flower, 2004).

GC induce the expression and secretion of ANX-A1 in several cell types. In the hamster, dexamethasone (DEX), a synthetic GC, causes an increase in cell associated ANX-A1 levels in all types of peripheral blood leukocytes with a more marked response in the neutrophil (Mancuso *et al.*, 1995). Interestingly, in human volunteers, hydrocortisone administration causes a significant increase in levels of both intracellular and cell surface ANX-A1 (Goulding *et al.*, 1990). This effect is not confined to humans as was shown by the fact that the levels of ANX-A1 are decreased in rat peritoneal cells by the administration of a GC receptor antagonist, RU486 (Peers

et al., 1993). Accordingly, adrenalectomised rats also show a decrease in ANX-A1 mRNA and protein in the lung (Vishwanath *et al.*, 1992). As ANX-A1 is strongly induced by GC it led to the suggestion that ANX-A1 could act as a cellular mediator of the anti-inflammatory actions of GC (Flower, 1988). This effect was originally attributed to the capability of ANX-A1 to inhibit PLA_2 activity. This inhibition would block arachidonic acid production and the downstream eicosanoid production. As eicosanoids have an important role in pain, fever and inflammation it was thought that ANX-A1's ability to inhibit release/synthesis of these mediators was mediating the anti-inflammatory effects of the GC. Figure 1.7 shows the effect of GC and ANX-A1 on the generation of eicosanoids from membrane phospholipids.

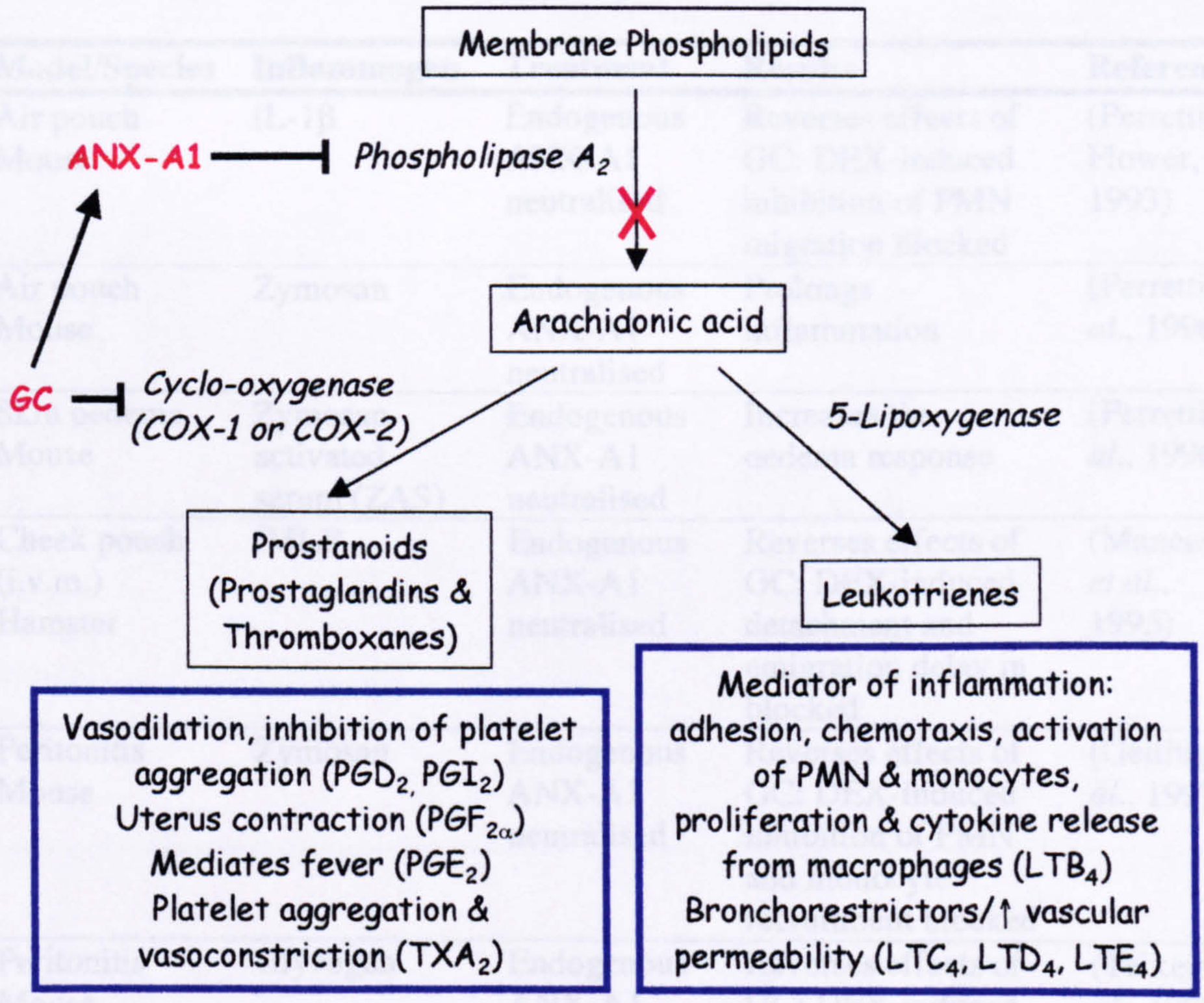

Figure 1.7. The effect of glucocorticoids and ANX-A1 on eicosanoid formation. Figure adapted from Nussey & Whitehead, 2001; Rang *et al.*, 2003.

Many experiments have been carried out to examine the role of endogenous ANX-A1 and the effects of exogenous ANX-A1 and its N-terminal derived peptides in inflammation. Table 1.1. summarises the findings of a number of these experiments. Some of these studies will be described in more detail in the following sections.

Table 1.1. The anti-inflammatory effects of ANX-A1 in models of inflammation.

i.c.v., intracerebroventricular injection, i.p., intraperitoneal, i.pl. intraplantar injection, I/R, ischaemia-reperfusion, i.s.,intrascrotal, i.v., intravenous, i.v.m., intravital microscopy

Endogenous ANX-A1

Model/Species	Inflammogen	Treatment	Results	Reference
Air pouch Mouse	IL-1β	Endogenous ANX-A1 neutralised	Reverses effects of GC: DEX-induced inhibition of PMN migration blocked	(Perretti & Flower, 1993)
Air pouch Mouse	Zymosan	Endogenous ANX-A1 neutralised	Prolongs inflammation	(Perretti *et al.*, 1996a)
Skin oedema Mouse	Zymosan-activated serum (ZAS)	Endogenous ANX-A1 neutralised	Increases the oedema response	(Perretti *et al.*, 1996a)
Cheek pouch (i.v.m.) Hamster	fMLP	Endogenous ANX-A1 neutralised	Reverses effects of GC: DEX-induced detachment and emigration delay in blocked	(Mancuso *et al.*, 1995)
Peritonitis Mouse	Zymosan	Endogenous ANX-A1 neutralised	Reverses effects of GC: DEX-induced inhibition of PMN and monocyte recruitment blocked	(Getting *et al.*, 1997)
Peritonitis Mouse	Glycogen	Endogenous ANX-A1 neutralised	Reverses effects of GC: DEX-induced inhibition of PMN recruitment blocked	(Teixeira *et al.*, 1998)

Pain Rat	Carrageenin TNF-α IL-1β	Endogenous ANX-A1 neutralised	Reverse effects of GC: DEX-induced anti-hyperalgesic effects blocked	(Ferreira *et al.*, 1997)
Arthritis model Rat	Adjuvant	Endogenous ANX-A1 neutralised	Reverse effects of GC: DEX-induced reduction on arthritis index, paw volume and cell influx blocked	(Yang *et al.*, 1999)
Arthritis model Rat	Carrageenin	Endogenous ANX-A1 neutralised	Reverse effects of GC: DEX-induced inhibition of PMN recruitment blocked	(Yang *et al.*, 1997)

Exogenous ANX-A1: hrANX-A1 (full length protein)

Model/Species	**Inflammogen**	**Treatment**	**Results**	**Reference**
Air pouch Mouse	IL-1β	hrANX-A1 (i.v.)	Reduces PMN accumulation in air pouch	(Perretti *et al.*, 1993; Perretti & Flower, 1993)
Mesentery (i.v.m.) Rat	LPS	hrANX-A1 (i.v.)	Attenuates LPS-induced cell adhesion and emigration	(Allcock *et al.*, 2001)
Mesentery (i.v.m.) Mouse	Zymosan	hrANX-A1 (s.c.)	Reduced extent of zymosan-induced cell adhesion and emigration	(Lim *et al.*, 1998)
Mesentery (i.v.m.) Mouse	Zymosan	hrANX-A1 (i.v.)	Caused adherent cell detachment	(Lim *et al.*, 1998)
Paw oedema Rat	Carrageenin	hrANX-A1 (i.pl.)	Inhibited carrageenin-induced paw oedema	(Cirino *et al.*, 1989a)

Exogenous ANX-A1: Peptide Ac2-26

Model/Species	Inflammogen	Treatment	Results	Reference
Air pouch Mouse	IL-1β	Ac2-26 (i.v.)	Reduces PMN migration into air pouch	(Perretti *et al.*, 1993)
Cheek pouch (i.v.m.) Hamster	fMLP	Ac2-26 (i.v.)	Mimicked GC (DEX) i.e. increased emigration time	(Mancuso *et al.*, 1995)
Mesentery (i.v.m.) Mouse	Zymosan	Ac2-26 (s.c.)	Reduced extent of zymosan-induced cell adhesion and emigration	(Lim *et al.*, 1998)
Mesentery (i.v.m.) Rat	IL-1β	Ac2-26 (s.c.)	Reduced IL-1β-induced cell adhesion and emigration	(Cuzzocrea *et al.*, 1997)
Mesentery (i.v.m.) Mouse	I/R of mesenteric vessels	Ac2-26 (i.v.)	Reduces I/R-induced cell adhesion and emigration, induces adherent cell detachment	(Gavins *et al.*, 2003)
Peritonitis Mouse	Zymosan	Ac2-26 (s.c.)	Reduces zymosan-induced PMN influx into cavity	(Getting *et al.*, 1997)
Circulatory shock	I/R of splanchic organs	Ac2-26 (s.c.) (i.v.)	Reduces the I/R-induced decrease in blood pressure/ decrease leukocyte accumulation in intestines	(Cuzzocrea *et al.*, 1997)
Pain Rat	Carrageenin TNF-α IL-1β	Ac2-26 (i.pl.)	Reduced the intensity of hyperalgesia	(Ferreira *et al.*, 1997)
Arthritis model Rat	Carrageenin	Ac2-26 (i.v.)	Reduces carrageenin-induced recruitment of PMN into joint	(Yang *et al.*, 1997)

Exogenous ANX-A1: Fragment 1-188

Model/Species	Inflammogen	Treatment	Results	Reference
Air pouch Mouse	IL-1β	Fragment 1-188 (i.v.)	Reduces IL-1β-induced PMN accumulation in air pouch	(Perretti *et al.*, 1993)
Fever Rat	IL-1β	Fragment 2-188 (i.c.v.)	Reduces IL-1β-induced increase in colonic temperature	(Carey *et al.*, 1990)
Brain Rat	Occlusion of MCA	Fragment 1-188 (i.c.v.)	Inhibition of neuronal damage (infarct size) and oedema	(Relton *et al.*, 1991)

Endogenous ANX-A1

The effects of endogenous ANX-A1 were first examined by passive immunisation experiments using neutralising anti-serum or monoclonal antibodies. Application of the cytokine IL-1 into an experimental air pouch caused leukocyte emigration, as a basic model of leukocyte accumulation and inflammation. DEX is anti-inflammatory in this model by inhibiting the influx of cells into the air pouch. When endogenous ANX-A1 is blocked by a passive immunisation protocol with a neutralising sheep serum the anti-migratory effects of i.v. DEX are blocked (Perretti & Flower, 1993). This suggests that endogenous ANX-A1 has a specific role in DEX-induced inhibition of cell migration. These anti-migratory actions of ANX-A1 are unlikely to be due to the blockade of inflammatory mediator generation. This was shown again using an IL-1β-induced inflammation in a mouse air pouch model. The use of drugs that block eicosanoid producing pathways downstream of arachidonic acid (indomethacin, the

cyclooxygenase (COX) inhibitor and BWA4C, the selective 5-lipoxygenase inhibitor) do not have an anti-migratory effect in this model (Perretti & Flower, 1993).

So, these results challenged the previous idea that PLA_2 inhibition by ANX-A1 was the sole mechanism for the anti-inflammatory actions of the glucocorticoids. Recently it has become clear that it is likely that many of the anti-inflammatory actions of ANX-A1 are due to interference with granulocyte recruitment, migration and/or activation, at sites of inflammation brought about by other mechanisms.

From Table 1.1 it can be seen that in a variety of models of acute inflammation, performed in different species and with different inflammogens, anti-annexin antibodies have been reported to reverse the anti-inflammatory effects of the GC *in vivo*. Altogether these experiments indicate an important role for endogenous ANX-A1 in GC-induced inhibition of leukocyte recruitment and consequent tissue damage.

To examine more closely the ability of GC and endogenous ANX-A1 to influence leukocyte movement, intravital microscopy studies were carried out initially in the hamster cheek pouch model. When fMLP was used as an inflammatory stimulus to activate the hamster cheek pouch microcirculation there was a reduction in rolling velocities of WBC and an increase in the number of adherent and emigrating cells (i.e. an easily quantifiable inflammation). DEX was shown to have no effect on cell rolling and adhesion, however it influenced the fate of adherent cells such that a higher proportion detached from the vessel wall and returned to the blood flow, rather than emigrating through the wall into the surrounding tissue (Mancuso *et al.*, 1995). Cells that did emigrate took longer to do so. The use of an anti-ANX-A1 serum 24 hr before

DEX challenge reversed (almost to control levels) the delay in emigration and caused less cells to detach from the vessel wall. So DEX brings about this anti-inflammatory effect by affecting the leukocyte transmigration process and this seems to be mediated by endogenous ANX-A1.

Interestingly this relationship was not restricted to the neutrophils, as seen with experiments conducted to study endogenous ANX-A1 and its role in the anti-migratory action of GC on monocyte recruitment. In a model of murine peritonitis induced by zymosan DEX could reduce 24 hr monocyte recruitment in a dose-dependent fashion. Passive immunisation against full length hrANX-A1 rendered the steroid inactive in reducing cell recruitment (Getting *et al.*, 1997). This suggests that DEX may act *via* ANX-A1 on monocyte recruitment in the same way as it does in neutrophils. Indeed, when U937 cells were transfected with an ANX-A1 cDNA to augment protein expression a reduced degree of transmigration towards SDF-1α/CXCL12 was measured (Perretti *et al.*, 2002). The most recent data indicate that endogenous ANX-A1 is capable of inhibition of monocyte emigration reinforcing the previous *in vivo* study conducted in the mouse.

As GC have been shown to inhibit recruitment of eosinophils (Teixeira *et al.*, 1995) a study was carried out to evaluate the role of endogenous ANX-A1 in the recruitment of this cell type. DEX could inhibit both acute and delayed-onset recruitment of eosinophils from the circulation into sites of cutaneous inflammation (in a mouse model of allergic reaction in the skin) however this effect was shown to be independent of ANX-A1 (Teixeira *et al.*, 1998). So although endogenous ANX-A1 can be clearly demonstrated to have a role in mediating the anti-migratory effects of DEX with

respect to neutrophil and monocyte recruitment this is not the mechanism that DEX utilises to inhibit eosinophil recruitment.

Exogenous ANX-A1

After the cloning and sequencing of ANX-A1, human recombinant ANX-A1 (hrANX-A1) was available in substantial amounts. The protein could be administered exogenously and was clearly shown to mimic several of the anti-inflammatory effects of GC in a variety of models (Table 1.1.). As each annexin possesses a unique N-terminus it is thought that this might confer specificity of activity. Thus, peptides have been synthesised and tested, the idea being that they may be easier to prepare and administer compared to handling of the full-length protein. Many studies have shown that peptide Ac2-26 (corresponding to 25 amino acids of the 41 amino acid N-terminus) and a truncated version of ANX-A1, fragment 1-188, are effective at inhibiting leukocyte recruitment mimicking the effects of hrANX-A1 (see Table 1.1.). Although fragment 1-188 was shown to exhibit anti-migratory action in an IL-1β air pouch model it was not as efficacious as the full length protein (fragment 1-188 inhibited IL-1β-induced neutrophil accumulation by a maximum of 49% whereas full length hrANX-A1 inhibited accumulation by almost 90%) (Perretti & Flower, 1993). Peptide Ac2-26 also inhibited leukocyte migration in the IL-1β air pouch model, with a similar efficacy to whole length hrANX-A1 (around 90% inhibition of leukocyte recruitment) although it was approximately two orders of magnitude less potent than the full length parent protein (Perretti *et al.*, 1993). This study also suggested that the peptide was acting *via* the same mechanism as the native ANX-A1 as when inactive ANX-A1 was given

intravenously (which did not alter IL-1β-induced neutrophil migration) it completely blocked the effect of the peptide (Perretti *et al.*, 1993).

One important finding of these original studies was that both hrANX-A1 and peptide Ac2-26 could cause adherent cells to detach from activated endothelium such that, rather than emigrate, these cells returned to the blood stream. This was shown in both the inflamed hamster cheek pouch (Mancuso *et al.*, 1995) and in the mouse mesentery after inflammation induced by zymosan (Lim *et al.*, 1998) and during the course of this thesis, by I/R (Gavins *et al.*, 2003). This suggests that exogenous ANX-A1 could be reducing cell emigration to the site of inflammation by causing detachment of adherent cells. As discussed before, endogenous ANX-A1 could also be acting in this manner (Mancuso *et al.*, 1995).

ANX-A1 has also been demonstrated to have a role in another facet of inflammation, that is, pain. In a model of mechanical hyperalgesia (rat paw pressure test) DEX was shown to reduce the hyperalgesic effects of agents such as carrageenin, TNF-α and IL-1β. Passive immunisation against ANX-A1 abolished the anti-hyperalgesic effect of DEX in this model. Hyperalgesic responses could also be inhibited by pre-treatment with peptide Ac2-26 (Ferreira *et al.*, 1997). More recently, administration of the peptide has been shown to inhibit nociceptive behaviour in the mouse formalin paw test: injection of formain into hind paw causes a biphasic response consisting of licking and biting the paw. Peptide Ac2-26 could inhibit the later phase of the nociceptive response (Pieretti *et al.*, 2004).

1.2.4. Mechanisms of Action

Experimental work using FACS analysis, confocal microscopy and western blotting has shown that in human neutrophils, ANX-A1 was mainly found intracellularly with only small amounts on the cell surface. Neutrophil adhesion to endothelial monolayers (stimulated by either fMLP, IL-8 or PAF) causes intracellular ANX-A1 to be translocated to the cell surface (much larger amounts of intact, 37 kDa ANX-A1 could now be detected) where it is kept in a Ca^{2+} dependent manner (Oliani *et al.*, 2001; Perretti *et al.*, 1996b). After adhesion, neutrophils lost a majority (>50%) of their staining for cell-associated ANX-A1. ANX-A1 could now be detected in the supernatant from the adherent cells, although this was not the intact 37 kDa protein but a cleaved form of the protein that was only 33 kDa in size. So the surface bound ANX-A1 on adherent cells is subjected to proteolysis and a 33 kDa 'clipped' form of the protein is released into the media (Perretti *et al.*, 1996b). These data suggest that externalised ANX-A1 may be involved in the negative regulation of neutrophil migration. The idea of a specific 'lipocortinase' has also been suggested, which might 'clip' the N-terminal region of ANX-A1 releasing the inactive 33 kDa form (Perretti *et al.*, 1996b). The enzyme(s) responsible for this action has yet to be identified. However several enzymes have been shown to cleave the N-terminal region of ANX-A1 including elastase (Huang *et al.*, 1987; Smith *et al.*, 1990), calpain (Ando *et al.*, 1989; Liu *et al.*, 1995), cathepsin D (Ando *et al.*, 1989) and plasmin (Huang *et al.*, 1987) though it is not yet defined which one is present in the microenvironment of the adherent neutrophil thus which one would be biologically relevant.

Experiments were then performed to look at the cellular distribution of ANX-A1 in emigrating cells during an actual inflammatory response. A model of acute peritonitis in the rat was induced by i.p. injection of carrageenin for 4 hr. Mesenteries were stained and neutrophils in the vasculature and tissues were examined. ANX-A1 was found in the nucleus, cytoplasm and plasma membrane of intravascular neutrophils. The majority of ANX-A1 in the plasma membrane of adherent cells is the intact, 37 kDa form of the protein (Oliani *et al.*, 2001) backing up what was found *in vitro* (Perretti *et al.*, 1996b). Cells that had emigrated from the vessels were found to contain mainly the clipped 33 kDa isoform of the protein and this was located in vacuoles. This has led to the proposal that *in vivo* endogenous ANX-A1 acts as an autocrine inhibitor that controls the emigration process in pathophysiological situations (membrane bound ANX-A1 affects adherent cells from which it is secreted). The proteolytic cleavage of ANX-A1 that can occur on the cell surface may regulate the action of this protein and may be somehow involved in the regulation of the cell emigration process.

It is still unclear how ANX-A1 is released from neutrophils as the protein lacks a signal sequence which would be necessary to target ANX-A1 to the classical secretory pathway. An *in vitro* study has established that in resting human neutrophils there is co-localization of ANX-A1 with gelatinase granules (but not with secretory vesicles or lysosomes) a large proportion of which is found in the matrix of the granules. On adhesion (of neutrophils to monolayers of endothelial cells) there is an externalization of ANX-A1 and it is found in a punctate pattern on the neutrophil surface (Perretti *et al.*, 2000). *In vivo*, it was demonstrated that adherent cells (in the vasculature) had co localization of ANX-A1 and gelatinase and once cells had emigrated (found outside of

the vasculature) only a very low amount of gelatinase was found, indicating that exocytosis of this enzyme had occurred (Oliani *et al.*, 2001). As gelatinase granules are mobilised during neutrophil extravasation (Borregaard & Cowland, 1997) this may be a mechanism for externalising a large proportion of ANX-A1 from activated neutrophils.

Experiments were suggesting that leukocytes might contain binding sites for ANX-A1 on their surface and that these were mediating the effects of exogenous ANX-A1. A study was carried out to assess binding of human ANX-A1 to cells although this used an indirect method to quantify binding in which binding of ANX-A1 was detected using a specific mAb and flow cytometric analysis. Human monocytes, but not lymphocytes, were shown to exhibit Ca^{2+}-dependent, trypsin-sensitive ANX-A1 binding and two specific binding sites were found using immunoprecipitation studies (Goulding *et al.*, 1996). As specific proteinaceous binding sites for ANX-A1 are found on the surface of human monocytes and neutrophils (Euzger *et al.*, 1999) a recent breakthrough in the field is the proposition that ANX-A1 is likely to be an agonist at the formyl peptide receptor (FPR), the prototype of the family of seven transmembrane domain G-protein-coupled receptors. The first study used an N-terminal derived peptide of ANX-A1, Ac9-25, and found that it was triggering signalling pathways in neutrophils (Walther *et al.*, 2000). This was an *in vitro* study and a variety of experiments demonstrated that Ac9-25 was acting on FPR in a similar manner to another ligand of the receptor, fMLP. The transcellular Ca^{2+} signals, which are initiated when fMLP binds to its receptor, FPR, were also increased when Ac9-25 was added to cells. Activation of chemoattractant receptors by their agonists can lead to heterologous and homologous desensitisation i.e. the down-regulation of cell responses to a second challenge by an agonist. This desensitisation of Ca^{2+} mobilisation was seen

not only in response to fMLP, but also Ac9-25. Peptide Ac9-25 caused desensitisation of Ca^{2+} mobilisation in neutrophils and stopped them responding to chemotactic gradients. These authors proposed that this mechanism could possibly have a role in decreasing cell emigration. Antagonists of fMLP were also shown to abolish the inhibitory effect of Ac9-25 on neutrophil transendothelial migration using a two-chamber system (Walther *et al.*, 2000). Application of antagonists of FPR, in a model of mouse peritonitis, blocked the anti-inflammatory properties of Ac2-26 and Ac2-12. Indication for binding of ANX-A1 to murine FPR was obtained by a set of *ex-vivo* experiments with FPR knockout mice (Perretti *et al.*, 2001). However, this issue is not as clear-cut as first thought and FPR may not be the only receptor involved in the biological action of ANX-A1. In fact a variant of FPR termed FPR-like 1 (FPRL1), may also be involved in the anti-inflammatory mechanism of ANX-A1 (Gavins *et al.*, 2003).

1.2.5. ANX-A1 Knockout Mice

ANX-A1 knockout (ANX-$A1^{-/-}$) mice have been recently generated in our laboratory (Hannon *et al.*, 2002). The mice were produced using a dual-purpose vector which both inactivates the ANX-A1 gene and can report on the activity of the promoter with Lac-Z staining. The mice produced were healthy, viable and reproduced normally, with the mutated gene being passed on in the Mendelian fashion. Although the ANX-$A1^{-/-}$ mice were generated prior to the start of this PhD no research was published on the topic until 2002. Since then a small number of papers have been published beginning to report on the phenotype of ANX-$A1^{-/-}$ mice (Hannon *et al.*, 2002) (Wells *et al.*, in

press) and their inflammatory responses (Hannon *et al.*, 2002; Roviezzo *et al.*, 2002; Yang *et al.*, 2004; Yona *et al.*, 2004).

The initial paper on the ANX-A1$^{-/-}$ mice (Hannon *et al.*, 2002) has shown that the mice displayed altered levels of other annexins. In particular, annexins 2, 4, 5 and 6 were up-regulated in the lung of the ANX-A1$^{-/-}$ mice, whereas higher levels of 2 and 4 were found in the thymus of male mice with no difference in the female thymus. A strong up-regulation of COX-2 and cPLA$_2$ was seen in the lung and thymus of ANX-A1$^{-/-}$ mice irrespective of the sex. As many studies have shown the anti-inflammatory effects of ANX-A1 in models of acute inflammation these were the first types of studies to be carried out with the ANX-A1$^{-/-}$ mice to examine the effects of removing the ANX-A1 gene. Previous studies have shown that administration of the exogenous ANX-A1 mimetic, Ac2-26, can reduce neutrophil influx into the peritoneal cavity inflamed with zymosan (Getting *et al.*, 1997). Conversely, blockade of endogenous ANX-A1 reverses the anti-inflammatory actions of DEX in this model (Getting *et al.*, 1997). When the ANX-A1$^{-/-}$ mice were studied it was shown that the mice had a significantly greater cell emigration into the peritoneal cavity at all of the time-points examined (2, 4 and 24 hr) when compared to the wild type (ANX-A1$^{+/+}$). Heterozygote mice showed intermediate levels of emigration between the ANX-A1$^{+/+}$ and the ANX-A1$^{-/-}$ at the early time-points (2 and 4 hr) but more similar emigration numbers to the ANX-A1$^{+/+}$ at the 24 hr time-point (Hannon *et al.*, 2002). An increased IL-1β production by ANX-A1$^{-/-}$ mice was also noted after 2 hr zymosan peritonitis. ANX-A1$^{-/-}$ mice were found to be resistant to the anti-inflammatory effects of GC (DEX) in this model. Whereas DEX could reduce neutrophil migration in the peritoneal cavity of ANX-A1$^{+/+}$ mice by almost 50%, the GC could only reduce emigration in the

ANX-A1$^{-/-}$ mice by 22% and this difference was not significant. This data reinforces the idea that endogenous ANX-A1 may play a tonic inhibitory role in acute inflammation.

A second model of acute inflammation was studied in the ANX-A1$^{-/-}$ mice. An increase in paw inflammation in response to carrageenin-induced inflammation was also found. In particular, although ANX-A1$^{-/-}$ mice showed a similar time course for carrageenin-induced paw swelling they displayed an enhanced sensitivity and had greater swelling at most of the time-points examined (Hannon *et al.*, 2002). This fits with previous, similar studies showing that, in a model of carrageenin-induced paw swelling in the rat, exogenous ANX-A1 could inhibit paw oedema (Cirino *et al.*, 1989b).

A third study has utilised the ANX-A1$^{-/-}$ mice to monitor chronic inflammation. A model of antigen-induced arthritis (AIA) was used in which ANX-A1$^{+/+}$ mice show significant inflammation of the knee joint as demonstrated by a number of histopathologic features including pannus formation, synovitis (synovial lining hypercellularity), exudation of inflammatory cells into the joint space, cartilage damage and also bone damage. In this model, ANX-A1$^{-/-}$ mice showed exacerbation of AIA with a greater degree of synovitis, exudation of inflammatory cells and bone damage. As is seen in the previous study, the anti-inflammatory actions of GC are markedly attenuated in these mice. In the ANX-A1$^{+/+}$ mice DEX significantly reduced overall severity of AIA by 31% whereas ANX-A1$^{-/-}$ mice were relatively insensitive to DEX, with an overall severity inhibition of 13% (Yang *et al.*, 2004). These data suggest that endogenous ANX-A1 also has a role in more chronic models of inflammation.

Most recently the characterisation of macrophages from ANX-A1$^{-/-}$ mice has been studied (Yona *et al.*, 2004). They have been shown to have defects in the phagocytosis process that is dependent on the stimulus used. For example, peritoneal macrophages from ANX-A1$^{-/-}$ mice had a reduction in the phagocytosis of non-opsonised, but not opsonised, zymosan or IgG complexes. Macrophages from ANX-A1$^{-/-}$ mice did not appear to be morphologically different to macrophages from the ANX-A1$^{+/+}$, however they were shown to ingest or associate with significantly lower numbers of zymosan particles compared to the ANX-A1$^{+/+}$. This suggests a role for endogenous ANX-A1 during macrophage phagocytosis, at least under certain conditions.

1.3. Scope of the thesis

1.3.1. Aims

This thesis focuses on two main models of acute inflammation in the mouse with particular attention to the leukocyte recruitment process in ANX-A1$^{-/-}$ mice. The aims of this thesis were:

1. To use a simple model of acute inflammation (peritonitis) to assess leukocyte recruitment. The technique was modified by the addition of a cell staining protocol so that flow cytometry could be utilised to identify recruited cell populations in a more objective way to simple cell counting. This model could then be used to compare leukocyte recruitment between the ANX-A1$^{-/-}$ and ANX-A1$^{+/+}$ mice.

2. To learn the technique of intravital microscopy in the mouse cremaster muscle (from a visit to Dr. Granger's Laboratory in Louisiana, USA) with the intention being to set up and apply this technique to the current problem under investigation.

3. To determine if exogenous ANX-A1 has a role to play in leukocyte recruitment in the cremaster muscle intravital preparation.

4. To utilise intravital microscopy of the mouse cremaster muscle to dissect the recruitment process and to determine if differences existed between the ANX-A1$^{+/+}$ and ANX-A1$^{-/-}$ mice.

5. To examine leukocyte recruitment in transgenic ANX-A1 over-expressing mice to complement data obtained in the ANX-A1$^{-/-}$ mice.

1.3.2. Hypothesis

The hypothesis this project has explored is that major alterations in the inflamed microcirculation of ANX-A1$^{-/-}$ mice will occur. Based on previous pharmacological studies it is likely these mice will have an exacerbated inflammatory response when compared to their equivalent ANX-A1$^{+/+}$ mice.

Methods

2. Methods

Two main models were used in this study to assess leukocyte recruitment in inflammation: mouse peritonitis and intravital microscopy of the mouse cremaster. Leukocyte transmigration can be studied *in vivo* using a number of different techniques. The most common method is to quantify the migration of leukocytes into a body cavity such as the peritoneal cavity, or the pleural cavity, after the local administration of a pro-inflammatory stimulus such as zymosan, thioglycollate (non-specific) or IL-1β (specific inflammatory mediator). This study makes use of both zymosan- and IL-1β-induced peritonitis with the addition of a cell staining protocol so that flow cytometry could be utilised to identify the recruited cell populations. This technique provided valuable information on leukocyte recruitment to sites of inflammation however it did not identify the different stages of leukocyte recruitment. So, a technique of intravital microscopy of the mouse cremaster muscle was also used, to visualise potential alterations in the leukocyte recruitment process in the microcirculation of ANX-A1$^{-/-}$ mice.

2.1. Flow Cytometry

2.1.1. Animals

ANX-A1$^{-/-}$ and ANX-A1$^{+/+}$ animals were recently generated in our own laboratory (Hannon *et al.*, 2002) on a C57BL/6 background. The animals were viable, healthy and bred normally. No differences were found between the ANX-A1$^{+/+}$ and the ANX-A1$^{-/-}$ animals with respect to their appearance, behaviour or weight (Hannon *et al.*, 2002). Transgenic ANX-A1 over-expressing (ANX-A1^{TG}) mice and negative littermate control (ANX-A1^{LM}) mice were generated at Imperial College by Dr. Nic Wells and were a gift to the department. Transgenic mice were created on a C57BL/10 x CBA/Ca background using a transgene containing murine ANX-A1 cDNA with a chicken beta-actin promoter and cytomegalovirus enhancer. Over-expression of ANX-A1 does not appear to produce obvious effects on development or survival of these mice.

All mice were maintained on a standard chow pellet diet with tap water *ad libitum*. Animals were housed in cages in a room with controlled lighting (lights on 8:00 to 20:00 hr) in which the temperature was maintained at 21-23°C. Male and female animals were used and weighed between 25 and 35 g. Animal work was performed according to Home Office regulations (guidance from the Animals (Scientific Procedures) Act, 1986).

2.1.2. Model of Mouse Peritonitis

The peritoneal cavity was used as a site for the administration of inflammatory stimuli. Leukocytes were then collected in lavage fluids at selected time-points (4 or 24 hr).

Zymosan Preparation

Zymosan type A (500 mg) was mixed with 50-200 ml of phosphate buffered saline (PBS) and boiled (and continually stirred) in a conical flask for approximately 30 min. After cooling on ice the suspension was washed 3 times by centrifugation in PBS at 400 *g* for 15 min at 4°C. The resulting pellet was re-suspended in 10 ml PBS (500 mg zymosan in 10 ml PBS) and aliquoted into sterile eppendorf tubes at 100-500 µl volumes. These were then centrifuged at 400 *g* for 3 min and the supernatant discarded. The zymosan was then stored at -20°C until required.

Zymosan-Induced Peritonitis

Peritonitis was induced in mice using an i.p. injection of 1 mg zymosan in 0.5 ml sterile PBS. The dose of zymosan chosen was used in previous experiments performed in our laboratories and has been shown to cause a marked degree of leukocyte extravasation (Getting *et al.*, 1997; Hannon *et al.*, 2002; Perretti *et al.*, 1992)After the injection mice were left for selected time-points (4 and 24 hr) before being killed by carbon dioxide (CO_2) exposure and the leukocytes collected as described below (section 2.1.3.). Cells were also collected from untreated animals as controls. Figure 2.1. is a summary of the time-points examined.

IL-1β-Induced Peritonitis

Peritonitis was induced in mice using an i.p. injection of 10 ng IL-1β in 0.5 ml sterile PBS. The dose of IL-1β given has been used in previous experiments performed in our laboratory (Ajuebor *et al.*, 1998b). After the injection mice were left for selected time-points (Figure 2.1.) before being killed by CO_2 exposure and the leukocytes collected by the method described below (See section 2.1.3.).

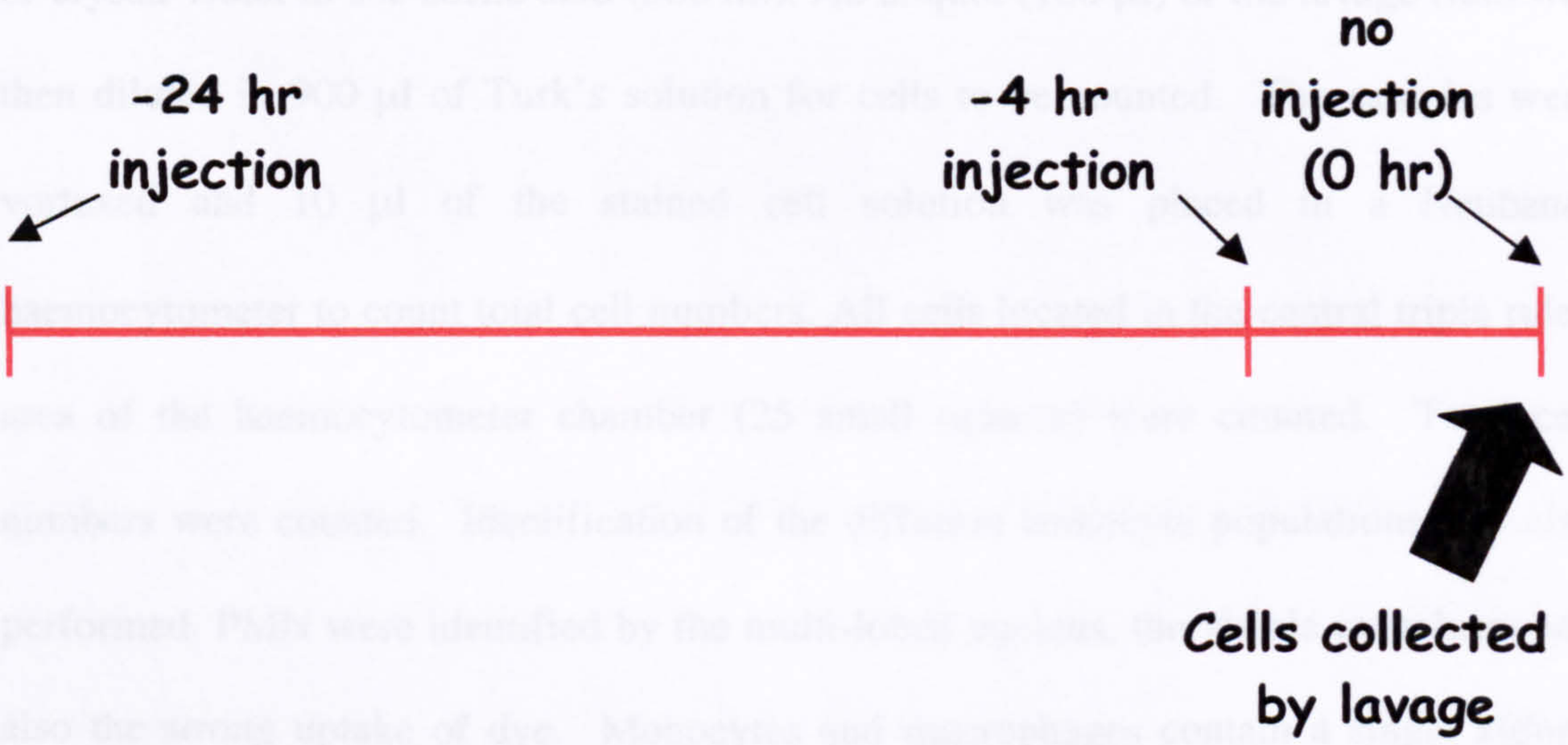

Figure 2.1. A summary of peritonitis time-points examined. Injection was either 10 ng IL-1β in 0.5 ml sterile PBS or 1 mg zymosan in 0.5 ml sterile PBS.

2.1.3. Collection of Peritoneal Lavage Fluids

Immediately after the animals were killed by CO_2 exposure, a small incision was made in the fur at the abdominal midline, the skin removed from either side and the peritoneal cavity exposed. The cavity was then injected with 3 ml of PBS containing 3 mM ethylenediaminetetra-acetic acid sodium salt (EDTA) and 25 U/ml heparin. The

cavity was gently massaged to ensure any loosely adherent cells were recovered and then the cavity was opened by a small incision in the abdominal muscle. The lavage fluid was collected using a 1 ml Pasteur pipette. Usually 1.5-2.5 ml of lavage fluid could be recovered. Samples were placed into polypropylene tubes and kept on ice.

Differential Cell Counting

Turk's solution (0.01% crystal violet in acetic acid) was prepared by dissolving 50 mg of crystal violet in 3% acetic acid (500 ml). An aliquot (100 µl) of the lavage fluid was then diluted in 900 µl of Turk's solution for cells to be counted. The samples were vortexed and 10 µl of the stained cell solution was placed in a Neubauer haemocytometer to count total cell numbers. All cells located in the central triple ruled area of the haemocytometer chamber (25 small squares) were counted. Total cell numbers were counted. Identification of the different leukocyte populations was also performed. PMN were identified by the multi-lobed nucleus, the visible cytoplasm and also the strong uptake of dye. Monocytes and macrophages contain a single kidney shaped nucleus and a larger cytoplasm and cells stained a paler blue. Lymphocytes contain a large round nucleus and only a small cytoplasm and these cells also stain a dark blue (see figure 2.2.). The number of cells recovered from the peritoneal cavity of each mouse could then be calculated using the following formula:

Number of cells counted in central triple ruled area (25 small squares) **x 10^4** (dilution factor on slide) **x 10** (dilution in Turk's) **= number of cells per ml of fluid**

Number of cells per ml of fluid x volume of liquid recovered = number of cells recovered from animal

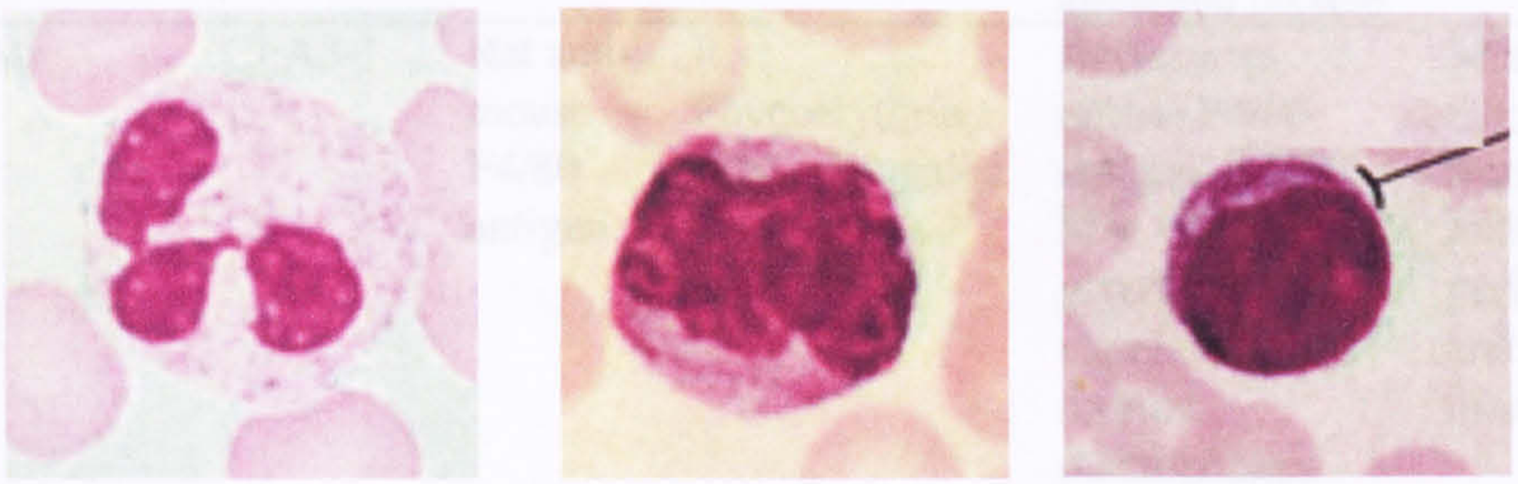

Figure 2.2. Cell types found in the lavage fluids by a peritoneal cavity wash.
Photos obtained from www.vh.org

2.1.4. Antibodies

A mixture of antibodies was used to label the cells collected from the peritoneal cavity. Figure 2.3. is a table showing details of these antibodies and the cell markers they recognise. Figure 2.4. is a diagram explaining the differential staining of peritoneal cells.

Abbreviation	Ab clone number	Details	Conjugated?	Ab specificity	Cells recognized by the Ab.
CD11b Ab	M1/70	Rat anti-mouse CD11b mAb	Biotin conjugated	Recognizes the170kDa α_M chain of Mac-1 (CD11b/CD18, $\alpha_M\beta_2$ integrin)	Monocytes, PMN and NK cells
Gr-1 Ab	RB6-8C5	Rat anti-mouse Ly-6G (Gr-1) and Ly-6C mAb	Fluorescein isothiocyanate (FITC) conjugated	Recognizes the LY-6G (Gr-1-myeloid differentiation antigen), a 21-25-kDa GPI anchored protein	Granulocytes (neutrophils and eosinophils)
F4/80 Ab	CI:A3-1	Rat anti-mouse F4/80 antigen	R. Phycoerythrin (PE) conjugated	Recognises mouse F4/80 antigen, a 160-kDa glycoprotein expressed by murine macrophages and blood monocytes	Murine macrophages from sites including peritoneal cavity and blood monocytes
Isotype control	A95-1	Rat IgG_{2b}. κ isotype standard	Biotin conjugated	Isotype-matched negative control for CD11b Ab	

Figure 2.3. Summary of antibodies used to stain peritoneal cells.

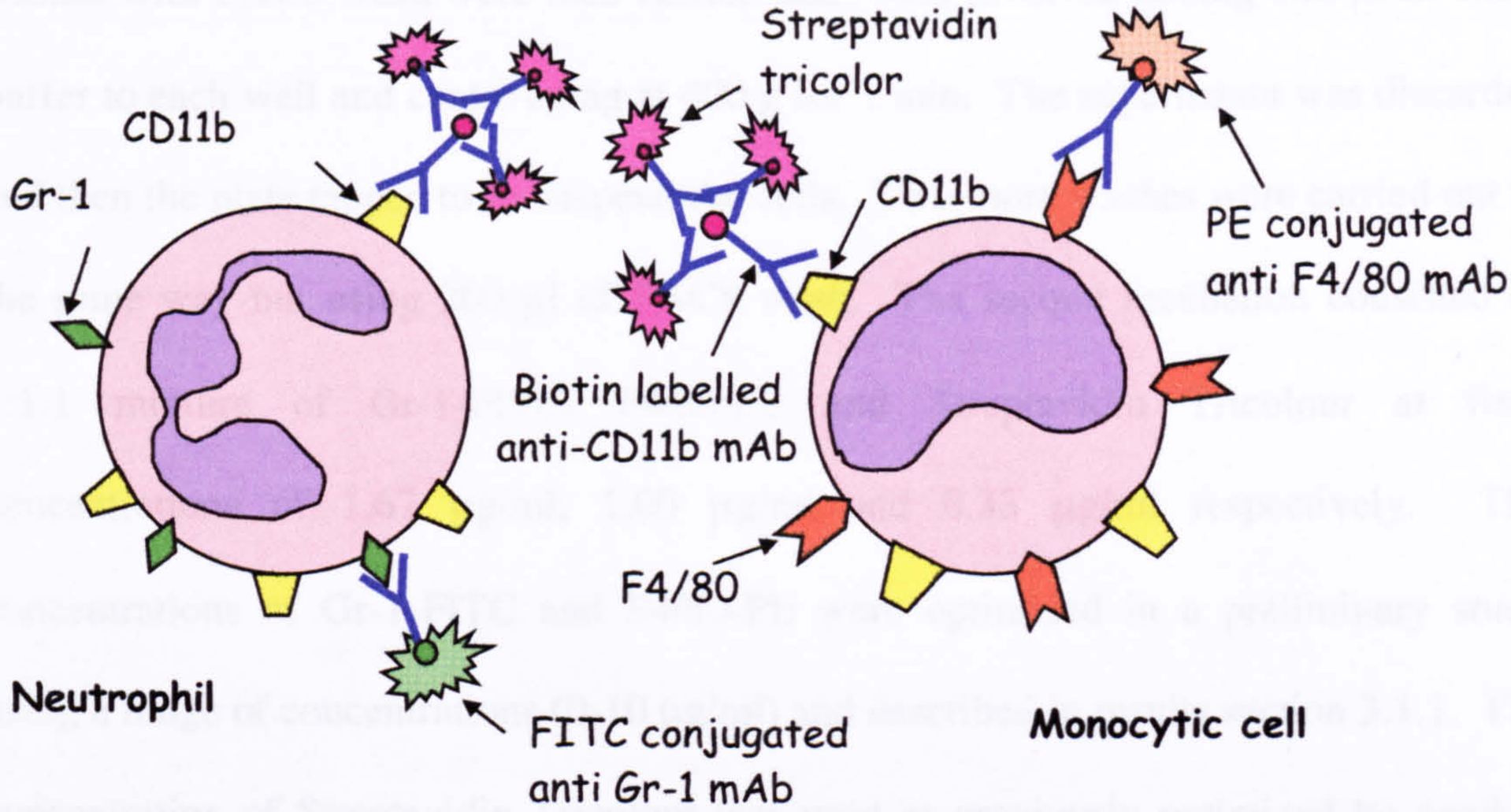

Figure 2.4. Diagram showing fluorescent labelling of peritoneal cells.

2.1.5. Cell Staining

After differential cell counting, lavage fluids were centrifuged at 400 *g* for 10 min, the supernatant collected into eppendorfs and frozen at -80°C for later analysis of mediator concentrations. The resulting pellet was re-suspended in FACS wash (PBS containing 0.2% bovine serum albumin (BSA) and 0.1% sodium azide (NaN_3)) to make cells up to a concentration of 4×10^7 cells/ml. Aliquots of cells (10 µl) were seeded onto a 96-well plate (spare cells were spun down and the resulting pellets frozen at -80°C for later analysis of protein concentrations by western blotting). A 1:1 mixture of 50 µl blocking IgG (human γ globulin, 6 mg/ml, made up in FACS wash) and either the CD11b antibody or the isotype control, both at a final concentration of 5 µg/ml were placed on the cells. These concentrations were used as they have been previously optimised by another group who demonstrated the technique to this department (Henderson *et al.*, 2001). The plate was put on ice and incubated for 30 min. Three

washes with FACS wash were then carried out. This involved adding 100 µl of wash buffer to each well and centrifuging at 400 *g* for 1 min. The supernatant was discarded and then the plate tapped to re-suspend the cells. Two more washes were carried out in the same way but using 200 µl of FACS wash. The second incubation consisted of 1:1:1 mixture of Gr-1-FITC, F4/80-PE and Streptavidin Tricolour at final concentrations of 1.67 µg/ml, 1.00 µg/ml and 0.33 µg/ml respectively. The concentrations of Gr-1-FITC and F4/80-PE were optimized in a preliminary study using a range of concentrations (0-10 µg/ml) and described in results section 3.1.1. The concentration of Streptavidin Tricolour was used as previously optimized by another group (Henderson *et al.*, 2001). The antibodies were added to the cells, which were then incubated, covered and on ice, for 30 min. Cells were again washed three times with FACS wash. The cells were re-suspended with 200 µl FACS wash and then fixed with 200 µl of cold cell fixative (CellFIX™, 1/10 dilution of stock). The flow cytometric analysis either followed immediately after this step or the next morning (tubes were stored wrapped in foil, overnight in the fridge). The cell staining steps are summarized in figure 2.5.

INCUBATION 1			
WELL		**BIgG**	**Antibody**
Main wells		50 µl	50 µl biotin CD11b
Unstained well		50 µl	50 µl FACS wash
Isotype control		50 µl	50 µl isotype control
FITC only	Single	50 µl	50 µl FACS wash
PE only	colour	50 µl	50 µl FACS wash
Tricolour only	controls	50 µl	50 µl biotin CD11b

INCUBATION 2				
Well	**FITC**	**PE**	**Tricolour**	**FACS wash**
Main wells	50 µl	50 µl	50 µl	
Unstained well				150 µl
Isotype control	50 µl	50 µl	50 µl	
FITC only	50 µl			100 µl
PE only		50 µl		100 µl
Tricolour only			50 µl	100 µl

Figure 2.5. Summary of cell staining steps for flow cytometry protocol. Final concentrations of reagents: biotin CD11b, isotype control : 5 µg/ml, BIgG (blocking IgG, human γ globulin): 3 mg/ml, FITC conjugated Gr-1: 1.67 µg/ml, PE conjugated F4/80: 1 µg/ml, streptavidin tricolour (secondary for CD11b): 0.33 µg/ml.

2.1.6. Flow Cytometric Analysis

Analysis of single cell suspensions by flow cytometry was completed using a FACScan flow cytometer (Becton Dickinson). Contaminants (red blood cells, dead cells, and debris) were gated out at the time of analysis, using forward and side scatter gating. FITC fluorescence was detected through the FL-1 channel; PE florescence through the FL-2 channel and Tricolour was assessed using the FL-3 channel. Data was acquired and analysed using the CellQuest© application on a Power Macintosh G3 computer. For each sample a minimum of 10,000 events were analysed. Gates were constructed around two populations, the FL-1 positive events (Gr-1 positive) and around FL-2 positive events (F4/80 positive events). The criteria examined were the percentage of total events each population contained and also the level of CD11b expression found in each of these populations. Figure 2.6 is a representative dot plot from the FACS machine after treatment with an inflammogen in a wild type mouse. This dot plot is

separating events based on the scatter in the FL1 and FL2 channels, FL1 being the channel for Gr-1 and FL2 the channel for F4/80. Three distinct populations are seen and gated so that the percentage of total events in each cloud can be determined. The Gr-1 positive events are neutrophils, the F4/80 positive events are monocytic cells and the events that are negative for both Gr-1 and F4/80 are mainly lymphocytes, with some dead cells and cell debris though most of this would have gated out at the time of data acquisition.

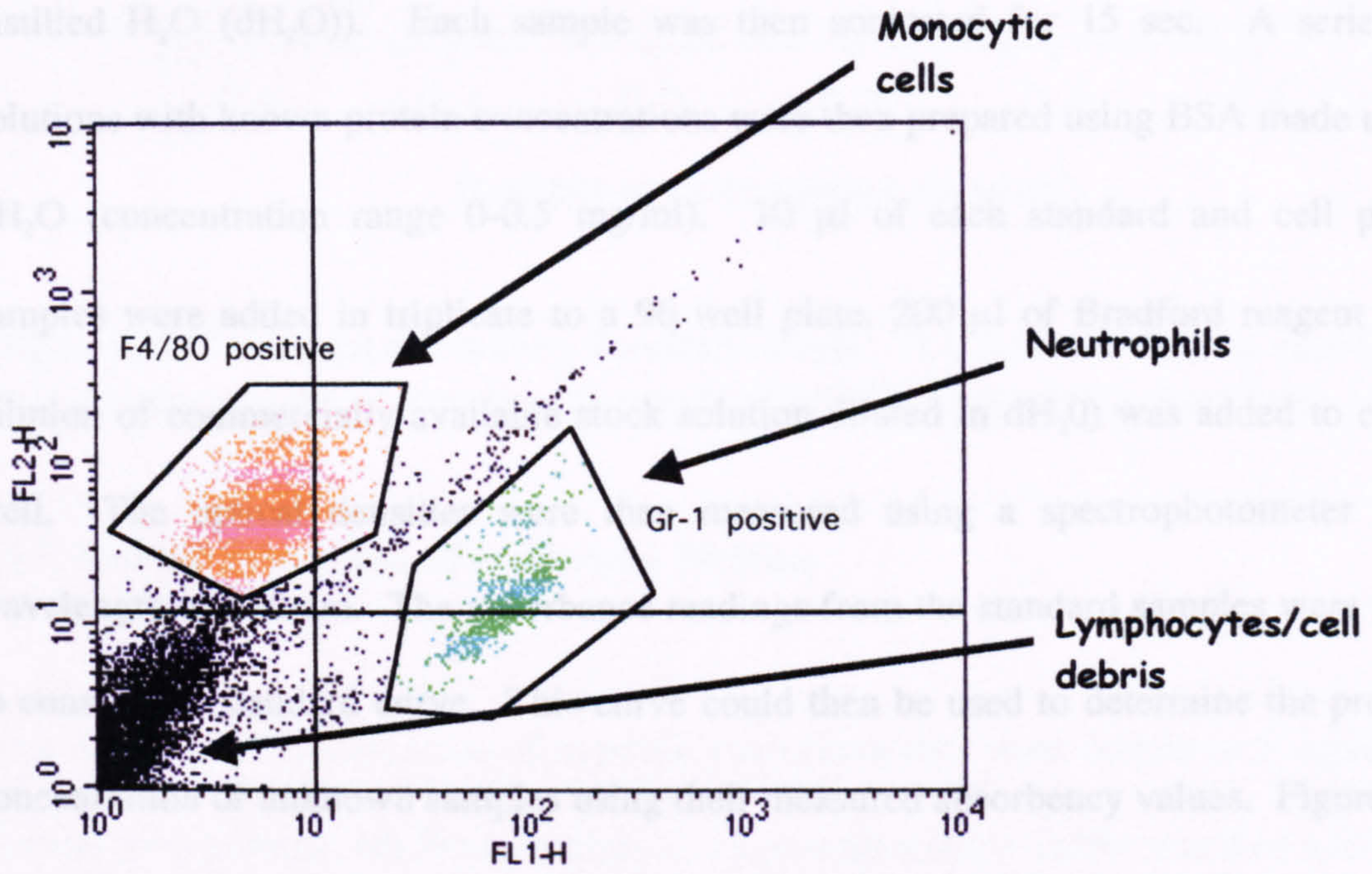

Figure 2.6. R epresentative dot plot from the FACS machine. Figure showing the events separated on the basis of Gr-1 and F4/80 Ab staining. Three distinct populations are seen: green, Gr-1 positive events (neutrophils), orange, F4/80 positive events (monocytic cells) and black, lymphocytes and some cell debris.

2.2. *In Vitro* Techniques: Protein and Mediator Generation in Peritoneal Samples

2.2.1 Bradford Assay for Protein

Cell pellets collected during peritonitis experiments were frozen at –80°C. Analysis of protein content was made with the widely used Bradford assay (Bradford, 1976). The samples were thawed at 4°C and then immediately re-suspended in protease inhibitory buffer (complete mini EDTA-free protease inhibitory cocktail tablet made up in 7 ml distilled H_2O (dH_2O)). Each sample was then sonicated for 15 sec. A series of solutions with known protein concentrations were then prepared using BSA made up in dH_2O (concentration range 0-0.5 mg/ml). 10 µl of each standard and cell pellet samples were added in triplicate to a 96 well plate. 200 µl of Bradford reagent (1:5 dilution of commercially available stock solution diluted in dH_20) was added to every well. The optical densities were then measured using a spectrophotometer at a wavelength of 570 nm. The absorbance readings from the standard samples were used to construct a standard curve. This curve could then be used to determine the protein concentration of unknown samples using their measured absorbency values. Figure 2.7 shows a representative standard curve constructed for a Bradford assay from standard samples.

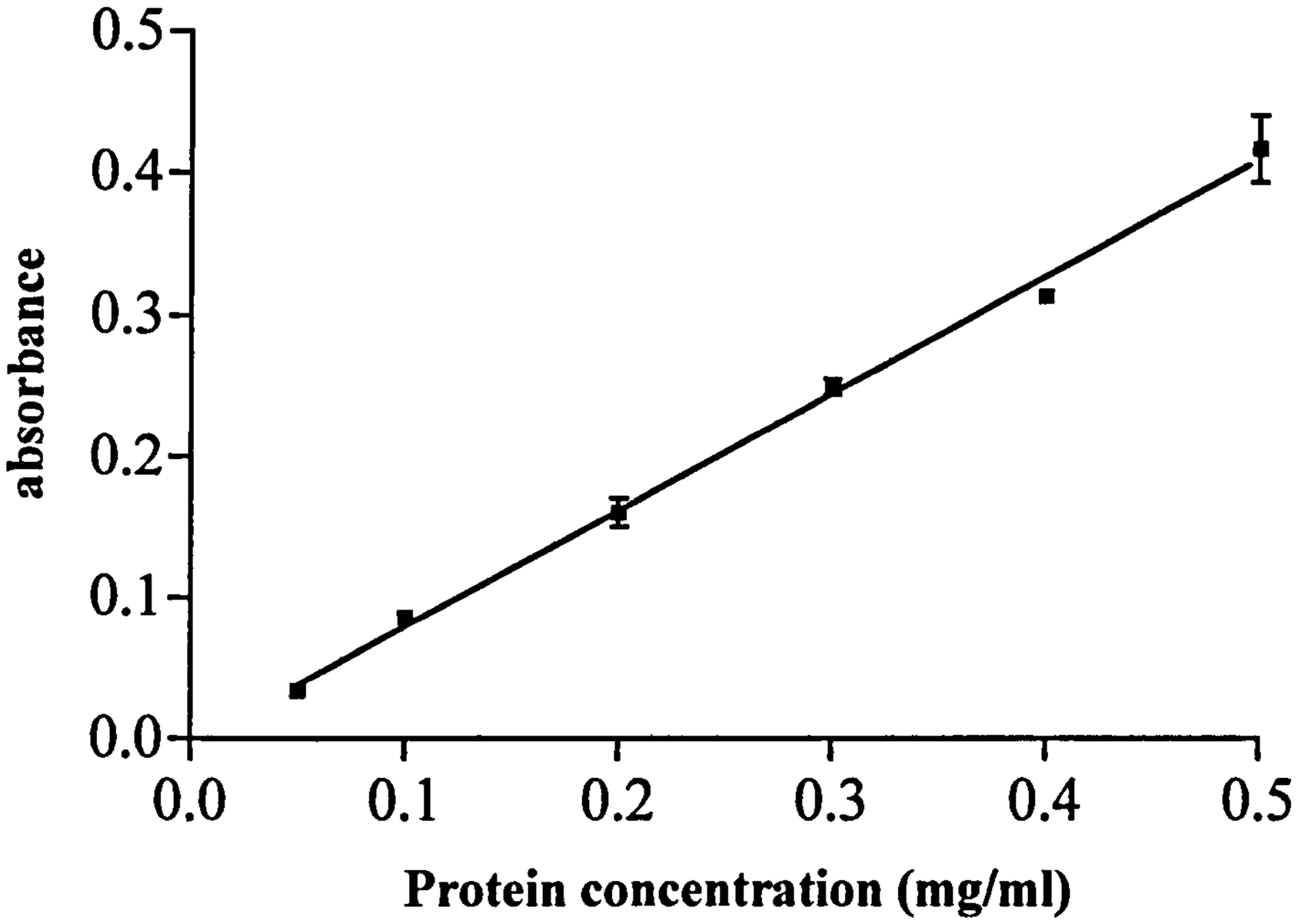

Figure 2.7. Standard curve for a Bradford assay. The curve can then be used to calculate the amount of protein in an sample of unknown protein concentration.

2.2.2. Sample Preparation for Western Blotting

Once the protein concentration of samples was known they were diluted to 2 mg/ml by dilution with protease inhibitory buffer. 2 x Laemmli sample buffer was then added to samples at a 1:1 ratio to yield a 1 x Laemmli buffer comprising 50 mM Tris HCl (pH 6.8), 100 mM dithiothretol (DTT), 2% sodium dodecyl sulphate (SDS), 0.1% bromophenol blue and 10% glycerol (Laemmli *et al.*, 1970). Samples were then boiled for 5 min. Prepared samples contained a final concentration of 1 mg/ml protein and were stored at -20°C.

2.2.3. SDS-PAGE (SDS Polyacrylamide Gel Electrophoresis) Western Blotting

Western blotting samples and prestained protein markers (broad range) were thawed at room temperature and markers boiled for 5 min. Samples were then loaded onto a 10% polyacrylamide gel comprising 3.3 ml protogel polyacrylamide, 2.5 ml resolving buffer (1.5 M Tris HCl pH 8.8), 2.9 ml dH_2O, 50 µl ammonium persulphate and 10 µl Temed and topped with a 4% stacking gel comprising 0.8 ml protogel polyacrylamide, 1.25 ml stacking buffer (0.5 M Tris HCl pH 6.8), 2.5 ml dH_2O, 50 µl ammonium persulphate and 10 µl Temed. Using a BioRad Mini-PROTEAN® III Electrophoresis system and a running buffer (25 mM Trizma Tris base, 192 mM glycine and 0.1% SDS in dH_2O) the gels were stacked and run at 100V until dye front reached the bottom of the gel (approximately 1 hr). The proteins in the gel were then transferred onto a nitrocellulose membrane (Hybond-C extra) via a system of wet transfer under 100 mA (taking approximately 1 hr) using transfer buffer (25 mM Tris base, 192 mM glycine and 20% methanol in dH_2O).

Following wet transfer the membrane was incubated overnight in a blocking solution of 5% milk in TBS-T (50 mM Tris HCl, 150 mM NaCl and 0.1% Tween 20 in dH_2O) at 4°C to prevent non-specific binding. The membrane was then washed 3 times (each wash 15 min) in TBS-T followed by incubation with a primary antibody (for ANX-A1 detection: 1:1000 rabbit anti-ANX-A1 antibody in TBS-T containing 5% milk, for α-tubulin detection: 1:5000 mouse anti-α-tubulin antibody in TBS-T containing 5% milk) for 1 hr at room temperature. The membrane was then washed 3 times (each wash 15 min) and incubated at room temperature for a further 1 hr with a peroxidase conjugated secondary antibody (ANX-A1 secondary: 1:2000 peroxidase conjugated goat anti-

rabbit antibody, α-tubulin secondary: 1:2000 peroxidase conjugated goat anti-mouse antibody). The membrane was washed as before. Membranes were then incubated for 1 min with enhanced chemiluminescence (ECL) reagent (1:1 mixture of two commercially available ECL reagents) before exposure to photographic film for approximately 1 min followed by developing and chemical fixation. Densitometric analysis was performed using the public domain NIH *Image* program (developed at the U.S. National Institutes of Health; http://rsb.info.nih.gov/nih-image/).

2.2.4. ELISA (Enzyme-Linked Immunosorbent Assay)

Ninety six well plates were coated with capture antibody (TNF ELISA: anti-mouse TNF antibody, KC ELISA: anti-mouse KC antibody) diluted in coating buffer (83 mM Na_2HPO_4, 134 mM NaH_2PO_4 in dH_2O, pH 6.5), sealed with parafilm and incubated overnight at 4°C. Following incubation plates were washed 3 times with wash buffer (PBS containing 0.05% Tween-20). After each wash the plate was inverted and blotted on paper towels to remove residual buffer. Next the plates were blocked to prevent non-specific binding using 200 µl assay diluent per well (PBS containing 10% FCS, pH 7.0) and incubated at room temperature for 1 hr. The plates were washed as before. Standards and samples (supernatants from peritonitis experiments, stored at -80°C, allowed to thaw at room temperature) were added to the wells (100 µl per well), the plates sealed and incubated at room temperature for 2 hr. Standards were prepared from a lyophilized sample reconstituted with 1 ml of deionised H_2O and stored in 50 µl aliquots at -80°C. For each experiment an aliquot was thawed at room temperature and then prepared into a series of standards made with assay diluent (range 0-1000 pg/ml). Assay diluent alone was used as the zero standard (0 pg/ml). After incubation of

samples and standards with the capture antibody the plates were washed as before but for a total of 5 washes. Detection antibody (biotinylated anti-mouse TNF/KC) and enzyme reagents (avidin-horseradish peroxidase conjugate) were added next for a 1 hr incubation at room temperature. Following the incubation the plates were washed for a total of 7 times and 100 μl of substrate solution (1:1 solution of tetramethylbenzidine and hydrogen peroxide) was added to each well, and incubated for 30 min at room temperature in the dark. Finally 50 μl of stop solution (1M sulphuric acid (H_2SO_4)) was added to each well. The optical densities were measured using a spectrophotometer at a wavelength of 450 nm within 30 min of addition of the stop solution. The absorbance readings from the standard samples were used to construct a standard curve on a logarithmic axis. This curve could then be used to determine the protein concentration of unknown samples using their measured optical densities. Figure 2.8 shows a representative standard curve obtained during an ELISA experiment for KC detection.

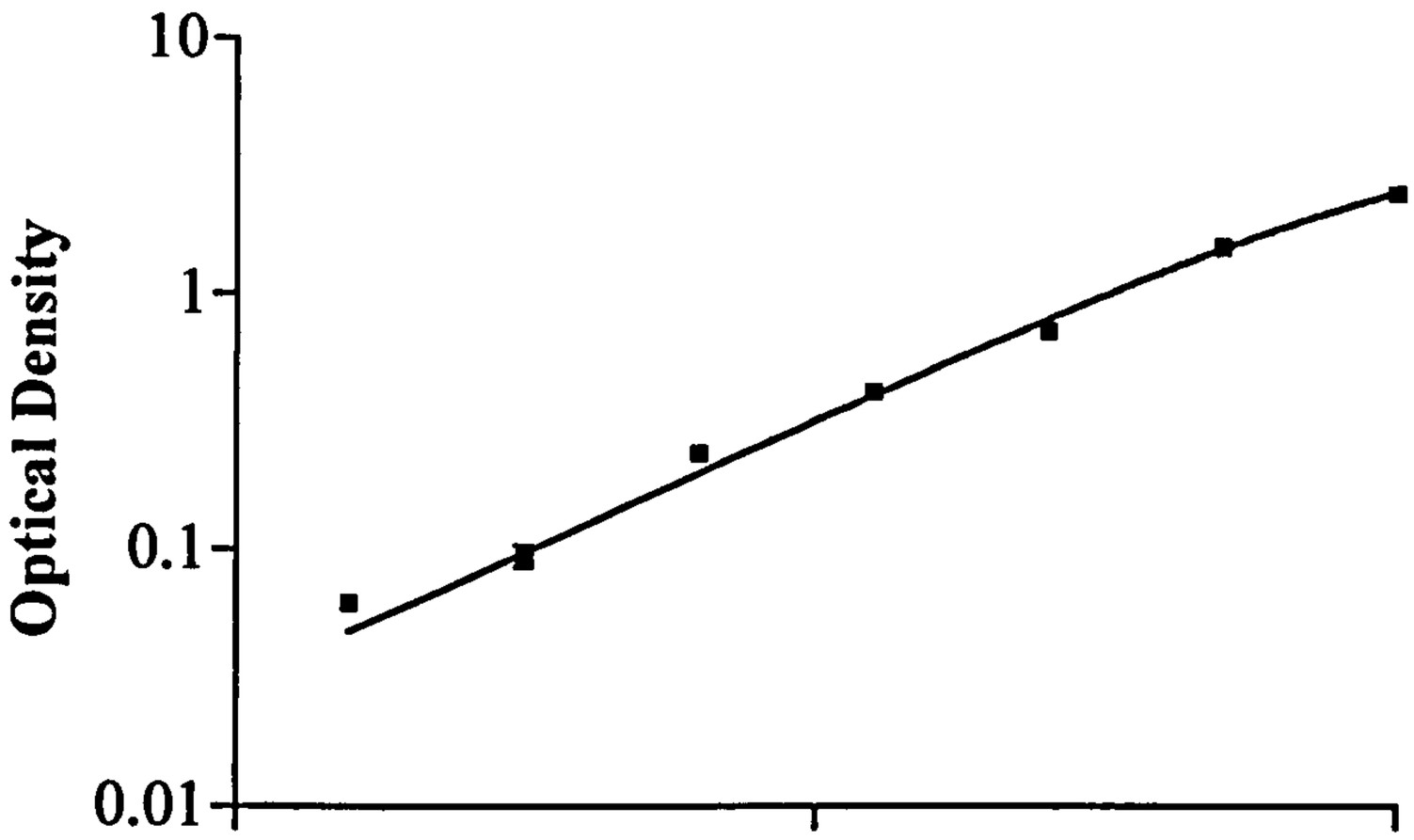

Figure 2.8. Standard curve for a KC ELISA. The curve is constructed from samples of known protein concentration.

2.3. Intravital Microscopy

2.3.1. Animals

ANX-A1$^{+/+}$ and ANX-A1$^{-/-}$ animals were generated in our own laboratory. FPR$^{-/-}$ mice were also bred on-site (breeding pairs donated by P.M. Murphy and J.L.Gao, NIH, Maryland, USA). C57BL/6 mice were purchased from B&K Universal and housed for a minimum of 1 week before being used for experiments. All animals were maintained on a standard chow pellet diet with tap water *ad libitum*. Animals were housed in cages in a room with controlled lighting (lights on 8:00 to 20:00) in which the temperature was maintained at 21-23°C. Male animals were used and weighed between 20 and 35 g. Animal work was performed according to Home Office regulations (guidance from the Animals (Scientific Procedures) Act, 1986).

2.3.2. Cremaster Muscle Preparation for Intravital Microscopy

Male mice were anaesthetised with one of two anaesthetic mixtures; either diazepam (6 mg/kg) subcutaneously in the neck followed immediately with an intramuscular injection of Hypnorm™ (0.7 mg/kg fentanyl citrate and 20 mg/kg fluanisone) in the thigh muscle, or a mixture of xylazine (7.5 mg/kg) and ketamine (150 mg/kg) made up in sterile H_2O and mixed before being injected i.p. In some cases the right jugular vein was cannulated for administration of saline, drugs and FITC-labelled albumin during the experiment. The neck area was shaved with electric clippers and the skin over the area removed. The salivary gland was moved to one side and the jugular vein was isolated from surrounding fat and tissues using tweezers. Using a silk suture the vein

was tied off proximally and a suture was loosely placed further down. A small incision was made in the vessel with micro scissors and the cannula (polyethylene tubing (PE10) connected to a 1 ml syringe) placed in and tied in place with silk suture. Next, the anterior aspect of the scrotum was gently shaved and all loose hair removed with a small piece of sticky tape. The mouse was placed onto the viewing stage. This was a specially made Perspex viewing stage consisting of a base plate with a central area containing a raised circular area (diameter: 24 mm, height: 15 mm) topped with a permanently attached glass cover slip. The central area has a raised edge to contain the buffer (which drips onto the preparation to keep it warm and moist). Excess buffer is drained away by suction (See Figure 2.9.). The stage was placed onto a heating pad to maintain body temperature at 37°C. An incision was made in the skin and fascia over the ventral aspect of the right scrotum. Care was taken not to touch the underlying tissue with any instruments used. Irrigation of exposed tissue started (as soon as tissue was exposed) with bicarbonate buffered solution (BBS). This solution consisted of 132 mM NaCl, 5 mM KCl, 2 mM $CaCl_2$, 1 mM $MgSO_4$, 20 mM $NaHCO_3$ made up in distilled water and heated to 37°C. This solution was regularly applied to the exposed tissue to keep it moist. The incision was extended up above the inguinal fold and to the distal end of the scrotum. The underlying connective tissue fascia was then carefully separated from around the cremaster sack avoiding touching the cremaster muscle. At this point the animal was positioned using a gel heating pack (to keep animal warm) in a supine position with the cremaster sack resting on the central glass region of the stage. A suture was used in the distal end of the cremaster sack to hold down and slightly extend the end of the sack. Using a cauteriser a line was scored down the centre of the cremaster sack and also from left to right along the top edge of the sack. The cauteriser was allowed to completely pierce the tissue at one point and then

scissors were placed in here and the scored lines cut along gently. The cremaster then started to lie flat on the glass stage. Four hooks (bent 6 gauge needles) attached to threads and taped down were used along the edges of the tissue (two on each side) to hold the cremaster down onto the glass stage. The small vessel connecting the testicle and cremaster was sealed using the cauteriser and then scissors used to cut the last remaining connections between the testicle and the cremaster muscle. The testicle was laid out to the side so as little as possible was covering the cremaster muscle. The preparation was then ready to view under the microscope. Figure 2.10. is a photographic summary of cremaster preparation. The preparation on the stage was then mounted on a Zeiss Axioskop 'FS' microscope with a water immersion objective lens (magnification of x 40; Carl Zeiss Ltd, Welwyn Garden City, UK) and an eyepiece (x 10 magnification; Carl Zeiss Ltd) was used to observe the microcirculation. The preparation was trans-illuminated with a 12-V, 100-W halogen light source. An optical Doppler Velocimeter (Microcirculation Research Institute, Texas A&M University, Dallas, Texas, USA) was attached to measure centre line RBC velocity. A Hitachi charge-coupled device colour camera (model KPC571; Tokyo, Japan) acquired images that were displayed onto a Sony Trinitron colour video monitor (model PVM 1440QM) and recorded on a Sony super-VHS video cassette recorder (model SVO-9500 MDP) for subsequent off-line analysis. A video time-date generator (model VTG-33; Tokyo, Japan) projected the time, date and stopwatch function, onto the monitor. The setup was connected so that warm BBS continuously dripped onto the tissue at a rate of 2 ml/min and was then removed using suction. Figure 2.11. shows the microscope set-up. The open cremaster muscle preparation was originally described in the early 1970's (Baez, 1973) for the rat and then the mouse. It has now been used extensively and reported in over 230 papers (PubMed search as of September 2004).

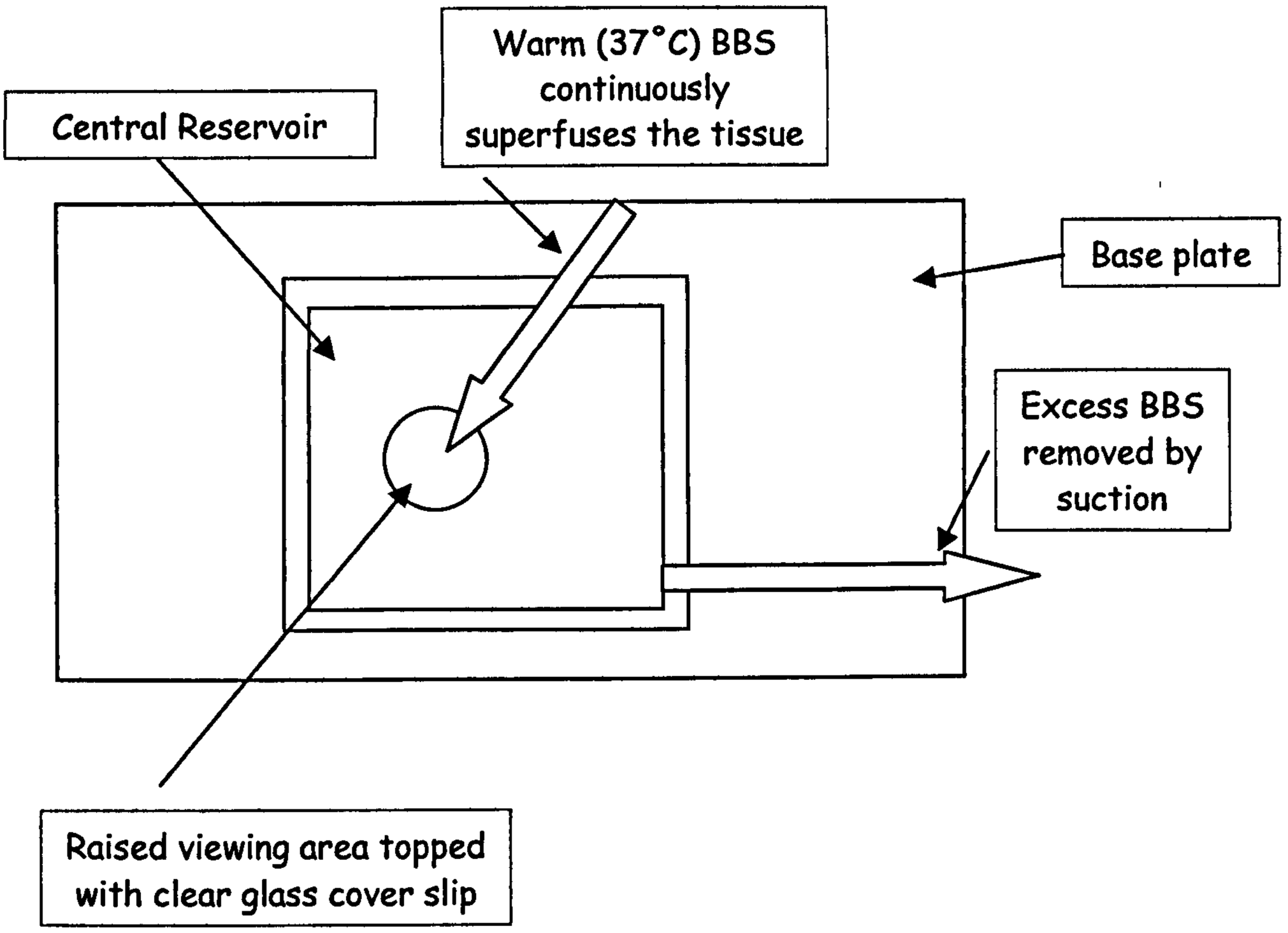

Figure 2.9. Diagram showing the specially designed Perspex stage used in this thesis.

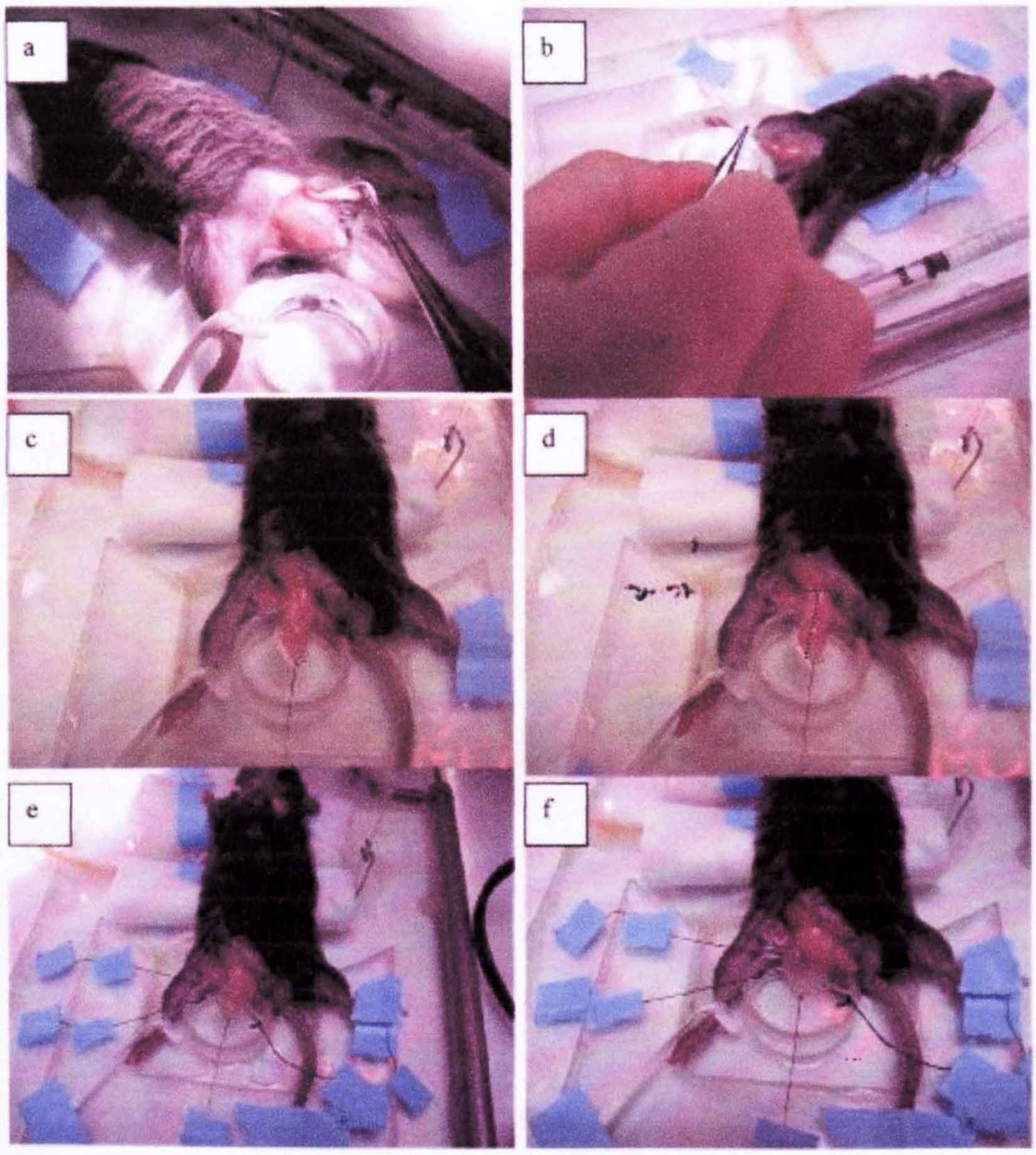

Figure 2.10. Photographic summary of the cremaster muscle preparation in mice. (a) The mouse taped to Perspex stage and skin removed from right scrotum to show testicle and surrounding cremaster (b) Cremaster and its contents after it is freed from surrounding fat and tissues (c) Cremaster and its contents extended and placed onto glass stage (d) Cremaster showing lines to be cut along (e) Cremaster sack after cutting and pins inserted to hold it in place (f) Testicle moved to side and cremaster ready for trans-illumination and observation.

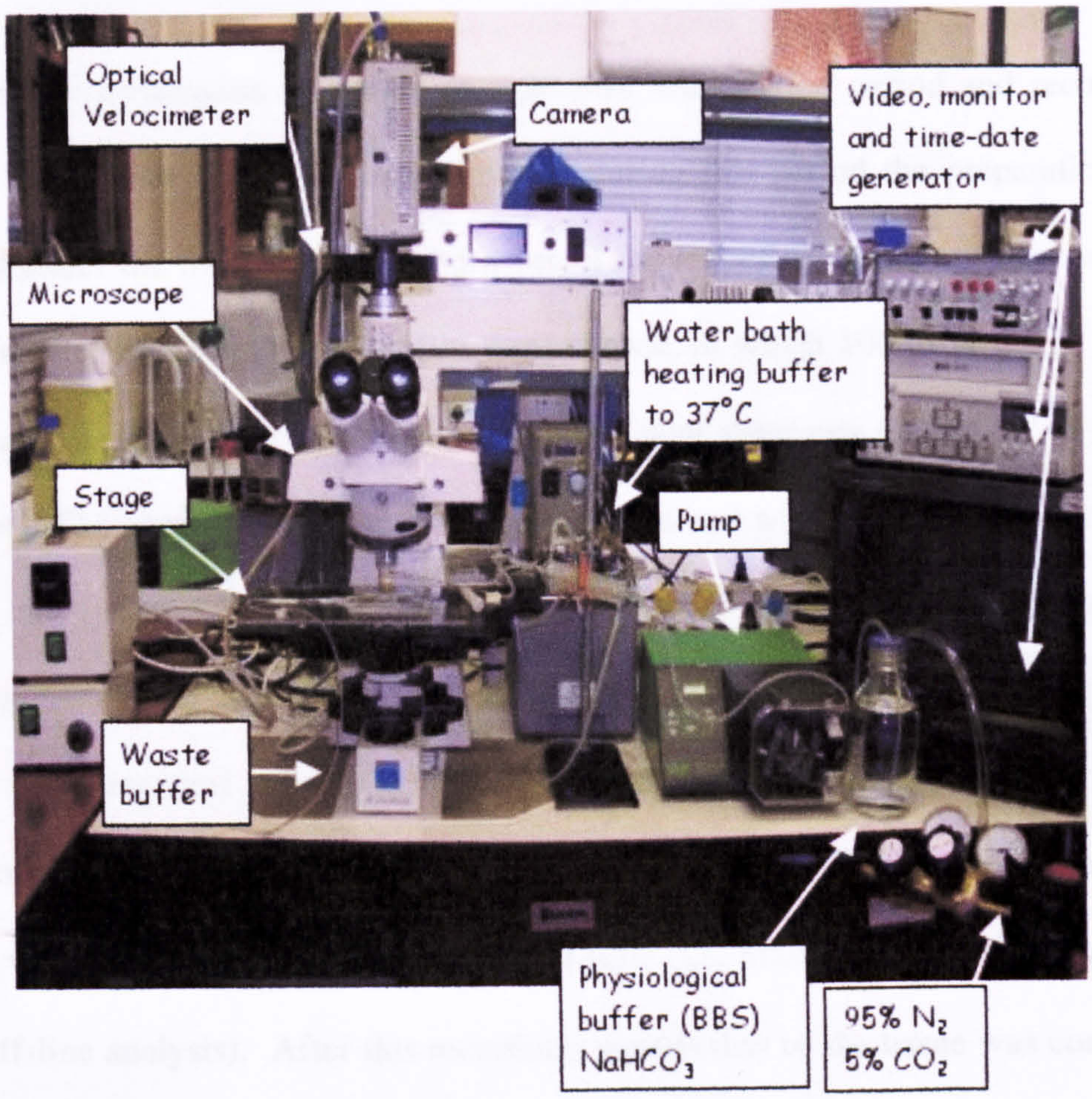

Figure 2.11. Intravital Microscopy Set Up.

2.3.3. PAF-Induced Inflammation

The cremaster preparation was allowed a 30 min stabilization period and recordings were not made until after this time, although during this period the preparation was examined under the microscope to find a vessel for recording. Post-capillary venules with a diameter between 20 and 40 μm were chosen, in which 100 μl length of vessel could clearly be seen. Also another criteria was a wall shear rate (WSR) of ~500 sec^{-1} or greater. The venule fitting the above parameters and with the smallest number of adherent and emigrated leukocytes at the end of the 30 min stabilization period was chosen to record. A 5 min recording was made and at the end of the recording the RBC velocity was measured using the Doppler velocimeter, and diameter noted. The number of cells that had emigrated into the surrounding tissue (50 μm either side of the 100 μm venule section) were counted in real-time (i.e. after recording the vessel not during off-line analysis). After this recording, superfusion of the tissue was continued with either normal BBS (vehicle control animals) or with a PAF solution (1 or 100 nM) made up in BBS. The concentration of PAF to be used was determined by experiments carried out previously in our laboratory (Tailor *et al.*, 1997) and by others (Zimmerman *et al.*, 1994). Recordings (5 min) were made every 15 min from the start of this superfusion with the same parameters measured as before and continued for 90 min. The video recordings were used subsequently for off-line analysis (see section 2.3.6).

Figure 2.12. is a summary of recordings made during PAF experiements.

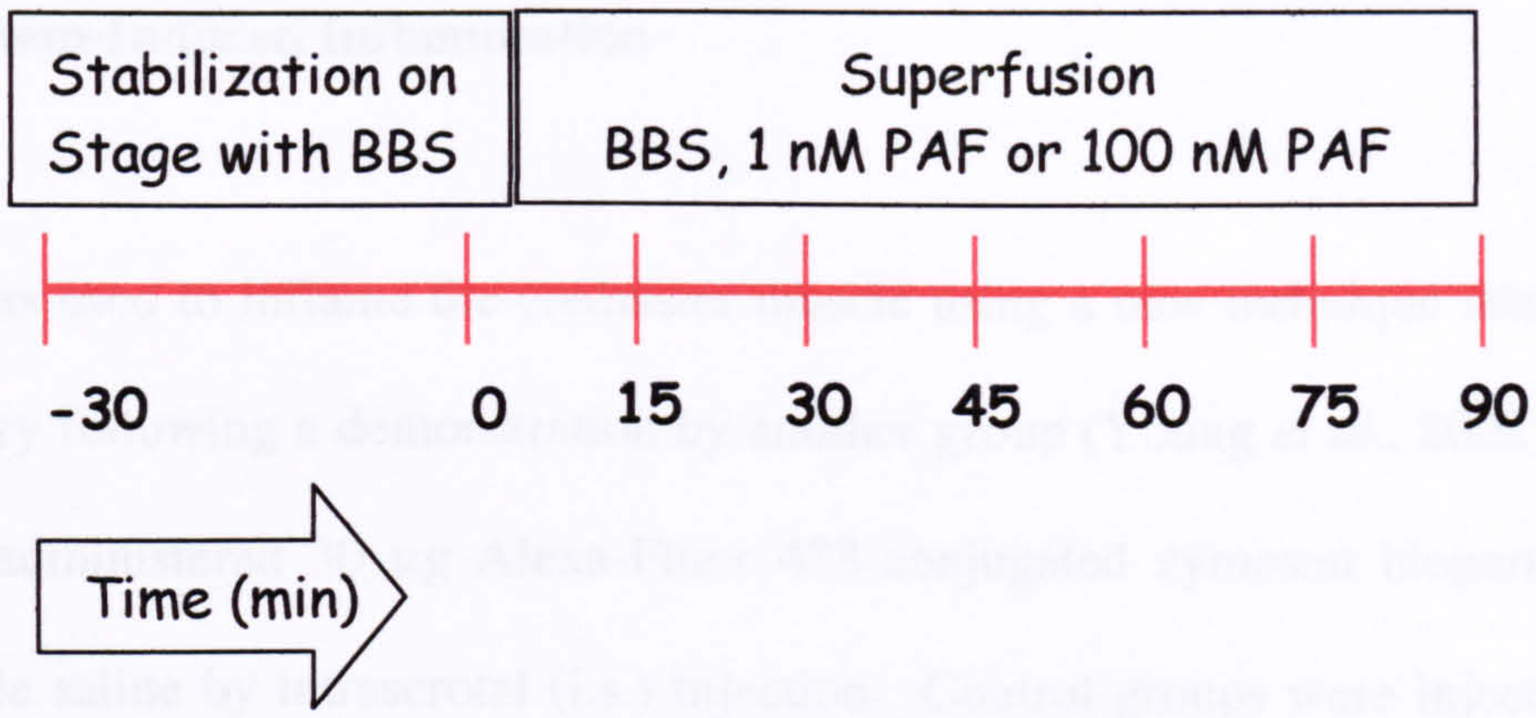

Figure 2.12. Summary of recordings made during PAF intravital experiments.

In the case of experiments designed to analyse cell detachment, after a 30 min stabilisation period a continuous video recording was made of a single vessel for 60 min during superfusion of the cremaster with 1 nM PAF. All analysis of these vessels was carried out off-line as described in section 2.3.6.

2.3.3.1. Effect of Ac2-26 in the Cremaster Muscle Inflamed with PAF

Male mice were first cannulated and then prepared for intravital microscopy of the cremaster muscle (see section 2.3.2.). After a 30 min stabilisation period and a basal recording (5 min) animals were either administered 200 μg peptide Ac2-26 (in 200 μl PBS) or 200 μl PBS alone via the cannula in the jugular vein (i.v.). Superfusion of the cremaster with a 100 nM PAF solution (made up in BBS) was then started. Recordings (5 min) were made every 15 min from the start of this superfusion with the same parameters measured as before and continued for 90 min. The video recordings were used subsequently for off-line analysis (see section 2.3.6).

2.3.4. Zymosan-Induced Inflammation

Zymosan was used to inflame the cremaster muscle using a new technique adapted by the laboratory following a demonstration by another group (Young *et al.*, 2002). Male mice were administered 30 μg Alexa-Fluor 488-conjugated zymosan bioparticles in 400 μl sterile saline by intrascrotal (i.s.) injection. Control groups were injected with i.s. saline (400 μl). These injections were performed under anaesthetic (either xylazine and ketamine (as above) or using inhaled halothane gas at a concentration of ~3%) following which the animal was allowed to recover. Later (approximately 4.5 hr after injection of zymosan), the mice were re-anaesthetised and the cremaster muscle prepared for intravital microscopy using the technique described above (section 2.3.2.). The cremaster preparation was allowed a 30 min stabilization period and recordings were not made until after this time, although during this period the preparation was examined under the microscope to find the vessels of choice to record. Post-capillary venules were chosen that had a diameter between 20 and 40 μm, in which 100 μl length of vessel could clearly be seen and with a WSR of ~500 s^{-1} or greater. One to three post-capillary venules were chosen for analysis from each mouse. A 5 min recording was made of each vessel and at the end of each recording the RBC velocity was measured using the Doppler velocimeter, and diameter noted. The number of cells that had emigrated into the surrounding tissue was counted (50 μm either side of the 100 μm venule section). A further experiment was carried out in which emigration was quantified at different distances from the vessel wall (0-50 μm, 50-100 μm and 100-150 μm: this was on both sides of the 100 μm length of vessel analysed).

In some cases a slightly different technique was used to that previously described following the method of another group (Young *et al.*, 2002). Briefly, after the animals were anaesthetised an incision was made across the bottom of the scrotal sack. Using gentle pressure the testicle was pushed down from the body cavity into the sac and out of the incision. Tweezers were used to pull away any fat clinging to the outside of the cremaster. The cremaster was then pinned to the stage using L-shaped pins and cut along the centre as previously described so the whole muscle could be pinned out flat to the stage. After a 10 min stabilization period post-capillary venules of 20–40 μm in diameter and 100 μm long were chosen. Leukocyte emigration was quantified in real-time per field of view (for 1-3 fields of view per vessel) in 1-3 vessels per animal. Figure 2.13 is a summary of the time course of this experiment. In some cases phagocytosis by emigrated leukocytes was also determined in real-time. This was done by direct observation and quantification of leukocytes under both bright light and fluorescence to see if the visible particles of zymosan were contained in the emigrated leukocyte. Data was normalised against the number of emigrated cells and so expressed as index of phagocytosis (%).

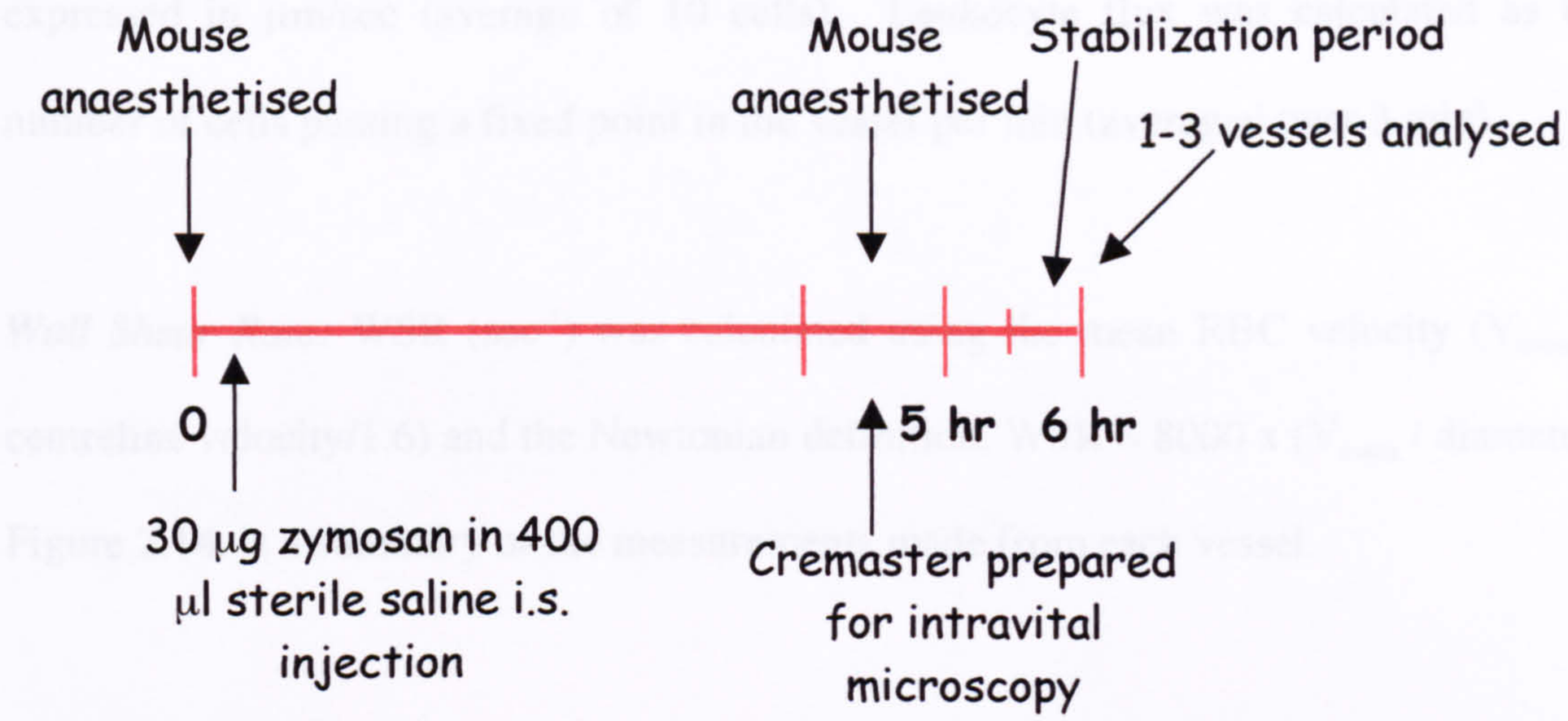

Figure 2.13. Summary of protocol for zymosan-induced inflammation in the cremaster muscle.

2.3.5. Post–Capillary Venule Leakage

In some cases post-capillary venule leakage was measured at the end of the experiment. FITC-labelled albumin (0.25 g/kg) dissolved in sterile saline was injected via the cannular in the jugular vein (approximately 100 μl per mouse). The FITC-albumin was allowed to circulate for 5 min before recording for 30 sec under a fluorescent light with an excitation filter of 450-490 nm and an emission filter of 525-620 nm. This was recorded for later off-line analysis (see section 2.3.6).

2.3.6. Off-line Analysis of Video Recordings

Cell adhesion, rolling velocity and flux: Cell adhesion was quantified by counting the number of adherent cells per 100 μm vessel length (adherent cells were stationary for 30 sec or longer) during each 5 min recording. Leukocyte rolling velocity was calculated by counting the time taken for a cell to travel a fixed length of the vessel and

expressed in μm/sec (average of 10 cells). Leukocyte flux was calculated as the number of cells passing a fixed point in the vessel per min (averaged over 3 min).

Wall Shear Rate: WSR (sec^{-1}) was calculated using the mean RBC velocity (V_{mean} = centreline velocity/1.6) and the Newtonian definition, WSR = 8000 x (V_{mean} / diameter). Figure 2.14. is a summary of the measurements made from each vessel.

Post-capillary venule leakage: Post-capillary venule leakage was measuring using mean fluorescence intensity measured on a Pentium 3 PC with video analysis software (*Image-Pro Plus,* Media Cybernetics, USA). Florescence was measured inside the vessel (Fl_{in}), 10 μm away from the outside of the vessel (Fl_{out}), and also in the background (Bk). Each measurement was made 3 times per vessel recording. The following formula was used to calculate index of albumin leakage (%):

$$[(Fl_{out}\text{-}Bk)/ (Fl_{in}\text{-}Bk)] \times 100$$

Detachment: Continuous video recordings (60 min) were used to examine the fate of adherent leukocytes. Using a method adapted from a previous study (Lim *et al.*, 1998) the fate of adherent cells was observed in 10 min periods over a total of 60 min. Each adherent cell was monitored to see if it detached or emigrated. The time taken for detachment of adherent cells was also recorded.

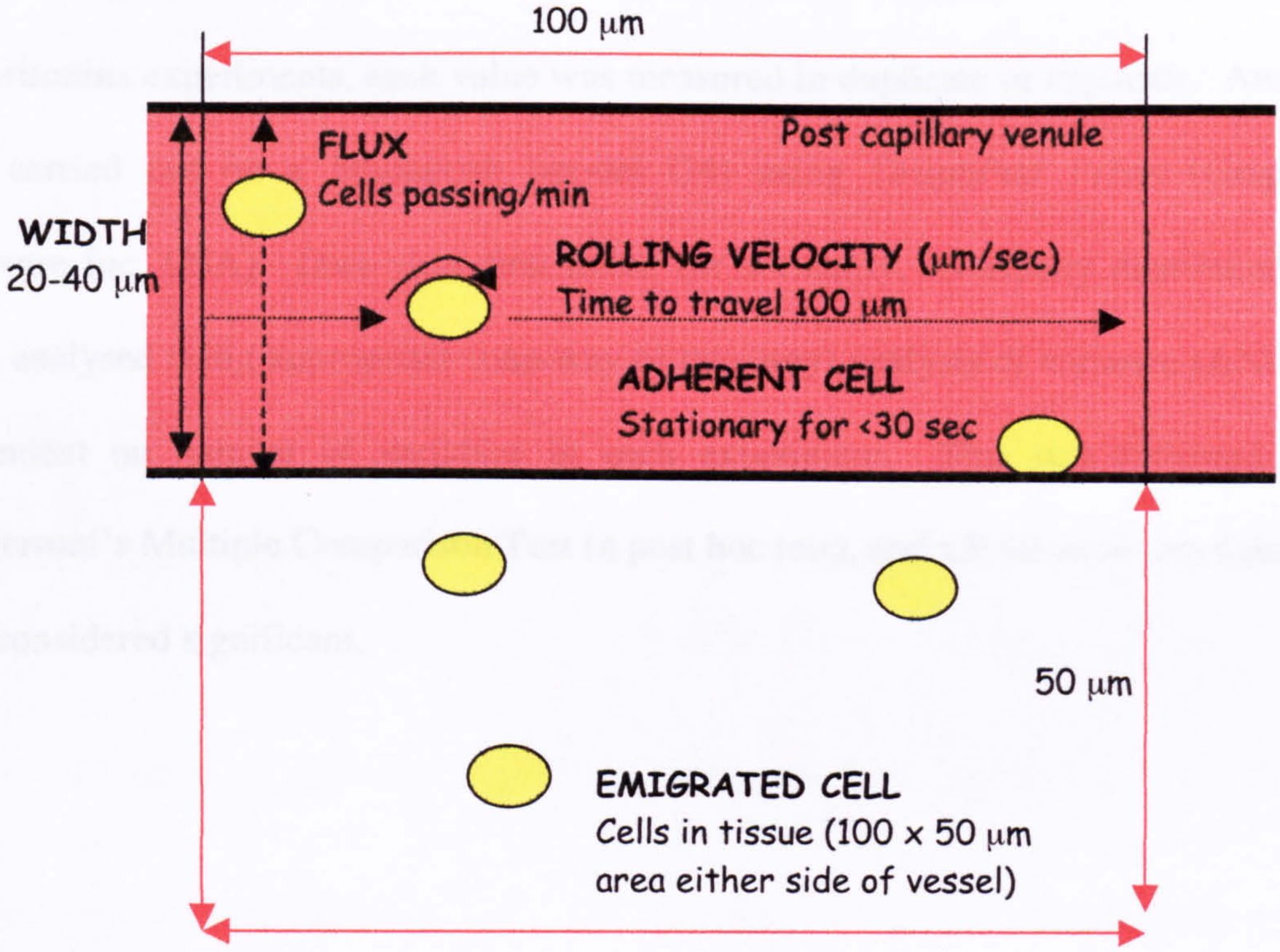

Figure 2.14. Summary diagram of measurements made.

2.4. Statistical Analysis

Data are expressed as mean ± standard error of the mean (SEM) for n mice. In the case of peritonitis experiments, each value was measured in duplicate or triplicate. Analysis was carried out on a Macintosh (model G4) using *GraphPad Prism* (GraphPad Software Inc, USA). Data were first tested for normality. Normally distributed data were analysed using appropriate (one-way or two-way) analysis of variance (ANOVA) dependent on number of variables in each experiment. This was followed by a Bonferroni's Multiple Comparison Test (a post hoc test), and a P value of less than 0.05 was considered significant.

2.5. Materials

Material	Supplier
Acetic acid	BDH, Leicestershire, UK
Alexa-Fluor 488-conjugated zymosan bioparticles	Molecular Probes (Invitrogen, Renfrewshire, UK)
Ammonium persulphate (APS)	Bio Rad, Hertfordshire, UK
Annexin 1 antibody (rabbit anti ANX-A1)	Zymed (Cambridge Bioscience, Cambridgeshire, UK)
Annexin 1 peptide (Ac2-26)	Advance Biotechnology Centre, Imperial College School of Medicine, London, UK
Biotin-conjugated rat anti mouse CD11b monoclonal Ab	Pharmingen (BD Biosciences, Oxfordshire, UK)
Biotin-conjugated rat IgG2b, κ monoclonal Ig isotype control	Pharmingen (BD Biosciences, Oxfordshire, UK)
Bovine serum albumin (BSA)	Sigma-Aldrich, Dorset, UK
Bradford Reagent	Sigma-Aldrich, Dorset, UK
Bromophenol blue	Sigma-Aldrich, Dorset, UK
Calcium chloride ($CaCl_2$)	Sigma-Aldrich, Dorset, UK
Cell FIX™	BD Biosciences, Oxfordshire, UK
Complete, Mini, EDTA-free protease inhibitor cocktail tablets	Roche Diagnostics, Sussex, UK
Crystal violet	Sigma-Aldrich, Dorset, UK
Diazepam	Roche, Hertfordshire, UK
Dithioretol (DTT)	Sigma-Aldrich, Dorset, UK
ECL™ western blotting detection reagent	Amersham Bioscience, Buckinghamshire, UK

Ethylenediaminetetraacetic acid (EDTA) sodium salt	Sigma-Aldrich, Dorset, UK
F4/80 antibody: PE conjugated (rat anti mouse)	Serotec, Oxfordshire, UK
FITC-conjugated rat anti-mouse Gr-1 monoclonal Ab	Pharmingen (BD Biosciences, Oxfordshire, UK)
Foetal calf serum (FCS)	Gibco (Invitrogen, Renfrewshire, UK)
Gas: nitrogen carbon dioxide mix	BOC gases, Lancastershire, UK
Glycerol	BDH, Leicestershire, UK
Heparin (sodium)	Leo Laboratories, Buckinghamshire, UK
Human γ Globulin	Sigma-Aldrich, Dorset, UK
Hydrochloric acid (HCl)	BDH, Leicestershire, UK
Hyperfilm™ ECL	Amersham Bioscience, Buckinghamshire, UK
Hypnorm™	Janssen, Buckinghamshire, UK
Ketamine (Ketaset)	Fort Dodge Animal Health, Hampshire, UK
Magnesium sulphate ($MgSO_4$)	Sigma-Aldrich, Dorset, UK
Mersilk 6-0 suture thread	Johnson and Johnson (3S Healthcare, London, UK)
Milk powder (Non fat)	Safeway, London, UK
Mouse KC ELISA set	R&D Systems, Oxfordshire, UK
Mouse TNF ELISA set	BD Biosciences, Oxfordshire, UK
Murine recombinant IL-1β	PeproTech, London, UK
Nitrocellulose membrane (Hybond™-C extra)	Amersham Bioscience, Buckinghamshire, UK

PAF (C16 form: $C_{26}H_{54}NO_7P$)	Sigma-Aldrich, Dorset, UK
Peroxidase-conjugated goat anti rabbit	Dako, Cambridgeshire, UK
Peroxidase conjugated goat anti mouse immunoglobulin	Dako, Cambridgeshire, UK
Phosphate buffered saline (PBS) tablets	Sigma-Aldrich, Dorset, UK
Polyethylene tubing (for cannulation)	BD Biosciences, Oxfordshire, UK
Potassium Chloride	BDH, Leicestershire, UK
Protogel (30% acrylamide/0.8% bisacyrlamide solution)	National Diagnostics, Yorkshire, UK
Prestained protein marker	New England Biolabs, Leicestershire, UK
Protogel resolving buffer (pH 8.8)	National Diagnostics, Yorkshire, UK
Protogel stacking buffer (pH 6.8)	National Diagnostics, Yorkshire, UK
Sodium Azide (NaN_3)	Sigma-Aldrich, Dorset, UK
Sodium Bicarbonate ($NaHCO_3$)	BDH, Leicestershire, UK
Sodium Chloride (NaCl)	BDH, Leicestershire, UK
Sodium dihydrogen orthophosphate dihydrate (NaH_2PO_4)	BDH, Leicestershire, UK
Sodium dodecyl sulphate (SDS)	Sigma-Aldrich, Dorset, UK
Sodium hydroxide (NaOH)	Sigma-Aldrich, Dorset, UK
di-Sodium hydrogen orthophoshate dihydrate (Na_2HPO_4)	BDH, Leicestershire, UK
Streptavidin Tri-color conjugate	Caltag Laboratories, Northamptonsire, UK
Sterile saline	Sigma-Aldrich, Dorset, UK
Sulphuric acid (H_2SO_4)	BDH, Leicestershire, UK
Suture thread	Pearsalls, Somerset, UK
Temed	National Diagnostics, Yorkshire, UK
Trizma® base	Sigma-Aldrich, Dorset, UK
Trizma® Hydrochloride	Sigma-Aldrich, Dorset, UK
Tubulin antibody (mouse monoclonal anti-α tubulin Ab)	Sigma-Aldrich, Dorset, UK
Tween 20 (Polyoxyethylene sorbitan	Sigma-Aldrich, Dorset, UK

monolaurate)	
Xyazine (Rompun)	Bayer, Suffolk, UK
Zymosan type A	Sigma-Aldrich, Dorset, UK

Results

3. Results

3.1. Peritonitis Model

As very few experiments had been carried out on the ANX-A1$^{-/-}$ mice prior to the start of this PhD the first set of experiments that were completed used a simple model of acute inflammation, the zymosan peritonitis model. As the main aim of this thesis was to examine leukocyte recruitment during inflammation, this was an ideal model for monitoring leukocyte trafficking in response to inflammatory stimuli. The zymosan peritonitis model had been previously well characterised in mice and was known to produce reliable and reproducible results. An additional step was added into the protocol, staining of the peritoneal cells with specific markers, so that flow cytometry could be utilised to identify the recruited cell populations.

3.1.1. Determination of Antibody Concentrations for Staining Mouse Peritoneal Cells

Preliminary studies were carried out to determine the optimum concentrations of antibodies to use to stain the cells collected from the peritoneal cavities of mice.

The titration curve for the Gr-1 Ab is shown in figure 3.1. The experiment used a pooled sample of peritoneal cells obtained from peritoneal washes of 3 x C57BL/6 mice (25-27g) that were treated i.p. with 1 mg zymosan (in 0.5 ml sterile PBS) 4 hr prior to the peritoneal wash. Each concentration of Gr-1 Ab was tested in duplicate.

The graph shows that the optimum concentration of antibody was 1.67 μg/ml. Higher concentrations of Ab offer no further advantage in terms of the levels of detection.

The titration curve for the F4/80 Ab is shown in figure 3.2. The experiment used a pooled sample of peritoneal cells obtained from the peritoneal washes of 2 x TO mice (32-35g) that were not treated with an inflammogen. This was because the F4/80 Ab stains monocytic cells that are found in a normal, untreated peritoneal cavity. Each concentration of Ab was tested in duplicate. There was a concentration dependent increase in F4/80 expression. Using this preliminary data it was decided that the final concentration of antibody to use to treat cells in further experiments would be 1 μg/ml as this concentration gave a significant signal above background. A concentration of 5 μg/ml may gain a stronger signal but was considered to be too expensive for routine work.

The concentrations of CD11b antibody, isotype control and streptavidin tricolour were previously optimised by another group and were adapted by us (Henderson *et al.*, 2001). IL-1β and zymosan doses were chosen as they have been successfully used in previous experiments performed in our laboratory (Ajuebor *et al.*, 1998; Perretti *et al.*, 1992).

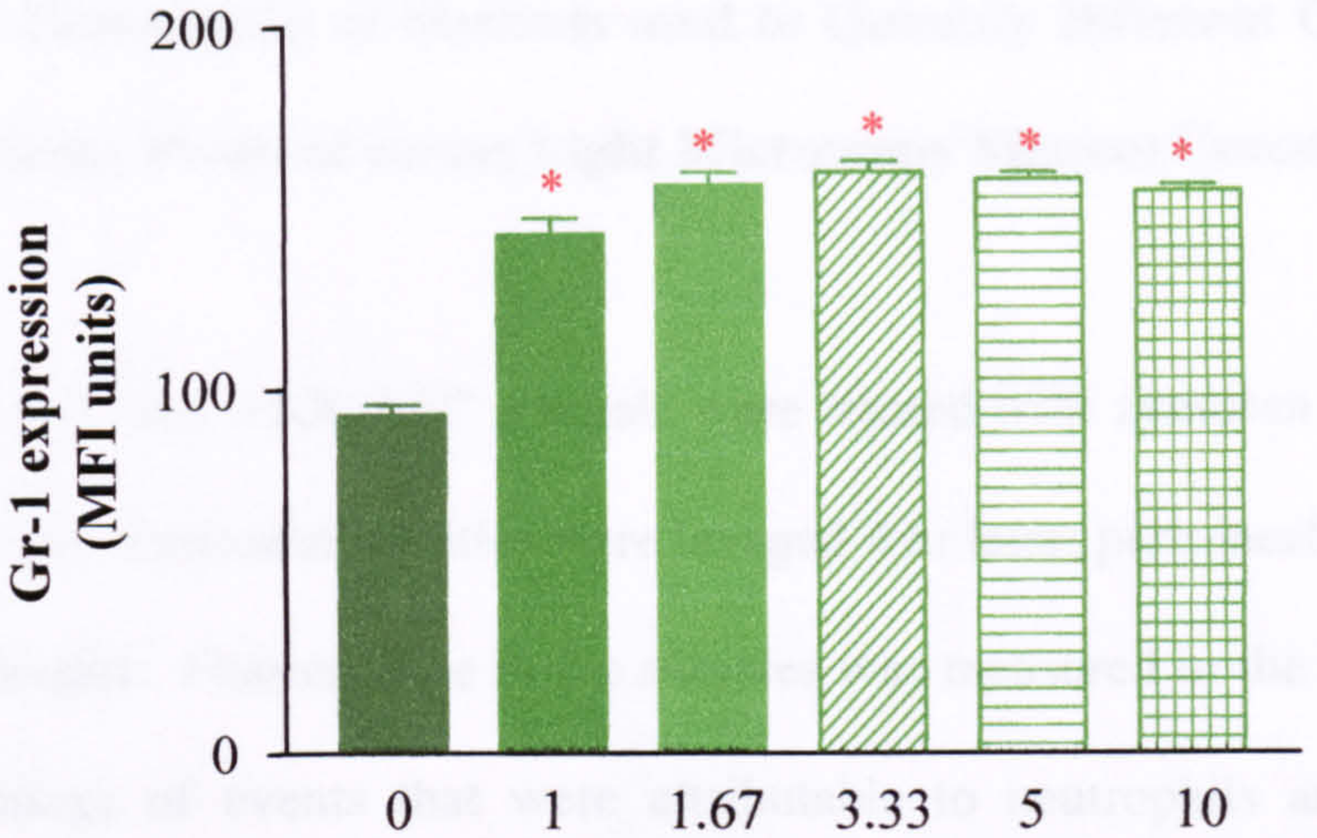

Figure 3.1. Titration curve for calculating the optimum concentration of Gr-1 Ab to stain mouse neutrophils. C57BL/6 mice were treated with 1 mg zymosan for 4 hr. Peritoneal cells were stained with Gr-1 Ab (0-10 μg/ml) and fluorescence measured. Values are mean±sem of triplicate analysis of n=3 mice, *P<0.05 vs. time 0.

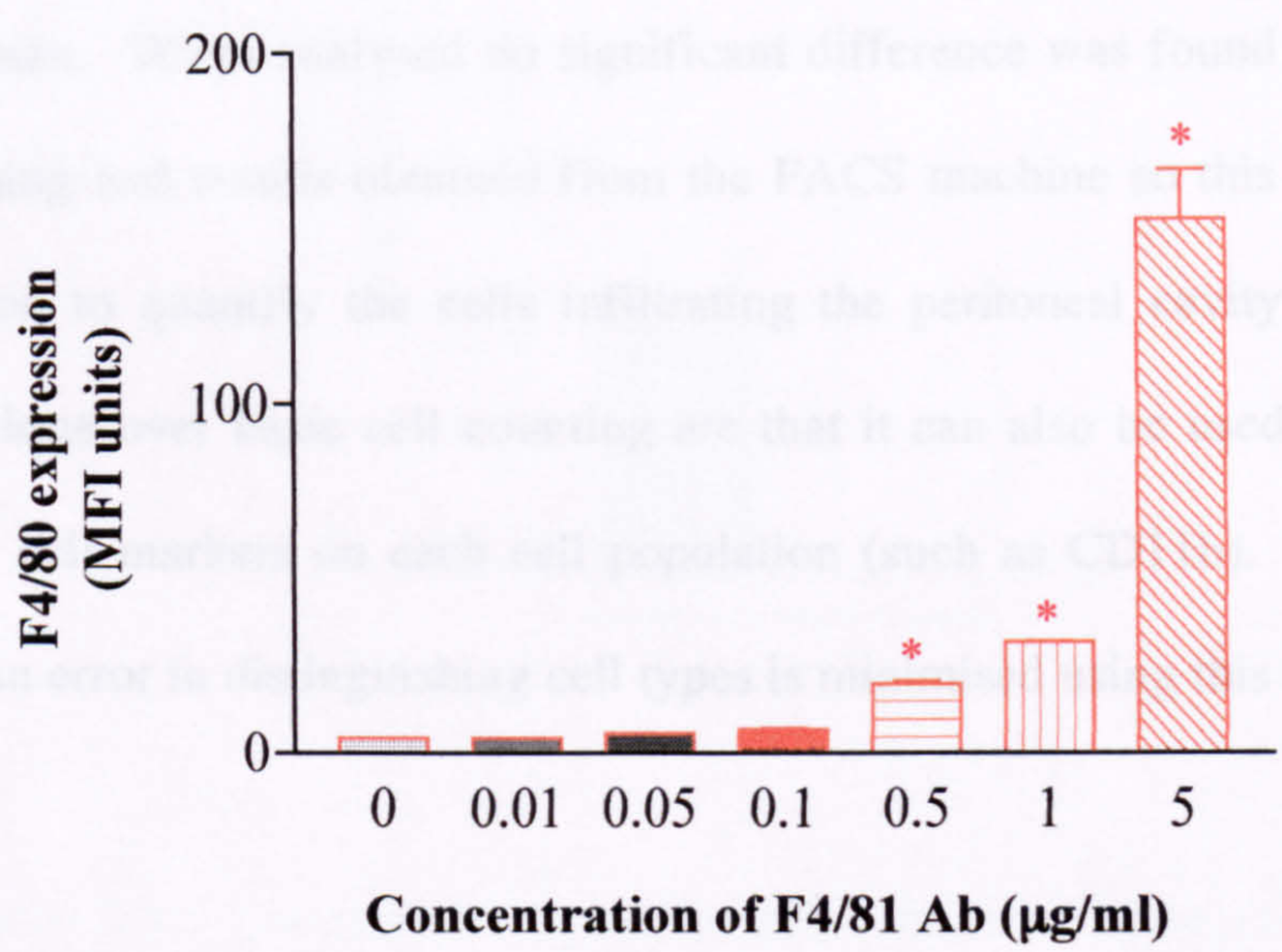

Figure 3.2. Titration curve for calculating the optimum concentration of F4/80 Ab to stain mouse mononuclear cells. Peritoneal cavities of TO mice were lavaged and peritoneal cells collected were stained with F4/80 Ab (0-5 μg/ml) and fluorescence measured. Values are mean±sem of triplicate analysis of n=2 mice, *P<0.05 vs. time 0.

3.1.2. Comparison of Methods used to Quantify Different Cell Populations: Flow Cytometry Protocol versus Light Microscopy Manual Counting

ANX-A1$^{-/-}$ and ANX-A1$^{+/+}$ animals were treated with zymosan (1 mg in 0.5 ml sterile PBS i.p.). Peritoneal cavities were lavaged 4 hr later; peritoneal samples were collected and stained. Fluorescence in the samples was measured in the FACS machine and the percentage of events that were attributable to neutrophils and monocytic cells, as assessed using the specific antibodies as markers for these cell types, was measured. Figure 3.3. is a comparison of results obtained by this method of distinguishing neutrophils and monocytic cells and the more widely used technique of visual cell counting using Turk's staining and a haemocytometer. Both graphs show the percentage of neutrophils found in the peritoneal cavity after 4 hr treatment with zymosan. When analysed no significant difference was found between results of cell counting and results obtained from the FACS machine so this was deemed a suitable method to quantify the cells infiltrating the peritoneal cavity. The benefits of this technique over basic cell counting are that it can also be used to assess the levels of other cell markers on each cell population (such as CD11b). Also the possibility of human error in distinguishing cell types is minimised using this technique.

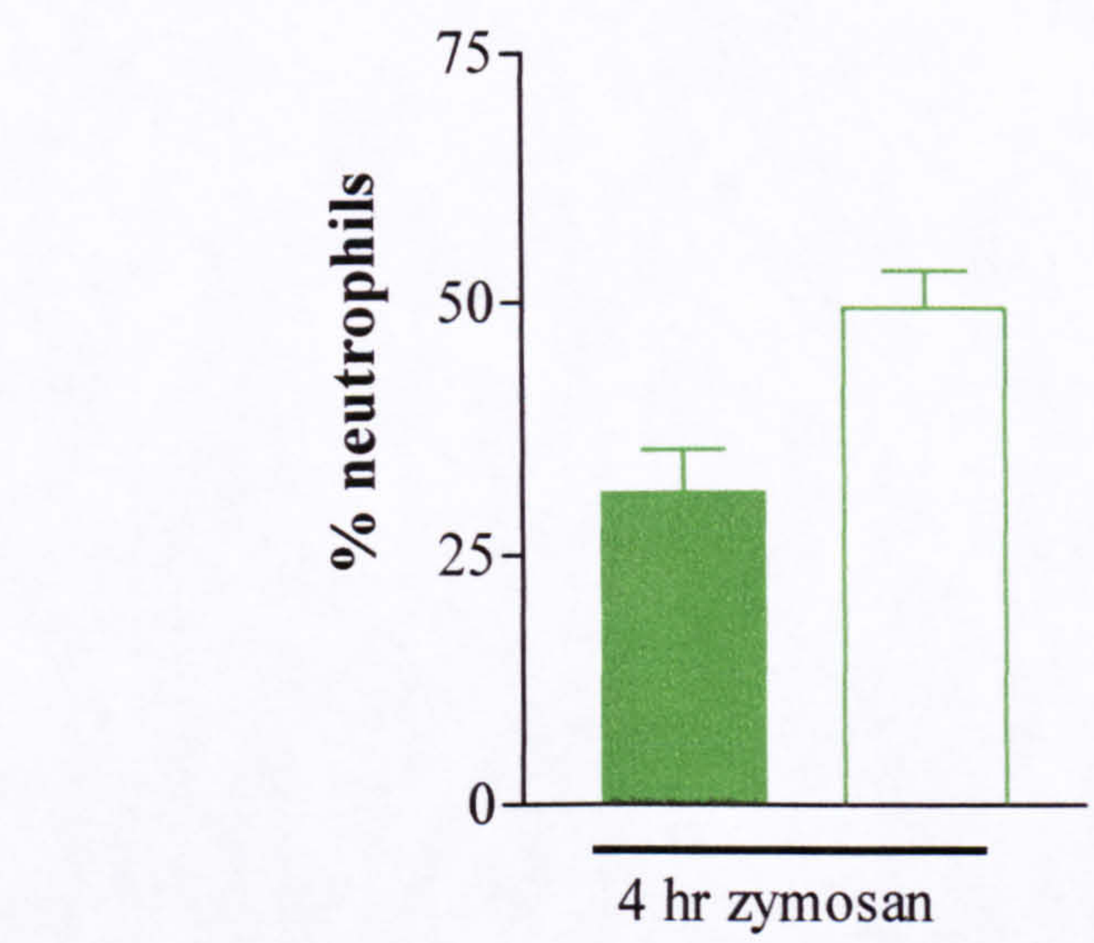

Figure 3.3. Comparison between data obtained by a simple cell count using a haemocytometer (a) and a count using the flow cytometer and fluorescently labelled cells (b). ANX-A1$^{+/+}$ ■ and ANX-A1$^{-/-}$ □ mice were treated i.p. for 4 hr with zymosan. Peritoneal cells were collected by lavage and either (a) differential cell counts were carried out on cells stained with Turk's solution or (b) the cells were stained with the appropriate fluorescent Abs for flow cytometric analysis.

3.1.3. Zymosan Peritonitis in ANX-A1$^{-/-}$ and ANX-A1$^{+/+}$ Mice

ANX-A1$^{+/+}$ and ANX-A1$^{-/-}$ mice were either treated i.p. with 1 mg zymosan (in 0.5 ml sterile PBS) or left as untreated controls. At selected time-points (4 or 24 hr) mice were killed and peritoneal cells collected and stained for flow cytometric analysis as described previously.

3.1.3.1. Gr-1 and F4/80 Positive Events

Figure 3.4 shows the levels of Gr-1 positive events found in the peritoneal cavity after zymosan treatment. Significantly higher levels of Gr-1 positive events (neutrophils) were found in the peritoneal cavity after 4 hr treatment with zymosan in both the ANX-A1$^{+/+}$ and ANX-A1$^{-/-}$ mice when compared to 0 hr. However, in the ANX-A1$^{-/-}$ there were significantly higher numbers of Gr-1 positive events (neutrophils) compared to the ANX-A1$^{+/+}$ at the 4 hr time-point (ANX-A1$^{+/+}$: 25.54±9.10 (n=7) vs. ANX-A1$^{-/-}$: 63.46±9.48 (n=8), $p<0.05$). At 24 hr the levels of Gr-1 positive events were decreased in the ANX-A1$^{+/+}$ (not significantly different to 0 hr) however in the ANX-A1$^{-/-}$ there were still significantly higher levels found at 24 hr compared to 0 hr.

When the F4/80 positive events (monocytic cells) in the peritoneal cavity were examined a different pattern was seen. Lower levels of F4/80 positive events (monocytic cells) were found in the peritoneal cavity after 4 hr treatment with zymosan in both the ANX-A1$^{+/+}$ and ANX-A1$^{-/-}$ mice compared to corresponding control animals. However, in the ANX-A1$^{-/-}$ mice there were significantly lower numbers of F4/80 positive events (monocytic cells) when compared to the ANX-A1$^{+/+}$ animals at

the 4 hr time-point (ANX-A1$^{+/+}$: 14.97±5.80 vs. ANX-A1$^{-/-}$: 0.32±0.12, n=8, P<0.05). This is seen in figure 3.5. In the ANX-A1$^{+/+}$ mice, the percentage of F4/80 positive cells increased at 24 hr back to basal levels (i.e. 24 hr value not significantly different to 0 hr value). In the ANX-A1$^{-/-}$ however, the percentage increased from that at 4 hr but did not returned back to basal levels.

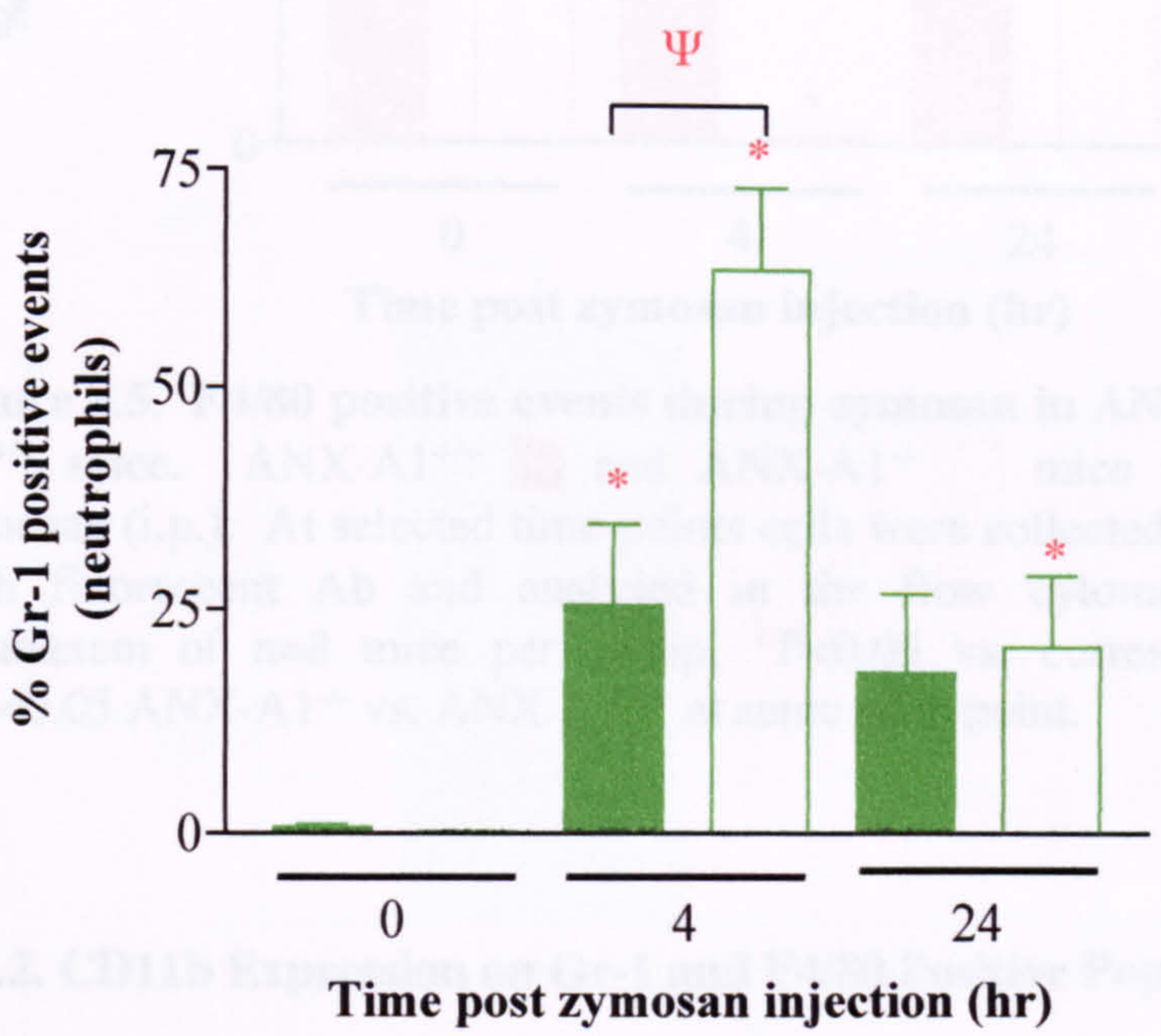

Figure 3.4. Gr-1 positive events during zymosan peritonitis in ANX-A1$^{-/-}$ and ANX-A1$^{+/+}$ mice. ANX-A1$^{+/+}$ ■ and ANX-A1$^{-/-}$ □ mice were treated with zymosan (i.p.). At selected time-points cells were collected by lavage, stained with fluorescent Ab and analysed in the flow cytometer. Values are mean±sem of n=7-8 mice per group, *P<0.05 vs. corresponding time 0, ΨP<0.05 ANX-A1$^{-/-}$ vs. ANX-A1$^{+/+}$ at same time-point.

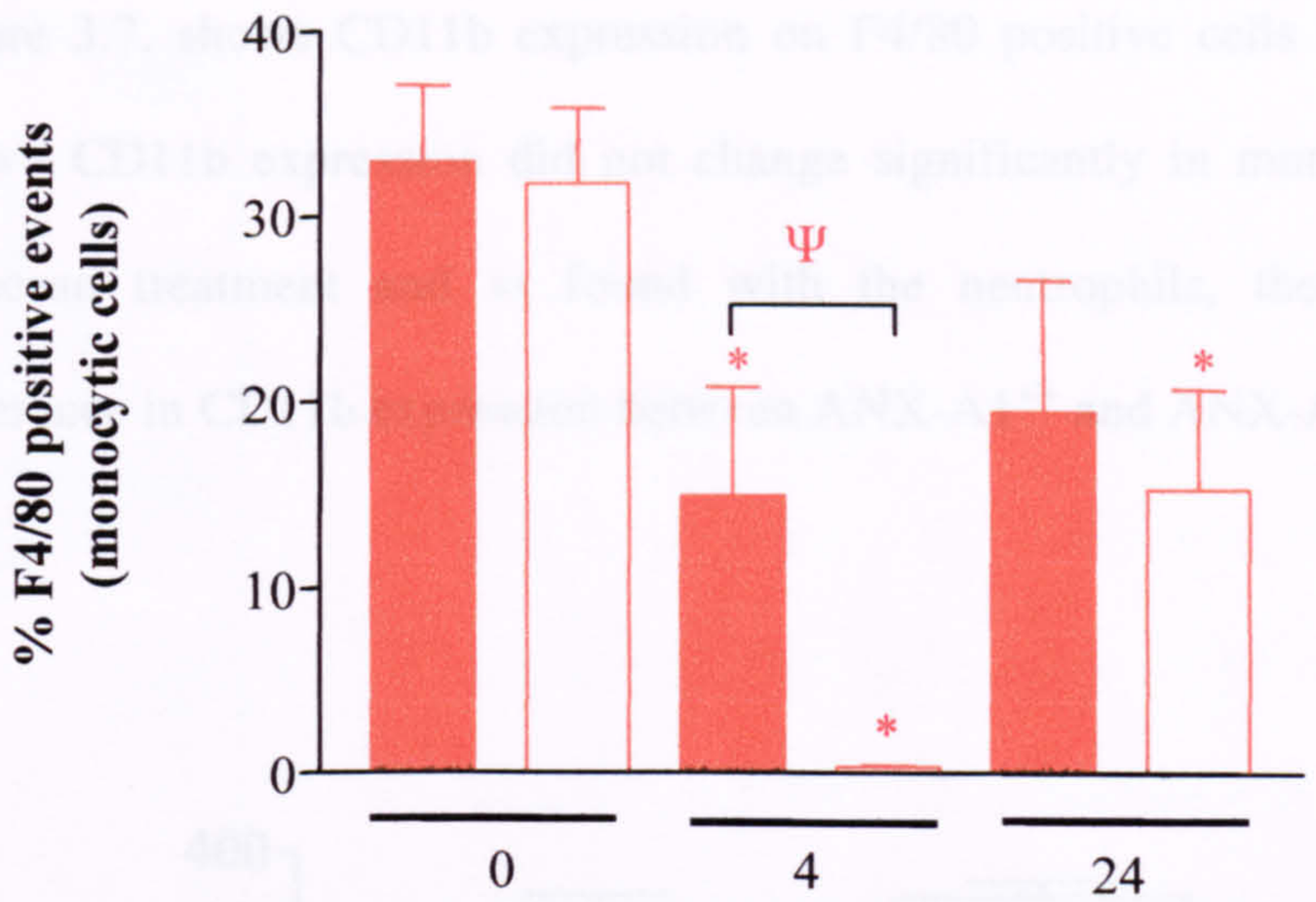

Figure 3.5. F4/80 positive events during zymosan in ANX-A1$^{-/-}$ and ANX-A1$^{+/+}$ mice. ANX-A1$^{+/+}$ ■ and ANX-A1$^{-/-}$ □ mice were treated with zymosan (i.p.). At selected time-points cells were collected by lavage, stained with fluorescent Ab and analysed in the flow cytometer. Values are mean±sem of n=8 mice per group, *P<0.05 vs. corresponding time 0, ΨP<0.05 ANX-A1$^{-/-}$ vs. ANX-A1$^{+/+}$ at same time-point.

3.1.3.2. CD11b Expression on Gr-1 and F4/80 Positive Populations

The level of CD11b expression was measured on both the Gr-1 positive population and the F4/80 positive population collected from the peritoneal cavity of ANX-A1$^{-/-}$ and ANX-A1$^{+/+}$ mice treated with zymosan for 4 hr or left as untreated controls. The levels of CD11b were measured as mean fluorescence intensity (MFI).

Figure 3.6. shows CD11b expression on Gr-1 positive cells (neutrophils). As shown there was no significant difference in CD11b levels found on neutrophils after 4 hr zymosan treatment between ANX-A1$^{+/+}$ and ANX-A1$^{-/-}$ mice.

Figure 3.7. shows CD11b expression on F4/80 positive cells (monocytic cells). As shown CD11b expression did not change significantly in monocytic cells after 4 hr zymosan treatment and as found with the neutrophils, there was no significant difference in CD11b expression between ANX-A1$^{+/+}$ and ANX-A1$^{-/-}$ mice.

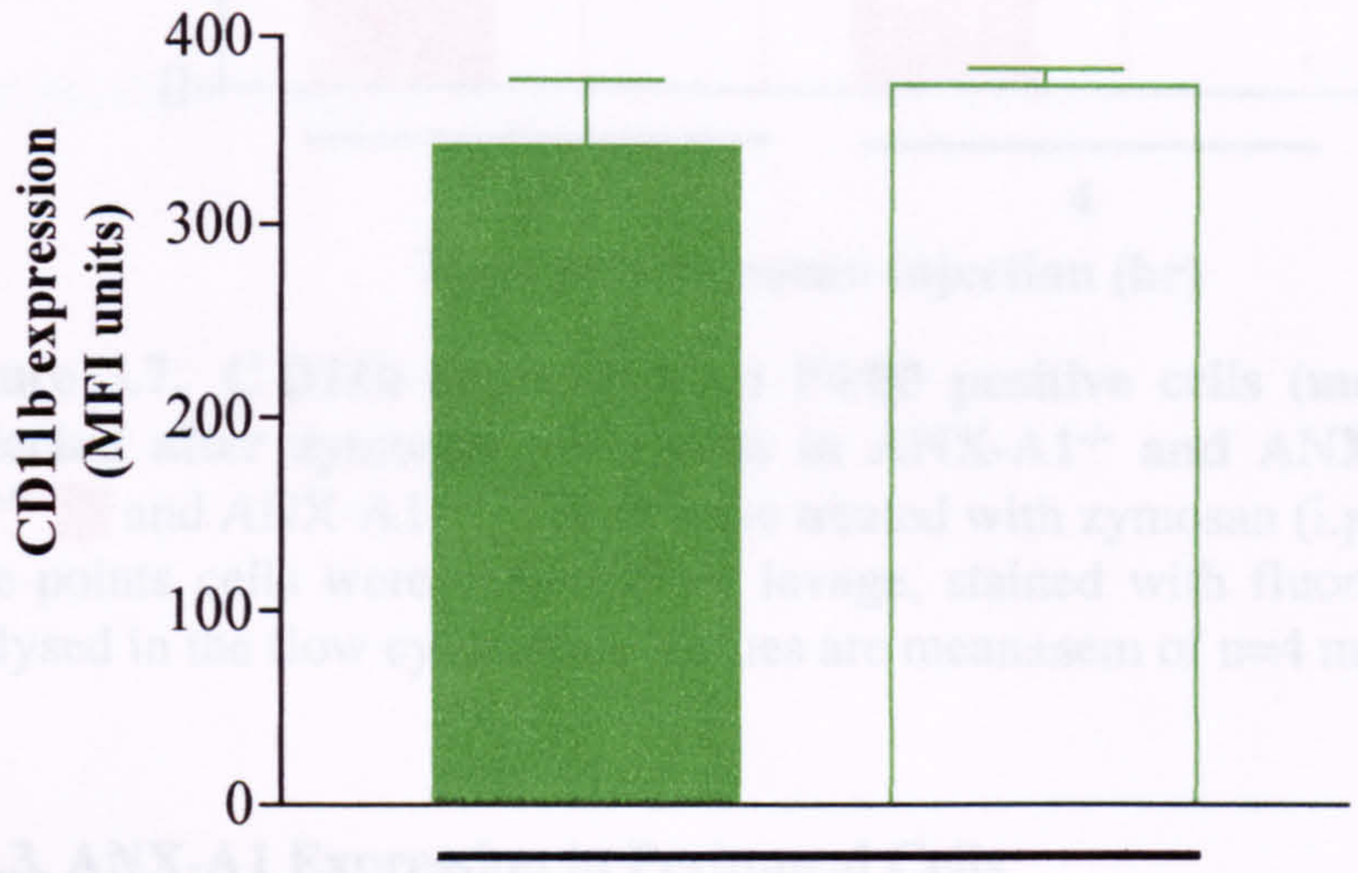

Figure 3.6. C D11b expression on Gr-1 positive cells (neutrophils) collected after zymosan peritonitis in ANX-A1$^{-/-}$ and ANX-A1$^{+/+}$ mice. ANX-A1$^{+/+}$ ■ and ANX-A1$^{-/-}$ □ mice were treated with zymosan (i.p.) for 4 hr. Cells were collected by lavage, stained with fluorescent Ab and analysed in the flow cytometer. Values are mean±sem of n= 4 mice per group.

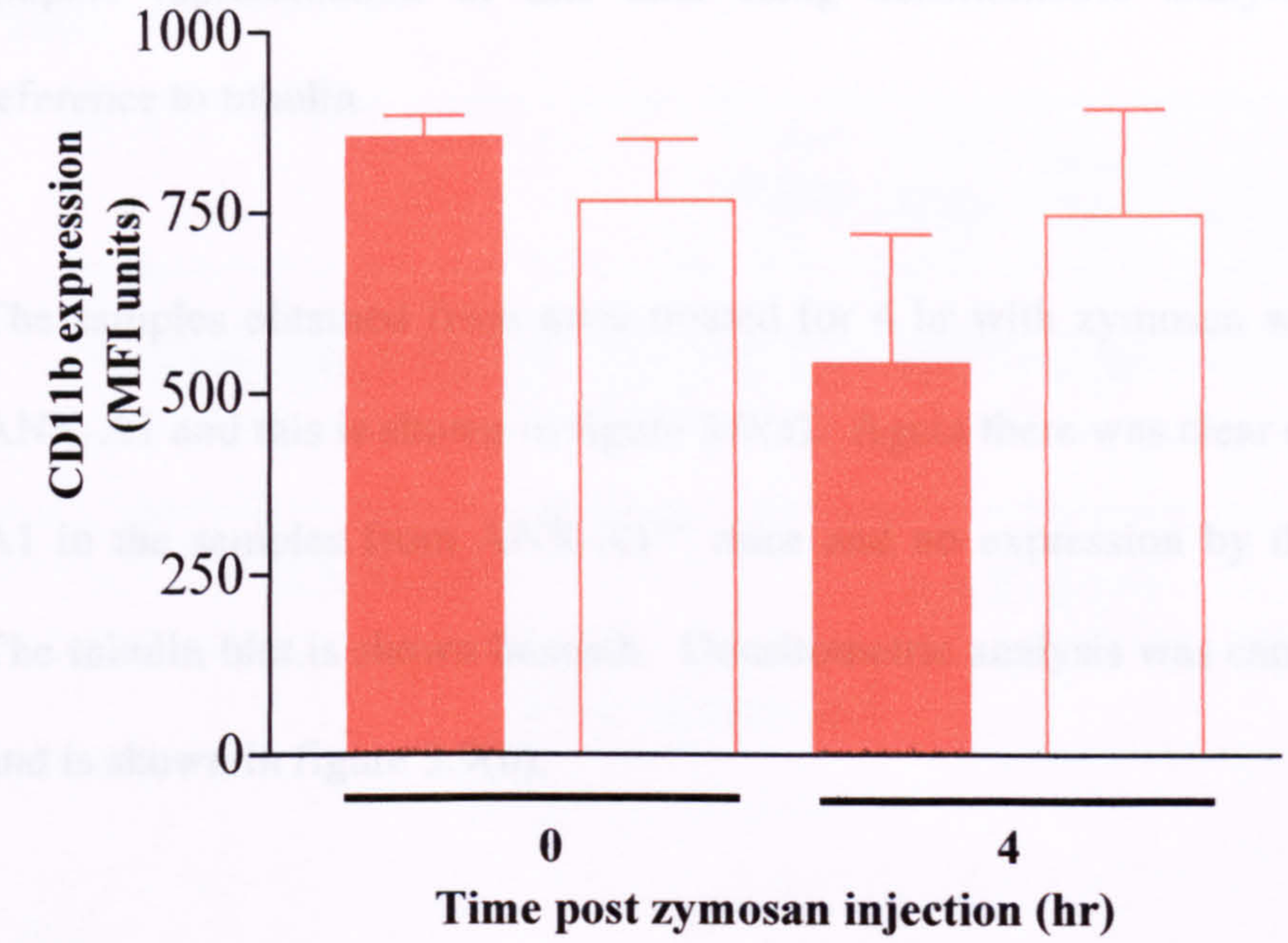

Figure 3.7. C D11b expression on F4/80 positive cells (monocytic cells) collected after zymosan peritonitis in ANX-A1$^{-/-}$ and ANX-A1$^{+/+}$. ANX-A1$^{+/+}$ ■ and ANX-A1$^{-/-}$ □ mice were treated with zymosan (i.p.). At selected time-points cells were collected by lavage, stained with fluorescent Ab and analysed in the flow cytometer. Values are mean±sem of n=4 mice per group.

3.1.3.3. ANX-A1 Expression in Peritoneal Cells

ANX-A1$^{-/-}$ and ANX-A1$^{+/+}$ mice were either treated with 1 mg zymosan i.p. for 4 hr or left as untreated controls. Cells collected from the peritoneal cavity were frozen at – 80°C and later thawed for western blot analysis.

Figure 3.8(a) shows the levels of ANX-A1 expression by peritoneal cells of untreated ANX-A1$^{-/-}$ and ANX-A1$^{+/+}$ mice (these would mainly be resident macrophages as determined by flow cytometry). ANX-A1 was clearly expressed by cells collected from ANX-A1$^{+/+}$ mice and was absent from the ANX-A1$^{-/-}$ cell lysates. Levels of tubulin are shown below to demonstrate equal protein loading. Figure 3.8(b) is a

graphic representation of this data using densitometric analysis normalised with reference to tubulin.

The samples obtained from mice treated for 4 hr with zymosan were also blotted for ANX-A1 and this is shown in figure 3.9(a). Again there was clear expression of ANX-A1 in the samples from ANX-A1$^{+/+}$ mice and no expression by the ANX-A1$^{-/-}$ mice. The tubulin blot is shown beneath. Densitometric analysis was carried out on the blots and is shown in figure 3.9(b).

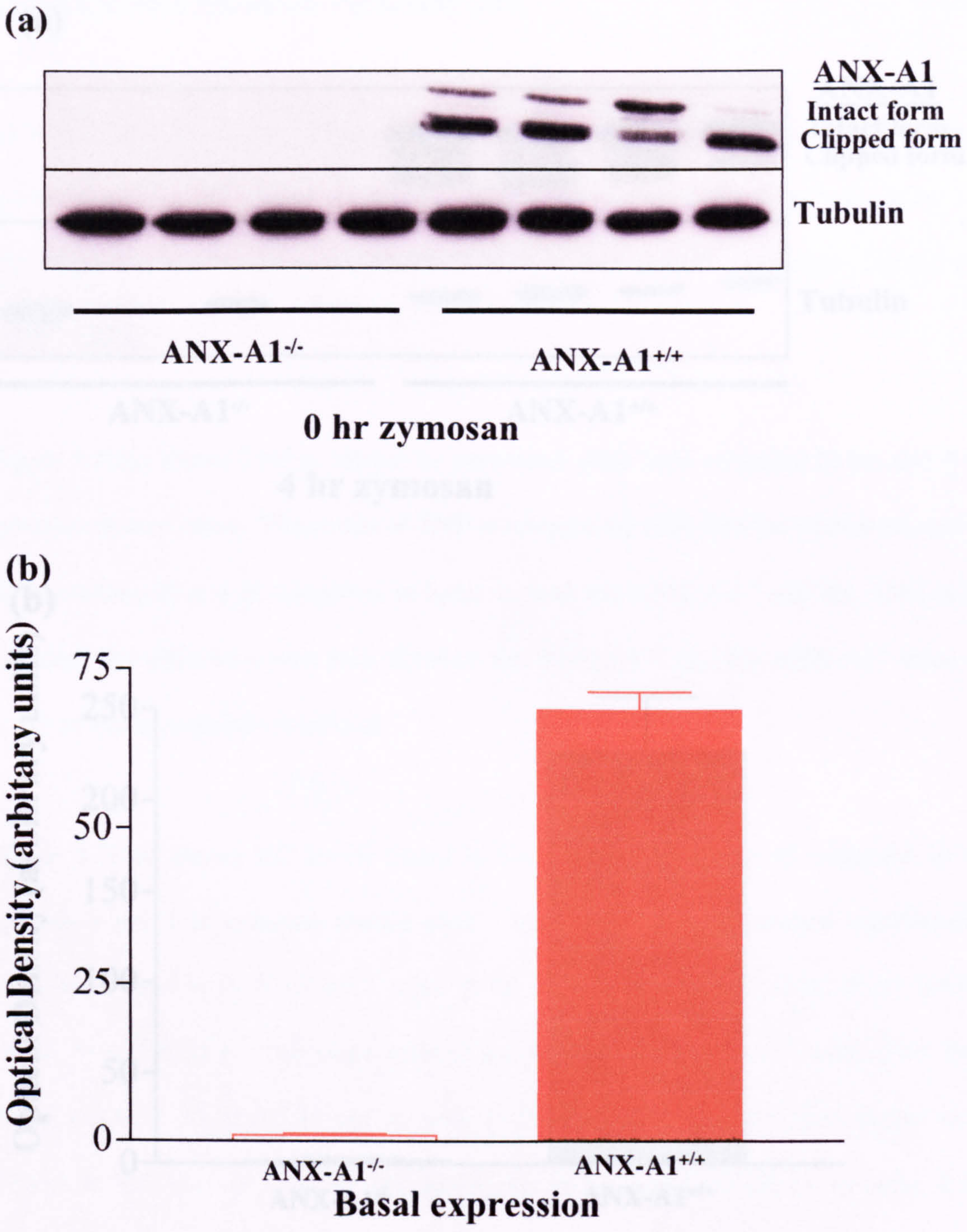

Figure 3.8. ANX-A1 expression on peritoneal cells collected from untreated (basal) ANX-A1$^{-/-}$ and ANX-A1$^{+/+}$ mice. Peritoneal cavities of untreated ANX-A1$^{+/+}$ ■ and ANX-A1$^{-/-}$ □ and mice were lavaged, cell lysates were analysed by western blotting for ANX-A1 and tubulin expression (a) Western blot results (b) Densitometry data from western blots. Values are mean±sem of n=4 mice per group.

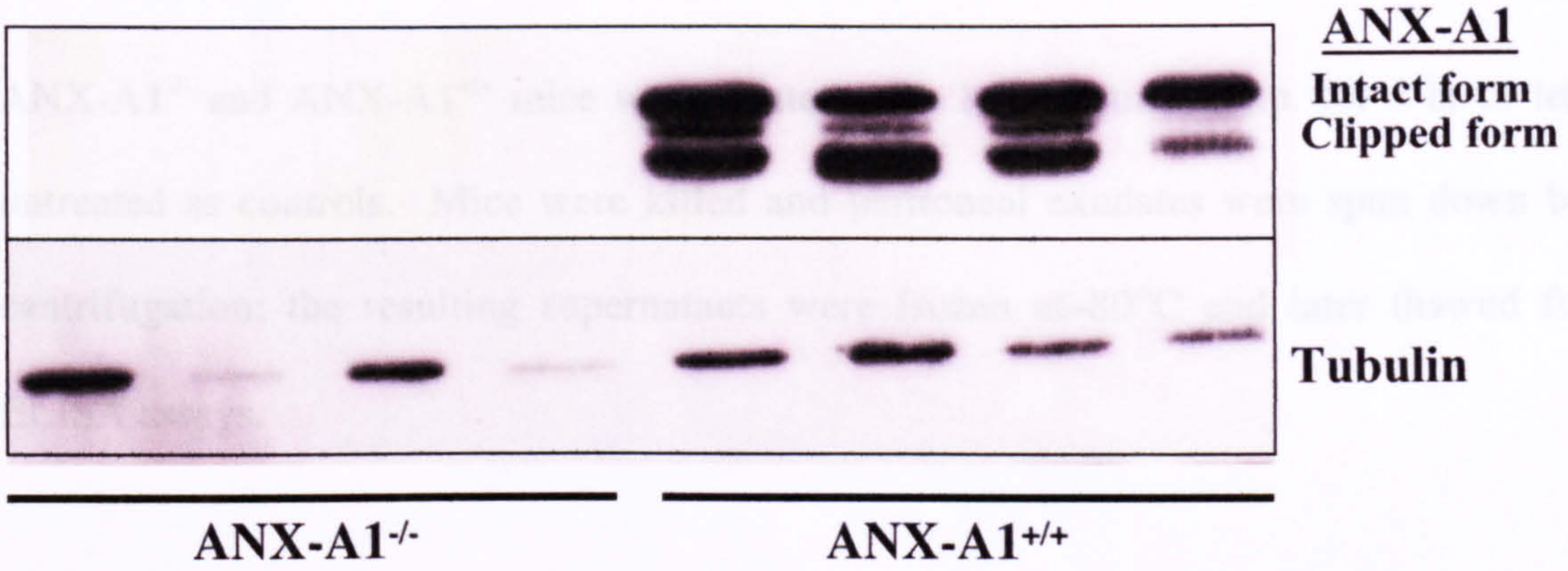

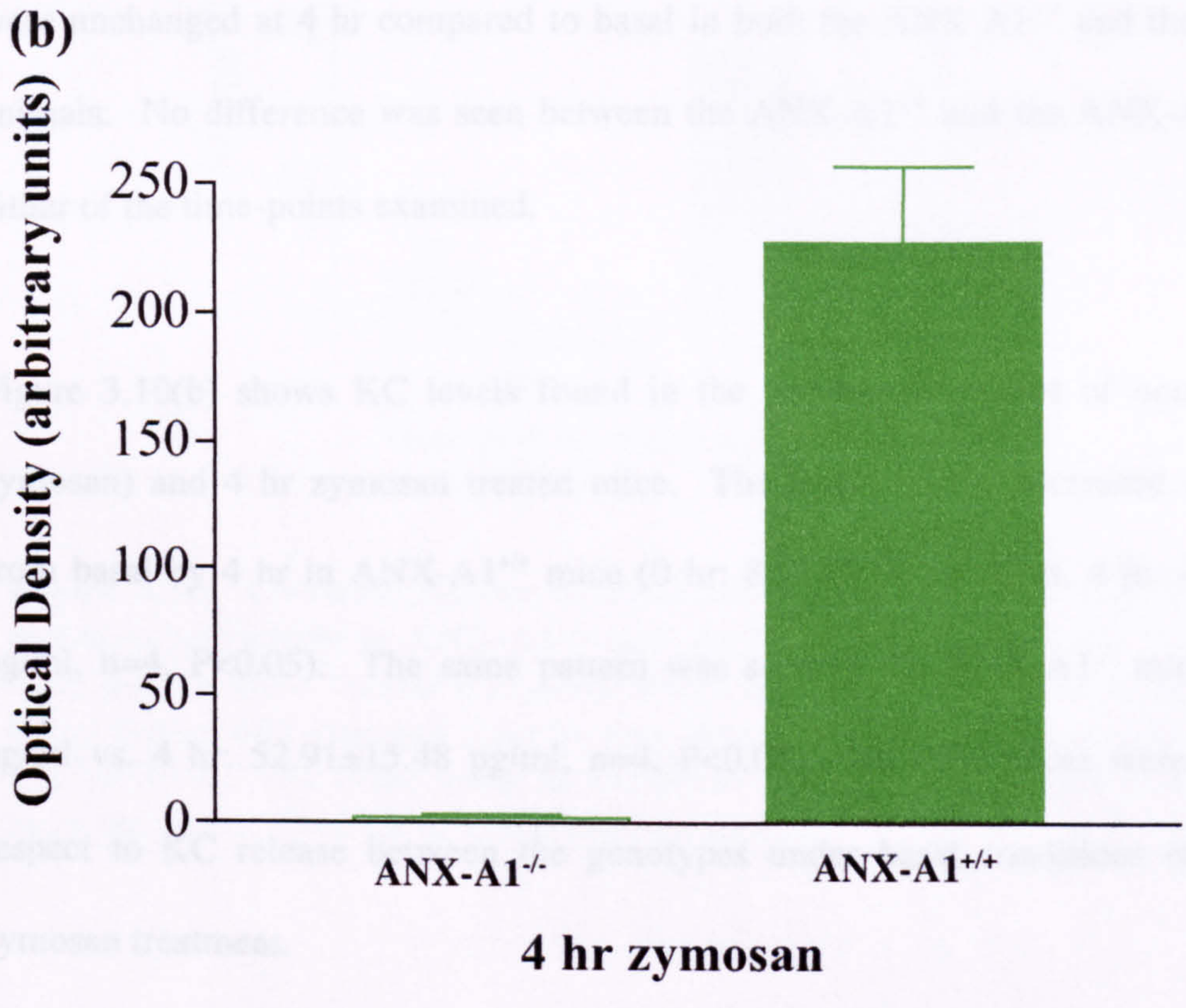

Figure 3.9. ANX-A1 expression on peritoneal cells collected after zymosan peritonitis in ANX-A1$^{-/-}$ and ANX-A1$^{+/+}$ mice. ANX-A1$^{+/+}$ ■ and ANX-A1$^{-/-}$ □ mice were treated with zymosan (i.p.) for 4 hr, collected cells were later analysed by western blotting for ANX-A1 and tubulin expression (a) Western blot results (b) Densitometry data from western blots. Values are mean±sem of n=4 mice per group.

3.1.3.4. Cytokine Release by Peritoneal Cells

ANX-A1$^{-/-}$ and ANX-A1$^{+/+}$ mice were treated with 1 mg zymosan i.p. for 4 hr or left untreated as controls. Mice were killed and peritoneal exudates were spun down by centrifugation; the resulting supernatants were frozen at–80°C and later thawed for ELISA assays.

Figure 3.10(a) shows TNF-α release by peritoneal cells from untreated (0 hr) and 4 hr zymosan treated mice. The levels of TNF-α released by cells into the peritoneal cavity were unchanged at 4 hr compared to basal in both the ANX-A1$^{+/+}$ and the ANX-A1$^{-/-}$ animals. No difference was seen between the ANX-A1$^{+/+}$ and the ANX-A1$^{-/-}$ mice at either of the time-points examined.

Figure 3.10(b) shows KC levels found in the peritoneal cavities of untreated (0 hr zymosan) and 4 hr zymosan treated mice. The levels of KC increased significantly from basal by 4 hr in ANX-A1$^{+/+}$ mice (0 hr: 8.93±5.18 pg/ml vs. 4 hr: 46.11±14.63 pg/ml, n=4, $P<0.05$). The same pattern was seen in the ANX-A1$^{-/-}$ mice (0hr: 0±0 pg/ml vs. 4 hr: 52.91±15.48 pg/ml, n=4, $P<0.05$). No differences were found with respect to KC release between the genotypes under basal conditions or after 4 hr zymosan treatment.

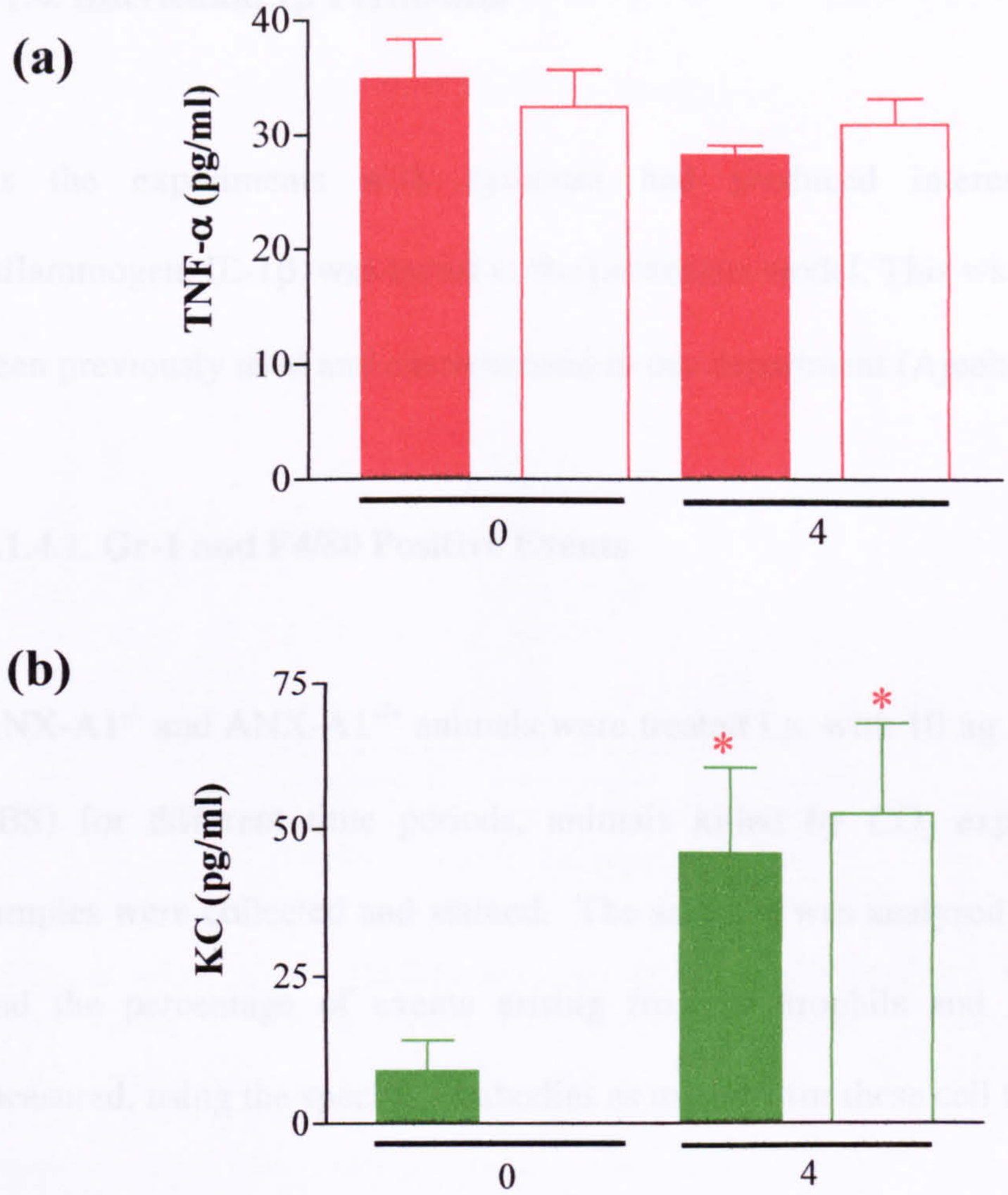

Figure 3.10. Cytokine release by cells into the peritoneal cavity during zymosan peritonitis in ANX-A1$^{+/+}$ and ANX-A1$^{-/-}$ mice. ANX-A1$^{+/+}$ (solid bars) and ANX-A1$^{-/-}$ (clear bars) mice were either left as untreated controls (0 hr) or treated with zymosan (i.p.) for 4 hr. Measurement of cytokine release (a) TNF-α (b) KC was made using an ELISA kit. Values are mean±sem of n=4 mice per group, *P<0.05 vs. corresponding time 0.

3.1.4. Interleukin 1β Peritonitis

As the experiments with zymosan had produced interesting results another inflammogen, IL-1β, was tested in the peritonitis model, This was also a model that had been previously used and characterised in our department (Ajuebor *et al.*, 1998).

3.1.4.1. Gr-1 and F4/80 Positive Events

ANX-A1$^{-/-}$ and ANX-A1$^{+/+}$ animals were treated i.p. with 10 ng IL-1β (in 0.5ml sterile PBS) for different time periods, animals killed by CO_2 exposure then peritoneal samples were collected and stained. The samples was analysed in the FACS machine and the percentage of events arising from neutrophils and monocytic cells were measured, using the specific antibodies as markers for these cell types.

Figure 3.11 shows the Gr-1 positive events (neutrophils) found in the peritoneal cavity after treatment with IL-1β. Higher levels of Gr-1 positive events (neutrophils) were found in the peritoneal cavity after 4 hr treatment with IL-1β in both the ANX-A1$^{+/+}$ and ANX-A1$^{-/-}$ mice. These numbers returned to basal levels after 24 hr treatment in both the ANX-A1$^{+/+}$ and the ANX-A1$^{-/-}$ animals. This is similar to the pattern seen with zymosan treatment. However when using IL-1β no significant difference between ANX-A1$^{+/+}$ and ANX-A1$^{-/-}$ mice was seen at any of the time-points.

The F4/80 positive events (monocytic cells) found after IL-1β treatment are displayed in figure 3.12. Treatment with IL-1β for 4 or 24 hr had no effect on levels of

monocytic cells found in the peritoneal cavity. No difference was seen in monocytic cell numbers between the two ANX-A1 genotypes.

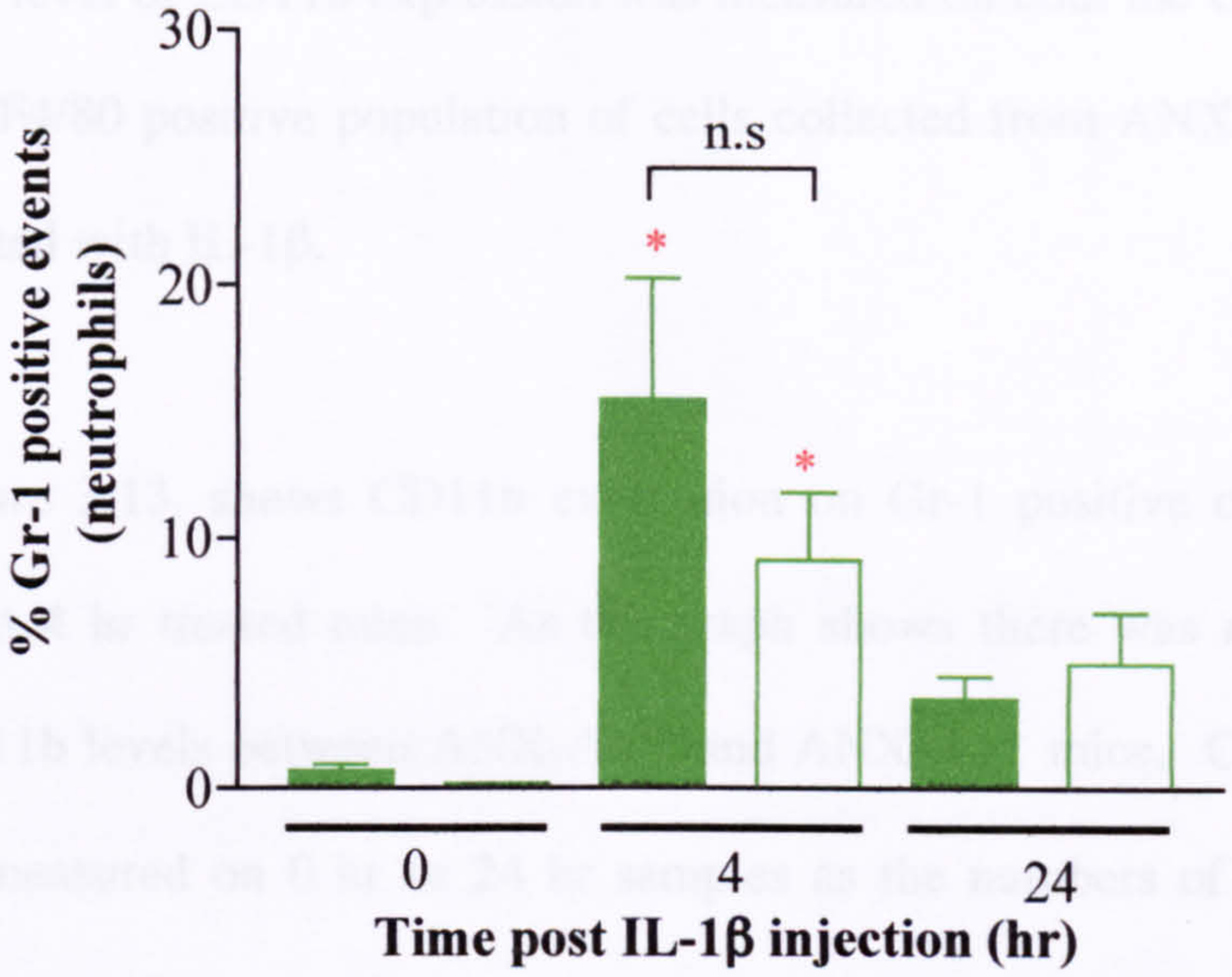

Figure 3.11. Gr-1 positive events during IL-1β peritonitis in ANX-A1$^{-/-}$ and ANX-A1$^{+/+}$ mice. ANX-A1$^{+/+}$ ■ and ANX-A1$^{-/-}$ □ mice were treated with IL-1β (i.p.). At selected time-points cells were collected by lavage, stained with fluorescent Ab and analysed in the flow cytometer. Values are mean±sem of n=8 mice per group, *P<0.05 vs. corresponding time 0, n.s, no significant difference.

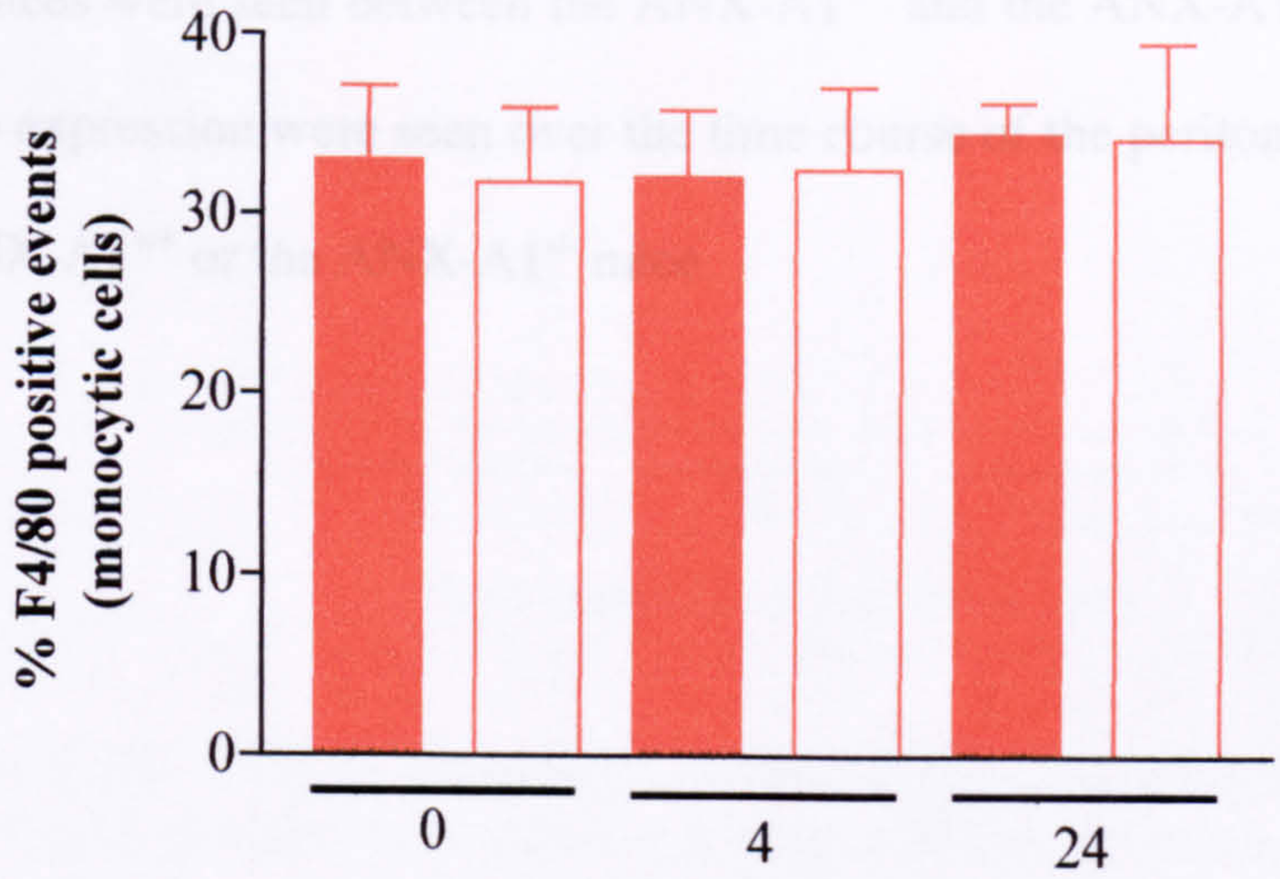

Figure 3.12. F4/80 positive events during IL-1β peritonitis in ANX-A1$^{-/-}$ and ANX-A1$^{+/+}$ mice. ANX-A1$^{+/+}$ ■ and ANX-A1$^{-/-}$ □ mice were treated with IL-1β (i.p.). At selected time-points cells were collected by lavage, stained with fluorescent Ab and analysed in the flow cytometer. Values are mean±sem of n=8 mice per group.

3.1.4.2. CD11b Expression on Gr-1 and F4/80 Positive Populations

The level of CD11b expression was measured on both the Gr-1 positive population and the F4/80 positive population of cells collected from ANX-A1$^{-/-}$ and ANX-A1$^{+/+}$ mice treated with IL-1β.

Figure 3.13. shows CD11b expression on Gr-1 positive cells (neutrophils) collected from 4 hr treated mice. As the graph shows there was no significant difference in CD11b levels between ANX-A1$^{+/+}$ and ANX-A1$^{-/-}$ mice. CD11b expression could not be measured on 0 hr or 24 hr samples as the numbers of neutrophils found at those time-points were too low to get an accurate result.

Figure 3.14. shows CD11b expression on F4/80 positive cells (monocytic cells). As with CD11b expression on Gr-1 positive cells it can be seen that no significant differences were seen between the ANX-A1$^{+/+}$ and the ANX-A1$^{-/-}$ mice. No changes in CD11b expression were seen over the time course of the peritonitis experiment in either the ANX-A1$^{+/+}$ or the ANX-A1$^{-/-}$ mice.

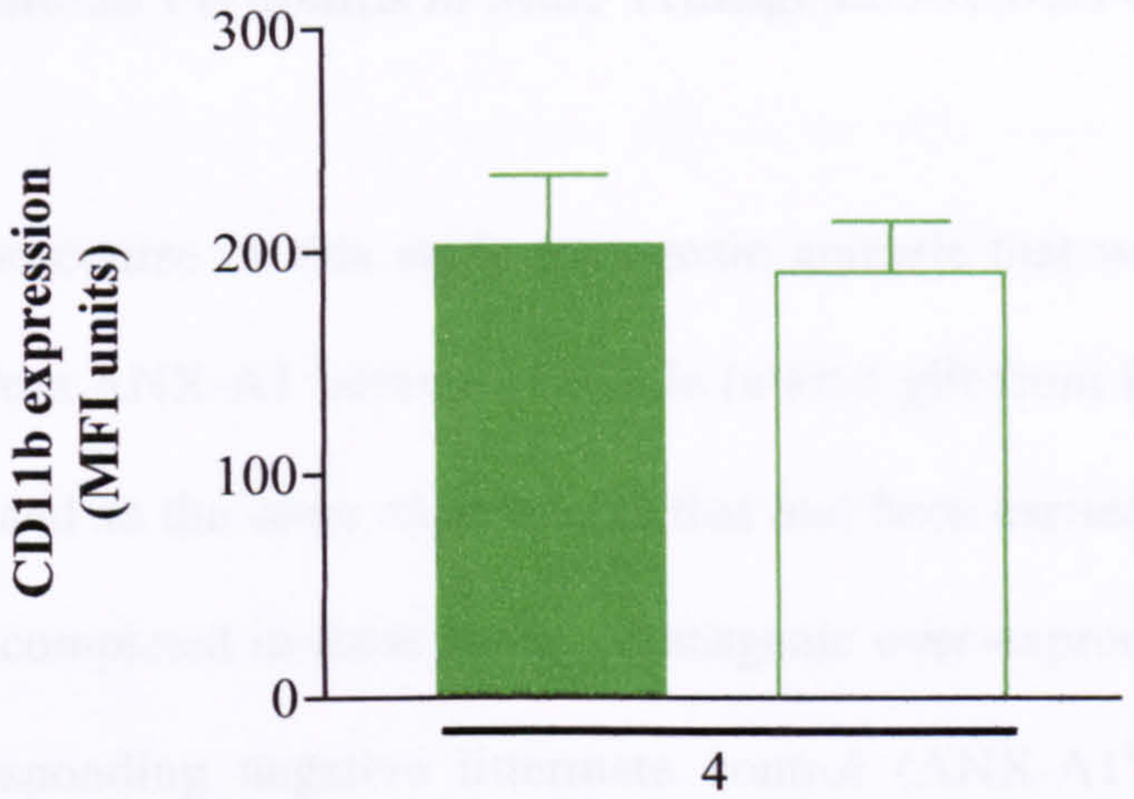

Figure 3.13. CD11b expression on Gr-1 positive cells (neutrophils) after IL-1β peritonitis in ANX-A1$^{-/-}$ and ANX-A1$^{+/+}$ mice. ANX-A1$^{+/+}$ ■ and ANX-A1$^{-/-}$ □ mice were treated with IL-1β (i.p.) for 4 hr. Cells were collected by lavage, stained with fluorescent Ab and analysed in the flow cytometer. Values are mean±sem of n=7-8 per group.

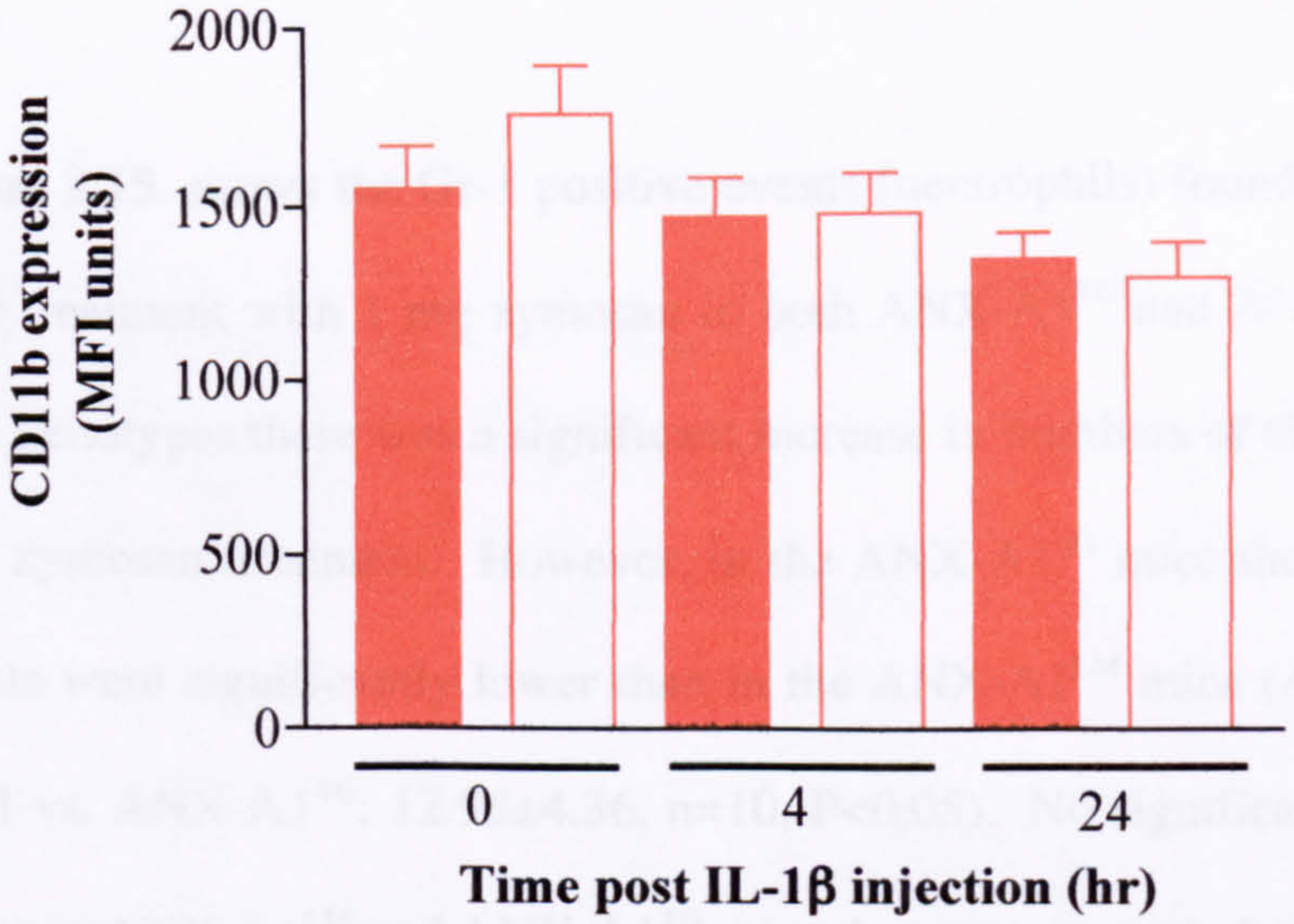

Figure 3.14. CD11b expression on F4/80 positive cells (monocytic cells) after IL-1β peritonitis in ANX-A1$^{-/-}$ and ANX-A1$^{+/+}$ mice. ANX-A1$^{+/+}$ ■ and ANX-A1$^{-/-}$ □ mice were treated with zymosan (i.p.). At selected time-points cells were collected by lavage, stained with fluorescent Ab and analysed in the flow cytometer. Values are mean±sem of n=8 mice per group.

3.1.5. Zymosan Peritonitis in Male Transgenic ANX-A1 Over-Expressing Mice

During the course of this study transgenic animals that were genetically modified to over-express ANX-A1 became available (a kind gift from Dr. Wells, Imperial College, London) and so the same experiments that had been carried out in the ANX-A1$^{-/-}$ mice could be completed in these mice. Transgenic over-expressing (ANX-A1^{TG}) mice and the corresponding negative littermate control (ANX-A1^{LM}) mice were used. The zymosan peritonitis model was chosen as this gave interesting results in the ANX-A1$^{-/-}$ animals. The majority of experiments were carried out in male animals but as some females were also available, a few experiments were also performed in these mice.

3.1.5.1. Gr-1 and F4/80 Positive Events

Figure 3.15. shows the Gr-1 positive events (neutrophils) found in the peritoneal cavity after treatment with 1 mg zymosan in both ANX-A1^{TG} and ANX-A1^{LM} male mice. In both genotypes there was a significant increase in numbers of Gr-1 positive events after 4 hr zymosan treatment. However, in the ANX-A1^{TG} mice the levels of Gr-1 positive events were significantly lower than in the ANX-A1^{LM} mice (ANX-A1^{LM}: 26.50±4.53, n=11 vs. ANX-A1^{TG}: 12.98±4.36, n=10, $P<0.05$). No significant difference was found between ANX-A1^{LM} and ANX-A1^{TG} mice that were untreated controls.

Figure 3.16. shows the F4/80 positive events (monocytic cells) found in the peritoneal cavity after treatment with zymosan in male ANX-A1^{LM} and ANX-A1^{TG} mice. In the ANX-A1^{LM} mice there was a significant decrease in numbers of F4/80 positive events after 4 hr zymosan treatment. In the ANX-A1^{TG} mice the levels of F4/80 positive

events did not decrease at the 4 hr time-point and were not significantly different to basal values. However there was no significant difference between the ANX-A1^{LM} and the ANX-A1^{TG} mice at this time-point. The graph also shows there was no significant difference between the ANX-A1^{LM} and ANX-A1^{TG} mice with respect to the untreated controls (0 hr time-point).

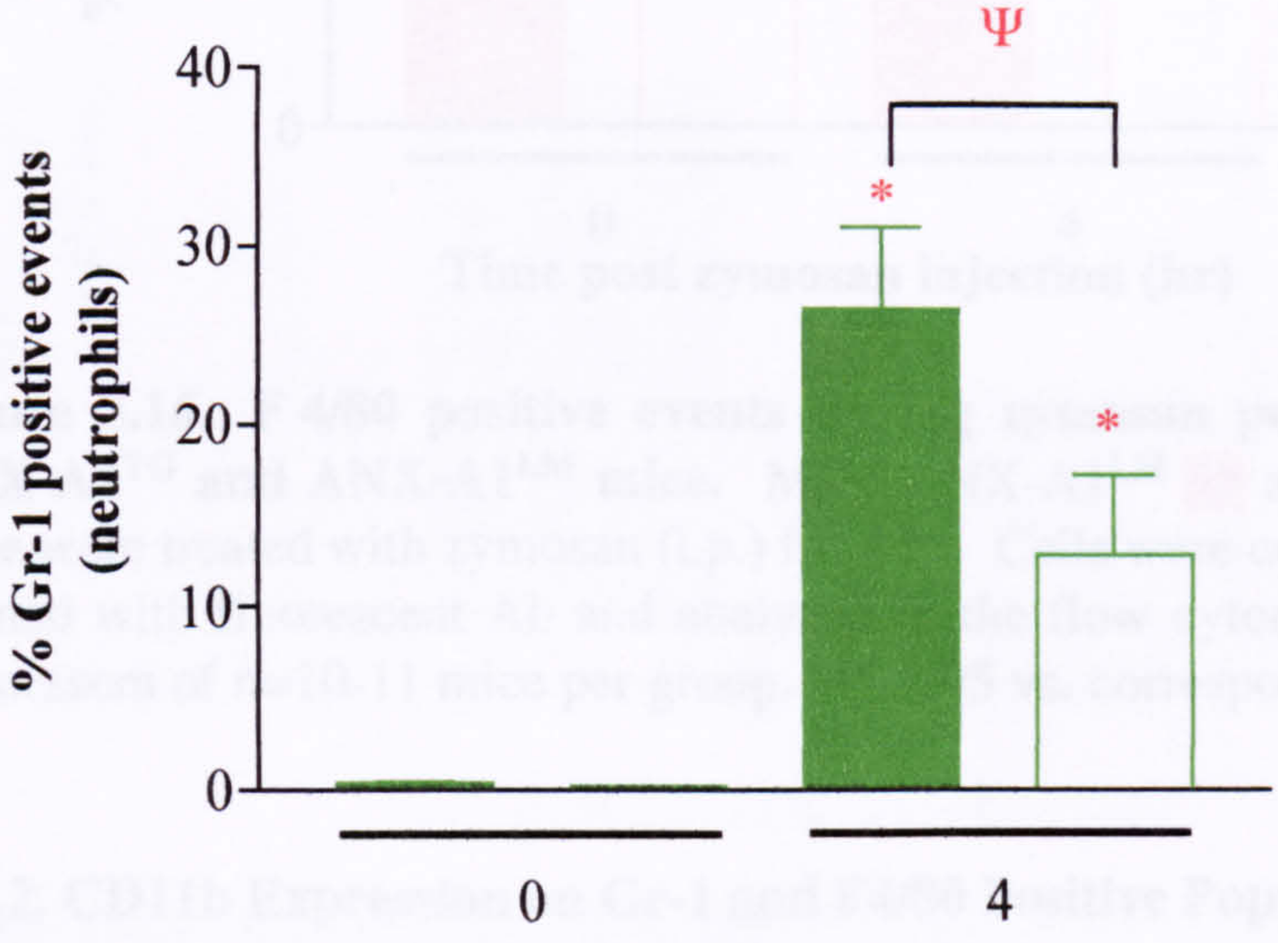

Figure 3.15. Gr-1 positive events during zymosan peritonitis in male ANX-A1^{TG} and ANX-A1^{LM} mice. Male ANX-A1^{LM} ■ and ANX-A1^{TG} □ mice were treated with zymosan (i.p.) for 4 hr. Cells were collected by lavage, stained with fluorescent Ab and analysed in the flow cytometer. Values are mean±sem of n=10-11 mice per group, *P<0.05 vs. corresponding time 0, ΨP<0.05 ANX-A1^{TG} vs. ANX-A1^{LM} at same time-point.

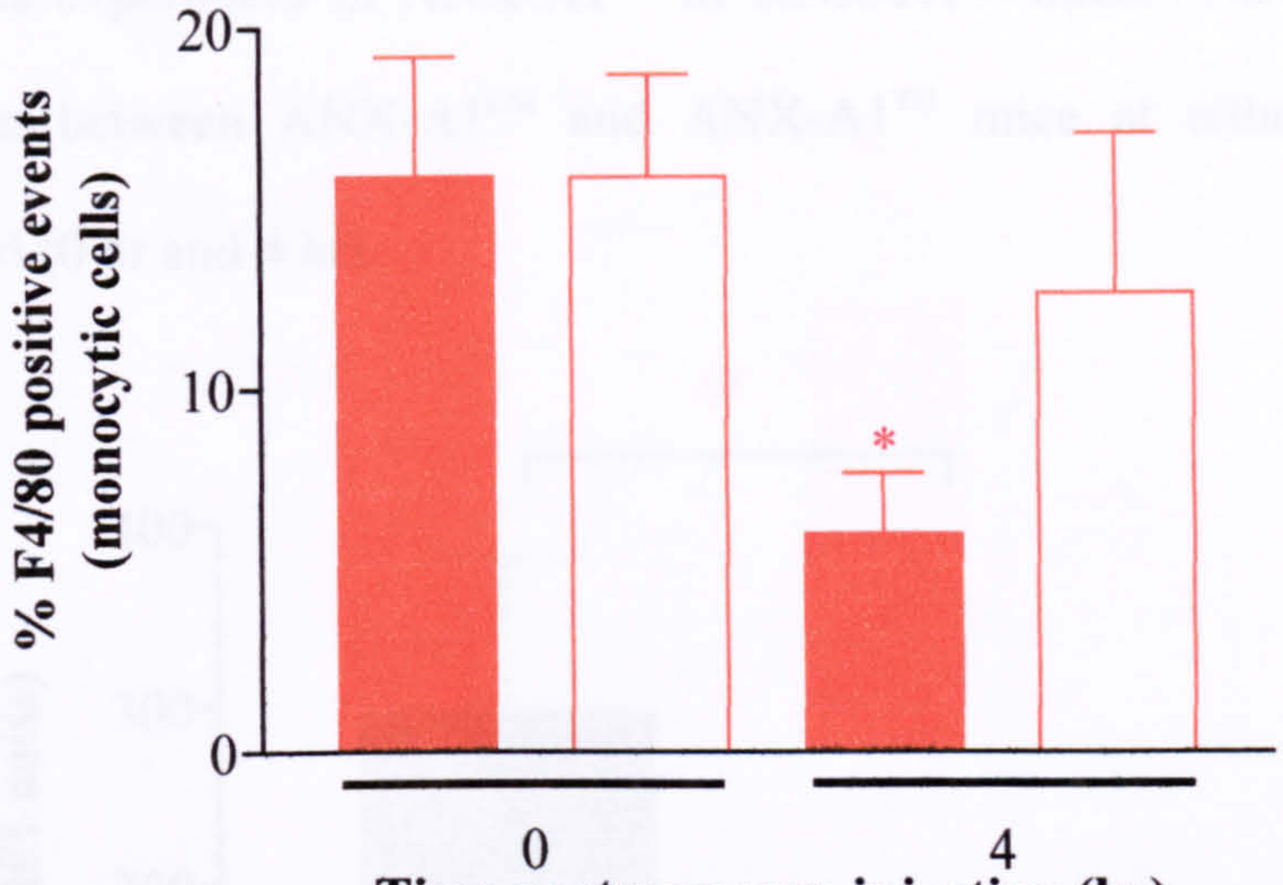

Figure 3.16. F 4/80 positive events during zymosan peritonitis in male ANX-A1^{TG} and ANX-A1^{LM} mice. Male ANX-A1^{LM} ■ and ANX-A1^{TG} □ mice were treated with zymosan (i.p.) for 4 hr. Cells were collected by lavage, stained with fluorescent Ab and analysed in the flow cytometer. Values are mean±sem of n=10-11 mice per group, *P<0.05 vs. corresponding time 0.

3.1.5.2. CD11b Expression on Gr-1 and F4/80 Positive Populations

The level of CD11b expression was measured on both the Gr-1 positive population and the F4/80 positive population of cells collected after treatment of ANX-A1^{TG} and ANX-A1^{LM} mice with zymosan.

Figure 3.17. shows CD11b expression on Gr-1 positive cells (neutrophils) 4 hr post zymosan injection. There were significantly higher levels of CD11b expressed on Gr-1 positive cells from ANX-A1^{LM} mice compared to cells from ANX-A1^{TG} mice (ANX-A1^{LM}: 296±85 vs. ANX-A1^{TG}: 107±51, n=7, P<0.05).

CD11b expression on F4/80 positive cells (monocytic cells) is shown in figure 3.18. No significant changes in CD11b expression were seen over the course of the

peritonitis experiment in ANX-A1^{LM} or ANX-A1^{TG} mice. No significant difference was seen between ANX-A1^{LM} and ANX-A1^{TG} mice at either of the time-points examined (0 hr and 4 hr).

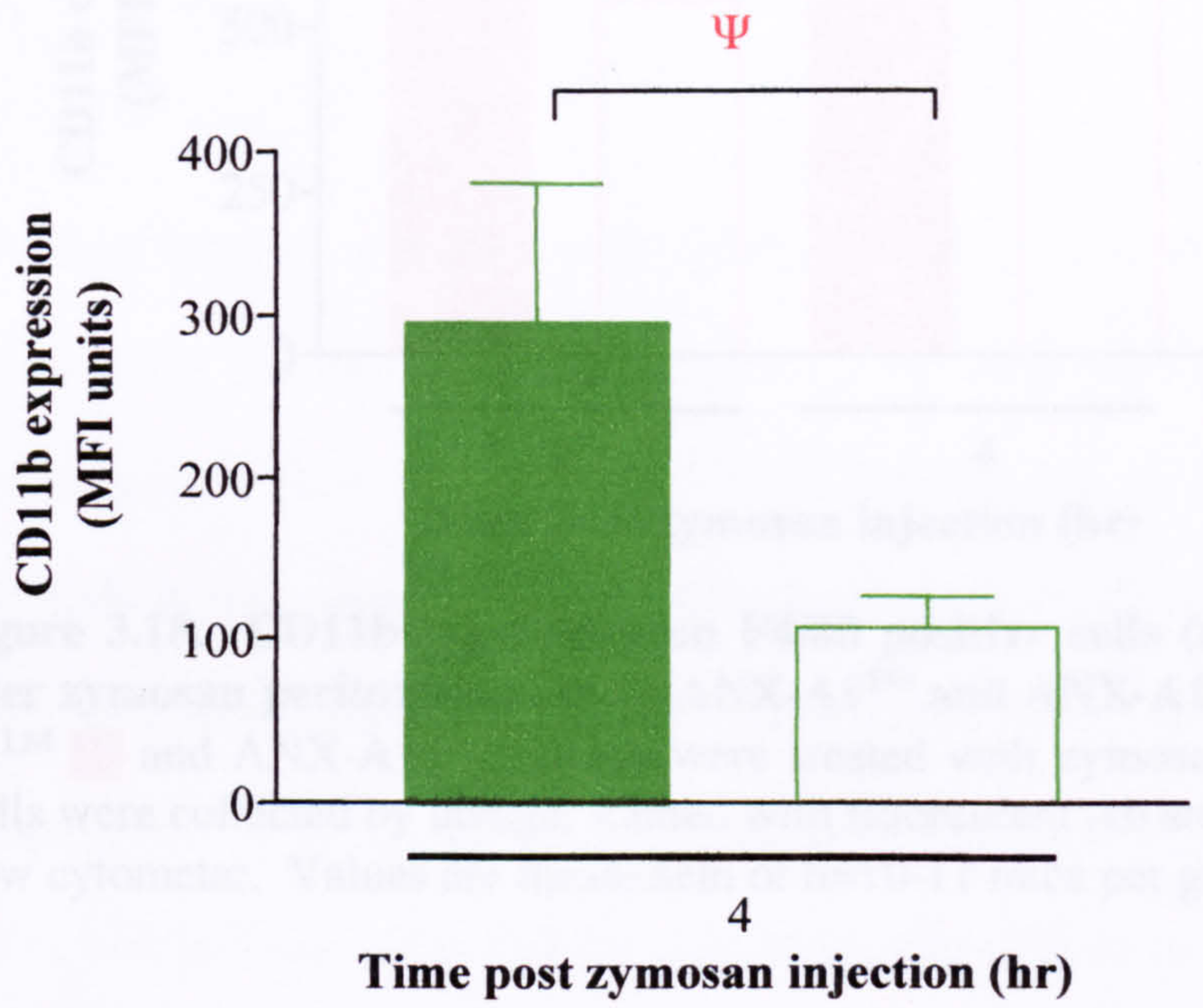

Figure 3.17. CD11b expression on Gr-1 positive cells (neutrophils) after zymosan peritonitis in male ANX-A1^{TG} and ANX-A1^{LM} mice. Male ANX-A1^{LM} ■ and ANX-A1^{TG} □ mice were treated with zymosan (i.p.) for 4 hr. Cells were collected by lavage, stained with fluorescent Ab and analysed in the flow cytometer. Values are mean±sem of n=7 mice per group, ΨP<0.05 ANX-A1^{TG} vs. ANX-A1^{LM}.

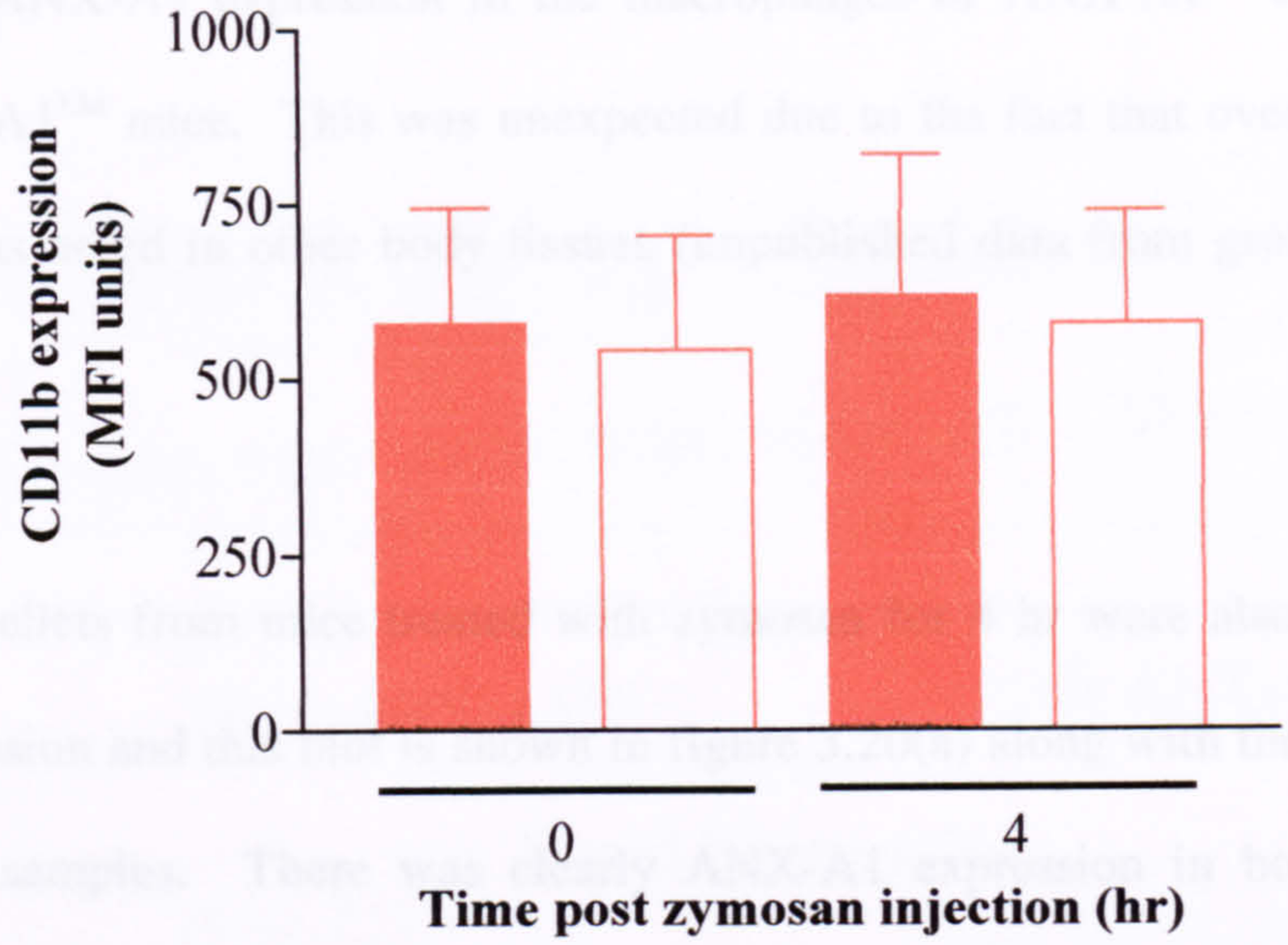

Figure 3.18. CD11b expression on F4/80 positive cells (monocytic cells) after zymosan peritonitis in male ANX-A1^{TG} and ANX-A1^{LM} mice. ANX-A1^{LM} ■ and ANX-A1^{TG} □ mice were treated with zymosan (i.p.) for 4 hr. Cells were collected by lavage, stained with fluorescent Ab and analysed in the flow cytometer. Values are mean±sem of n=10-11 mice per group.

3.1.5.3. ANX-A1 Expression in Peritoneal Cells

Male ANX-A1^{TG} and ANX-A1^{LM} mice were treated with 1 mg zymosan i.p. (in 0.5 ml sterile PBS) for 4 hr or left untreated as controls. Cells collected from the peritoneal cavity were frozen at –80°C and later thawed for Western blot analysis.

Figure 3.19(a) shows the levels of ANX-A1 expression by peritoneal cells from untreated (control) ANX-A1^{TG} and ANX-A1^{LM} mice (these cells would mainly be resident macrophages). ANX-A1 was found to be present in cells from both ANX-A1^{TG} and ANX-A1^{LM} mice. It was visually unclear if there was a difference in expression of the protein in either genotype so figure 3.19(b) shows a densitometric analysis of the blot. Data shown are normalised so expressed as a percentage of tubulin, see figure 3.19(a). The data from the densitometric analysis does not show

more ANX-A1 expression in the macrophages of ANX-A1^{TG} mice compared to the ANX-A1^{LM} mice. This was unexpected due to the fact that over-expression of ANX-A1 was noted in other body tissues (unpublished data from group who generated the mice).

Cell pellets from mice treated with zymosan for 4 hr were also blotted for ANX-A1 expression and this blot is shown in figure 3.20(a) along with the blot for tubulin from these samples. There was clearly ANX-A1 expression in both genotypes. Some samples show the typical ANX-A1 double band and some do not but this does not seem to be connected to which genotype the samples are obtained from. Figure 3.20(b) is an attempt to see if a correlation exists between the band density obtained from the western blot and the amount of Gr-1 positive events found in the peritoneal cavity of the same mice. Even though only a few samples could be assessed it shows a correlation exists between the two variables, i.e. the samples with less Gr-1 positive events had a lower optical density (and a single band on the western blot)

Figure 3.20(c) is a graphical representation of the data from the blot. There was no difference in the optical density of bands from either genotype and therefore ANX-A1 expression between the ANX-A1^{TG} and ANX-A1^{LM} mice on cells from the inflamed peritoneal cavity.

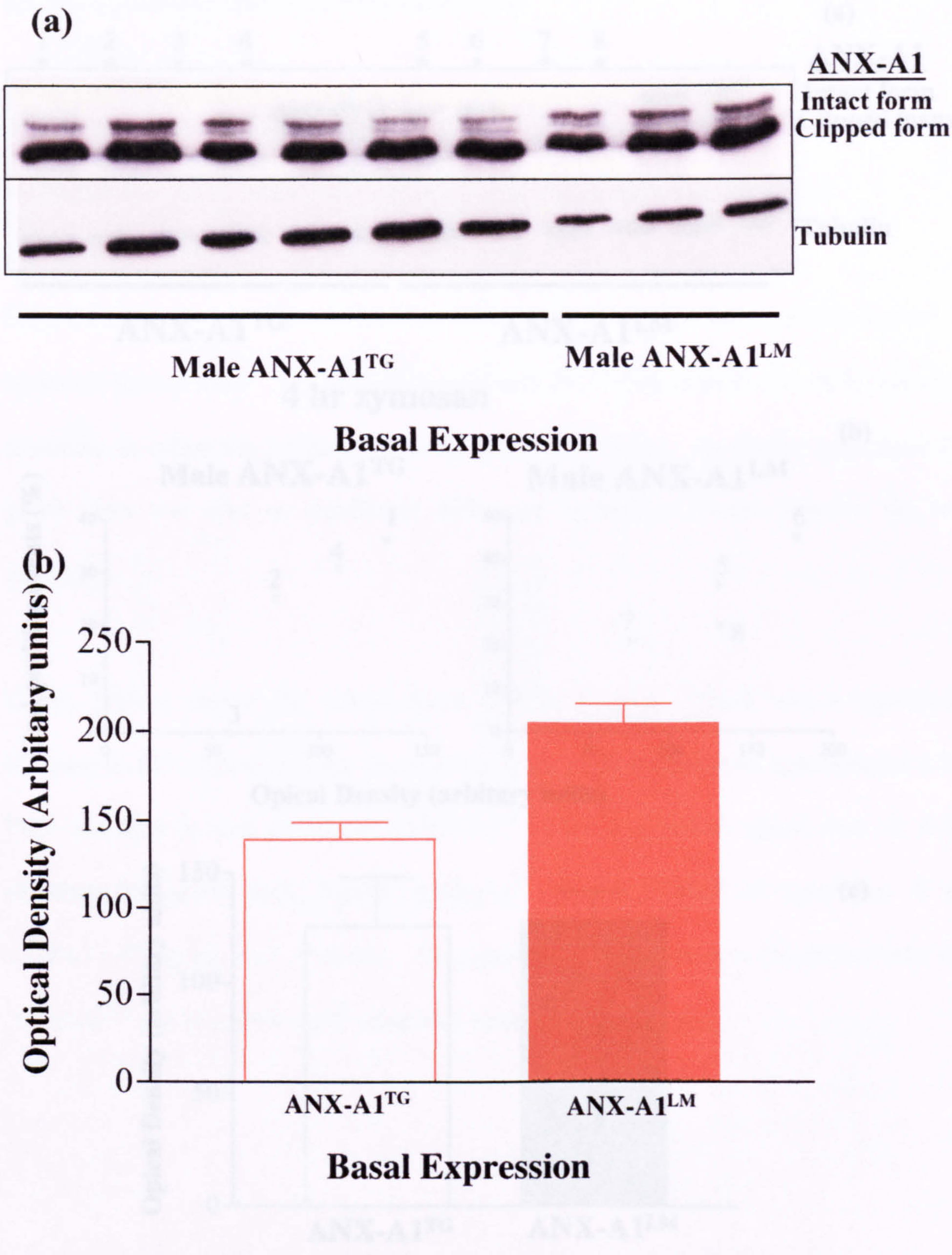

Figure 3.19. ANX-A1 expression on cells from peritoneal cavities of untreated (basal) male ANX-A1^{TG} and ANX-A1^{LM} mice. Peritoneal cavities of untreated male ANX-A1^{TG} □ and ANX-A1^{LM} ■ mice were lavaged, cell lysates were analysed by western blotting for ANX-A1 and tubulin expression (a) Western blot results (b) Densitometry data from western blots. Values are mean±sem of n=3-6 mice per group.

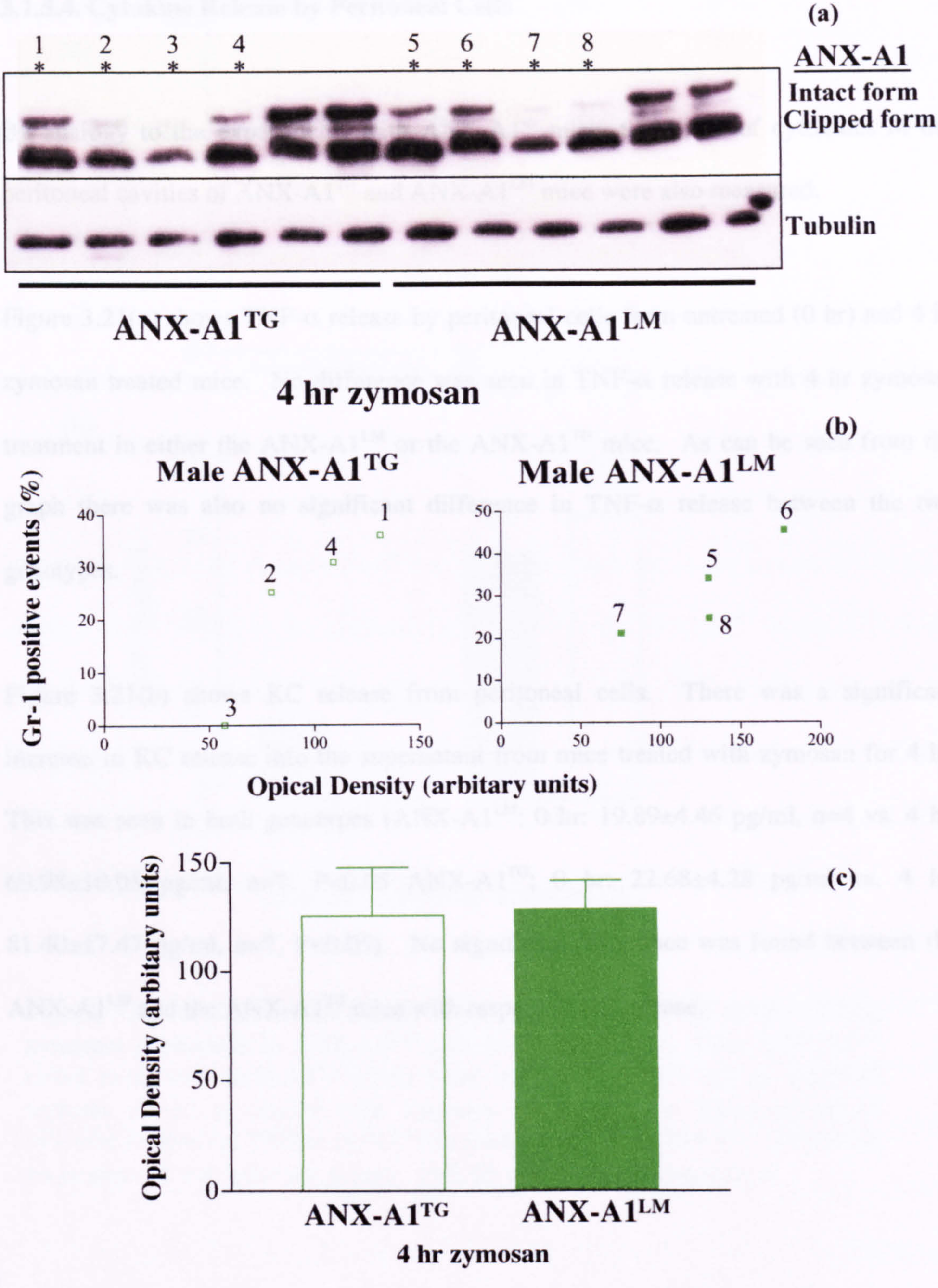

Figure 3.20. ANX-A1 expression on cells from peritoneal cavities of zymosan treated ANX-A1^{TG} and ANX-A1^{LM} mice. Male ANX-A1^{TG} □ and ANX-A1^{LM} ■ mice were treated with zymosan (i.p.) for 4 hr, collected cells were later analysed by western blotting for ANX-A1 and tubulin expression. (a) Western blot results (b) Correlation between band optical density and % Gr-1 positive events in these samples (c) Densitometry data from western blots. Values are mean±sem of n=6 mice per group.

3.1.5.4. Cytokine Release by Peritoneal Cells

By analogy to the experiments with ANX-A1$^{-/-}$ mice, the levels of cytokines in the peritoneal cavities of ANX-A1^{TG} and ANX-A1^{LM} mice were also measured.

Figure 3.21(a) shows TNF-α release by peritoneal cells from untreated (0 hr) and 4 hr zymosan treated mice. No difference was seen in TNF-α release with 4 hr zymosan treatment in either the ANX-A1^{LM} or the ANX-A1^{TG} mice. As can be seen from the graph there was also no significant difference in TNF-α release between the two genotypes.

Figure 3.21(b) shows KC release from peritoneal cells. There was a significant increase in KC release into the supernatant from mice treated with zymosan for 4 hr. This was seen in both genotypes (ANX-A1^{LM}; 0 hr: 19.89±4.46 pg/ml, n=4 vs. 4 hr: 69.98±10.05 pg/ml, n=7, $P<0.05$ ANX-A1^{TG}; 0 hr: 22.68±4.28 pg/ml vs. 4 hr: 81.40±17.47 pg/ml, n=7, $P<0.05$). No significant difference was found between the ANX-A1^{LM} and the ANX-A1^{TG} mice with respect to KC release.

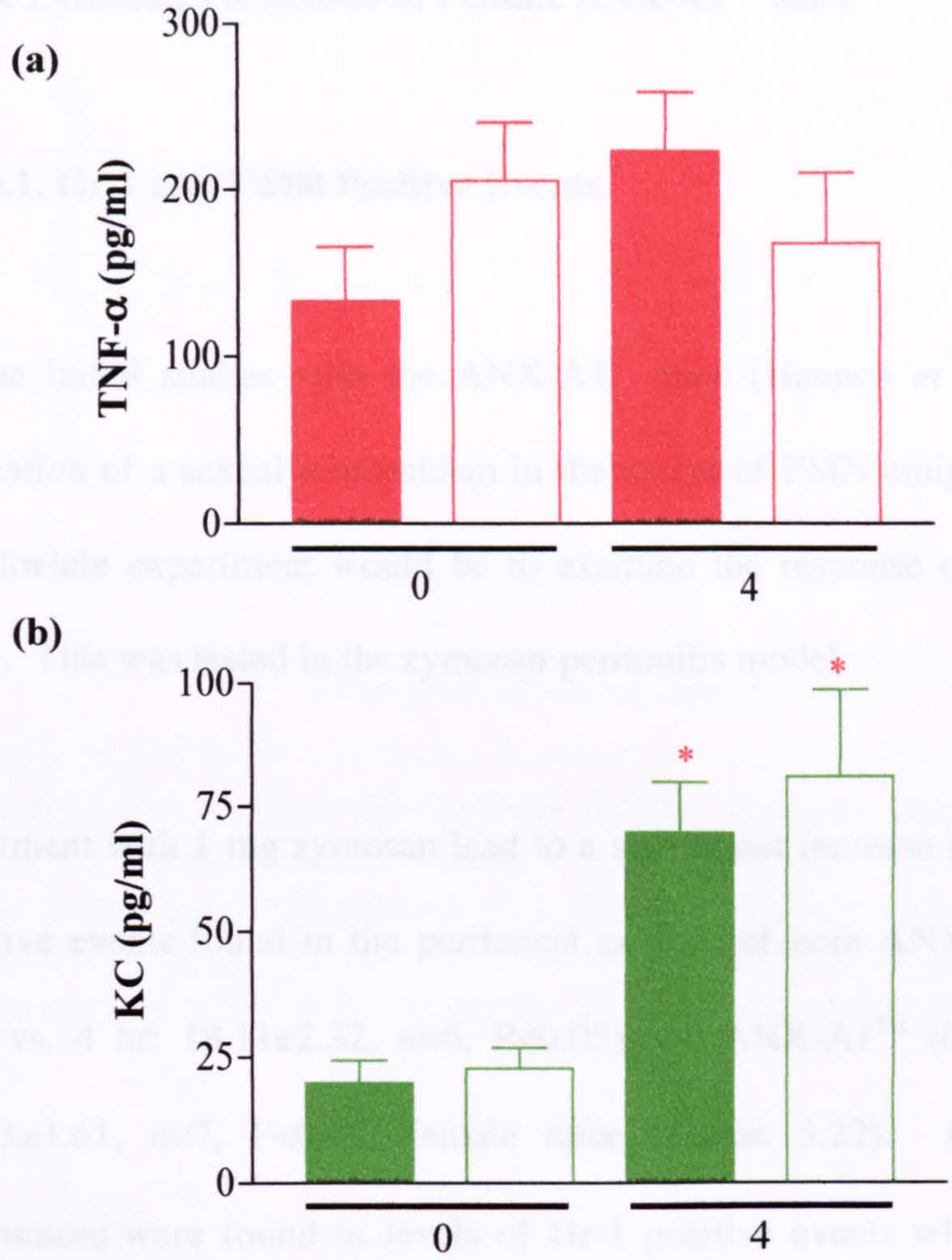

Figure 3.21. Cytokine release by cells into the peritoneal cavity during zymosan peritonitis in ANX-A1^{LM} and ANX-A1^{TG} mice. Male ANX-A1^{LM} (solid bars) and ANX-A1^{TG} (clear bars) mice were either left as untreated controls (0 hr) or treated with zymosan (i.p.) for 4 hr. Measurement of cytokine release (a) TNF-α (b) KC was made using an ELISA kit. Values are mean±sem of n=8 mice per group, *P<0.05 vs. corresponding time 0.

3.1.6. Zymosan Peritonitis in Female ANX-A1^{TG} Mice

3.1.6.1. Gr-1 and F4/80 Positive Events

In the initial studies with the ANX-A1$^{-/-}$ mice (Hannon *et al.*, 2002) there was an indication of a sexual dimorphism in the extent of PMN emigration. It was decided a worthwhile experiment would be to examine the response of the female ANX-A1^{TG} mice. This was tested in the zymosan peritonitis model.

Treatment with 1 mg zymosan lead to a significant increase in the percentage of Gr-1 positive events found in the peritoneal cavities of both ANX-A1^{LM} (0 hr: 0.13±0.05, n=8 vs. 4 hr: 18.11±2.32, n=6, $P<0.05$) and ANX-A1^{TG} (0 hr: 0.15±0.06, n=8 vs. 22.03±3.61, n=7, $P<0.05$) female mice (Figure 3.22). However, no significant differences were found in levels of Gr-1 positive events when the ANX-A1^{LM} mice were compared to the ANX-A1^{TG} mice at either the 0 hr or the 4 hr time-point.

Figure 3.23 shows that the levels of F4/80 positive events found in the peritoneal cavity after 4 hr treatment with zymosan were significantly decreased when compared to the levels found in untreated control mice (0 hr zymosan) in ANX-A1^{LM} mice (0 hr: 24.41±4.45, n=8 vs. 4hr: 2.95±1.39, n=6, $P<0.05$). The same pattern was seen in ANX-A1^{TG} mice (0 hr: 22.39±5.35, n=8 vs. 4 hr: 1.86±0.69, n=7, $P<0.05$). No significant difference was seen between the female ANX-A1^{LM} and ANX-A1^{TG} mice at either 0 hr or 4 hr.

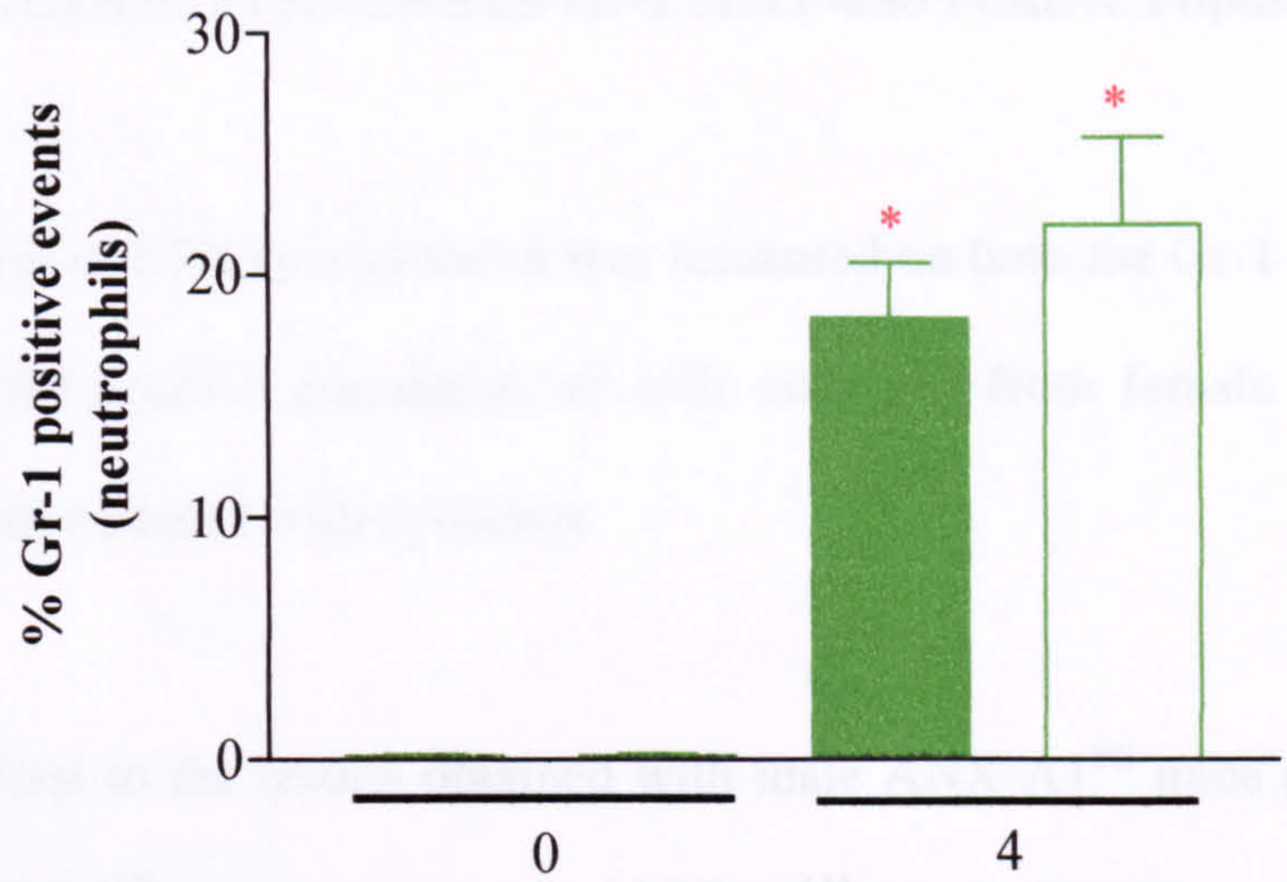

Figure 3.22. Gr-1 positive events during zymosan peritonitis in female ANX-A1^{TG} and ANX-A1^{LM} mice. Female ANX-A1^{LM} ■ and ANX-A1^{TG} □ mice were treated with zymosan (i.p.) for 4 hr. Cells were collected by lavage, stained with fluorescent Ab and analysed in the flow cytometer. Values are mean±sem of n=6-8 mice per group, *P<0.05 vs. corresponding time 0.

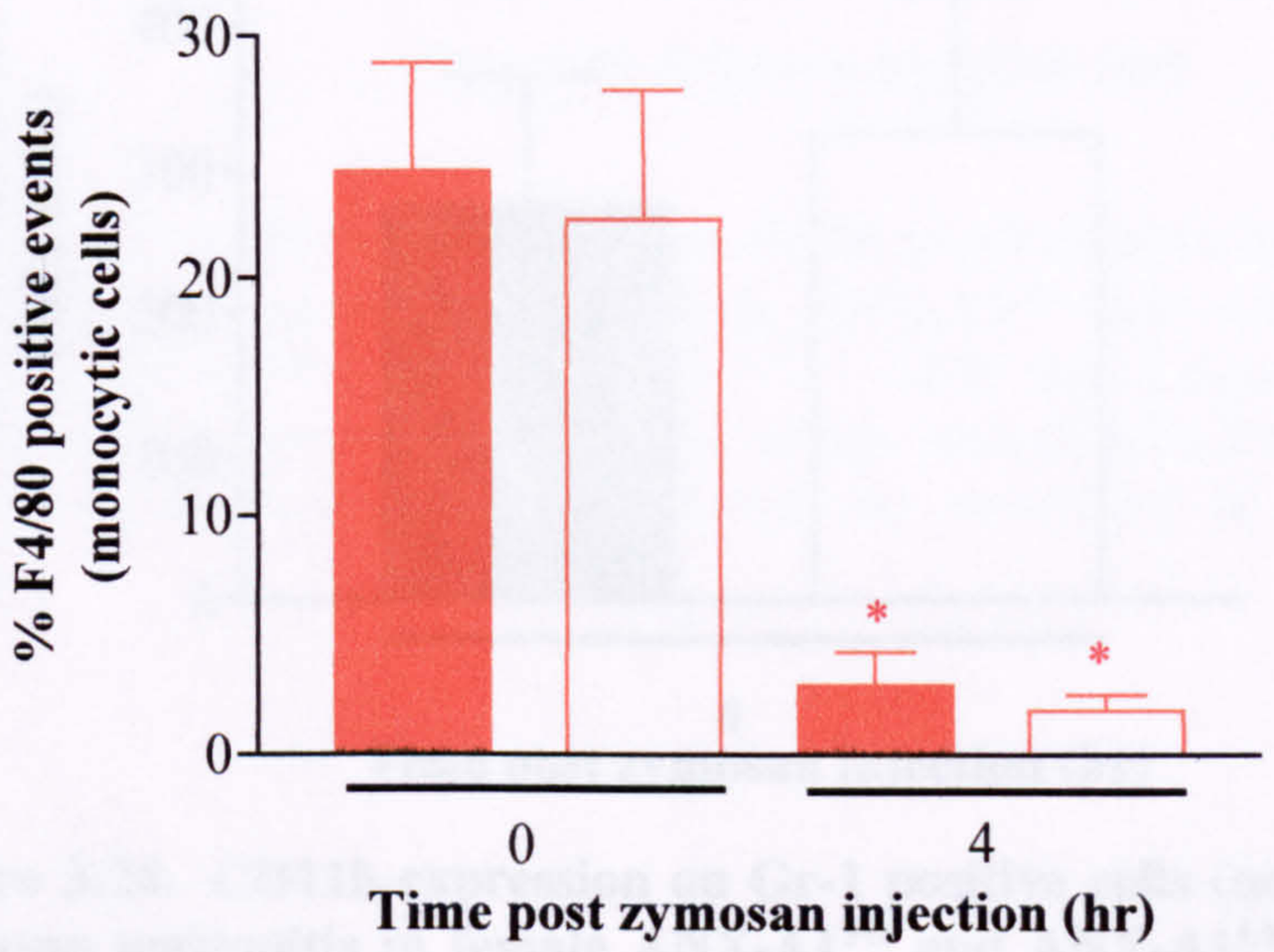

Figure 3.23. F4/80 positive events during zymosan peritonitis in female ANX-A1^{TG} and ANX-A1^{LM} mice. Female ANX-A1^{LM} ■ and ANX-A1^{TG} □ mice were treated with zymosan (i.p.) for 4 hr. Cells were collected by lavage, stained with fluorescent Ab and analysed in the flow cytometer. Values are mean±sem of n=6-8 mice per group, *P<0.05 vs. corresponding time 0.

3.1.6.2. CD11b Expression on Gr-1 and F4/80 Positive Populations

The level of CD11b expression was measured on both the Gr-1 positive population and the F4/80 positive population of cells collected from female ANX-A1^{TG} and ANX-A1^{LM} mice treated with zymosan.

In contrast to the results obtained with male ANX-A1^{TG} mice (lower CD11b on PMN of ANX-A1^{TG} mice compared to ANX-A1^{LM} mice), CD11b expression on Gr-1 positive cells (neutrophils) after 4 hr zymosan treatment was not significantly different between ANX-A1^{LM} and ANX-A1^{TG} female mice (Figure 3.24).

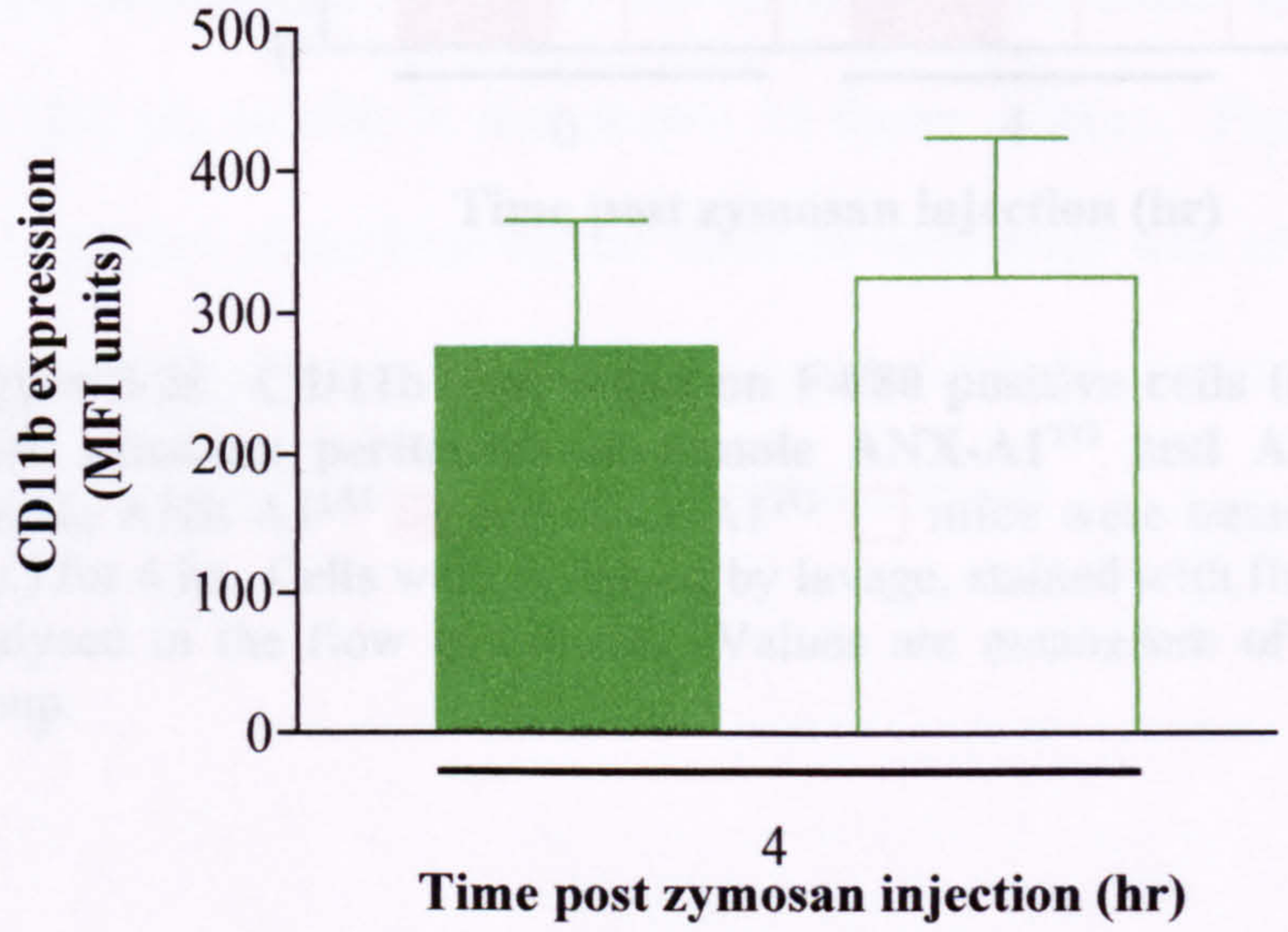

Figure 3.24. CD11b expression on Gr-1 positive cells (neutrophils) after zymosan peritonitis in female ANX-A1^{TG} and ANX-A1^{LM} mice. Female ANX-A1^{LM} ■ and ANX-A1^{TG} □ mice were treated with zymosan (i.p.) for 4 hr. Cells were collected by lavage, stained with fluorescent Ab and analysed in the flow cytometer. Values are mean±sem of n=6-7 mice per group.

Figure 3.25 shows CD11b expression on F4/80 positive events (monocytic cells). Expression was not altered by 4 hr treatment with zymosan in either the ANX-A1^{LM} or the ANX-A1^{TG} mice. CD11b expression was not significantly different between the genotypes basally (0 hr) or after 4 hr zymosan treatment.

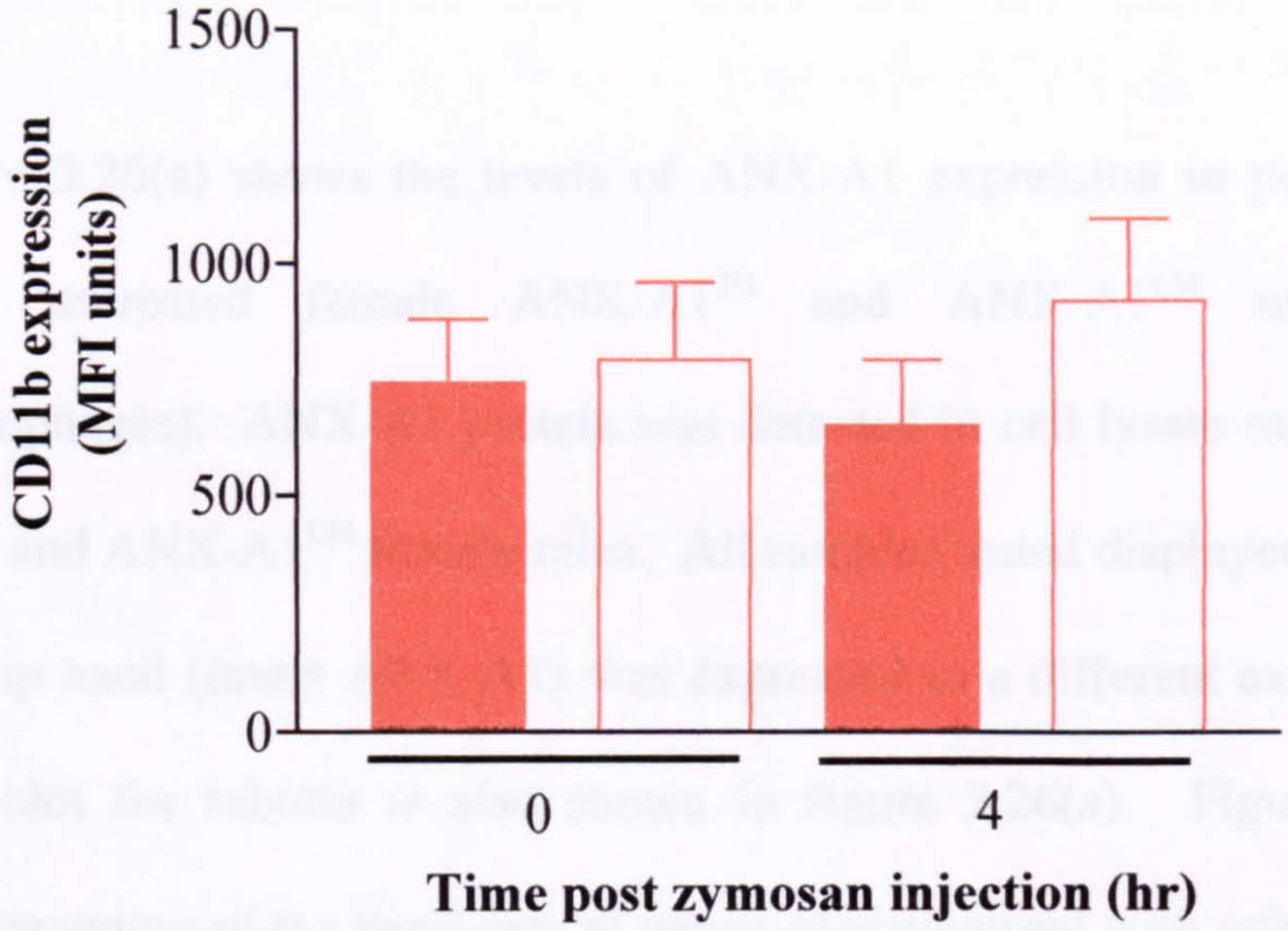

Figure 3.25. CD11b expression on F4/80 positive cells (monocytic cells) after zymosan peritonitis in female ANX-A1^{TG} and ANX-A1^{LM} mice. Female ANX-A1^{LM} ■ and ANX-A1^{TG} □ mice were treated with zymosan (i.p.) for 4 hr. Cells were collected by lavage, stained with fluorescent Ab and analysed in the flow cytometer. Values are mean±sem of n=6-7 mice per group.

3.1.6.3. ANX-A1 Expression in Peritoneal Cells

Female ANX-A1^{TG} and ANX-A1^{LM} mice were treated i.p. with 1 mg zymosan (in 0.5 ml sterile PBS) for 4 hr or left untreated as controls. Peritoneal cells collected from the peritoneal cavity were frozen at –80°C and later thawed for western blot analysis.

Figure 3.26(a) shows the levels of ANX-A1 expression in peritoneal cells collected from untreated female ANX-A1^{TG} and ANX-A1^{LM} mice (mainly resident macrophages). ANX-A1 protein was detected in cell lysate samples from both ANX-A1^{TG} and ANX-A1^{LM} female mice. All samples tested displayed double bands however the top band (intact ANX-A1) was expressed to a different extent in individual mice. The blot for tubulin is also shown in figure 3.26(a). Figure 3.25(b) is graphical representation of the band optical densities normalised with reference to tubulin, and as can be seen there was no difference in the ANX-A1 expression between ANX-A1^{LM} and ANX-A1^{TG} female mice under basal conditions.

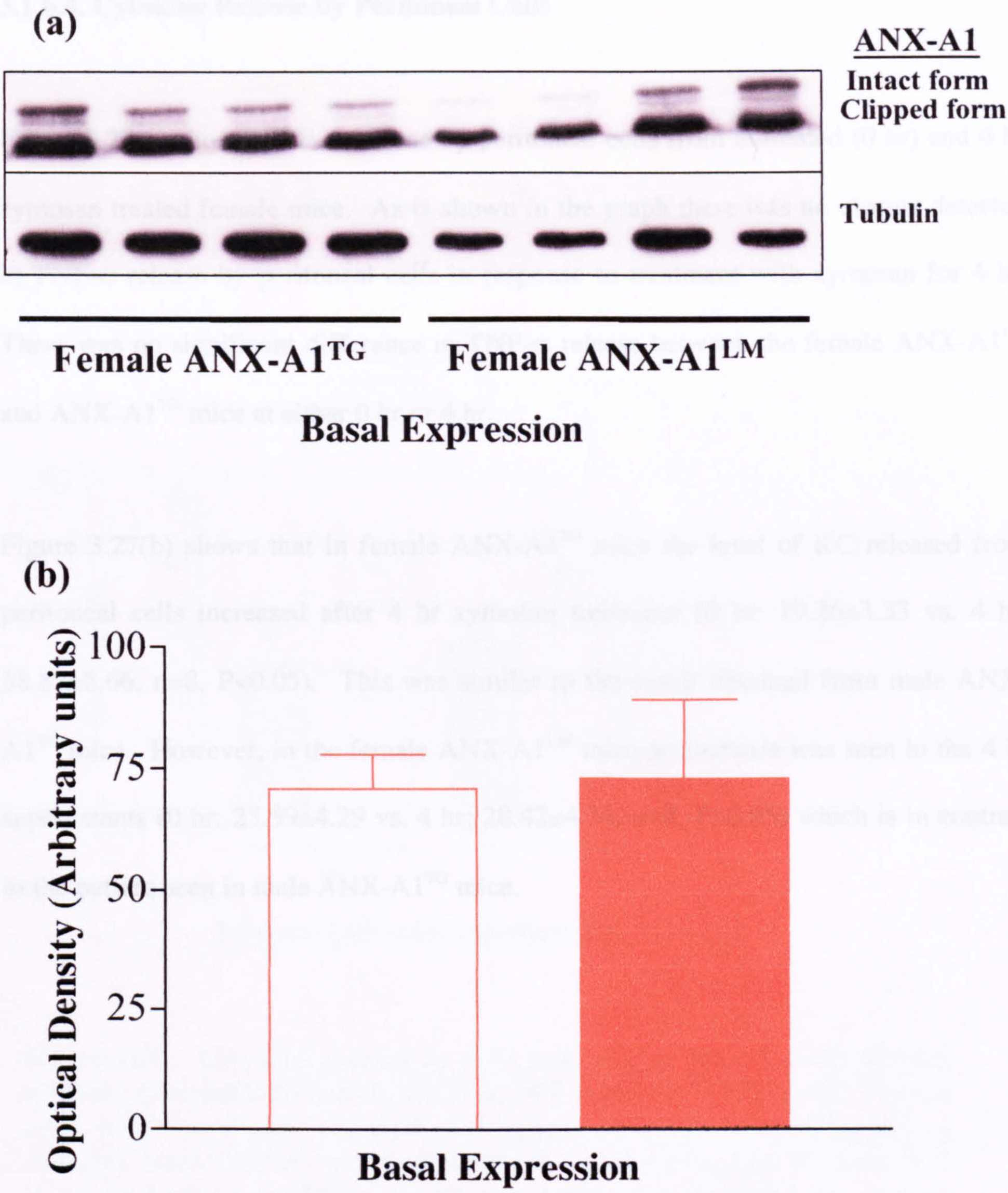

Figure 3.26. ANX-A1 expression on on cells from peritoneal cavities of untreated (basal) female ANX-A1^{TG} and ANX-A1^{LM} mice. Peritoneal cavities of untreated female ANX-A1^{TG} □ and ANX-A1^{LM} ■ mice were lavaged, cell lysates were analysed by western blotting for ANX-A1 and tubulin expression (a) Western blot results (b) Densitometry data from western blots. Values are mean±sem of n=4 mice per group.

3.1.6.4. Cytokine Release by Peritoneal Cells

Figure 3.27(a) shows TNF-α release by peritoneal cells from untreated (0 hr) and 4 hr zymosan treated female mice. As is shown in the graph there was no change detected in TNF-α release by peritoneal cells in response to treatment with zymosan for 4 hr. There was no significant difference in TNF-α release between the female ANX-A1^{LM} and ANX-A1^{TG} mice at either 0 hr or 4 hr.

Figure 3.27(b) shows that in female ANX-A1^{TG} mice the level of KC released from peritoneal cells increased after 4 hr zymosan treatment (0 hr: 19.26±3.33 vs. 4 hr: 38.85±8.66, n=8, $P<0.05$). This was similar to the result obtained from male ANX-A1^{TG} mice. However, in the female ANX-A1^{LM} mice no increase was seen in the 4 hr supernatants (0 hr: 25.59±4.29 vs. 4 hr: 28.42±4.74, n=8, $P>0.05$) which is in contrast to the pattern seen in male ANX-A1^{TG} mice.

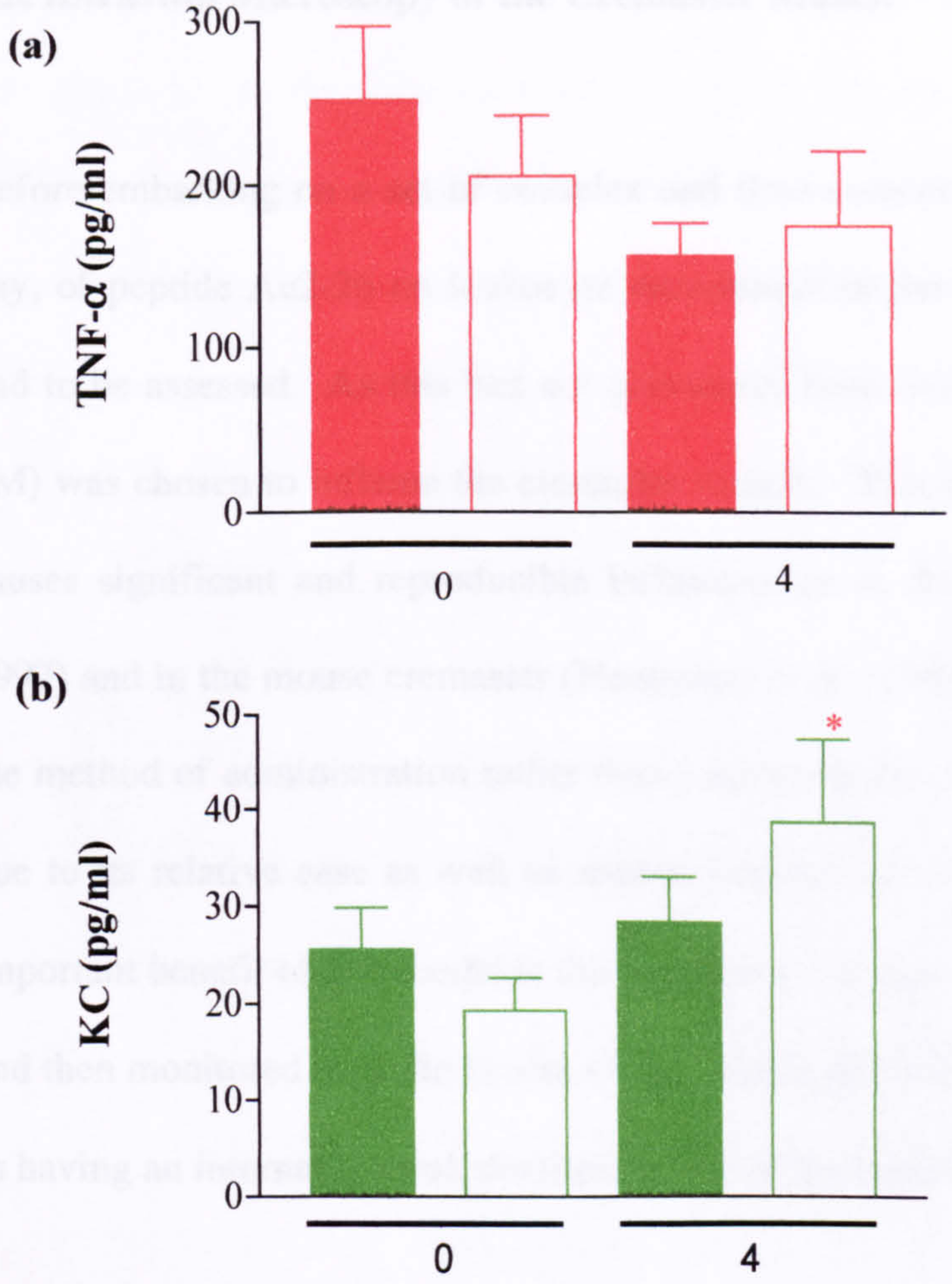

Figure 3.27. Cytokine release by cells into the peritoneal cavity during zymosan peritonitis in female ANX-A1 WT and ANX-A1^{TG} mice. Female ANX-A1^{LM} (solid bars) and ANX-A1^{TG} (clear bars) mice were either left as untreated controls (0 hr) or treated with zymosan (i.p.) for 4 hr. Measurement of cytokine release (a) TNF-α (b) KC was made using an ELISA kit. Values are mean±sem of n=8 mice per group, *P<0.05 vs. corresponding time 0.

3.2. Intravital Microscopy of the Cremaster Muscle

Before embarking on a set of complex and time-consuming experiments the effect, if any, of peptide Ac2-26 on leukocyte recruitment in the cremaster muscle preparation had to be assessed. As this had not previously been described, PAF superfusion (100 nM) was chosen to inflame the cremaster muscle. This concentration was chosen as it causes significant and reproducible inflammation in the rat mesentery (Tailor *et al.*, 1997) and in the mouse cremaster (Henninger *et al.*, 1997). Superfusion was chosen as the method of administration rather than local intrascrotal injection of an inflammogen due to its relative ease as well as animal licensing restrictions at that time. Another important benefit of this model is the fact that a vessel is chosen in an untreated animal and then monitored over the course of the developing inflammatory response so as well as having an internal control, the time course of the response could also be measured.

3.2.1. Effect of Ac2-26 in the Cremaster Muscle Preparation

C57BL/6 mice were prepared for intravital microscopy of the cremaster muscle and after a 30 min stabilisation period were either treated with 200 μg peptide Ac2-26 (in 200 μl PBS) or 200 μl PBS alone via a cannula in the jugular vein (i.v.). The cremaster was then superfused with 100 nM PAF for a total of 90 min.

Rolling Velocity

The effect of Ac2-26 on leukocyte rolling velocity is shown in figure 3.28. The data are presented as a percentage of the rolling velocity measured at time 0 (basal) for clarity. In PBS treated (vehicle control) mice the rolling velocity of leukocytes was

significantly reduced over the 90 min time course of 100 nM PAF superfusion from 30 min onwards. In the mice treated with peptide Ac2-26 there was also a reduction in cell rolling velocity over the PAF time course and this was significant at 30, 60, 75 and 90 min. There were no significant differences between the two treatment groups at any of the time-points measured.

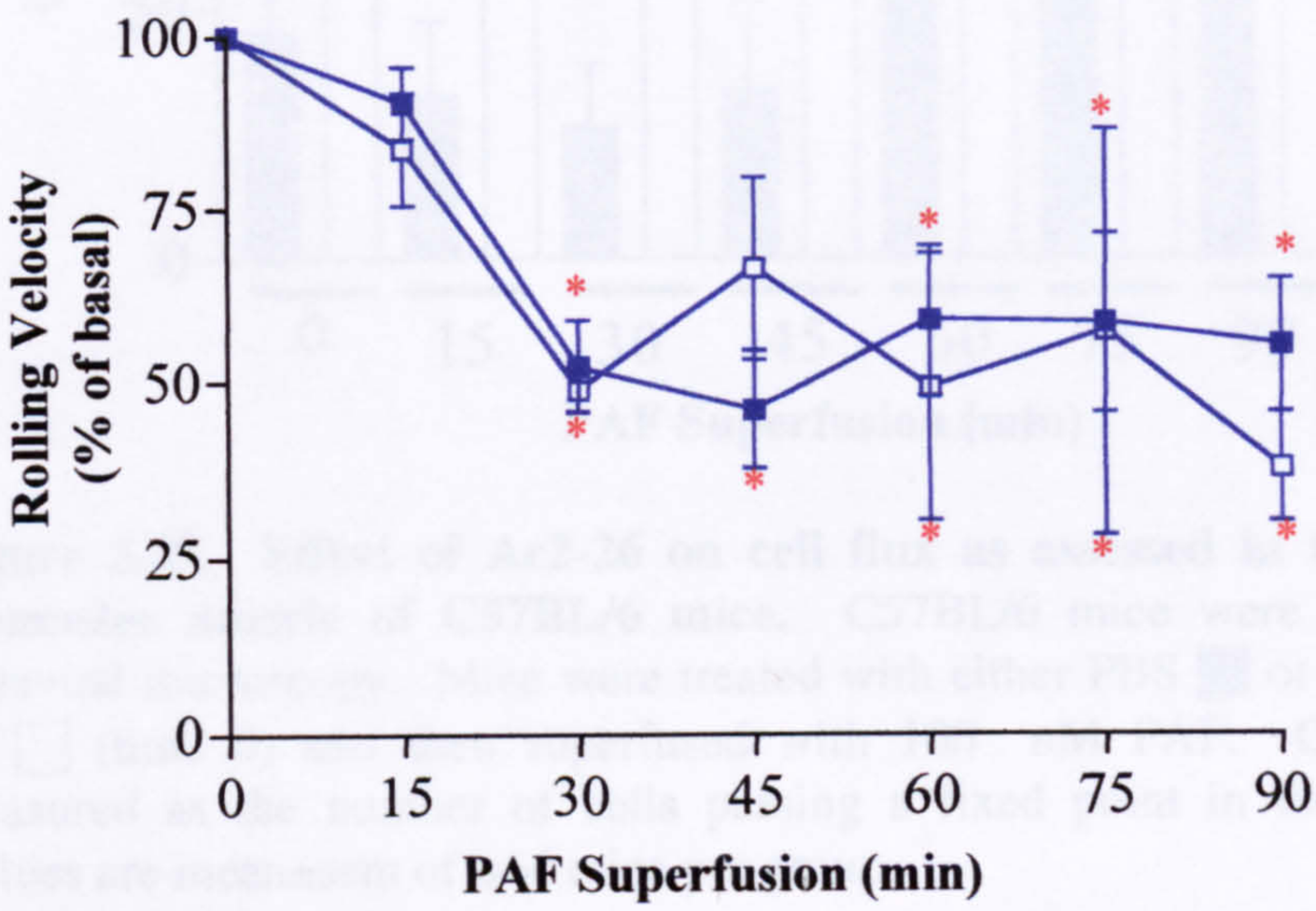

Figure 3.28. Effect of Ac2-26 on cell rolling velocity as assessed in the inflamed cremaster muscle of C57BL/6 mice. C57BL/6 mice were prepared for intravital microscopy. Mice were treated with either PBS ■ or 200 g Ac2-26 □ (time 0) and then superfused with 100 nM PAF. Rolling velocity is shown as % of basal rolling velocity (basal rolling velocity in PBS and Ac2-26 treated mice was 41±8 and 89±20 μm/sec respectively). Values are mean±sem of n=4 mice per group, *P<0.05 vs. corresponding time 0.

Cell Flux

Figure 3.29. shows the effect of 100 nM PAF on cell flux in vehicle control (PBS treated) and peptide Ac2-26 treated mice. In the vehicle control group cell flux was not significantly altered over 90 min of PAF superfusion. The same was seen in the peptide treated group. There were also no significant differences between the treatment groups at any of the time-points measured. The large error bars on the graph show that cell flux was highly variable in both the peptide treated and vehicle control animals.

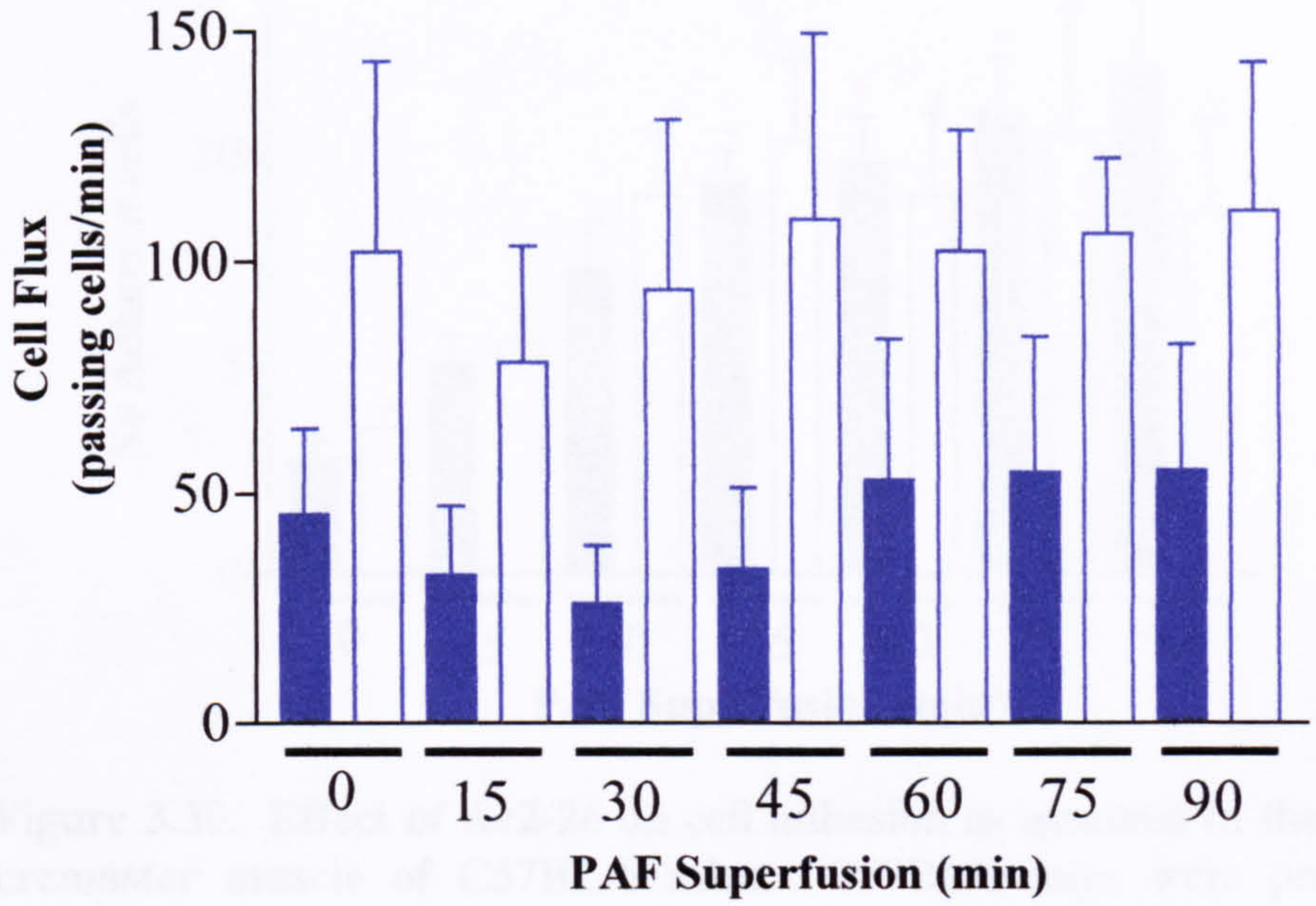

Figure 3.29. Effect of Ac2-26 on cell flux as assessed in the inflamed cremaster muscle of C57BL/6 mice. C57BL/6 mice were prepared for intravital microscopy. Mice were treated with either PBS ■ or 200 μg Ac2-26 □ (time 0) and then superfused with 100 nM PAF. Cell flux was measured as the number of cells passing a fixed point in the vessel/min. Values are mean±sem of n=4 mice per group.

Adhesion

Figure 3.30 shows that cell adhesion was increased in a time-dependent manner when the cremaster muscle was superfused with 100 nM PAF. In the vehicle control animals the number of adherent cells was significantly higher than the basal level (0 min) from 45 min of PAF superfusion onwards. The treatment of mice with Ac2-26 caused no significant change in adhesion which still increased in a time-dependent manner in these mice (also significant from 45 min onwards). No significant differences were seen between the two treatments at any of the time-points measured.

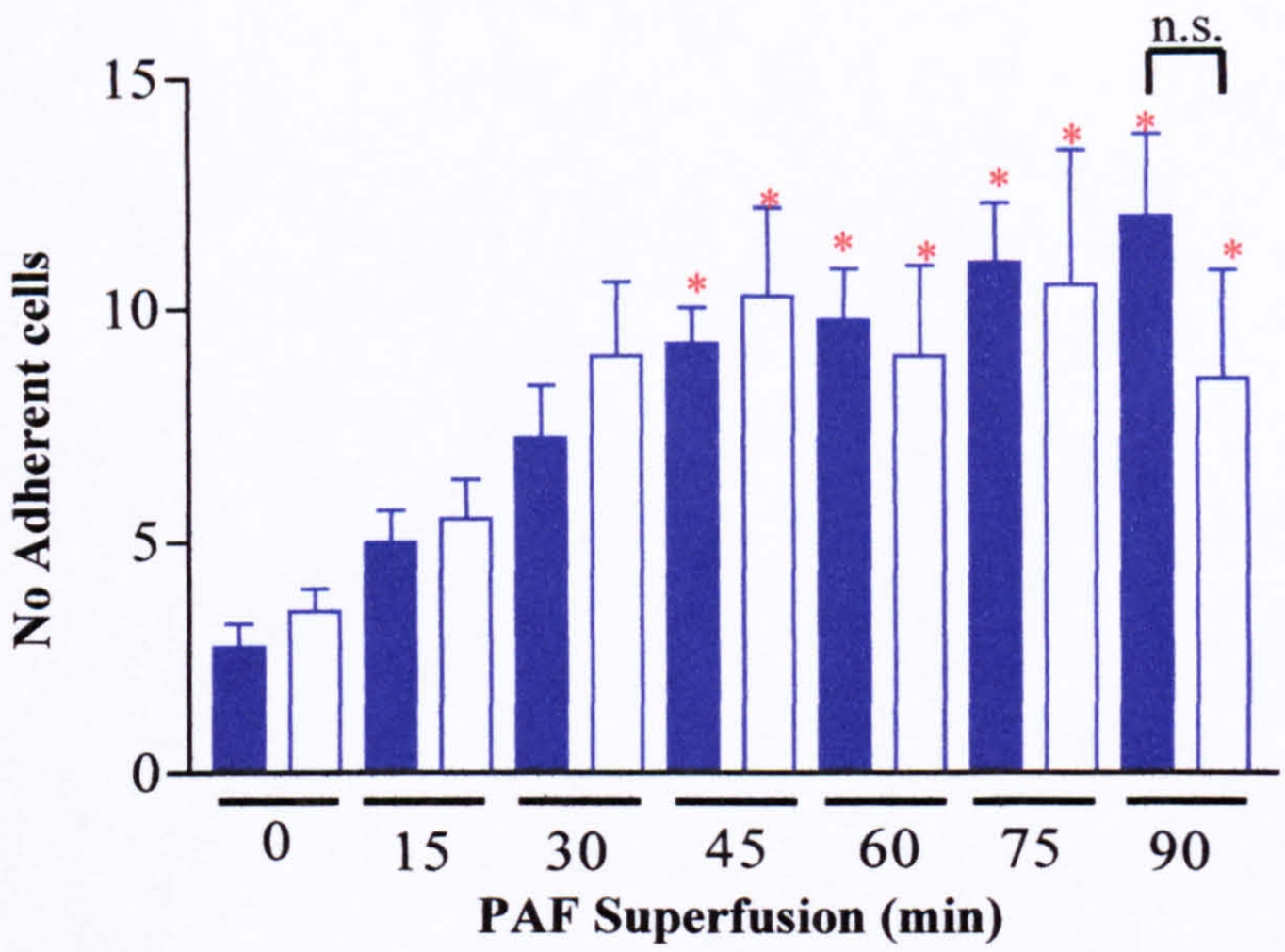

Figure 3.30. Effect of Ac2-26 on cell adhesion as assessed in the inflamed cremaster muscle of C57BL/6 mice. C57BL/6 mice were prepared for intravital microscopy. Mice were treated with either PBS ■ or 200 μg Ac2-26 □ (time 0) and then superfused with 100 nM PAF. Adhesion is measured as the number of cells stationary for >30 sec. Values are mean±sem of n=4 mice per group, *P<0.05 vs. corresponding time 0, n.s, no significant difference between KO vs. WT at same time-point.

Emigration

PAF also caused a time-dependent increase in the number of cells that emigrated from the vessel into the surrounding tissues in vehicle control mice. The profile of this response is shown in figure 3.31, showing a significant increase compared to basal from 30 min onwards. In animals treated with Ac2-26 there was a significant attenuation of this increase. Numbers of emigrated cells were significantly lower in peptide treated mice compared to the vehicle control at 75 and 90 min time-points. Calculated inhibitions of 43% and 54% were obtained for the peptide Ac2-26 group at 75 and 90 min PAF superfusion. The degree of inhibition becomes even more marked if calculations are made on net values, i.e. subtracting the spontaneous emigration measured before PAF superfusion which gives a calculated inhibition of 67% and 79% respectively. Another way of assessing this event was by comparing the areas under

the curve, showing that overall the treatment with Ac2-26 causes a 35% decrease in cell emigration. It can be also be seen that the number of emigrated cells in the peptide treated animals was not increased from basal (0 min) at any of the time-points measured.

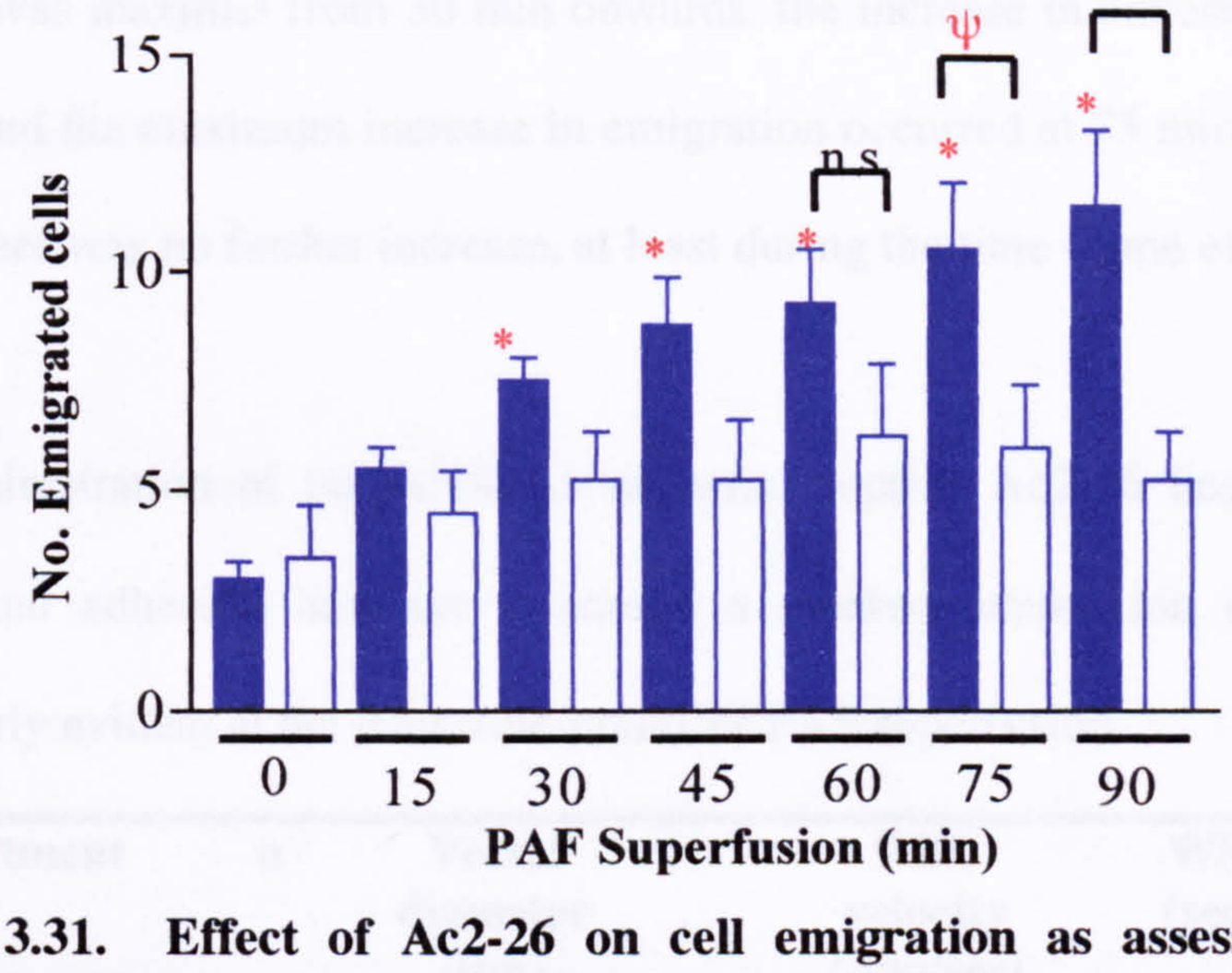

Figure 3.31. Effect of Ac2-26 on cell emigration as assessed in the inflamed cremaster muscle of C57BL/6 mice. C57BL/6 mice were prepared for intravital microscopy. Mice were treated with either PBS ■ or 200 μg Ac2-26 □ (time 0) and then superfused with 100 nM PAF. Emigration is measured as number of cells either side of 100 μm vessel. Values are mean±sem of n=4 mice per group, *P<0.05 vs. corresponding time 0, ψP<0.05 KO vs. WT mice at same time-point, n.s, no significant difference.

Haemodynamic parameters

The haemodynamic parameters measured in post-capillary venules of mice inflamed with 100 nM PAF are shown in table 3.1. Superfusion with 100 nM PAF had no significant effects on RBC velocity or WSR over the 90 min time course. The treatment of mice with Ac2-26 did not cause any significant changes to these parameters either.

Summary

The superfusion of 100 nM PAF in C57BL/6 mice caused a significant and measurable inflammation in the cremaster muscle. An effect on cell flux was not apparent, however there was a significant decrease in cell rolling velocity associated with a time-dependent increase in cell adhesion and emigration. The effect of PAF on cell rolling velocity was maximal from 30 min onwards, the increase in adhesion was maximal at 45 min and the maximum increase in emigration occurred at 75 min. After these time-points there was no further increase, at least during the time frame examined.

The administration of the ANX-A1 mimetic, peptide Ac2-26 had no effect on cell rolling and adhesion however it caused a marked attenuation of cell emigration, particularly evident at the later time-points of PAF superfusion.

Treatment	n	Vessel diameter (μm)		RBC velocity (mm/sec)	WSR (sec^{-1})
100 nM PAF + PBS (Vehicle control)	4	28.90 ± 3.39	0	2.68 ± 0.52	480 ± 92
			15	2.60 ± 0.57	457 ± 89
			30	2.55 ± 0.58	443 ± 93
			45	2.60 ± 0.63	452 ± 97
			60	2.85 ± 0.80	492 ± 122
			75	2.48 ± 0.44	435 ± 72
			90	2.33 ± 0.46	406 ± 69
100 nM PAF + Ac2-26	4	36.46 ± 2.25	0	3.85 ± 0.94	530 ± 133
			15	3.33 ± 0.54	453 ± 68
			30	3.18 ± 0.67	434 ± 91
			45	3.65 ± 0.89	496 ± 121
			60	3.23 ± 0.91	447 ± 131
			75	3.33 ± 0.88	463 ± 128
			90	2.53 ± 0.21	351 ± 37

Table 3.1. Effect of Ac2-26 on haemodynamic parameters of 100 nM PAF inflamed cremasteric venules of C57BL/6 mice. C57BL/6 mice were prepared for intravital microscopy. Mice were treated with either with either PBS (200 μl) or Ac2-26 (200 μg in 200 μl PBS) i.v. (after time 0 recording). The tissue was then superfused with 100 nM PAF. Vessel diameter and RBC velocity were measured and WSR calculated. Values are mean±sem of n=4 mice per group.

3.2.2. Effect of PAF on Leukocyte Recruitment in ANX-A1$^{-/-}$ and ANX-A1$^{+/+}$ Mice

Once it had been established that the microcirculation of the cremaster was susceptible to the effects of ANX-A1 by using the peptido-mimetic Ac2-26, then the first series of experiments were to examine leukocyte-endothelium interactions in ANX-A1$^{-/-}$ and ANX-A1$^{+/+}$ mice when no inflammatory stimulus was used. The response measured under these conditions is prompted by the trauma produced by the tissue manipulation during exposure of the cremaster muscle.

3.2.2.1. Basal leukocyte recruitment

ANX-A1$^{-/-}$ and ANX-A1$^{+/+}$ mice were prepared for intravital microscopy of the cremaster muscle. To assess basal levels of leukocyte recruitment a suitable vessel was chosen and then recorded for 90 min of the experiment. During this time the tissue was superfused with BBS to keep the conditions as physiological as possible

Rolling Velocity

Figure 3.32 shows cell rolling velocity in both the ANX-A1$^{+/+}$ and ANX-A1$^{-/-}$ mice under basal conditions. The data are presented as a percentage of basal rolling velocity. As can be clearly seen the cell rolling velocity in ANX-A1$^{+/+}$ mice was quite consistent over the time course of the experiment. The same pattern was seen in the ANX-A1$^{-/-}$ mice and the rolling velocity neither increased nor decreased significantly over the 90 min. No significant difference was seen between the two genotypes.

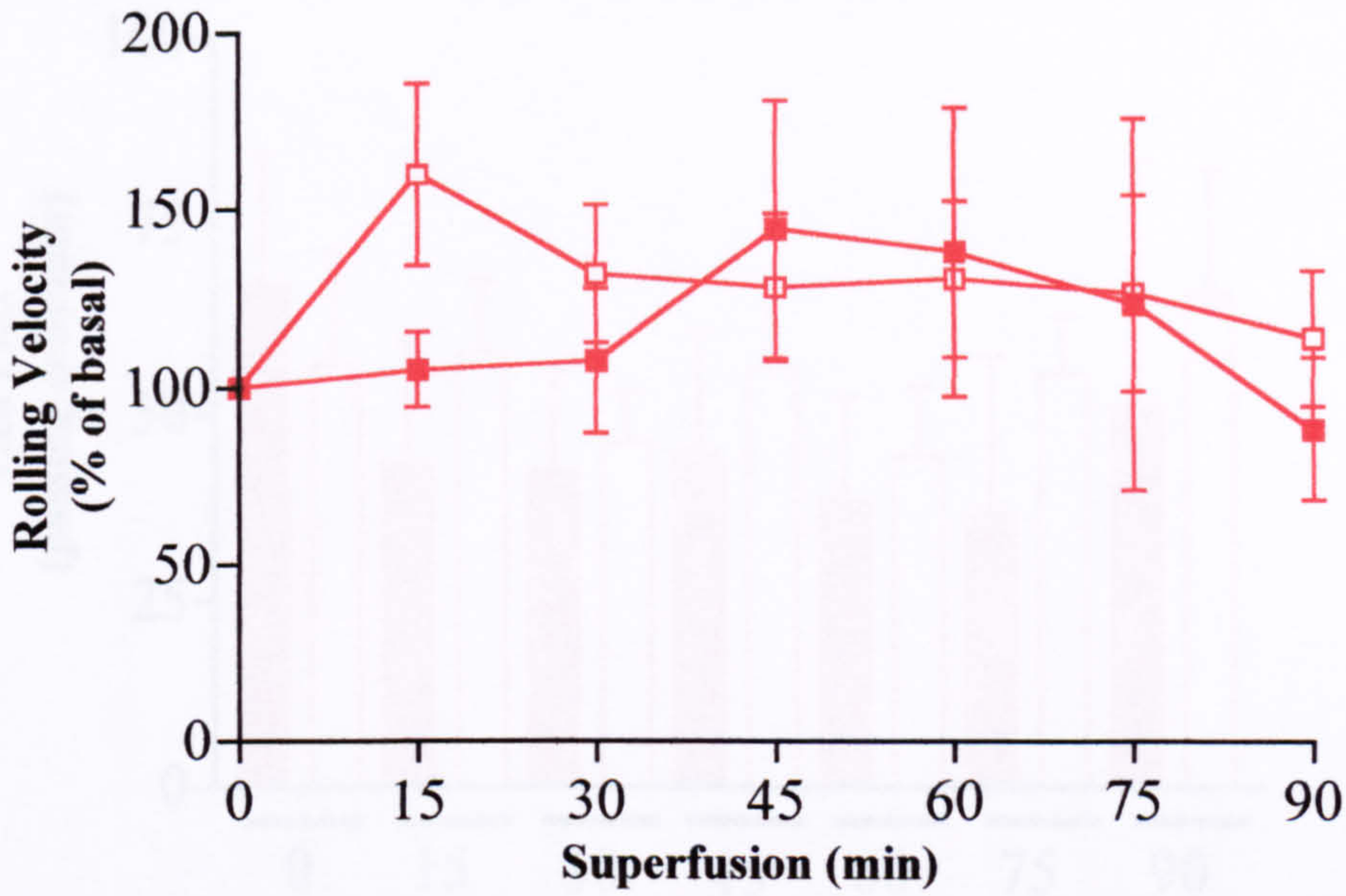

Figure 3.32. Basal cell rolling velocity as assessed in the cremaster muscle of ANX-A1$^{-/-}$ and ANX-A1$^{+/+}$ mice. ANX-A1$^{+/+}$ ■ and ANX-A1$^{-/-}$ □ mice were prepared for intravital microscopy. The tissue was superfused with BBS for 90 min. Rolling velocity is shown as % of basal rolling velocity (basal rolling velocity in ANX-A1$^{+/+}$ and ANX-A1$^{-/-}$ mice was 60±18 and 47±5 μm/sec respectively). Values are mean±sem of n=6 mice per group.

Cell Flux

Cell flux is measured as the number of cells passing a fixed point in the vessel per min. The basal cell flux in ANX-A1$^{+/+}$ and ANX-A1$^{-/-}$ mice is shown in figure 3.33. As it can be seen, the cell flux in both the ANX-A1$^{+/+}$ and the ANX-A1$^{-/-}$ mice was quite consistent over the time course of the experiment. However, the values obtained for each mouse analysed were quite variable as shown by the relatively large error bars. There was no difference in the extent of cell flux when ANX-A1$^{+/+}$ animals were compared to ANX-A1$^{-/-}$ mice at any of the time-points measured.

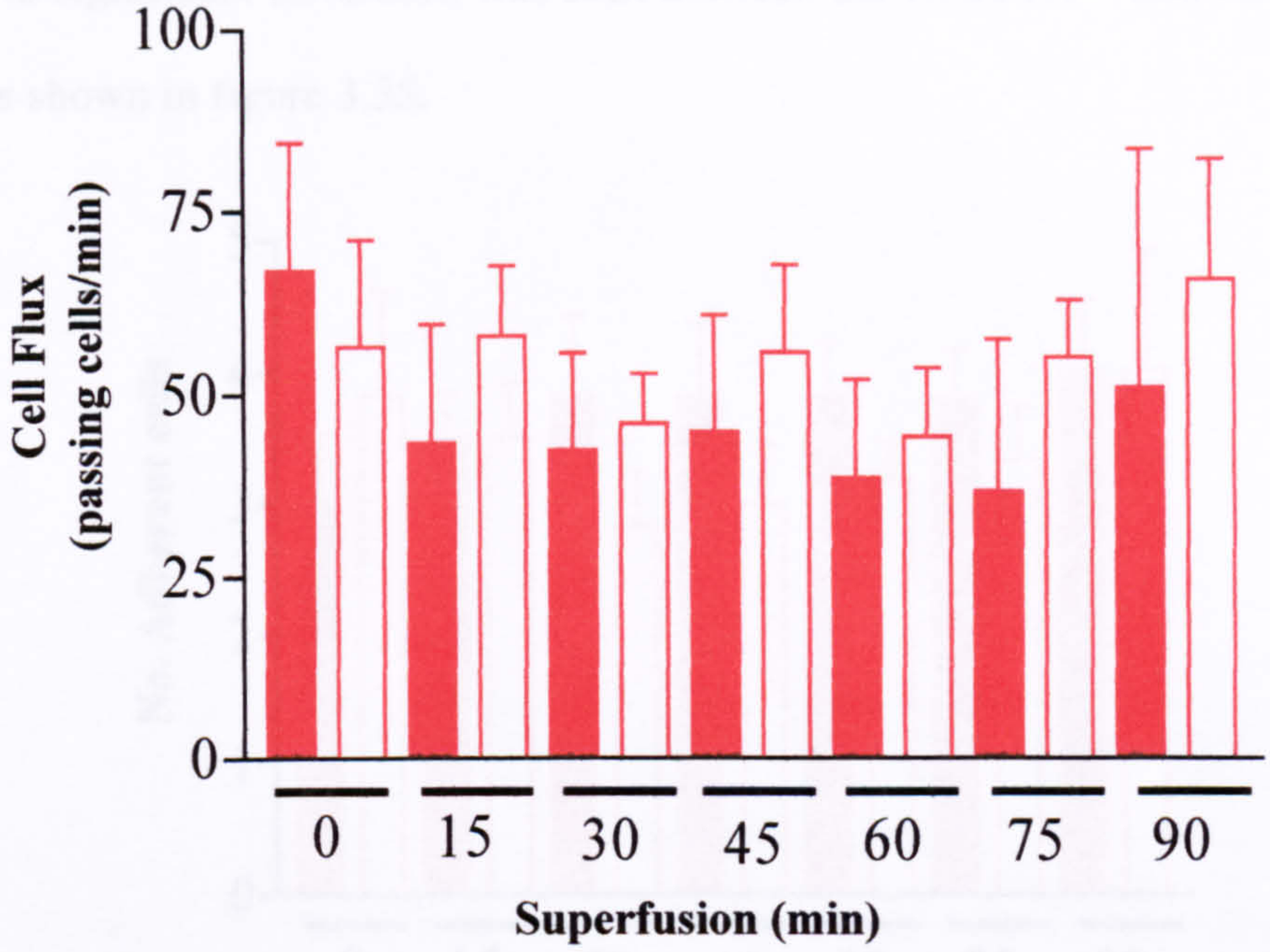

Figure 3.33. Basal cell flux as assessed in the cremaster muscle of ANX-A1$^{-/-}$ and ANX-A1$^{+/+}$ mice. ANX-A1$^{+/+}$ ■ and ANX-A1$^{-/-}$ □ mice were prepared for intravital microscopy. The tissue was superfused with BBS for 90 min. Cell flux was measured as the number of cells passing a fixed point in the vessel/min. Values are mean±sem of n=6 mice per group.

Adhesion

The basal levels of cell adhesion in the ANX-A1$^{-/-}$ and the ANX-A1$^{+/+}$ mice are shown in figure 3.34. Between 3 and 4 adherent cells were found consistently over the time course in both the ANX-A1$^{+/+}$ and ANX-A1$^{-/-}$ mice and these levels did not significantly increase or decrease over the 90 min time course. No significant difference was seen when comparing the two genotypes.

Emigration

Basal cell emigration shows a similar pattern to cell adhesion however, with a smaller proportion of emigrated cells compared to adherent cells. The number of emigrated cells was consistent over the time course in both the ANX-A1$^{+/+}$ and ANX-A1$^{-/-}$ mice.

No significant difference was seen between the ANX-A1$^{+/+}$ and ANX-A1$^{-/-}$ mice. This is shown in figure 3.35.

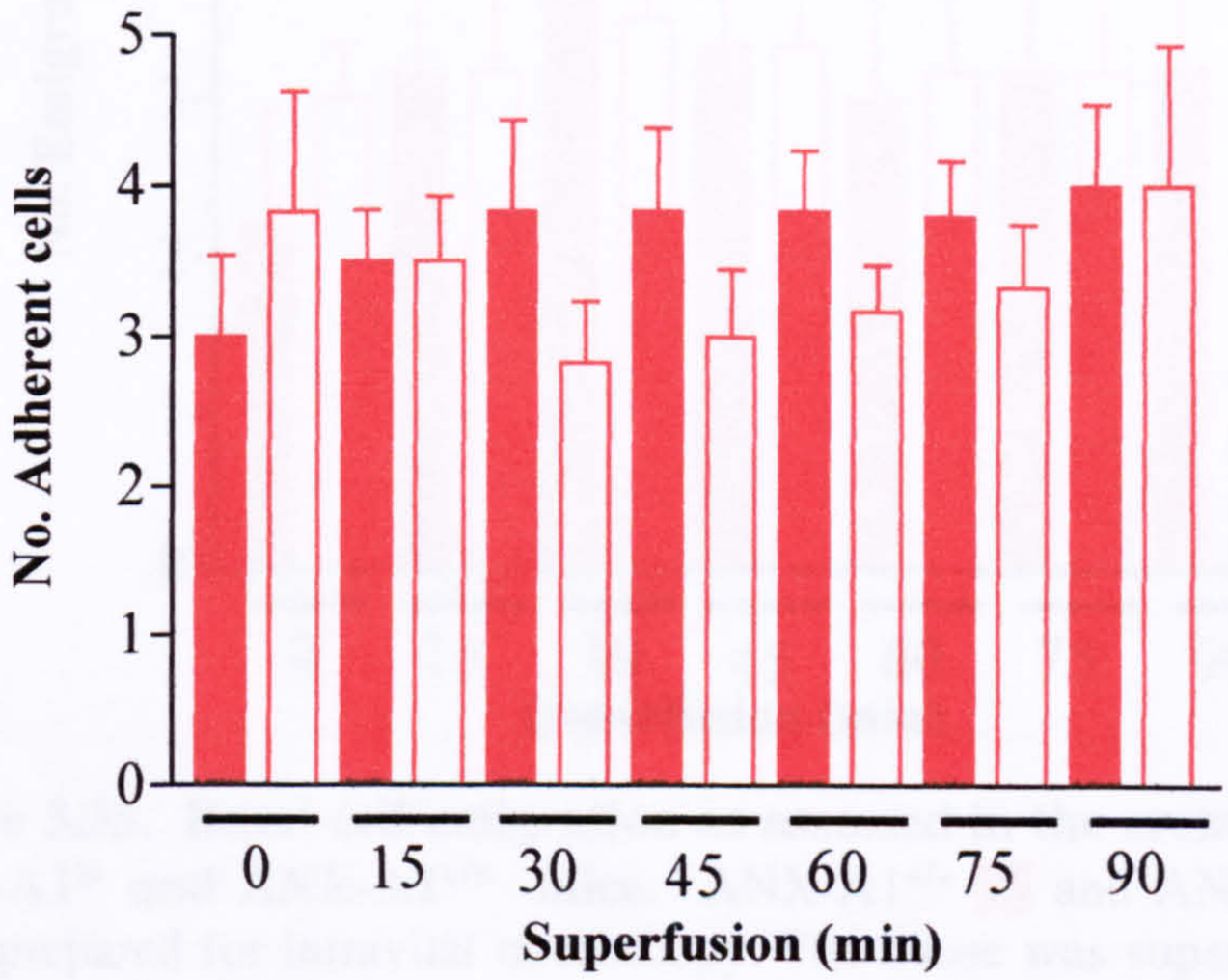

Figure 3.34. Basal cell adhesion as assessed in the cremaster muscle of ANX-A1$^{-/-}$ and ANX-A1$^{+/+}$ mice. ANX-A1$^{+/+}$ ■ and ANX-A1$^{-/-}$ □ mice were prepared for intravital microscopy. The tissue was superfused with BBS for 90 min. Adhesion is measured as number of cells stationary for >30 sec. Values are mean±sem of n=6 mice per group.

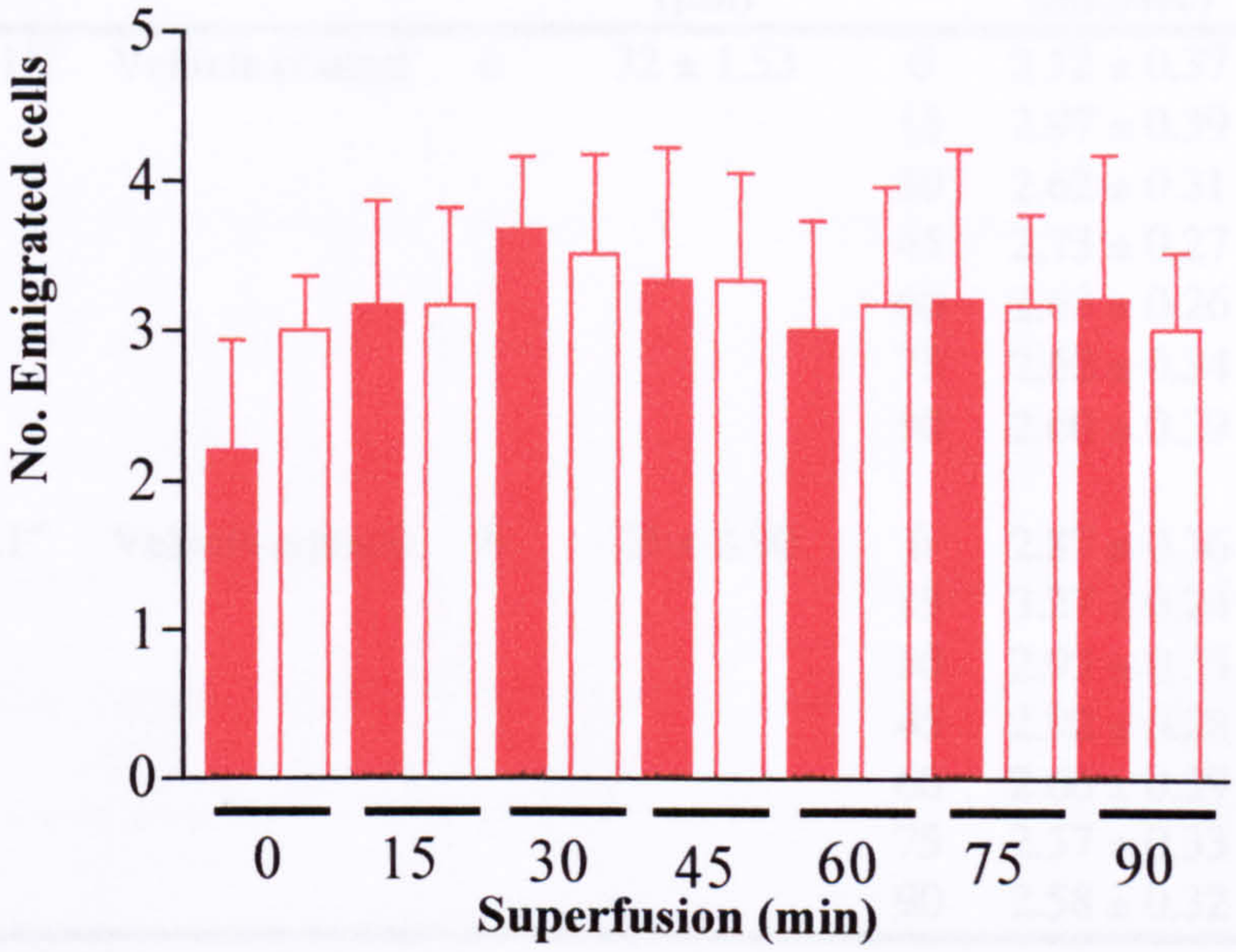

Figure 3.35. Basal cell emigration as assessed in the cremaster muscle of ANX-A1$^{-/-}$ and ANX-A1$^{+/+}$ mice. ANX-A1$^{+/+}$ ■ and ANX-A1$^{-/-}$ □ mice were prepared for intravital microscopy. The tissue was superfused with BBS for 90 min. Emigration is measured as number of cells either side of 100 μm vessel. Values are mean±sem of n=6 mice per group.

Haemodynamic parameters

The haemodynamic parameters measured in untreated post-capillary venules are shown in table 3.2. No significant differences were seen between the genotypes with respect to either RBC velocity or WSR at any of the time-points. These parameters were not significantly altered over the time course of the experiment in either the ANX-A1$^{+/+}$ or the ANX-A1$^{-/-}$ mice.

Genotype	Treatment	n	Vessel diameter (μm)		RBC velocity (mm/sec)	WSR (sec^{-1})
ANX-A1$^{+/+}$	Vehicle control	6	32 ± 1.53	0	2.52 ± 0.37	385 ± 47
				15	2.97 ± 0.39	466 ± 69
				30	2.62 ± 0.31	404 ± 42
				45	2.73 ± 0.27	425 ± 44
				60	2.63 ± 0.26	411 ± 47
				75	2.62 ± 0.34	411 ± 50
				90	2.60 ± 0.29	404 ± 36
ANX-A1$^{-/-}$	Vehicle control	6	29 ± 2.90	0	2.87 ± 0.36	496 ± 46
				15	3.27 ± 0.24	575 ± 54
				30	2.93 ± 0.35	509 ± 47
				45	2.92 ± 0.28	512 ± 40
				60	2.60 ± 0.39	440 ± 30
				75	2.57 ± 0.33	436 ± 25
				90	2.58 ± 0.32	438 ± 20

Table 3.2. Haemodynamic parameters in vehicle control (basal) cremasteric venules of ANX-A1$^{+/+}$ and ANX-A1$^{-/-}$ mice. ANX-A1$^{+/+}$ and ANX-A1$^{-/-}$ mice were prepared for intravital microscopy. The tissue was superfused with BBS for 90 min. Vessel diameter and RBC velocity were measured and WSR calculated. Values are mean±sem of n=6 per group.

Summary

When quantifying basal leukocyte recruitment in ANX-A1$^{-/-}$ and ANX-A1$^{+/+}$ a low level of cell adhesion and emigration could be measured but did not significantly increase over the 90 min time course of the experiment. Rolling velocity and cell flux were also unchanged and constant over the time course however these numbers were more variable than those obtained with cell emigration and adhesion. The preparation proved to be quite stable and apart from the initial mild activation due to tissue manipulation and maintaining the mouse on the stage produced no further activation. So, the next experiments examined the response of ANX-A1$^{-/-}$ mice to an inflammatory stimulus.

3.2.2.2. Effect of High Dose (100 nM) PAF

To examine the recruitment of leukocytes under inflammatory conditions PAF was chosen as an inflammatory stimulus. This agonist was chosen for the reasons outlined above (section 3.2.) and also because PAF is a direct acting leukocyte activator (the PAF receptor is found on blood leukocytes). This means that other cell types in the surrounding tissues (for example, tissue macrophages) should not be activated by PAF offering some degree of selectivity. Initial experiments were carried out to investigate potential defects in the leukocyte migration process due to absence of ANX-A1.

ANX-A1$^{-/-}$ and ANX-A1$^{+/+}$ mice were prepared for intravital microscopy of the cremaster muscle. A suitable vessel was chosen, superfused with a 100 nM PAF solution, and then recorded for 90 min of the experiment to assess leukocyte recruitment under inflammatory conditions.

Rolling Velocity Figure 3.36 shows the rolling velocity in ANX-A1$^{-/-}$ and ANX-A1$^{+/+}$ mice during 90 min of 100 nM PAF superfusion. The data are presented as a percentage of the basal rolling velocity (time 0). The ANX-A1$^{+/+}$ mice showed a significant decrease in cell rolling velocity over the time course which was significant from 30 min onwards. In the ANX-A1$^{-/-}$ mice, the rolling velocity also decreased. This was significant from 15 min onwards. No significant differences were found between the ANX-A1$^{+/+}$ and the ANX-A1$^{-/-}$ animals at any of the time-points examined.

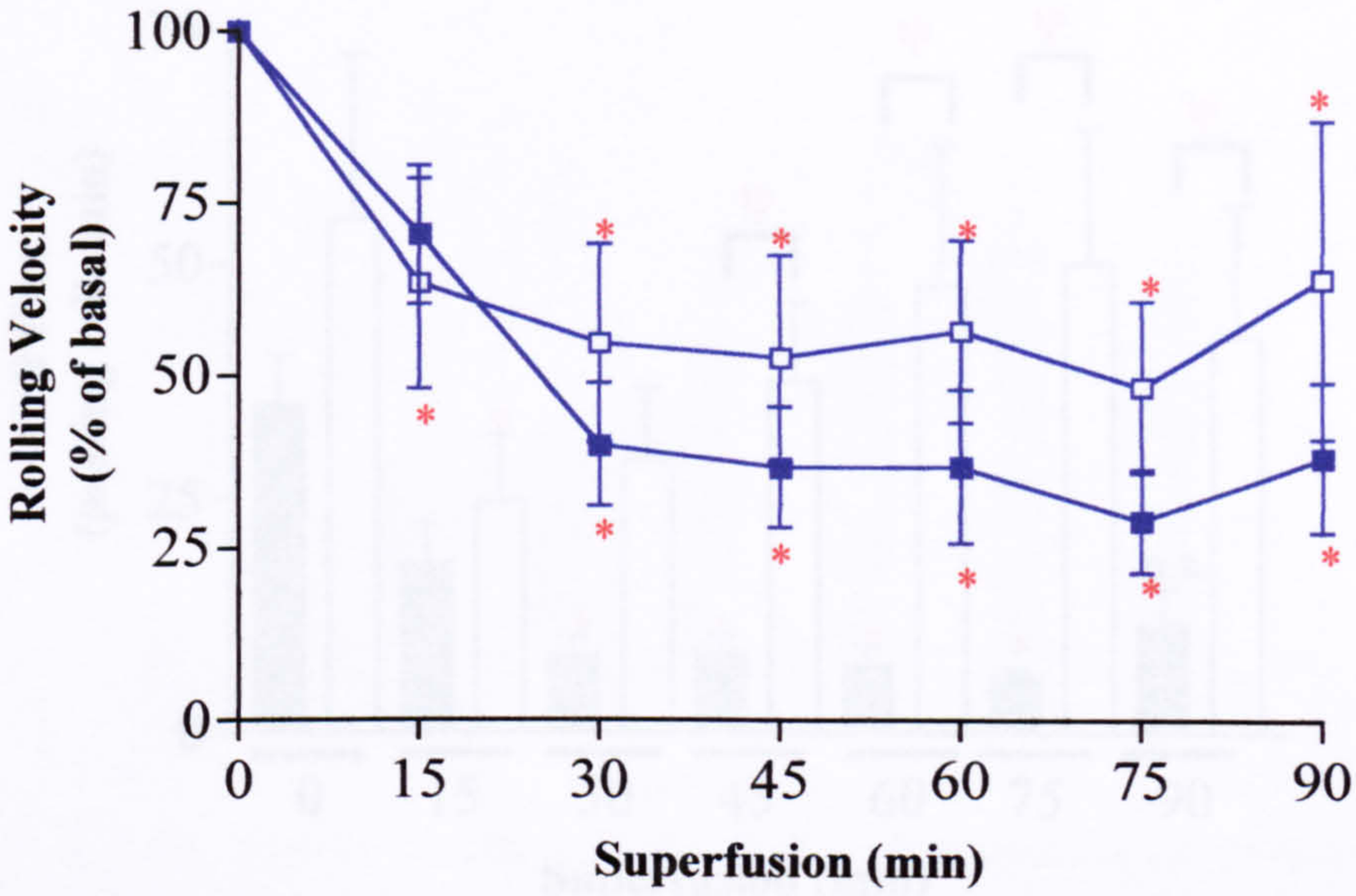

Figure 3.36. Effect of 100 nM PAF on cell rolling velocity as assessed in the cremaster muscle of ANX-A1$^{-/-}$ and ANX-A1$^{+/+}$ mice. ANX-A1$^{+/+}$ ■ and ANX-A1$^{-/-}$ □ mice were prepared for intravital microscopy. The tissue was superfused with 100 nM PAF for 90 min. Rolling velocity is shown as % of basal rolling velocity (basal rolling velocity in ANX-A1$^{+/+}$ and ANX-A1$^{-/-}$ mice was 60±16 and 73±11 μm/sec respectively). Values are mean±sem of n=6 mice per group, *P<0.05 vs. corresponding time 0.

Cell Flux

Cell flux in 100 nM PAF inflamed cremaster muscles of ANX-A1$^{-/-}$ and ANX-A1$^{+/+}$ mice is shown in figure 3.37. In the ANX-A1$^{+/+}$ mice a similar pattern to rolling velocity findings was seen, that is, a significant decrease in cell flux was measured over the time course which became significantly different from basal (0 min) from 30 min onwards (although it slightly increases again at 90 min). In the ANX-A1$^{-/-}$ animals the cell flux does not follow the same pattern as the ANX-A1$^{+/+}$ mice. Although the cell flux decreased significantly at 15 min it then increased again. It remained variable over the time course and was not significantly different from basal for the duration of the experiment. The cell flux was significantly different in the ANX-A1$^{-/-}$ animals compared to the ANX-A1$^{+/+}$ animals at 45, 60 and 75 and 90 min.

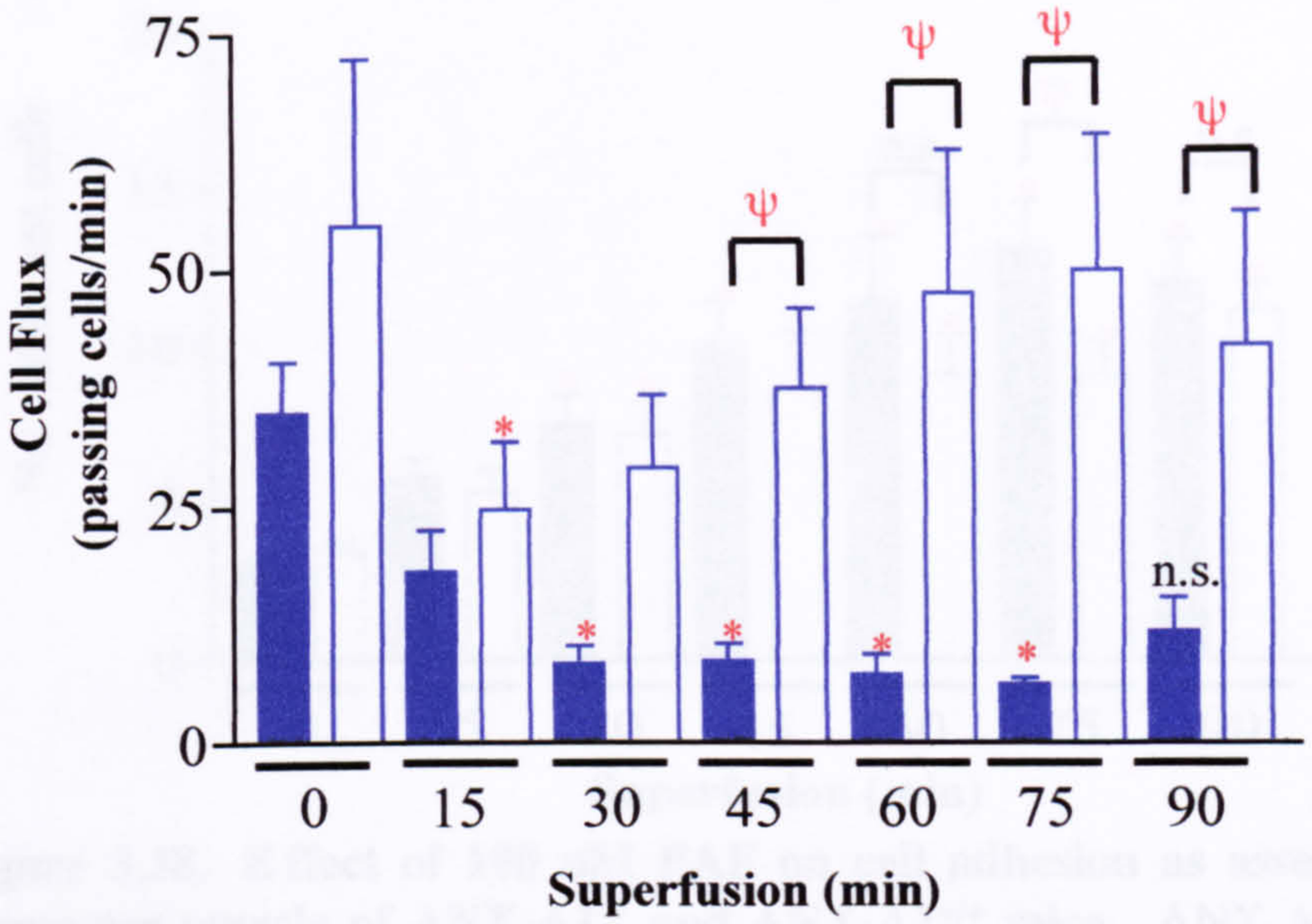

Figure 3.37. E ffect of 100 nM PAF on cell flux as assessed in the cremaster muscle of ANX-A1$^{-/-}$ and ANX-A1$^{+/+}$ mice. ANX-A1$^{+/+}$ ■ and ANX-A1$^{-/-}$ □ mice were prepared for intravital microscopy. The tissue was superfused with 100 nM PAF for 90 min. Cell flux was measured as the number of cells passing a fixed point in the vessel/min. Values are mean±sem of n=6 mice per group, *P<0.05 vs. corresponding time 0, ψP<0.05 ANX-A1$^{-/-}$ vs. ANX-A1$^{+/+}$ at same time-point, ns, no significant difference.

Adhesion

Adhesion of leukocytes induced by 100 nM PAF is shown in figure 3.38. In the ANX-A1$^{+/+}$ mice cell adhesion increased in a time-dependent manner. There were significantly higher numbers of adherent cells compared to basal (0 min) from 30 min onwards. A similar PAF induced time-dependent increase in cell adhesion was observed in the ANX-A1$^{-/-}$ mice which was also significant from 30 min onwards. No significant difference was calculated between the ANX-A1$^{+/+}$ and the ANX-A1$^{-/-}$ animals except at the 75 min time-point where significantly higher cell adhesion was attained in the ANX-A1$^{+/+}$ compared to the ANX-A1$^{-/-}$ mice (75 min; ANX-A1$^{+/+}$: 13.00±1.53 vs. ANX-A1$^{-/-}$: 9.00±1.10, n=6, P<0.05).

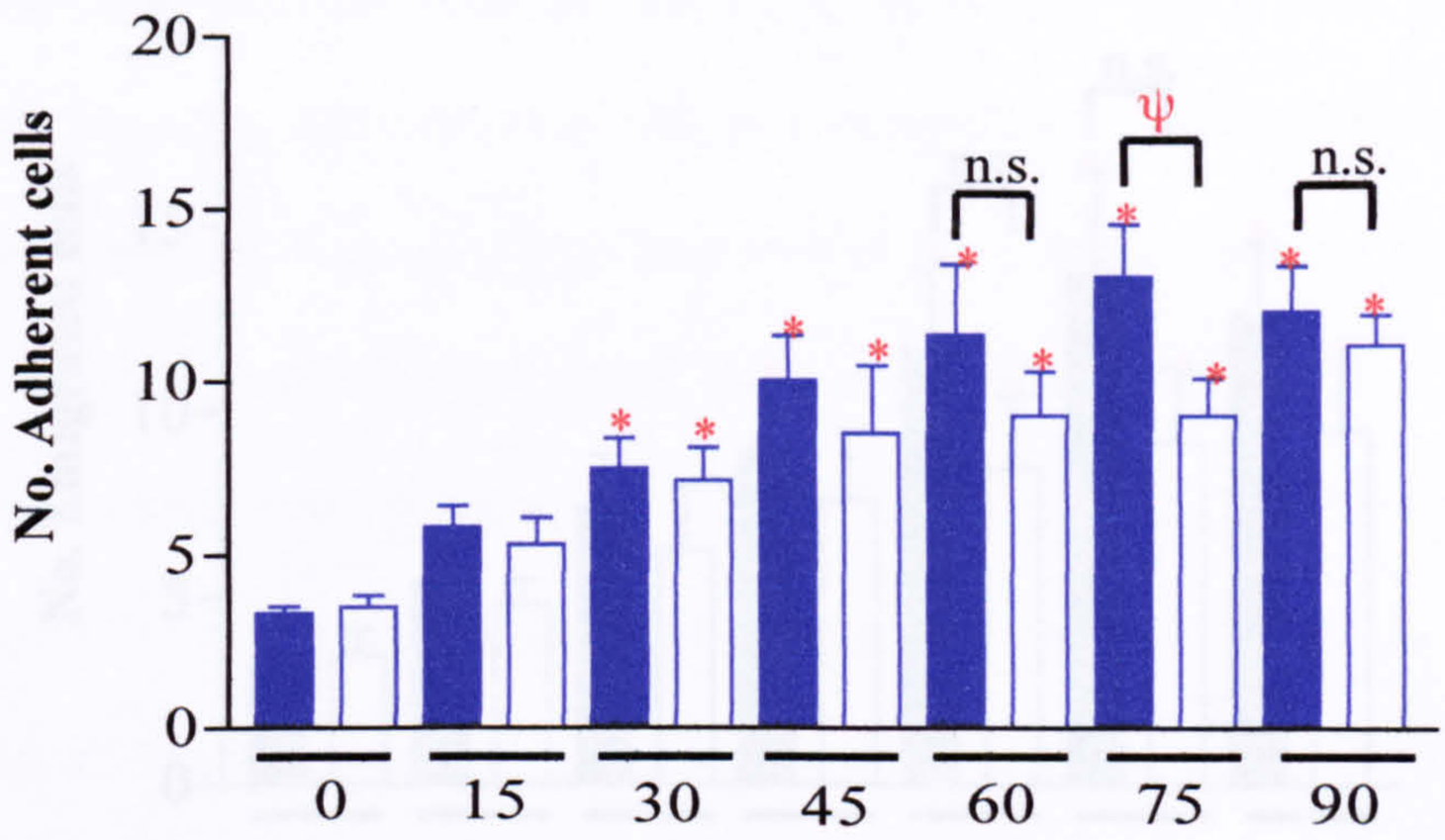

Figure 3.38. Effect of 100 nM PAF on cell adhesion as assessed in the cremaster muscle of ANX-A1$^{-/-}$ and ANX-A1$^{+/+}$ mice. ANX-A1$^{+/+}$ ■ and ANX-A1$^{-/-}$ □ mice were prepared for intravital microscopy. The tissue was superfused with 100 nM PAF for 90 min. Adhesion is measured as number of cells stationary for >30 sec. Values are mean±sem of n=6 mice per group, *P<0.05 vs. corresponding time 0, ψP<0.05 ANX-A1$^{-/-}$ vs. ANX-A1$^{+/+}$ at same time-point, n.s, no significant difference.

Emigration

Following PAF superfusion cell emigration increased significantly in a time-dependent manner in both the ANX-A1$^{+/+}$ and the ANX-A1$^{-/-}$ mice. In the ANX-A1$^{+/+}$ animals this was significant from 45 min and in the ANX-A1$^{-/-}$ mice from 60 min. Emigration shows a very similar pattern to that found with cell adhesion, that is, with no difference seen between the genotypes throughout the time course. At the later time-points (60, 75 and 90 min) consistently lower emigration was found in the ANX-A1$^{-/-}$ mice however this did not reach statistical significance at the 5% level. This is shown in figure 3.39.

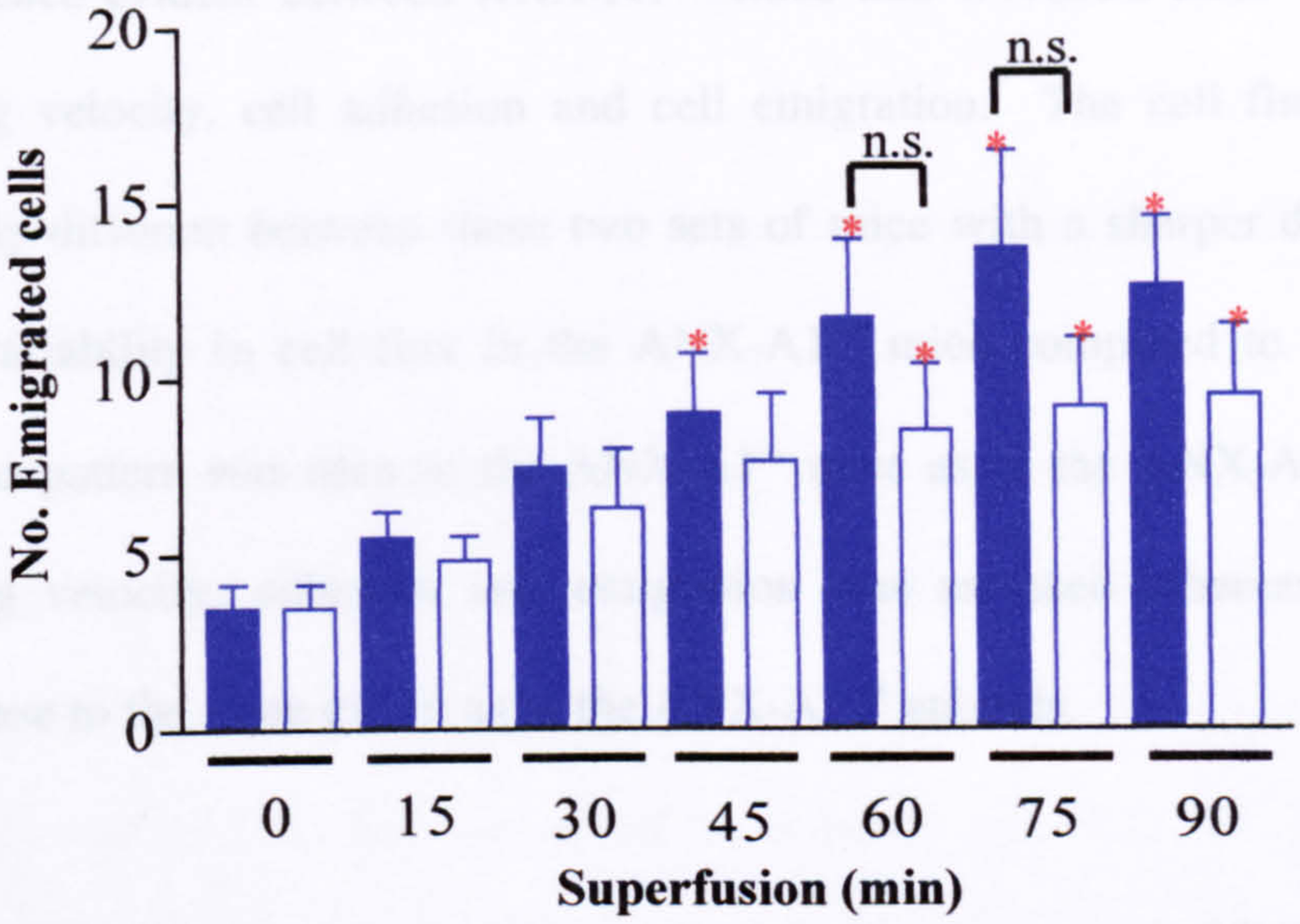

Figure 3.39. Effect of 100 nM PAF on cell emigration as assessed in the cremaster muscle of ANX-A1$^{-/-}$ and ANX-A1$^{+/+}$ mice. ANX-A1$^{+/+}$ ■ and ANX-A1$^{-/-}$ □ mice were prepared for intravital microscopy of the cremaster muscle. The tissue was superfused with 100 nM PAF for 90 min. Emigration is measured as number of cells either side of 100 μm vessel. Values are mean±sem of n=6 mice per group, *P<0.05 vs. corresponding time 0, n.s, no significant difference between ANX-A1$^{-/-}$ vs. ANX-A1$^{+/+}$ at same time-point.

Haemodynamic parameters

The haemodynamic parameters measured in post-capillary venules inflamed with 100 nM PAF are shown in table 3.3. RBC velocity and WSR were not significantly altered over the time course of the experiment in either the ANX-A1$^{+/+}$ or the ANX-A1$^{-/-}$ mice. No significant differences were seen between the genotypes with respect to either RBC velocity or WSR at any of the time-points measured.

Summary

When the cremaster microcirculation of ANX-A1$^{+/+}$ mice was activated with 100 nM PAF over a 90 min time course, there was significantly decreased cell rolling velocity and cell flux and increased cell adhesion and cell emigration. The data are essentially similar to those obtained in C57BL/6 mice as described in section 3.1 with no

difference evident between ANX-A1$^{+/+}$ mice and C57BL/6 mice with respect to cell rolling velocity, cell adhesion and cell emigration. The cell flux was found to be slightly different between these two sets of mice with a sharper decrease in flux and less variability in cell flux in the ANX-A1$^{+/+}$ mice compared to C57BL/6 mice. A similar pattern was seen in the ANX-A1$^{-/-}$ mice as in the ANX-A1$^{+/+}$ mice when cell rolling velocity, adhesion and emigration was assessed whereas cell flux did not decrease to the same extent as in the ANX-A1$^{+/+}$ animals.

Significant differences were not seen between the genotypes with respect to cell rolling velocity, adhesion or flux however, at the later time-points of the experiment there was significantly higher cell flux in the ANX-A1$^{-/-}$ mice compared to the ANX-A1$^{+/+}$ mice.

Genotype	Treatment	n	Vessel diameter (μm)		RBC velocity (mm/sec)	WSR (sec^{-1})
ANX-A1$^{+/+}$	100 nM PAF	6	32 ± 0.94	0	3.07 ± 0.44	488 ± 78
				15	2.53 ± 0.26	406 ± 51
				30	2.73 ± 0.27	432 ± 53
				45	2.92 ± 0.32	467 ± 64
				60	2.38 ± 0.23	378 ± 43
				75	2.70 ± 0.19	427 ± 42
				90	2.66 ± 0.26	408 ± 50
ANX-A1$^{-/-}$	100 nM PAF	6	35 ± 1.77	0	4.30 ± 0.73	603 ± 82
				15	3.70 ± 0.56	518 ± 56
				30	4.07 ± 0.75	566 ± 81
				45	3.63 ± 0.43	511 ± 43
				60	3.30 ± 0.30	466 ± 26
				75	3.60 ± 0.54	502 ± 53
				90	3.15 ± 0.55	455 ± 76

Table 3.3. Haemodynamic parameters of 100 nM PAF inflamed cremasteric venules of ANX-A1$^{+/+}$ and ANX-A1$^{-/-}$ mice. ANX-A1$^{+/+}$ and ANX-A1$^{-/-}$ mice were prepared for intravital microscopy of the cremaster muscle. The tissue was superfused with 100 nM PAF for 90 min. Vessel diameter and RBC velocity were measured and WSR calculated. Values are mean±sem of n=6 mice per group.

3.2.2.3. Effect of Low Dose (1 nM) PAF

In preliminary studies carried out in our department in parallel to these *in vivo* experiments, cells taken from ANX-A1$^{-/-}$ mice were more susceptible to *in vitro* activation when a low concentration of PAF was used, namely 1 nM. Therefore investigations using this lower dose of PAF in the cremaster preparation were carried out in order to highlight any potential changes between the genotypes. The experiments were carried out as before however this time the microcirculation was superfused with 1 nM PAF for up to 90 min.

Rolling Velocity

Figure 3.40 shows rolling velocity in ANX-A1$^{-/-}$ and ANX-A1$^{+/+}$ mice after treatment with 1 nM PAF. The data are presented as a percentage of basal cell rolling velocity (at time 0). The lower concentration of PAF (1 nM) was unable to significantly reduce cell rolling velocity in the ANX-A1$^{+/+}$ mouse as it did in the case with 100 nM PAF (see figure 3.36). A similar pattern was seen in the ANX-A1$^{-/-}$ mice at the start of superfusion, however at the later time-points (75 and 90 min) the rolling velocity was reduced significantly compared to basal. Thus, using the lower dose of PAF, a difference due to absence of the ANX-A1 gene began to emerge.

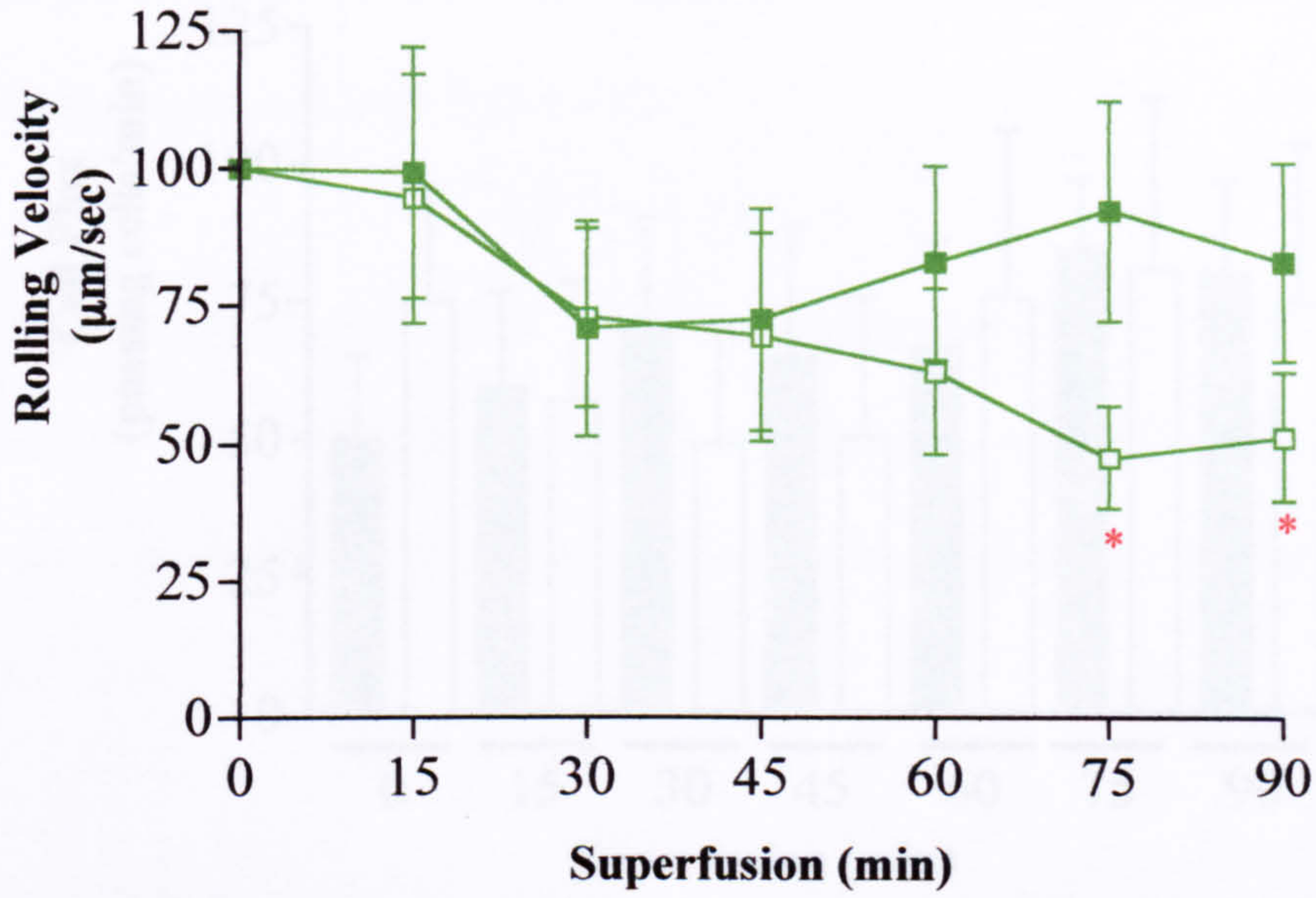

Figure 3.40. Effect of 1 nM PAF on cell rolling velocity as assessed in the cremaster muscle of ANX-A1$^{-/-}$ and ANX-A1$^{+/+}$ mice. ANX-A1$^{+/+}$ ■ and ANX-A1$^{-/-}$ □ mice were prepared for intravital microscopy. The tissue was superfused with 1 nM PAF for 90 min. Rolling velocity is shown as % of basal rolling velocity (basal rolling velocity in ANX-A1$^{+/+}$ and ANX-A1$^{-/-}$ mice was 50±15 and 75±20 µm/sec respectively). Values are mean±sem of n=6 mice per group, *P<0.05 vs. corresponding time 0.

Cell Flux

The values for cell flux measured during superfusion with 1 nM PAF is shown in figure 3.41. In contrast to the results obtained in ANX-A1$^{+/+}$ mice treated with 100 nM PAF (figure 3.37), superfusion with 1 nM PAF did not modify the cell flux over the 90 min treatment. The same holds true for the ANX-A1$^{-/-}$ mice though in this case this was not very different to the cell flux produced by 100 nM PAF treatment.

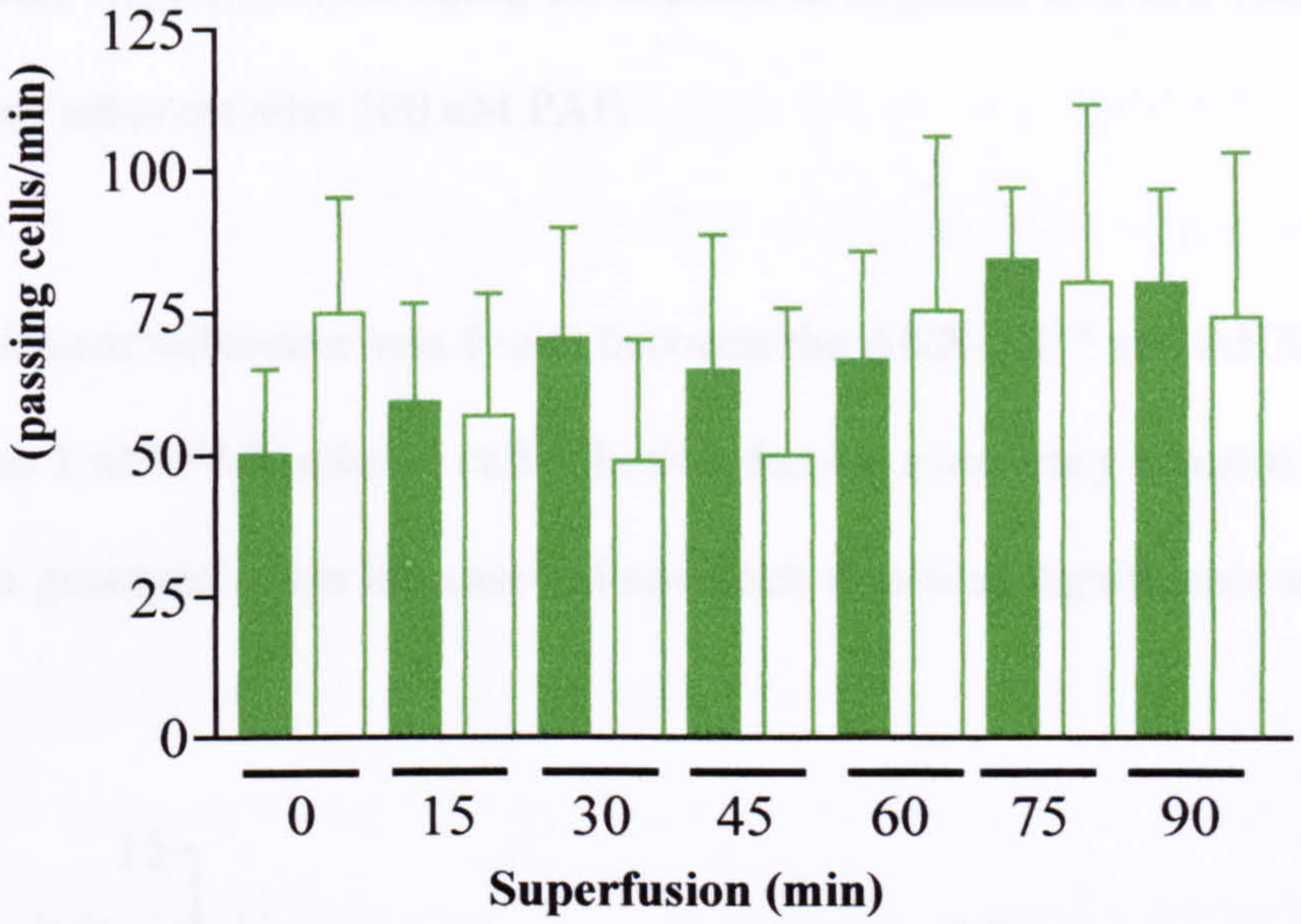

Figure 3.41. Effect of 1 nM PAF on cell flux as assessed in the cremaster muscle of ANX-A1$^{-/-}$ and ANX-A1$^{+/+}$ mice. ANX-A1$^{+/+}$ ■ and ANX-A1$^{-/-}$ □ mice were prepared for intravital microscopy. The tissue was superfused with 1 nM PAF for 90 min. Cell flux was measured as the number of cells passing a fixed point in the vessel/min. Values are mean±sem of n=6 mice per group.

Adhesion

The cell adhesion induced by 1 nM PAF is shown in figure 3.42. In ANX-A1$^{+/+}$ mice there was a time-dependent increase in cell adhesion over the time course which follows the profile obtained with the higher concentration of PAF, with a significant increase from 45 min onwards. However, it must be noted that lower numbers of adherent cells were found with 1 nM PAF compared to 100 nM PAF. For instance, at the 60 min time-point, 7.00±0.45 adherent cells were found in response to 1 nM PAF whereas 11.33±2.03 cells were found in response to 100 nM PAF (see figures 3.38 and 3.42). ANX-A1$^{-/-}$ mice also showed a time-dependent increase in cell adhesion over 90 min which was significantly different to time 0 from 30 min onwards. This is similar to the response to 100 nM PAF. However, in contrast to the ANX-A1$^{+/+}$ mice, emigration was not reduced in response to the lower dose of PAF. As an example, at the 60 min

time-point, 7.83±1.33 cells could be counted in response to 1 nM PAF and 9.00±1.27 cells were adherent after 100 nM PAF.

No significant difference was found between the ANX-A1$^{+/+}$ and ANX-A1$^{-/-}$ mice with respect to 1 nM PAF induced cell adhesion despite a tendency towards higher values in the latter genotype. This increase did not reach statistical significance at the 5% level.

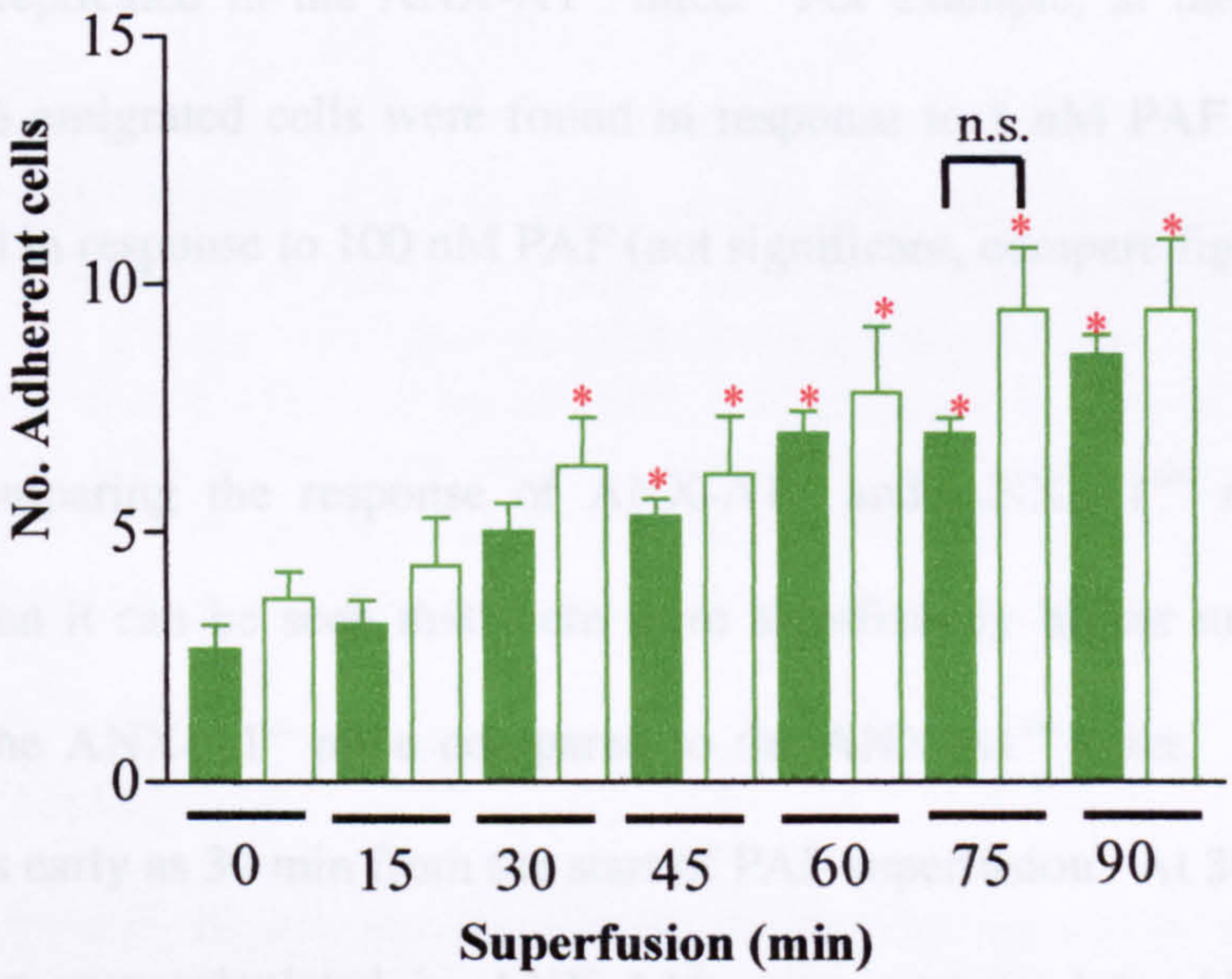

Figure 3.42. Effect of 1 nM PAF on cell adhesion as assessed in the cremaster muscle of ANX-A1$^{-/-}$ and ANX-A1$^{+/+}$ mice. ANX-A1$^{+/+}$ ■ and ANX-A1$^{-/-}$ □ mice were prepared for intravital microscopy. The tissue was superfused with 1 nM PAF for 90 min. Adhesion is measured as number of cells stationary for >30 sec. Values are mean±sem of n=6 mice per group, *P<0.05 vs. corresponding time 0, n.s, no significant difference between ANX-A1$^{-/-}$ vs. ANX-A1$^{+/+}$ at same time-point.

Emigration

Figure 3.43 reports the effect of 1 nM PAF on leukocyte emigration in ANX-A1$^{-/-}$ and ANX-A1$^{+/+}$ mice. Again, there was a time-dependent increase in cell emigration in both ANX-A1$^{+/+}$ and ANX-A1$^{-/-}$ mice. In the ANX-A1$^{+/+}$ there was significantly higher numbers of cells (compared to basal) from 30 min onwards. The numbers of emigrated

cells were significantly lower than those found to be emigrating in response to 100 nM PAF. For instance, at the 60 min time-point 5.00±0.45 emigrated cells were found in response to 1 nM PAF whereas 11.67±2.23 cells were counted in response to 100 nM PAF. In the case of the ANX-A1$^{-/-}$ animals, there was also a time-dependent increase in cell emigration in response to 1 nM PAF and this was significant from 15 min onwards. As was found in the case of cell adhesion, although the ANX-A1$^{+/+}$ mice showed a significantly lower degree of cell emigration in response to the lower dose of PAF this was not replicated in the ANX-A1$^{-/-}$ mice. For example, at the 60 min time-point, 7.50±0.56 emigrated cells were found in response to 1 nM PAF and 8.50±1.88 cells emigrated in response to 100 nM PAF (not significant, compare figure 3.39 and 3.43).

When comparing the response of ANX-A1$^{-/-}$ and ANX-A1$^{+/+}$ mice to 1 nM PAF superfusion it can be seen that there were significantly higher numbers of emigrated cells in the ANX-A1$^{-/-}$ mice compared to the ANX-A1$^{+/+}$ mice. This difference was evident as early as 30 min from the start of PAF superfusion. At 30 min 46% more cell emigration was calculated in ANX-A1$^{-/-}$ mice compared to ANX-A1$^{+/+}$ mice, this difference increases to over 50% more cell emigration in the ANX-A1$^{-/-}$ mice at the 60 min time-point. When comparisons were made on net values (subtracting the spontaneous emigration measured before PAF superfusion) the greater extent of emigration in the ANX-A1$^{-/-}$ mice becomes even more evident, for example, at 30 min, 75% more cell emigration was measured in the ANX-A1$^{-/-}$ mice compared to the ANX-A1$^{+/+}$ mice. When comparing the total overall increase in cell emigration, by examining area under the curve, 39% higher emigration could be calculated in ANX-A1$^{-/-}$ mice compared to ANX-A1$^{+/+}$ mice.

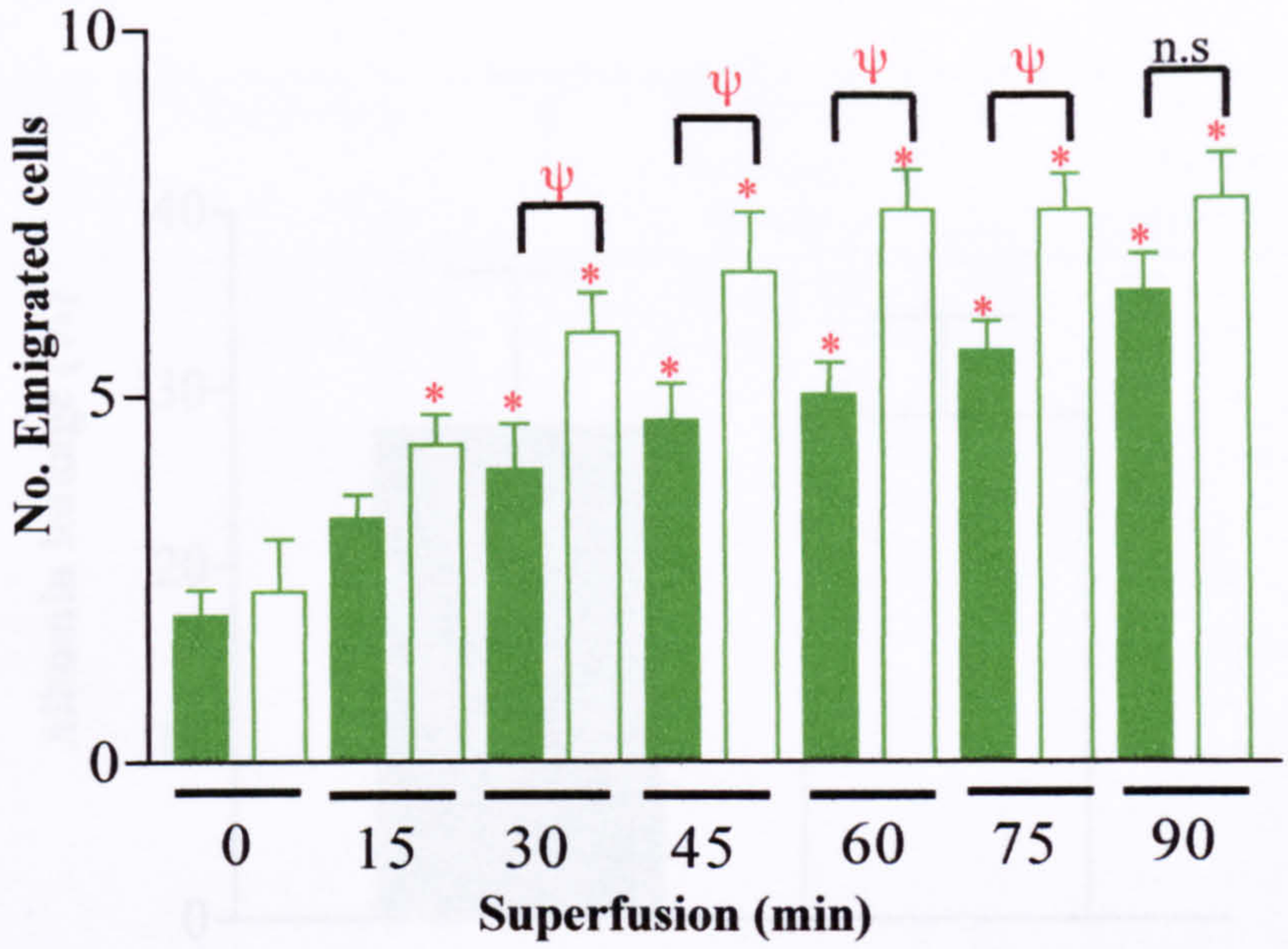

Figure 3.43. Effect of 1 nM PAF on cell emigration as assessed in the cremaster muscle of ANX-A1$^{-/-}$ and ANX-A1$^{+/+}$ mice. ANX-A1$^{+/+}$ ■ and ANX-A1$^{-/-}$ □ mice were prepared for intravital microscopy. The tissue was superfused with 1 nM PAF for 90 min. Emigration is measured as number of cells either side of 100 μm vessel. Values are mean±sem of n=6 mice per group, *P<0.05 vs. corresponding time 0, ψP<0.05 ANX-A1$^{-/-}$ vs. ANX-A1$^{+/+}$ at same time-point, n.s, no significant difference.

Albumin Leakage

As a significantly higher number of cells emigrated at 45 and 60 min in the ANX-A1$^{-/-}$ mice in response to 1 nM PAF compared to ANX-A1$^{+/+}$ mice, this later time-point was chosen to examine leakage of albumin into the surrounding tissue. Animals superfused with 1 nM PAF for 60 min were injected with FITC labelled albumin, and after 5 min a vessel was recorded for later analysis of albumin leakage. No significant difference in fluorescence leakage was found between the ANX-A1$^{+/+}$ and ANX-A1$^{-/-}$ mice and this is shown in figure 3.44.

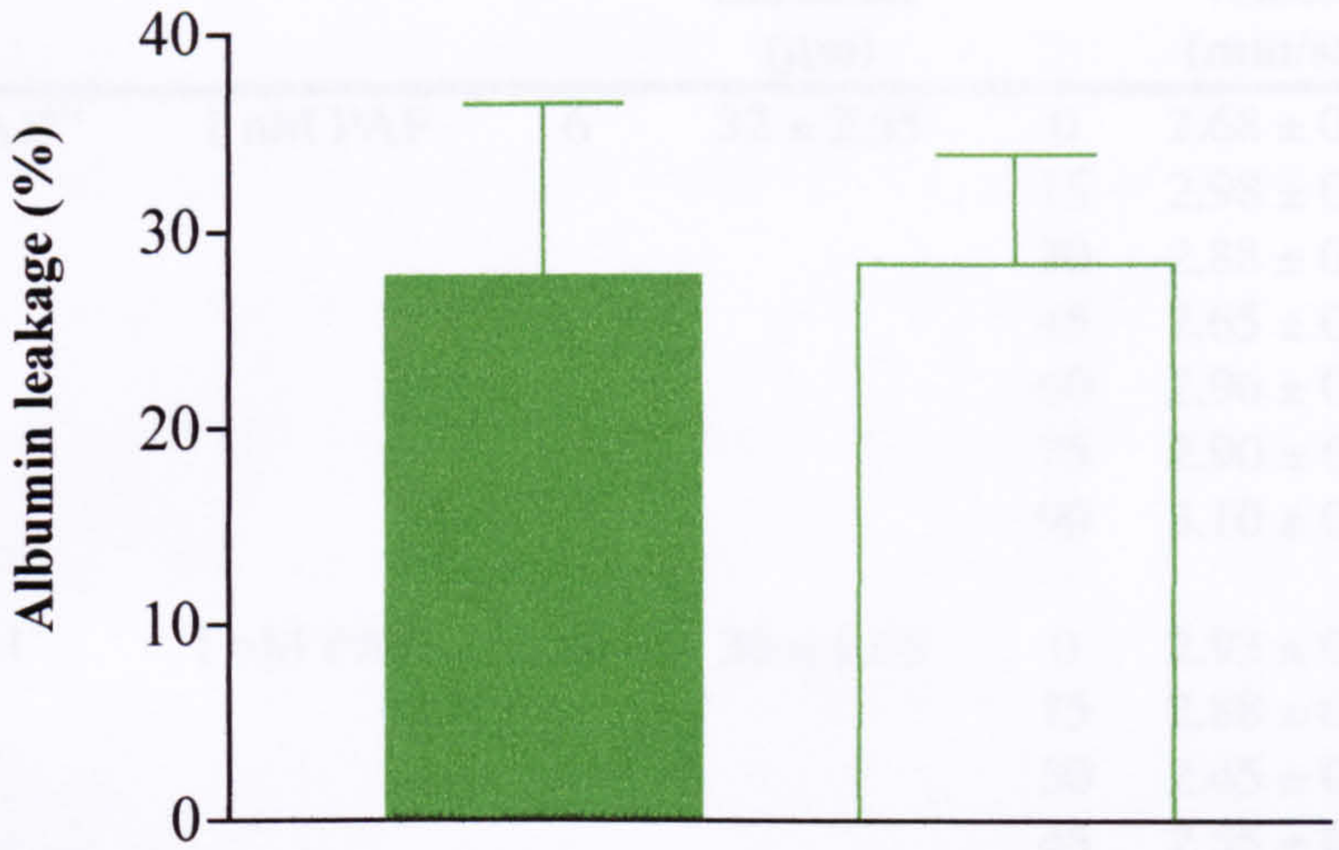

Figure 3.44. Effect of 1 nM PAF on albumin leakage as assessed in the cremaster muscle of ANX-A1$^{-/-}$ and ANX-A1$^{+/+}$ mice. ANX-A1$^{+/+}$ ■ and ANX-A1$^{-/-}$ □ mice were prepared for intravital microscopy of the cremaster muscle. The tissue was superfused with 1 nM PAF for 60 min. At 60 min FITC labelled albumin was injected 5 min prior to analysis of albumin leakage. Values are mean±sem of n=4-5 mice per group.

Haemodynamic parameters

The haemodynamic parameters were measured in post-capillary venules treated with 1 nM PAF and are shown in table 3.4. No significant differences were seen between the genotypes with respect to either RBC velocity or WSR at any of the time-points. These parameters were not significantly altered over the time course of the experiment in either the ANX-A1$^{+/+}$ or the ANX-A1$^{-/-}$ mice.

Genotype	Treatment	n	Vessel diameter (μm)		RBC velocity (mm/sec)	WSR (sec^{-1})
ANX-A1$^{+/+}$	1 nM PAF	6	32 ± 2.55	0	2.68 ± 0.35	432 ± 37
				15	2.98 ± 0.31	497 ± 61
				30	2.88 ± 0.34	474 ± 51
				45	2.65 ± 0.36	425 ± 44
				60	2.96 ± 0.28	459 ± 55
				75	2.90 ± 0.35	444 ± 46
				90	3.10 ± 0.52	467 ± 64
ANX-A1$^{-/-}$	1 nM PAF	6	30 ± 1.65	0	2.93 ± 0.34	492 ± 46
				15	2.88 ± 0.39	481 ± 50
				30	2.45 ± 0.32	419 ± 57
				45	2.55 ± 0.34	439 ± 63
				60	2.48 ± 0.34	425 ± 61
				75	2.48 ± 0.32	420 ± 51
				90	2.57 ± 0.36	432 ± 56

Table 3.4. Haemodynamic parameters in 1 nM PAF inflamed cremasteric venules of ANX-A1$^{+/+}$ and ANX-A1$^{-/-}$ mice. ANX-A1$^{+/+}$ and ANX-A1$^{-/-}$ mice were prepared for intravital microscopy. The tissue was superfused with 1 nM PAF for 90 min. Vessel diameter and RBC velocity were measured and WSR calculated. Values are mean±sem of n=6 mice per group.

Summary

In the ANX-A1$^{+/+}$ mouse superfusion with 1 nM PAF seemed to be unable to produce significant changes in cell rolling and cell flux however the numbers of adherent and emigrated cells did increase in a time-dependent manner over the 90 min time course. Although the adhesion and emigration response to 1 nM PAF was significant it was not as marked as when mice were treated with the high dose, 100nM, of PAF showing that the response was also concentration-dependent.

When examining cell rolling velocities in ANX-A1$^{-/-}$ mice a slight effect could be noted which was evident at the later time-points. This indicates that a difference due to the

absence of the ANX-A1 gene was now beginning to emerge. A time-dependent increase in cell adhesion and emigration was produced but in contrast to the ANX-A1$^{+/+}$ mice these responses were not reduced versions of the 100 nM PAF response. Cell adhesion and emigration was much higher after 1 nM PAF treatment, so much so that differences were not found between the 1 nM and 100 nM PAF superfused ANX-A1$^{-/-}$ animals. Due to this a significantly higher degree of cell emigration was observed in the ANX-A1$^{-/-}$ mice compared to the ANX-A1$^{+/+}$ mice. A role for ANX-A1 is now emerging in this more moderate model of inflammation.

3.2.2.4. Effect of 1 nM PAF on Leukocyte Recruitment: Cell Detachment Study

Experiments using 1 nM PAF had shown that leukocyte emigration was greater in ANX-A1$^{-/-}$ mice compared to ANX-A1$^{+/+}$ mice but that cell adhesion was not significantly affected. This may suggest an effect of endogenous ANX-A1 in the fate of the adherent leukocyte (as in the hamster cheek pouch microcirculation (Mancuso *et al.*, 1995)). So, the next set of experiments were designed so the cremaster muscle was superfused for up to 60 min with 1 nM PAF and, at 10 min intervals, cell detachment was monitored using a method adapted from a previous study (Lim *et al.*, 1998).

Adherent cells that detach

Figure 3.45 shows the numbers of adherent cells that detach. These are cells that are adherent for a minimum of 30 sec but then return to the main blood flow after this time rather than emigrating. The vessels were analysed in 10 min intervals over the 60 min time course. In the ANX-A1$^{+/+}$ mice the numbers of cells that detach were quite constant over 60 min even though the values were quite variable (large error bars). In

the ANX-A1$^{-/-}$ mice a similar trend was seen however, lower cell detachment was detected in the ANX-A1$^{-/-}$ mice compared to the ANX-A1$^{+/+}$ mice at the 0 min time-point, i.e. before superfusion with PAF began although due to the small numbers of cells involved, this was not statistically significant. No significant differences were found between the ANX-A1$^{+/+}$ and the ANX-A1$^{-/-}$ mice over the time course assessed.

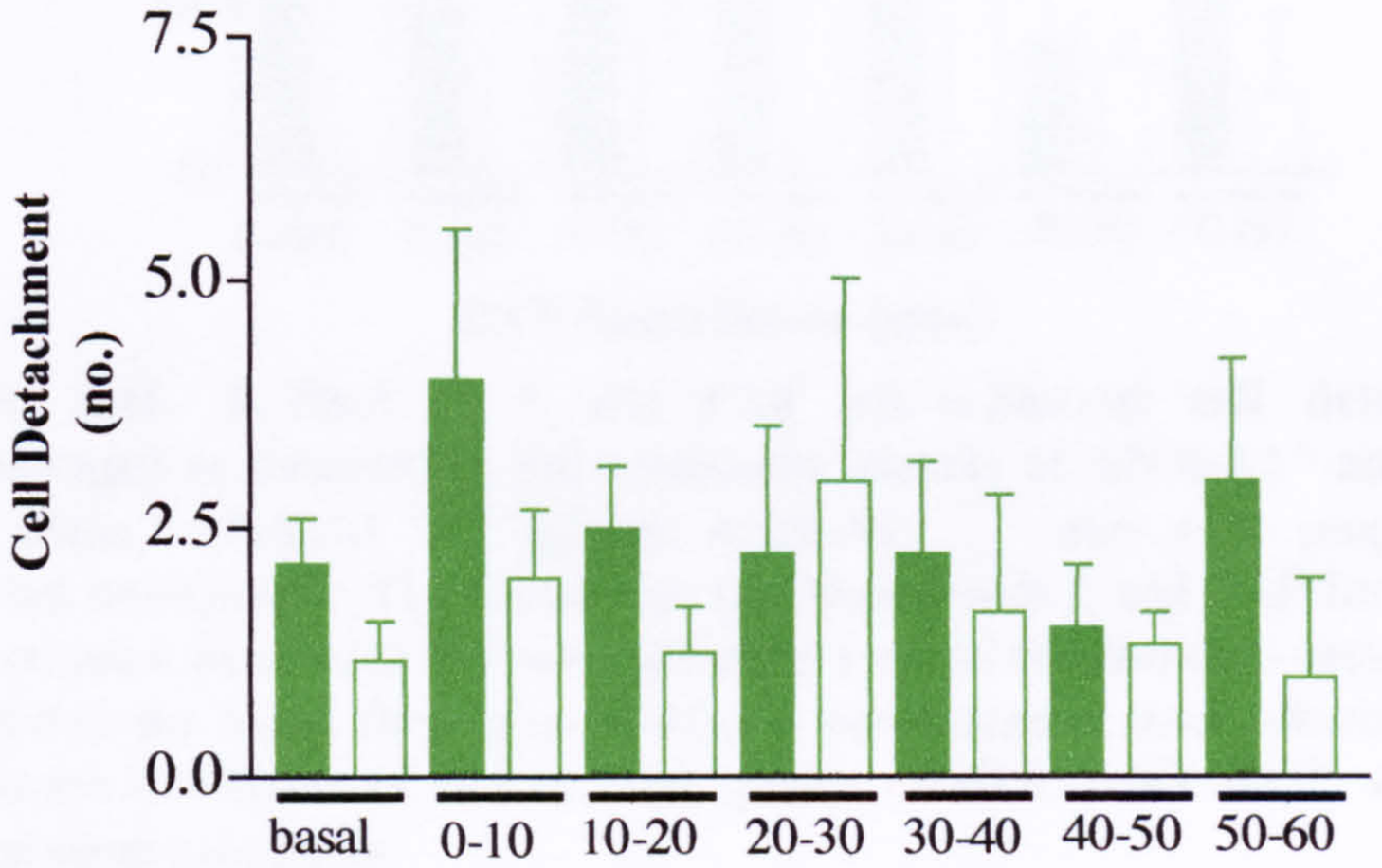

Figure 3.45. Effect of 1 nM PAF on adherent cell detachment as assessed in the cremaster muscle of ANX-A1$^{-/-}$ and ANX-A1$^{+/+}$ mice. ANX-A1$^{+/+}$ ■ and ANX-A1$^{-/-}$ □ mice were prepared for intravital microscopy. The tissue was superfused with 1 nM PAF for 60 min. Cells counted were those that were adherent for >30 sec and then detached and returned to the blood flow. Values are mean±sem of n=4 mice per group.

Figure 3.46 shows the above data as a percentage of adherent cells that detach. This shows that in ANX-A1$^{+/+}$ mice the percentage of cells that detach trends to be stable over the 60 min time course. In the ANX-A1$^{-/-}$ animals a significantly lower percentage of adherent cells detach at the 0 min time-point. Once superfusion began this effect was lost and for the rest of the time-course the percentage of detaching cells were not found to be significantly different between the genotypes.

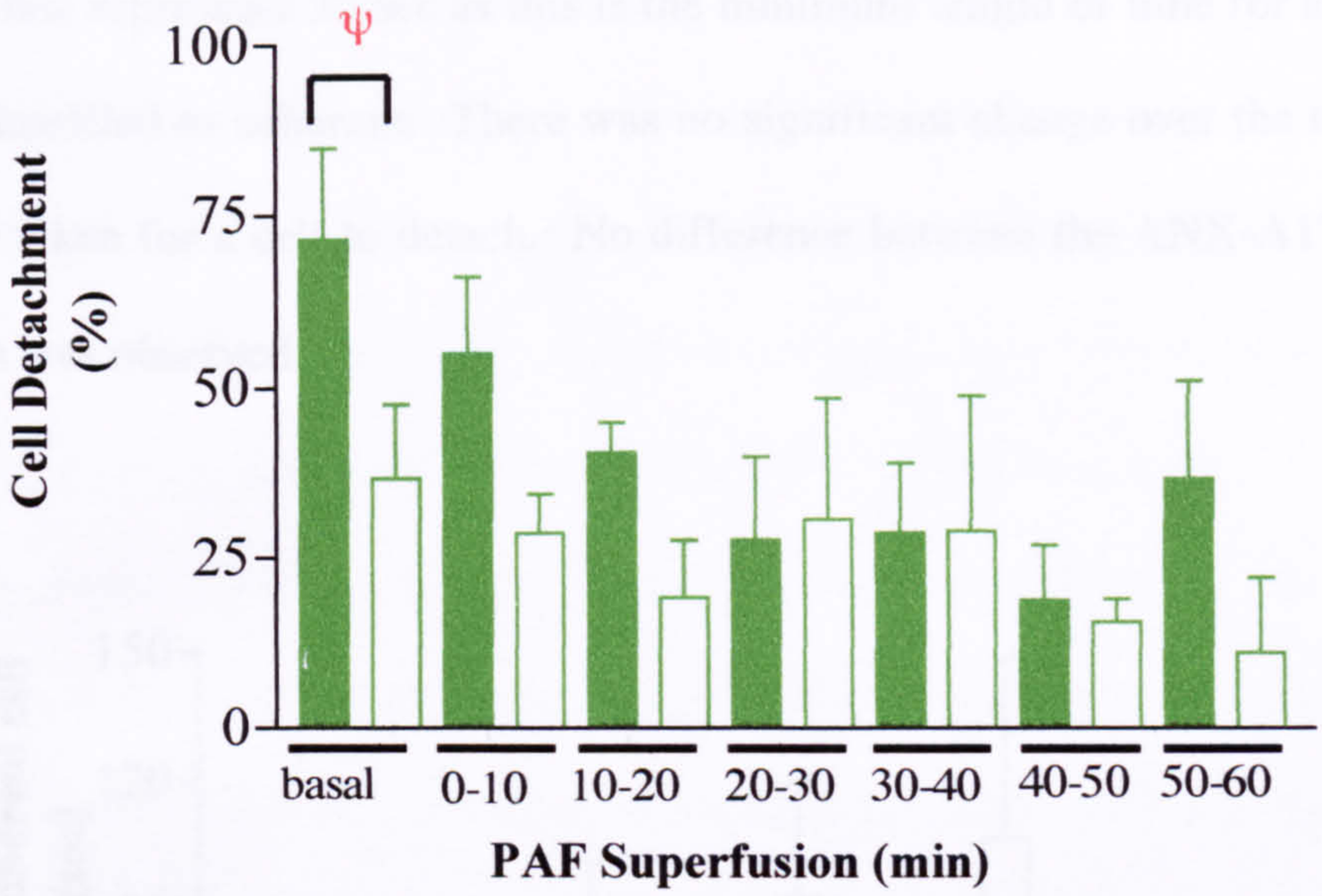

Figure 3.46. E ffect of 1 nM PAF on adherent cell detachment (percentage) as assessed in the cremaster muscle of ANX-A1$^{-/-}$ and ANX-A1$^{+/+}$ mice. ANX-A1 WT ■ and ANX-A1$^{-/-}$ □ mice were prepared for intravital microscopy. The tissue was superfused with 1 nM PAF for 60 min. Cells counted were those that were adherent for >30 sec and then detached and returned to the blood flow (expressed as a percentage of total adherent cells). Values are mean±sem of n=4 mice per group, ψP<0.05 ANX-A1$^{+/+}$ vs. ANX-A1$^{-/-}$ at same time-point.

Figure 3.47 is a graph to show the length of time it took for adherent cells to detach. The line represents 30 sec as this is the minimum length of time for a stationary cell to be classified as adherent. There was no significant change over the time course in the time taken for a cell to detach. No difference between the ANX-A1$^{+/+}$ and ANX-A1$^{-/-}$ mice was observed.

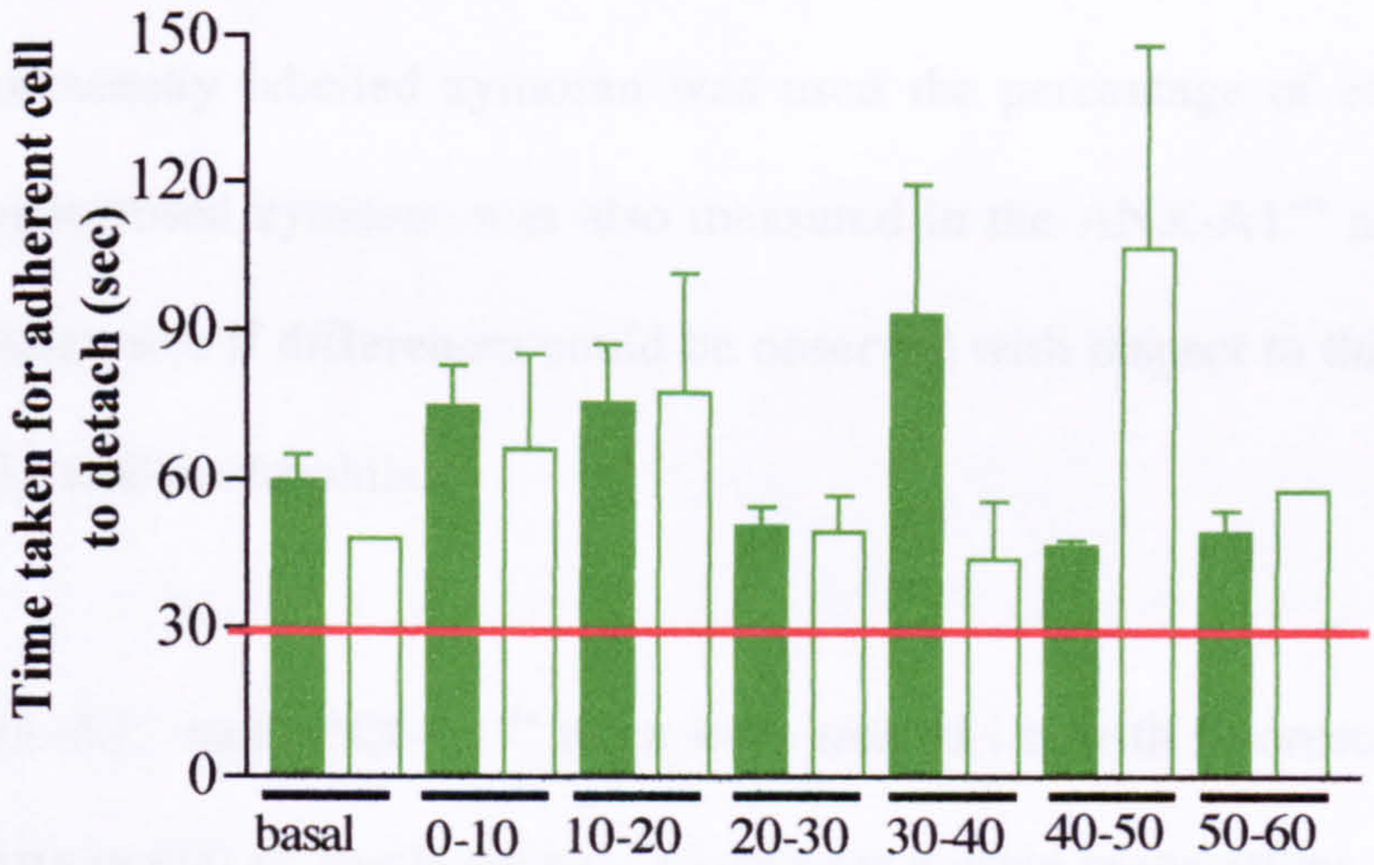

Figure 3.47. Effect of 1 nM PAF on adherent cell detachment time as assessed in the cremaster muscle of ANX-A1$^{-/-}$ and WT mice. ANX-A1$^{+/+}$ ■ and ANX-A1$^{-/-}$ □ mice were prepared for intravital microscopy. The tissue was superfused with 1 nM PAF for 60 min. Cells counted were those that were adherent for >30 sec and time taken to detach and return to the blood flow was measured. Values are mean±sem of n=4 mice per group.

3.2.3. Effect of Zymosan on Leukocyte Recruitment in ANX-A1$^{-/-}$ and ANX-A1$^{+/+}$ Mice

Next a series of experiments were performed in the cremaster muscle preparation using zymosan as an inflammogen. As zymosan-induced peritonitis promoted significantly higher levels of neutrophil emigration in the ANX-A1$^{-/-}$ mice the leukocyte recruitment process was examined in more detail using the mouse cremaster microcirculation. As fluorescently labelled zymosan was used the percentage of emigrated cells that had phagocytosed zymosan was also measured in the ANX-A1$^{+/+}$ and the ANX-A1$^{-/-}$ mice to determine if differences could be observed with respect to this important function of emigrated neutrophils.

ANX-A1$^{-/-}$ and ANX-A1$^{+/+}$ mice were treated i.s. with fluorescently labelled zymosan (30 μg in 400 μl sterile saline). Cremaster muscle preparations were carried out so that various vessels could be chosen and recorded 6 hr post zymosan injection. The first study was conducted in the laboratory of Dr. S. Nourshargh. The cremaster muscle was prepared using a slightly different protocol as described in the methods section (2.3.4). Cell emigration was analysed as well as the percentage of emigrated cells that had phagocytosed zymosan.

Study 1

Emigration

In the first set of experiments cell emigration was assessed in animals treated i.s. with either zymosan or saline for 6 hr. Figure 3.48 shows the number of emigrated cells counted in ANX-A1$^{-/-}$ and ANX-A1$^{+/+}$ mice after treatment with zymosan. The number of emigrated cells were counted in 1-3 fields of view for 1-3 vessels per animal. In the saline injected animals (vehicle control) there were very low numbers of cell emigration and no significant difference observed between ANX-A1$^{+/+}$ and ANX-A1$^{-/-}$ mice. After 6 hr zymosan treatment significant numbers of cells had emigrated into the tissues surrounding vessels in both the ANX-A1$^{+/+}$ and ANX-A1$^{-/-}$ mice (ANX-A1$^{+/+}$; saline: 3.52±0.60 vs. 6 hr zymosan: 26.52±2.47, n=3, P<0.05, ANX-A1$^{-/-}$; saline: 2.37±2.47 vs.6 hr zymosan: 40.81±2.38, n=3, p<0.05). When comparing the ANX-A1$^{+/+}$ to the ANX-A1$^{-/-}$ mice, significantly higher numbers of cells were found to have emigrated in ANX-A1$^{-/-}$ mice after 6 hr zymosan treatment compared to ANX-A1$^{+/+}$ mice (ANX-A1$^{+/+}$: 26.52±2.47 vs. ANX-A1$^{-/-}$: 40.81±2.38, n=3, P<0.05).

Phagocytosis

Figure 3.49 shows the percentage of emigrated cells that were found to have phagocytosed zymosan particles. The data is presented as index of phagocytosis as this normalises the phagocytosis for the number of emigrated cells that are in the tissue. No significant difference was found in the percentage of emigrated cells that had phagocytosed zymosan when comparing the ANX-A1$^{-/-}$ to the ANX-A1$^{+/+}$ mice.

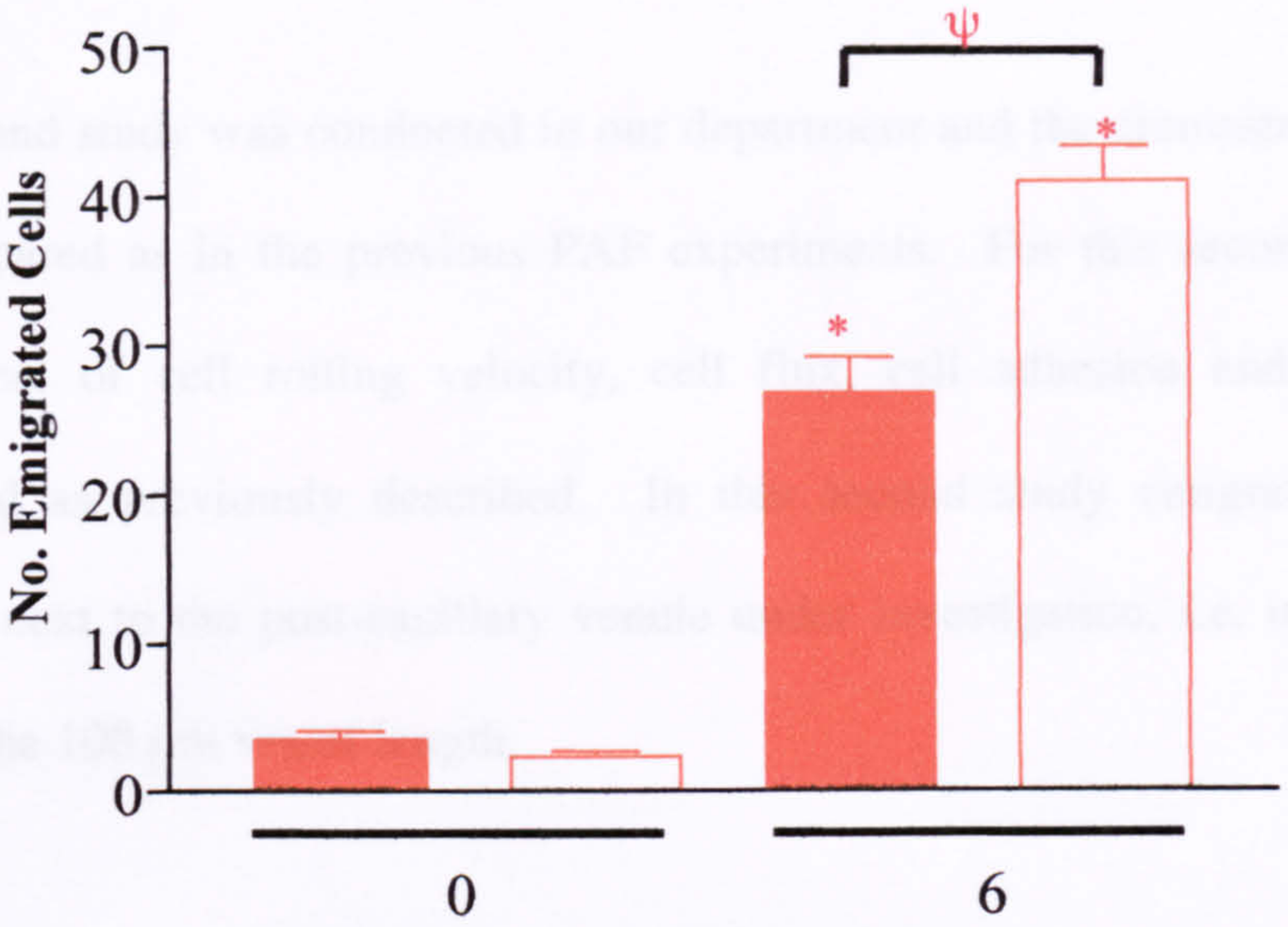

Figure 3.48. Effect of zymosan on cell emigration as assessed in the cremaster muscle of ANX-A1$^{-/-}$ and ANX-A1$^{+/+}$ mice. ANX-A1$^{+/+}$ ■ and ANX-A1$^{-/-}$ □ mice were injected i.s. with either saline (400 μl: 0hr zymosan) or zymosan (30 μg in 400 μl saline). Later mice were prepared for intravital microscopy so measurements were made at 6 hr post injection. Emigration was measured as number of cells per field of view (f.v). 3 f.v were analysed per vessel; 1-3 vessels were chosen per mouse. Values are mean±sem of n=3 mice per group, *P<0.05 vs. corresponding time 0, ψP<0.05 ANX-A1$^{-/-}$ vs. ANX-A1$^{+/+}$ at same time-point.

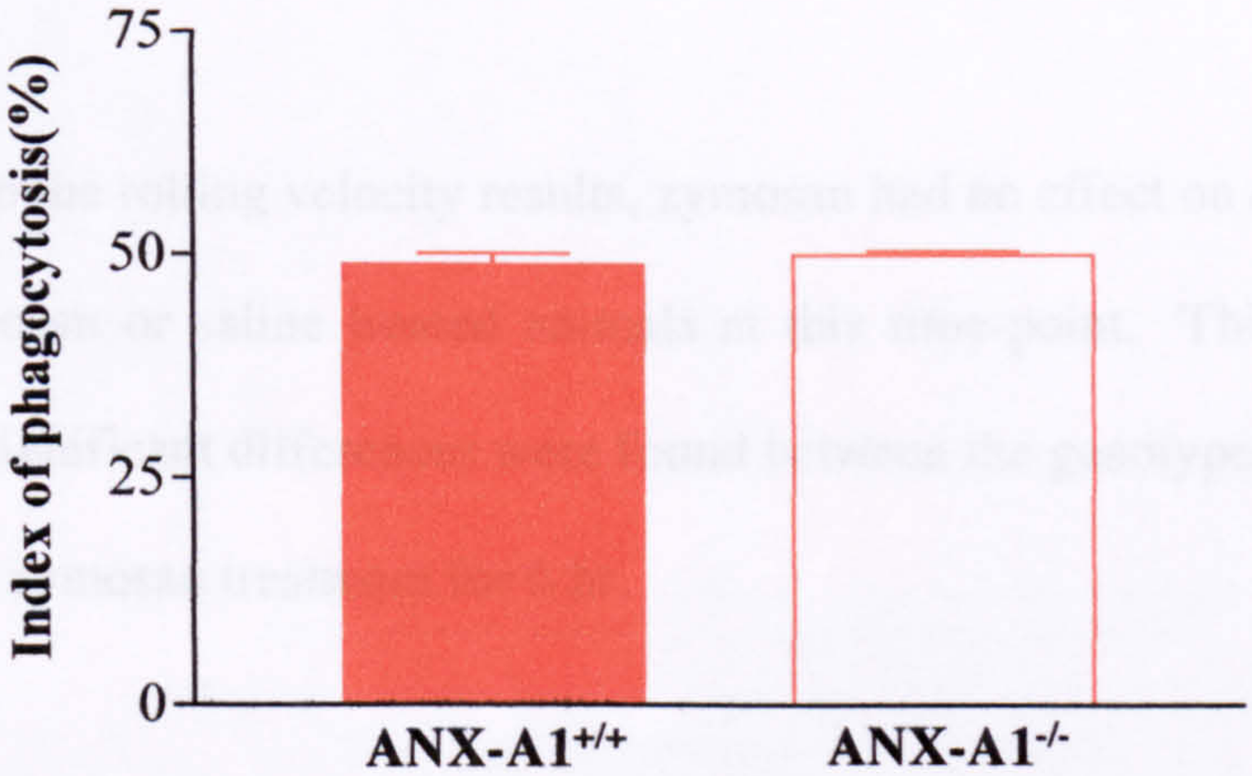

Figure 3.49. Effect of zymosan on phagocytosis by emigrated cells as assessed in the cremaster muscle of ANX-A1$^{-/-}$ and ANX-A1$^{+/+}$ mice. ANX-A1$^{+/+}$ ■ and ANX-A1$^{-/-}$ □ mice were injected with 30 μg fluorescent zymosan (i.s.). 6 hr post-zymosan emigrated cells (see above) were analysed for phagocytosis (number of emigrated cells containing fluorescent particles per field of view). Data was normalised for number of emigrated cells so expressed as index of phagocytosis (%). Values are mean±sem of n=3 mice per group.

Study 2

The second study was conducted in our department and the cremaster microcirculation was prepared as in the previous PAF experiments. For this second study the usual parameters of cell rolling velocity, cell flux, cell adhesion and emigration were measured as previously described. In this second study emigration was assessed directly next to the post-capillary venule under investigation, i.e. up to 50 μm either side of the 100 μm vessel length.

Rolling Velocity

Zymosan treatment had no significant effects on cell rolling velocity in ANX-A1$^{+/+}$ or ANX-A1$^{-/-}$ animals. This is shown in figure 3.50. No significant differences were found between the ANX-A1$^{+/+}$ and the ANX-A1$^{-/-}$ animals with respect to rolling velocity after saline (vehicle control) treatment or after 6 hr zymosan treatment.

Cell Flux

Similarly to the rolling velocity results, zymosan had no effect on cell flux in vessels of either zymosan or saline treated animals at this time-point. This is shown in figure 3.51. No significant differences were found between the genotypes after saline (vehicle control) or zymosan treatment for 6 hr.

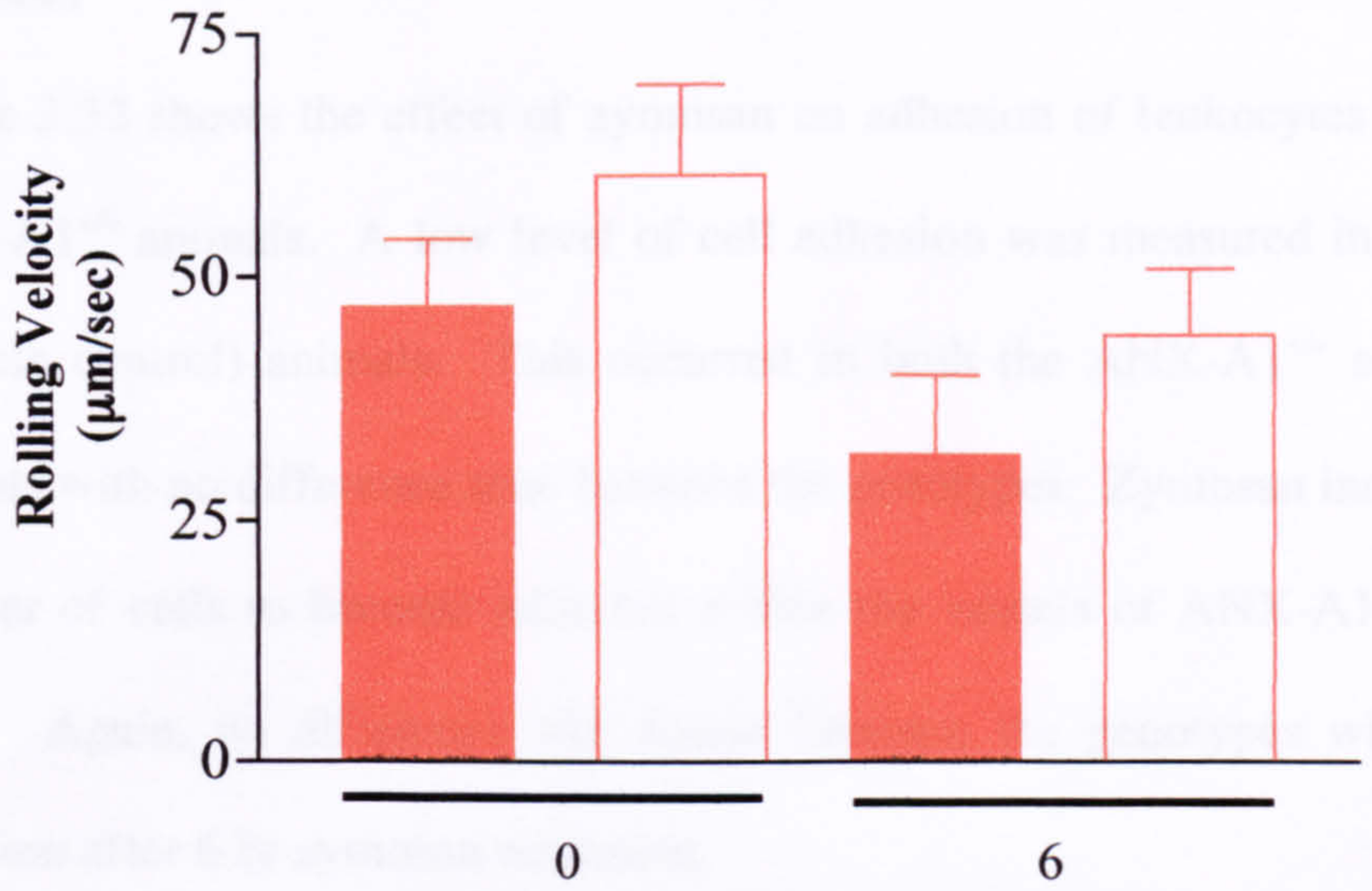

Figure 3.50. Effect of zymosan on cell rolling velocity as assessed in the cremaster muscle of ANX-A1$^{-/-}$ and ANX-A1$^{+/+}$ mice. ANX-A1$^{+/+}$ ■ and ANX-A1$^{-/-}$ □ mice were injected i.s. with with either saline (400 μl: 0hr zymosan) or zymosan (30 μg in 400 μl saline). Later mice were prepared for intravital microscopy so measurements were made at 6 hr post injection. Rolling velocity is measured as μm/sec. Values are mean±sem of n=4 mice per group.

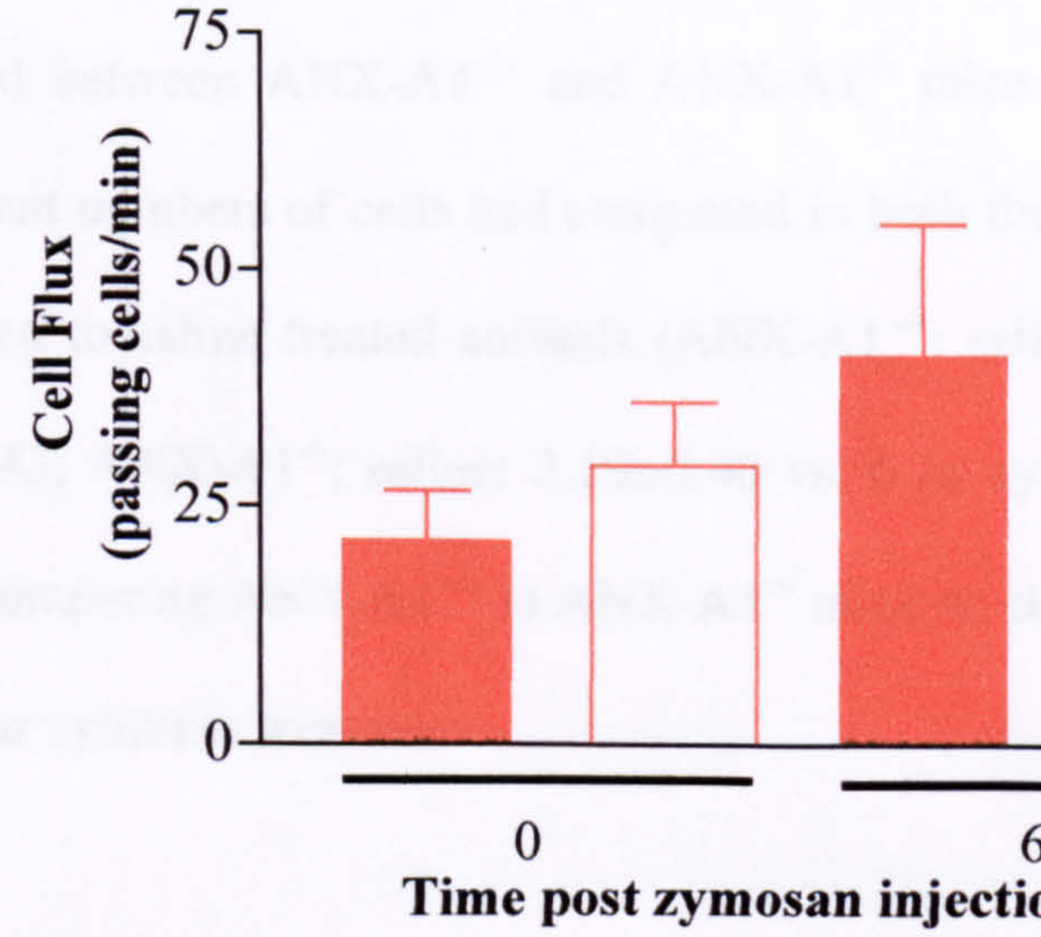

Figure 3.51. Effect of zymosan on cell flux as assessed in the cremaster muscle of ANX-A1$^{-/-}$ and ANX-A1$^{+/+}$ mice. ANX-A1$^{+/+}$ ■ and ANX-A1$^{-/-}$ □ mice were injected i.s. with with either saline (400 μl: 0hr zymosan) or zymosan (30 μg in 400 μl saline). Later mice were prepared for intravital microscopy so measurements were made at 6 hr post injection. Cell flux was measured as the number of cells passing a fixed point in the vessel/min. Values are mean±sem of n=4 mice per group.

Adhesion

Figure 3.52 shows the effect of zymosan on adhesion of leukocytes in ANX-A1$^{-/-}$ and ANX-A1$^{+/+}$ animals. A low level of cell adhesion was measured in the saline treated (vehicle control) animals. This occurred in both the ANX-A1$^{+/+}$ and the ANX-A1$^{-/-}$ animals with no difference seen between the genotypes. Zymosan induced a significant number of cells to become adherent within the vessels of ANX-A1$^{+/+}$ and ANX-A1$^{-/-}$ mice. Again, no difference was found between the genotypes with respect to cell adhesion after 6 hr zymosan treatment.

Emigration

In the second set of experiments cell emigration was measured as outlined earlier. Figure 3.53 shows the results of this experiment. In the saline injected animals (vehicle control) there were low numbers of emigrated cells and no significant difference observed between ANX-A1$^{+/+}$ and ANX-A1$^{-/-}$ mice. After 6 hr zymosan treatment significant numbers of cells had emigrated in both the ANX-A1$^{+/+}$ and ANX-A1$^{-/-}$ mice compared to saline treated animals (ANX-A1$^{+/+}$; saline: 1.83±0.39 vs. 6 hr zymosan: 9.67±1.43, ANX-A1$^{-/-}$; saline: 2.19±0.40 vs. 6 hr zymosan: 9.88±1.23, n=4, $P<0.05$). When comparing ANX-A1$^{+/+}$ to ANX-A1$^{-/-}$ mice no significant difference could be seen after 6 hr zymosan treatment.

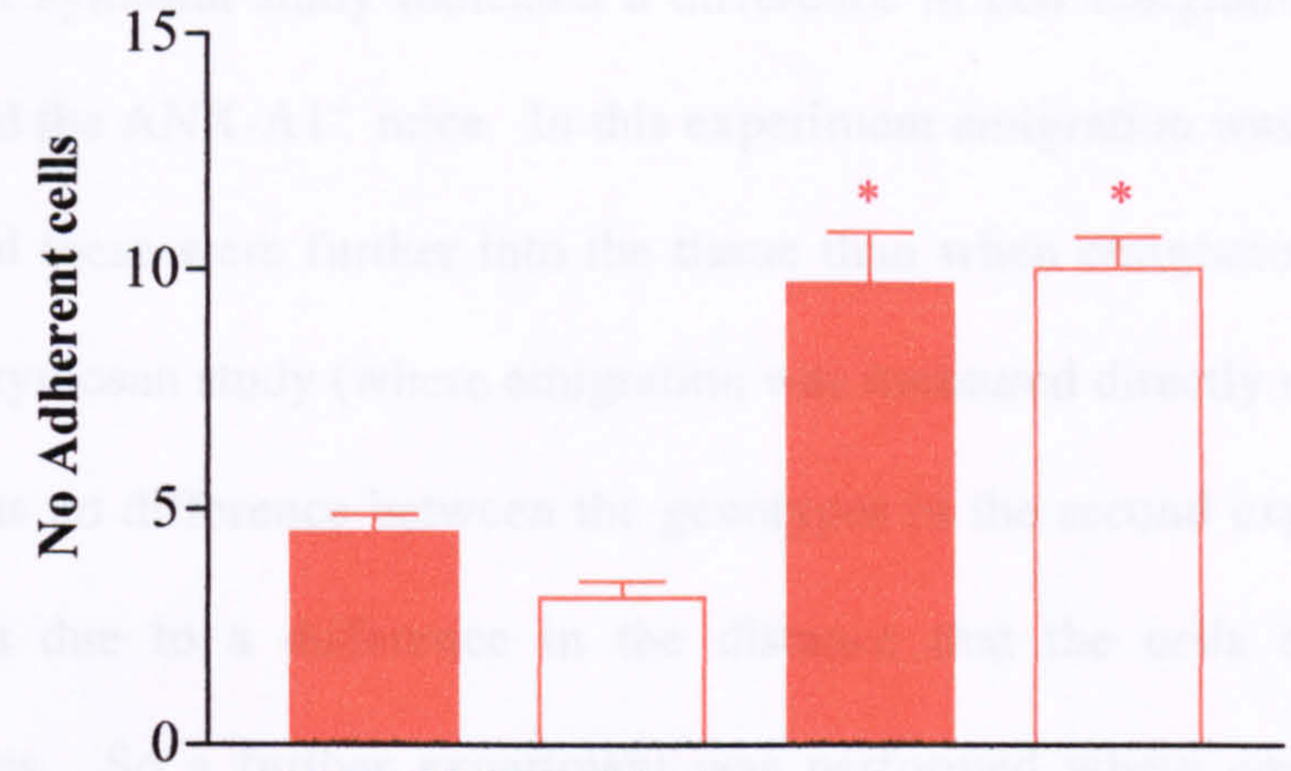

Figure 3.52. E ffect of zymosan on cell adhesion as assessed in the cremaster muscle of ANX-A1$^{-/-}$ and ANX-A1$^{+/+}$ mice. ANX-A1$^{+/+}$ ■ and ANX-A1$^{-/-}$ □ mice were injected with with either saline (400 µl: 0hr zymosan) or zymosan (30 µg in 400 µl saline). Later mice were prepared for intravital microscopy so measurements were made at 6 hr post injection. Adhesion is measured as number of cells stationary for >30 sec. Values are mean±sem of n=4 mice per group, *P<0.05 vs. corresponding time 0.

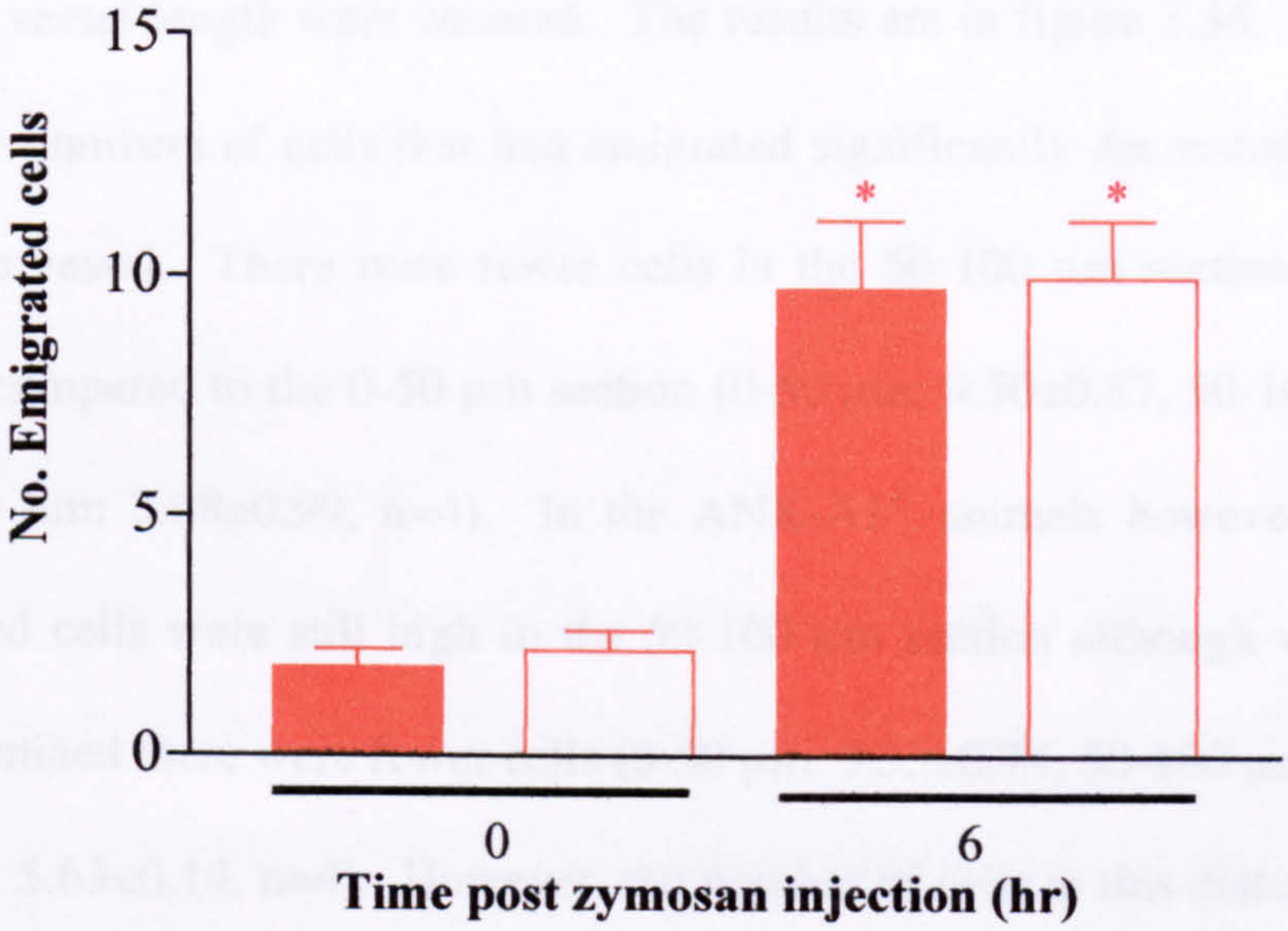

Figure 3.53. E ffect of zymosan on cell emigration as assessed in the cremaster muscle of ANX-A1$^{-/-}$ and ANX-A1$^{+/+}$ mice. ANX-A1$^{+/+}$ ■ and ANX-A1$^{-/-}$ □ mice were injected with with either saline (400 µl: 0hr zymosan) or zymosan (30 µg in 400 µl saline). Later mice were prepared for intravital microscopy of the cremaster muscle so measurements were made at 6 hr post injection. Emigration is measured as the number of cells either side of 100 µm vessel. Values are mean±sem of n=4 mice per group, *P<0.05 vs. corresponding time 0.

The first zymosan study indicated a difference in cell emigration between the ANX-A1$^{+/+}$ and the ANX-A1$^{-/-}$ mice. In this experiment emigration was examined per field of view and these were further into the tissue than when emigration was assessed in the second zymosan study (where emigration was measured directly next to the vessel). As there was no difference between the genotypes in the second experiment it is possible this was due to a difference in the distance that the cells emigrated in the two genotypes. So a further experiment was performed where emigration distance was taken into account as previously performed in the department (Tailor *et al.*, 1997).

Emigration Distance

Emigration was measured in animals treated with zymosan for 6 hr. Cells at different distances from the vessel wall (0-50 μm, 50-100 μm and 100-150 μm) on both sides of 100 μm vessel length were counted. The results are in figure 3.54. In the ANX-A1$^{+/+}$ mice the numbers of cells that had emigrated significantly decreased with the distance from the vessel. There were fewer cells in the 50-100 μm section and 100-150 μm section compared to the 0-50 μm section (0-50 μm: 9.50±0.87, 50-100 μm: 5.04±0.71, 100-150 μm: 3.08±0.99, n=4). In the ANX-A1$^{-/-}$ animals however, the numbers of emigrated cells were still high in the 50-100 μm section although when 100-150 μm was examined there were fewer cells (0-50 μm: 9.33±0.74, 50-100 μm: 6.42±0.44, 100-150 μm: 5.63±0.14, n=4). However, the number of cells at this distance (100-150 μm) was significantly higher in ANX-A1$^{-/-}$ mice compared to ANX-A1$^{+/+}$ mice. Overall, significantly higher numbers of emigrated cells (0-150 μm) were found in the ANX-A1$^{-/-}$ mice compared to the ANX-A1$^{+/+}$ mice (ANX-A1$^{+/+}$: 17.63±2.08 vs. ANX-A1$^{-/-}$: 21.38±0.95, n=4, $P<0.05$). In any case this difference was more modest than that measured in study 1.

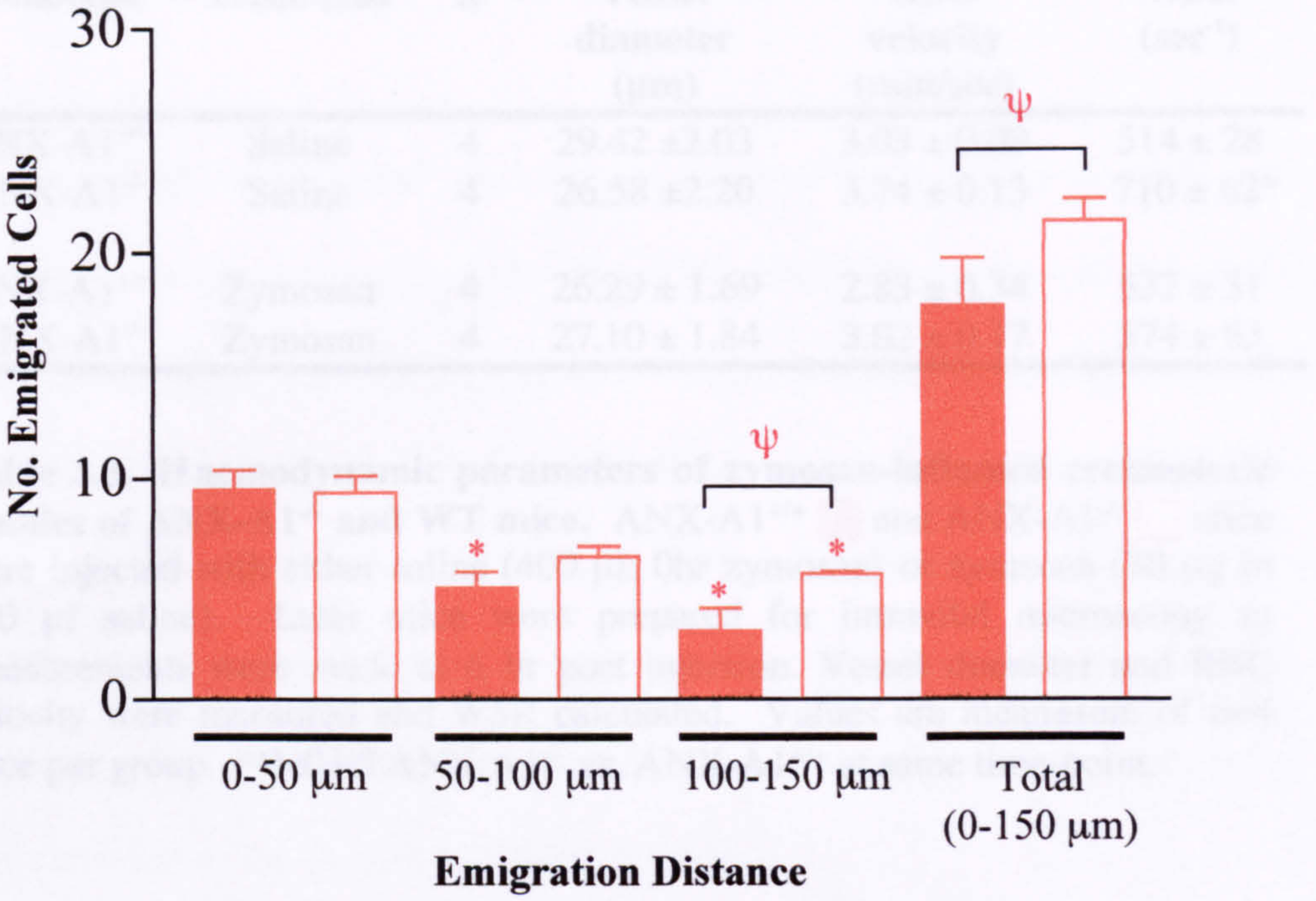

Figure 3.54. Effect of zymosan on cell emigration distance as assessed in the cremaster muscle of ANX-A1$^{-/-}$ and ANX-A1$^{+/+}$ mice. ANX-A1$^{+/+}$ ■ and ANX-A1$^{-/-}$ □ mice were injected with 30 μg zymosan (i.s.). Later mice were prepared for intravital microscopy so measurements were made at 6 hr post injection. Emigration was measured as number of cells at different distances either side of 100 μm vessel; 0-50, 50-100 and 100-150 μm. Values are mean±sem of n=4 mice per group, *P<0.05 vs. corresponding emigration at 0-50 μm, ψP<0.05 ANX-A1$^{-/-}$ vs. ANX-A1$^{+/+}$ at same distance.

Haemodynamic parameters

Table 3.5. shows the haemodynamic parameters measured in the ANX-A1$^{-/-}$ and ANX-A1$^{+/+}$ animals treated with saline or zymosan for 6 hr. The RBC velocity was not significantly different between the treatment groups or the genotypes. However, a significantly higher WSR was found in the saline treated ANX-A1$^{-/-}$ animals compared to the saline treated ANX-A1$^{+/+}$ animals (ANX-A1$^{-/-}$ saline: 710±62 sec^{-1} vs. ANX-A1$^{+/+}$ saline: 514±28 sec^{-1}, n=4, P<0.05). The WSR was not significantly different between the ANX-A1$^{+/+}$ and the ANX-A1$^{-/-}$ after 6 hr zymosan treatment.

Genotype	Treatment	n	Vessel diameter (μm)	RBC velocity (mm/sec)	WSR (sec^{-1})
ANX-A1$^{+/+}$	Saline	4	29.42 ±2.03	3.03 ± 0.09	514 ± 28
ANX-A1$^{-/-}$	Saline	4	26.58 ±2.20	3.74 ± 0.13	710 ± 62*
ANX-A1$^{+/+}$	Zymosan	4	26.29 ± 1.69	2.83 ± 0.34	532 ± 31
ANX-A1$^{-/-}$	Zymosan	4	27.10 ± 1.84	3.02 ± 0.17	574 ± 63

Table 3.5. Haemodynamic parameters of zymosan-inflamed cremasteric venules of ANX-A1$^{-/-}$ and WT mice. ANX-A1$^{+/+}$ ■ and ANX-A1$^{-/-}$ □ mice were injected with either saline (400 μl: 0hr zymosan) or zymosan (30 μg in 400 μl saline). Later mice were prepared for intravital microscopy so measurements were made at 6 hr post injection. Vessel diameter and RBC velocity were measured and WSR calculated. Values are mean±sem of n=4 mice per group. *P<0.05 ANX-A1$^{-/-}$ vs. ANX-A1$^{+/+}$ at same time-point.

Summary

Saline treatment for 6 hr seems to cause only a minimal degree of activation to vessels with only very low numbers of cells adhering and emigrating (not dissimilar to numbers found in untreated cremaster muscle preparation-see earlier data). Zymosan however, caused a marked increase in cell adhesion and emigration in both the ANX-A1$^{-/-}$ and ANX-A1$^{+/+}$ mice. Zymosan treatment did not affect cell rolling or cell flux, at least at the time-point examined. It seems as if the ANX-A1$^{-/-}$ mice became more activated than the ANX-A1$^{+/+}$ mice, with respect to cell emigration, however this was only seen when cell emigration was monitored further into the tissue than usually examined. The difference is unlikely to be due to differences in zymosan phagocytosis by emigrated cells as no difference was seen between the ANX-A1$^{+/+}$ and the ANX-A1$^{-/-}$ mice with respect to phagocytosis.

3.2.4. Effect of Ac2-26 in the Cremaster Muscle Preparation of $FPR^{-/-}$ Mice

As this model of intravital microscopy was proving to be a good for examining leukocyte recruitment and the role played by ANX-A1, a series of experiments were performed utilising the $FPR^{-/-}$ mice that were also available in our department. Previous experiments highlighted the fact that ANX-A1 is a likely agonist of the FPR and this may be the receptor through which ANX-A1 is exerting its actions. An examination of the effects of peptide Ac2-26 in the cremaster model was therefore a worthwhile experiment. In addition these experiments would complement those carried out with administration of the peptide to C57BL/6 mice.

$FPR^{-/-}$ mice were prepared for intravital microscopy of the cremaster muscle. Just prior to superfusion of 100 nM PAF mice were injected with 200 μg peptide Ac2-26 (in 200 μl of sterile PBS). Control mice were injected with 200 μl PBS alone. Superfusion of 100 nM PAF was then started and continued for 90 min.

Rolling Velocity

Rolling velocity in the $FPR^{-/-}$ mice in response to 100 nM PAF is shown in figure 3.55. Data is presented as a percentage of basal (0 min) cell rolling velocity. 100 nM PAF significantly reduced rolling velocity at the later time-points of 60 and 90 min in the vehicle control $FPR^{-/-}$ animals. This is different to the results obtained with the C57BL/6 mice controls for the $FPR^{-/-}$ mice. This is shown in figure 3.28 where the rolling velocity decreased from 30 min.

In the peptide treated $FPR^{-/-}$ mice cell rolling velocity was significantly lower than basal from 45 min onwards. Following peptide treatment in C57BL/6 mice the cell rolling became significantly slower than basal from 30 min (see figure 3.28). When comparing the two treatment groups (peptide and PBS treated controls) no differences were seen between them at any of the time-points measured.

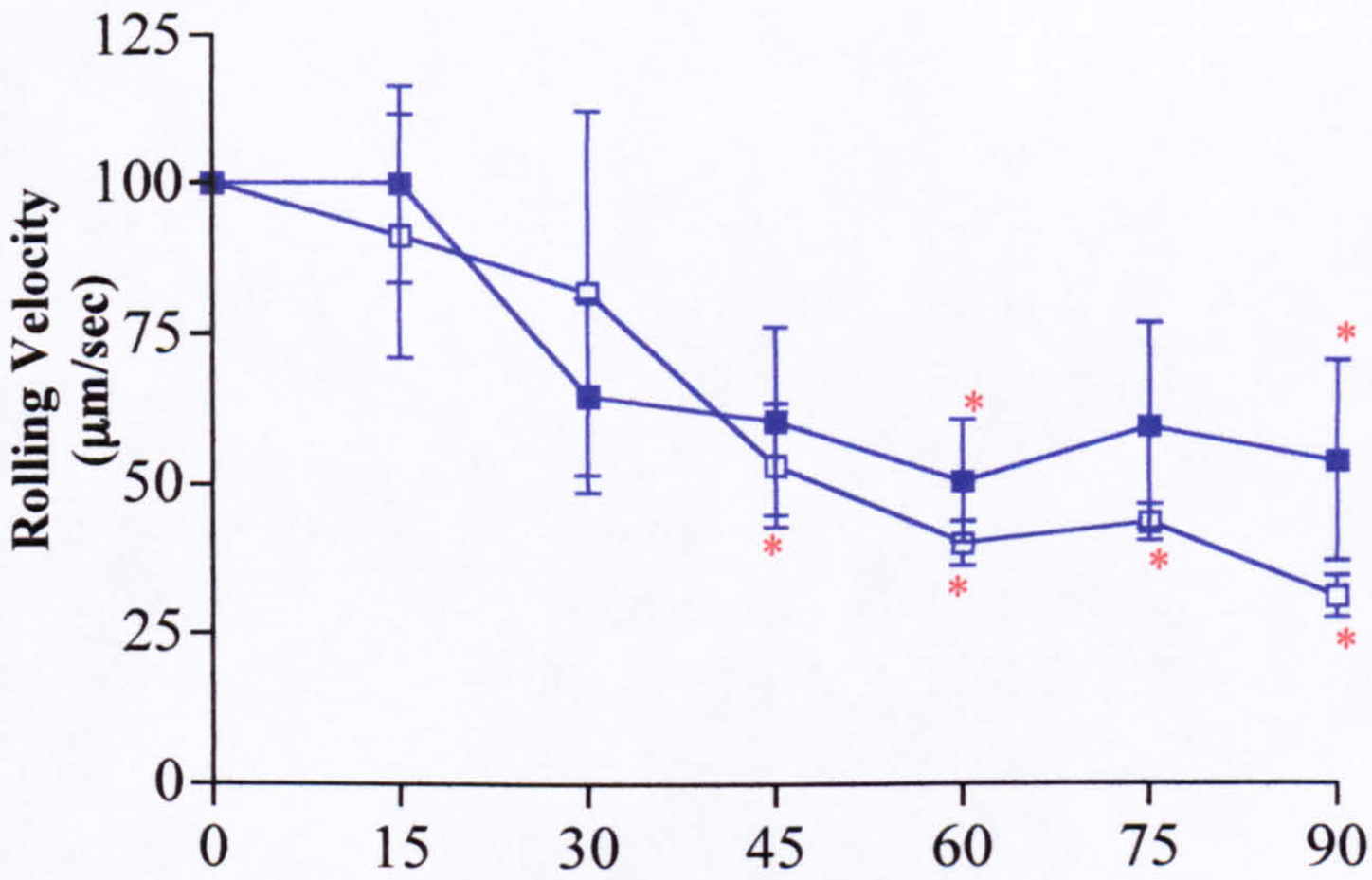

Figure 3.55. Effect of Ac2-26 on cell rolling velocity as assessed in the inflamed cremaster muscle of $FPR^{-/-}$ mice. $FPR^{-/-}$ mice were prepared for intravital microscopy. Mice were treated with either PBS ■ or 200 g Ac2-26 □ (time 0) and then superfused with 100 nM PAF. Rolling velocity is shown as % of basal rolling velocity. Values are mean±sem of n=4 mice per group), *P<0.05 vs. corresponding time 0.

Cell Flux

Figure 3.56 shows the cell flux in $FPR^{-/-}$ animals superfused with 100 nM PAF. Significant differences were not seen in cell flux over the time course in either the vehicle control animals (PBS treated) or the peptide treated group. Although a lower cell flux was noted in the peptide treated animals compared to the 0 min time point this

did not reach significance at any of the time points. This data fits with the cell flux seen in the C57BL/6 mice (figure 3.29).

No significant differences are found between the vehicle control group and the peptide treated mice except at the 90 min time-point (90 min; vc: 49.75±17.13 vs. pep: 11.58±4.40, n=4, P<0.05).

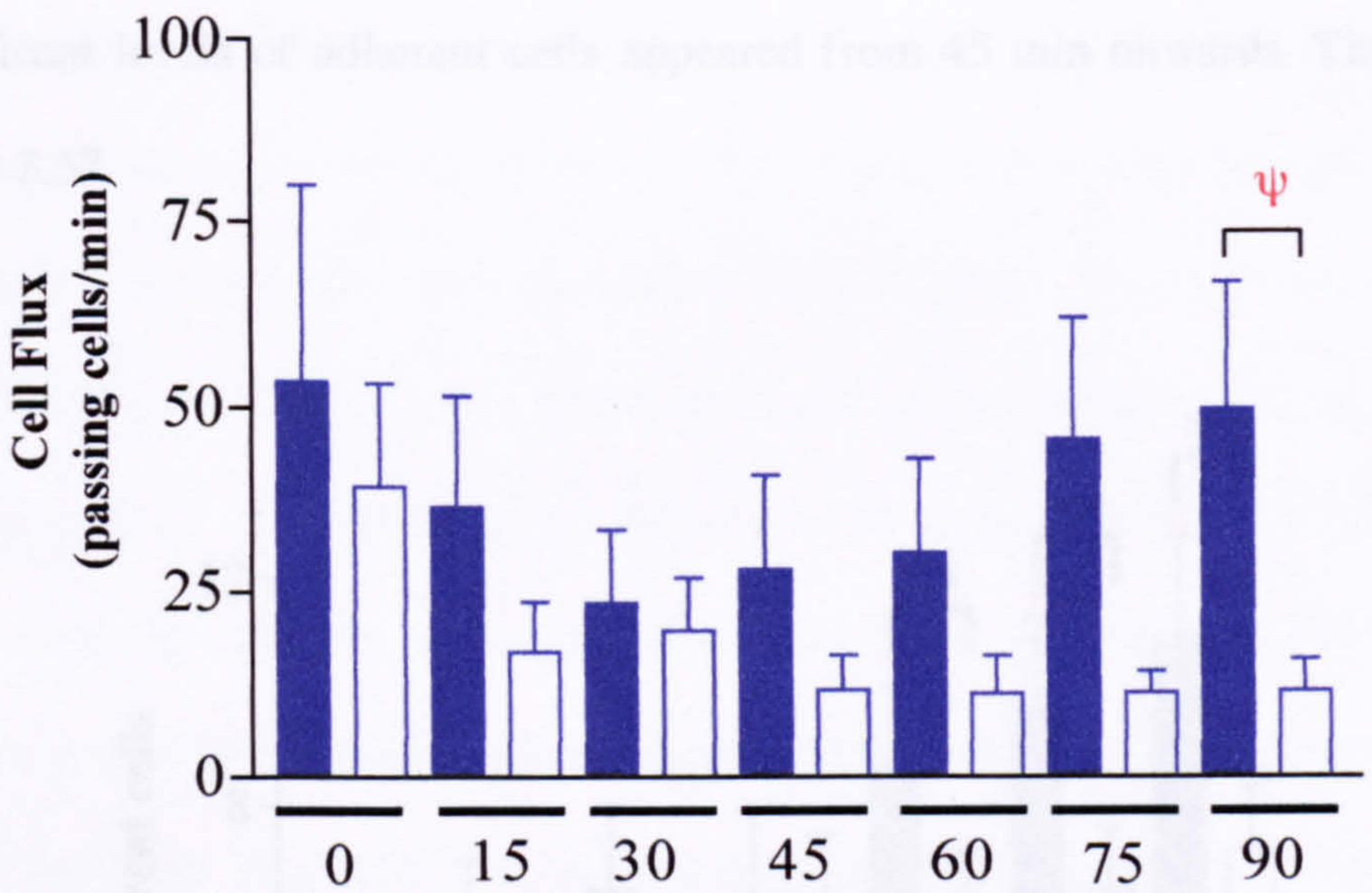

Figure 3.56. Effect of Ac2-26 on cell flux as assessed in the inflamed cremaster muscle of FPR$^{-/-}$ mice. FPR$^{-/-}$ mice were prepared for intravital microscopy. Mice were treated with either PBS ■ or 200 μg Ac2-26 □ (time 0) and then superfused with 100 nM PAF. Cell flux was measured as the number of cells passing a fixed point in the vessel/min. Values are mean±sem of n=4 mice per group, ψP<0.05 PBS vs. peptide at same time-point.

Adhesion

The high dose of PAF (100 nM) caused a time-dependent increase in the number of adherent cells in the FPR$^{-/-}$ mice. This is shown in figure 3.57. There were significantly higher numbers of adherent cells compared to basal (0 min) from 60 min onwards in the vehicle control group. This is only slightly different to the C57BL/6

mice in which adhesion becomes significantly higher than basal at the 45 min time-point (see figure 3.30).

Lower numbers of adherent cells were found in peptide treated mice compared to vehicle control animals, however, these values did not reach significance at the 5% level. The numbers of adherent cells only increased from basal at 90 min in the Ac2-26 treated mice. This was in contrast to the peptide-treated C57BL/6 mice where significant levels of adherent cells appeared from 45 min onwards. This is shown in figure 3.57.

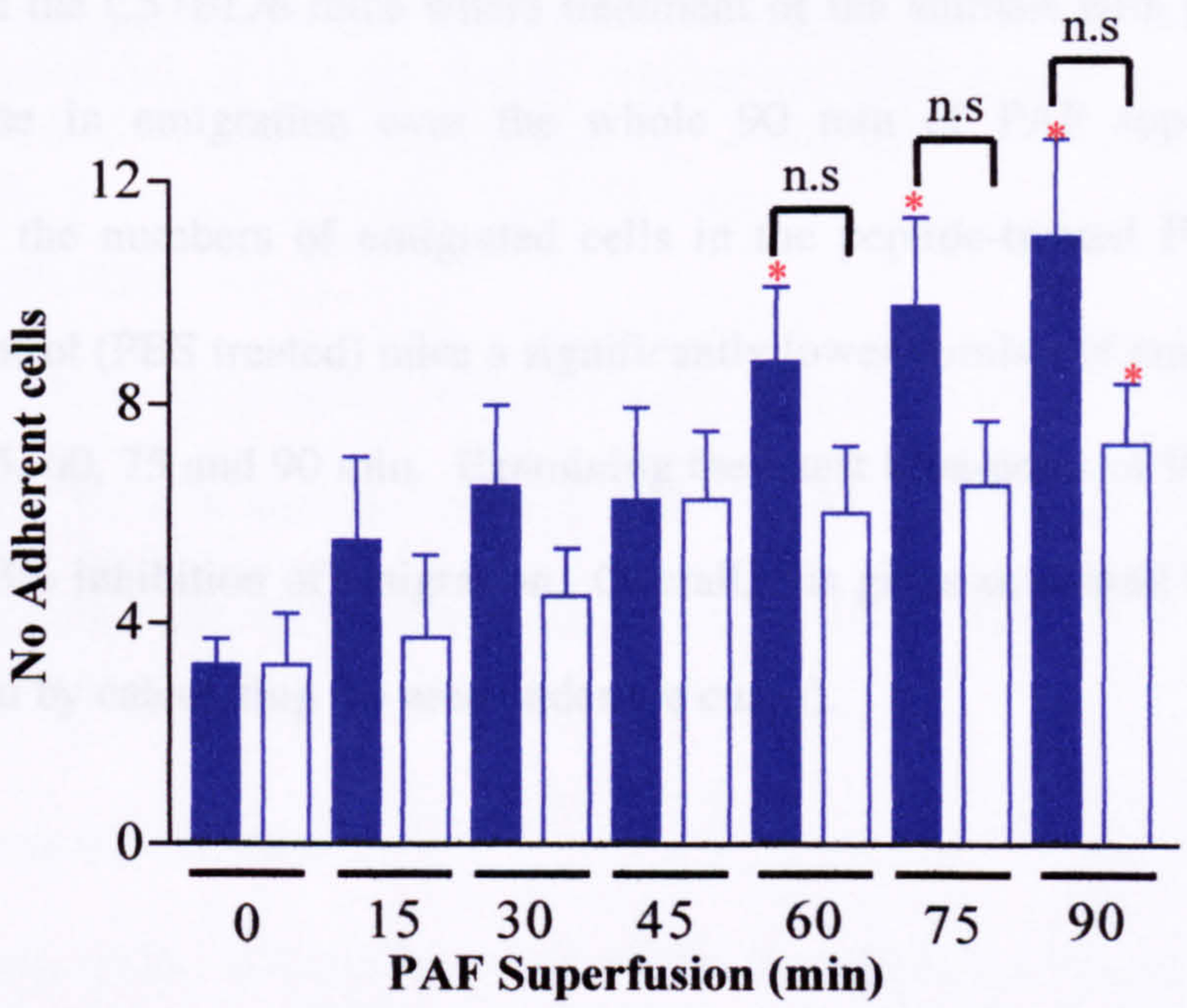

Figure 3.57. Effect of Ac2-26 on cell adhesion as assessed in the inflamed cremaster muscle of $FPR^{-/-}$ mice. $FPR^{-/-}$ mice were prepared for intravital microscopy. Mice were treated with either PBS ■ or 200 μg Ac2-26 □ (time 0) and then superfused with 100 nM PAF. Adhesion is measured as number of cells stationary for >30 sec. Values are mean±sem of n=4 mice per group, *P<0.05 vs. corresponding time 0.

Emigration

Figure 3.58 shows the effect of 100 nM PAF on cell emigration in $FPR^{-/-}$ mice. Vehicle-treated mice show that the number of cells that emigrated from the vessel increased over time up to 90 min. Numbers were significantly different to basal (0 min) from 30 min onwards. These results are comparable to those obtained in the C57BL/6 mice (see figure 3.31).

The injection of Ac2-26 before the start of PAF superfusion caused a significant attenuation of leukocyte recruitment. There was still a time-dependent increase in emigration but this was only significant from 60 min. This is in contrast to results obtained in the C57BL/6 mice where treatment of the animals with peptide abolished the increase in emigration over the whole 90 min of PAF superfusion. When comparing the numbers of emigrated cells in the peptide-treated $FPR^{-/-}$ mice to the vehicle control (PBS treated) mice a significantly lower number of emigrated cells were found at 45, 60, 75 and 90 min. Examining the latest time-point of 90 min the peptide caused a 53% inhibition of emigration. Overall, this gives an overall inhibition of 45% (as assessed by calculating the area under the curve).

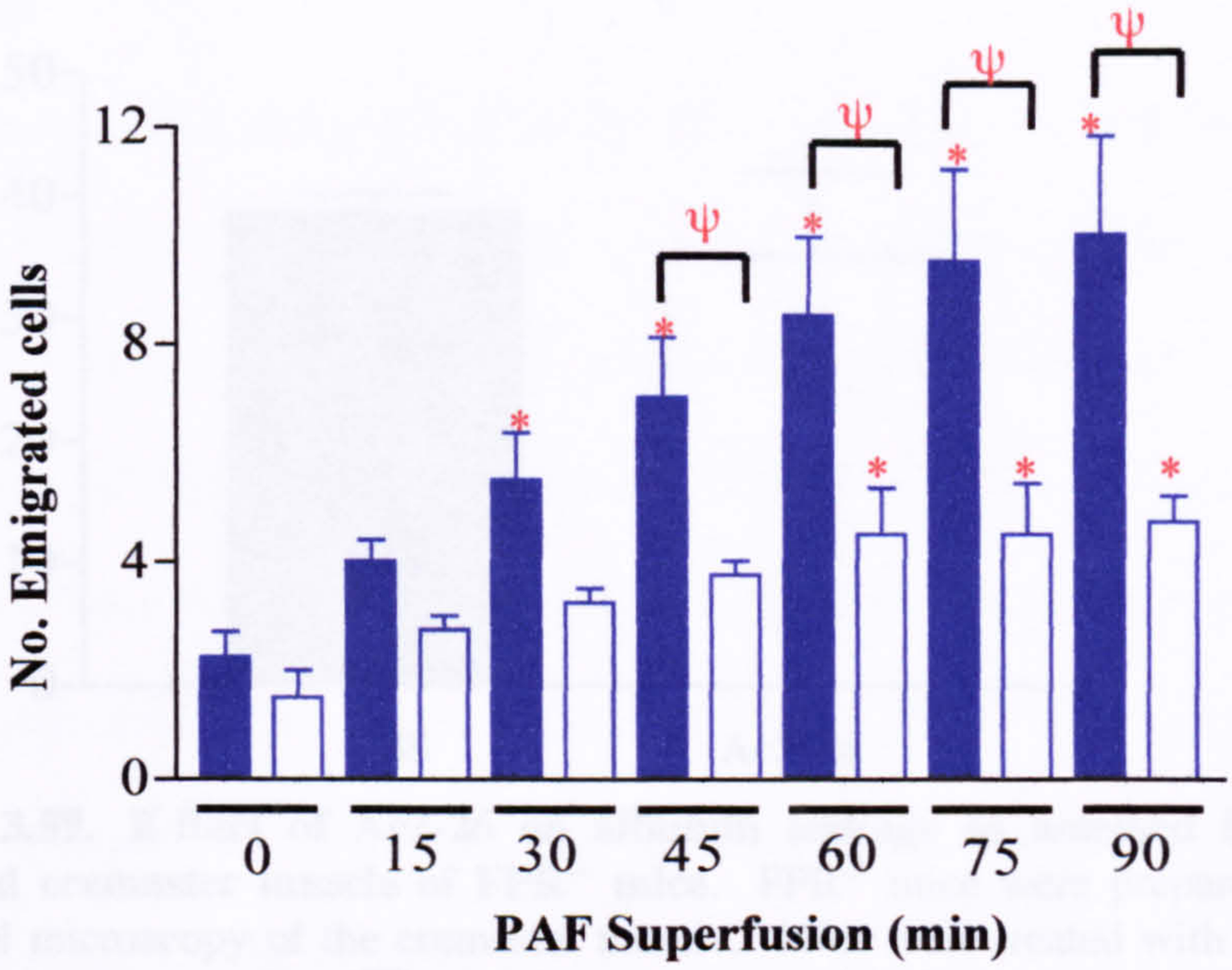

Figure 3.58. Effect of Ac2-26 on cell emigration as assessed in the inflamed cremaster muscle of FPR KO mice. $FPR^{-/-}$ mice were prepared for intravital microscopy. Mice were treated with either PBS ■ or 200 μg Ac2-26 □ (time 0) and then superfused with 100 nM PAF. Emigration is measured as number of cells either side of 100 μm vessel. Values are mean±sem of n=4 mice per group, *P<0.05 vs. corresponding time 0, ψP<0.05 PBS vs. peptide at same time-point

Albumin Leakage

Figure 3.59 shows the albumin leakage measured in vessels of PBS and Ac2-26 treated animals after 90 min superfusion with 100 nM PAF. No significant difference in albumin leakage was found between the mice treated with either PBS or peptide.

Haemodynamic parameters

The haemodynamic parameters measured in post-capillary venules of $FPR^{-/-}$ mice treated with either PBS or Ac2-26 and inflamed with 100 nM PAF are shown in table 3.6. Superfusion with 100 nM PAF had no significant effects on RBC velocity or WSR over the 90 min time course. The treatment of mice with Ac2-26 caused a slight decrease in RBC velocity and WSR although these differences were not significant.

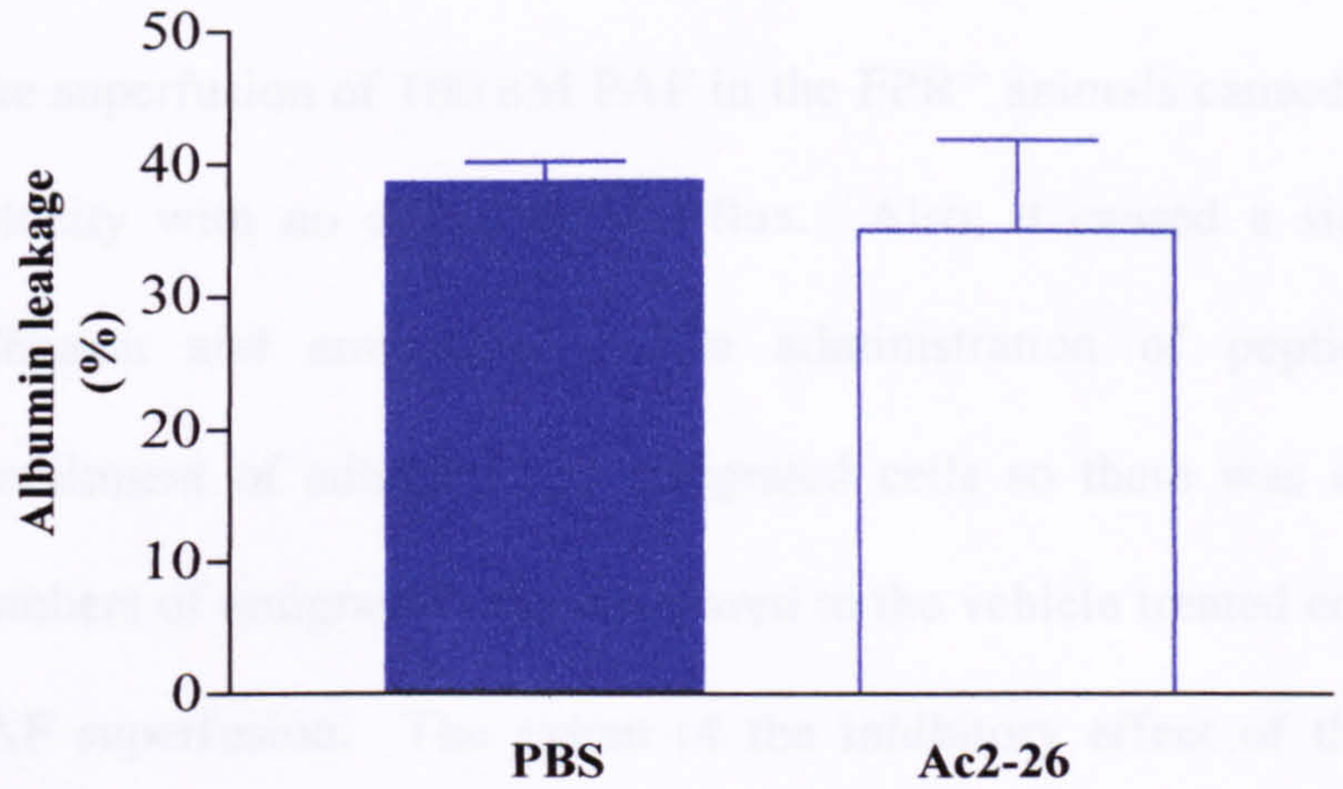

Figure 3.59. E ffect of Ac2-26 on albumin leakage as assessed in the inflamed cremaster muscle of FPR$^{-/-}$ mice. FPR$^{-/-}$ mice were prepared for intravital microscopy of the cremaster muscle. Mice were treated with either PBS ■ or 200 μg Ac2-26 □ (time 0) and then superfused with 100 nM PAF. At 90 min FITC labelled albumin was injected 5 min prior to analysis of albumin leakage. Values are mean±sem of n=3 mice per group.

Treatment	n	Vessel diameter (μm)		RBC velocity (mm/sec)	WSR (sec^{-1})
100 nM PAF + PBS (Vehicle control)	4	33.81 ± 0.98	0	4.50 ± 0.62	664 ± 86
			15	4.60 ± 0.71	677 ± 99
			30	4.58 ± 0.77	671 ± 100
			45	4.53 ± 1.71	664 ± 91
			60	5.20 ± 1.01	763 ± 137
			75	4.63 ± 0.94	679 ± 132
			90	4.90 ± 1.01	719 ± 140
100 nM PAF + Ac2-26	4	32.00 ± 1.86	0	2.93 ± 0.24	470 ± 62
			15	3.58 ± 0.57	572 ± 114
			30	3.73 ± 0.56	598 ± 120
			45	3.43 ± 0.40	548 ± 91
			60	3.23 ± 0.16	509 ± 43
			75	3.25 ± 0.16	513 ± 43
			90	3.25 ± 0.16	513 ± 43

Table 3.6. Effect of Ac2-26 on haemodynamic parameters of 100nM PAF inflamed cremasteric venules of FPR$^{-/-}$ mice. FPR$^{-/-}$ mice were prepared for intravital microscopy of the cremaster muscle. Mice were treated with either PBS or 200 μg Ac2-26 (time 0) and then superfused with 100 nM PAF. Vessel diameter and RBC velocity were measured and WSR calculated. Values are mean±sem of n=4 mice per group.

Summary

The superfusion of 100 nM PAF in the $FPR^{-/-}$ animals caused a decrease in cell rolling velocity with no effect on cell flux. Also, it caused a significant increase in cell adhesion and emigration. The administration of peptide Ac2-26 delayed the recruitment of adherent and emigrated cells so there was a significant reduction in numbers of emigrated cells compared to the vehicle treated controls over the 90 min of PAF superfusion. The extent of the inhibitory effect of the peptide Ac2-26 in the microcirculation of $FPR^{-/-}$ mice was quantitatively and qualitatively similar to that observed in the C57BL/6 mice.

Discussion

4. Discussion

The first year of this PhD study was spent learning the peritonitis model, the FACS and intravital microscopy techniques. Some problems were encountered during this PhD that were due to a shortage of ANX-A1$^{-/-}$ mice for experiments and there were also problems with animal licensing procedures. The next two years focused on the intravital technique which had been learnt during a one month visit to the laboratory of Dr. N. Granger in Louisiana State University, Shreveport, USA.

4.1. Flow Cytometry

- *More neutrophils and less monocytic cells are found in the peritoneal cavity of the ANX-A1$^{-/-}$ mouse after 4 hr zymosan peritonitis compared to the ANX-A1$^{+/+}$.*

Zymosan is a cell wall extract of the yeast, *Saccharomyces cerevisiae* that is widely used to promote inflammation, particularly in the peritoneal cavity where it induces a potent peritonitis. Zymosan initiates a complex inflammation via number of different pathways including stimulation of resident and infiltrating cells to release inflammatory mediators, activation of the alternative complement pathway and biosynthesis of eicosanoids. The zymosan-peritonitis model in the mouse has been well characterised (Ajuebor *et al.*, 1998a; Kolaczkowska *et al.*, 2001; Konno & Tsurufuji, 1983; Rao *et al.*, 1994). Administration of zymosan (1 mg by i.p. injection) produces a time dependent recruitment of inflammatory cells into the peritoneal cavity. Neutrophils begin to enter the cavity after the injection and increase up until 6 hr. By 24 hr the numbers are much lower (than at 6 hr) but not quite back to basal levels. The influx of

cells is maximal between 2 and 4 hr. Monocytic cells show an initial disappearance at 2 hr but then a steady increase over the rest of the 24 hr time course (Ajuebor *et al.*, 1998a; Kolaczkowska *et al.*, 2001).

The resident cells, macrophages and mast cells, are in close proximity to the post-capillary venules and are important in producing at least some of the initial signals responsible for the accumulation of cells in the peritoneal cavity. Experiments in which mast cells are depleted (by at least 95%) show a reduced PMN accumulation, likely due to the decreased levels of released chemokines (Ajuebor *et al.*, 1999). In line with this study, mast cell-deficient mice show a significantly lower degree of PMN influx in response to 6 hr zymosan treatment with decreased chemoattractant activity (measured in a chemotaxis assay) and decreased levels of inflammatory cytokines such as IL-1β and TNF-α compared to control mice. These defects were corrected in mast cell deficient mice by adoptive transfer of mast cells from congenic control mice (intraperitoneal transfer 3 weeks prior to peritonitis of cultured bone marrow-derived mast cells derived from congenic controls) (Kolaczkowska *et al.*, 2001). Peritoneal mesothelial cells are another resident cell type found in the peritoneal cavity that also contribute to inflammation in response to zymosan. They release cytokines and chemokines and zymosan also directly induces them to release NO (Yao *et al.*, 2004).

Many chemokines have been shown to involved in zymosan peritonitis and are rapidly released into the peritoneal cavity between 1 and 4 hr post zymosan injection with levels then returning towards basal by 24 hr. The CC chemokines, which are predominantly chemotactic for mononuclear cells, such as MIP-1α and MCP-1 have been shown to be produced as well as certain CXC chemokines such as MIP-2 and KC,

which are both chemotactic for neutrophils (Ajuebor *et al.*, 1998a; Ajuebor *et al.*, 1998c). Inflammatory cytokines such as TNF-α and IL-1β are also released in a similar pattern (Ajuebor *et al.*, 1998a; Kolaczkowska *et al.*, 2001; Perretti *et al.*, 1992). It has also been demonstrated that the anti-inflammatory cytokine IL-10 is released in this model (Ajuebor *et al.*, 1999). Therefore a balance between pro-inflammatory and anti-inflammatory signals in the peritoneal cavity regulates the response to zymosan.

Eicosanoids produced during zymosan peritonitis are also involved in the regulation of inflammatory cell recruitment, with release of LTC_4 arising predominately from resident cells and LTB_4 from both resident but mainly from infiltrating cells (Rao *et al.*, 1994). These are important in the inflammatory process as they can increase vascular permeability (LTC_4) and mediate many stages of inflammation including recruitment and activation of other inflammatory cells (LTB_4).

Work presented in this thesis uses the well-established protocol for zymosan-induced peritonitis although rather than having to manually distinguish and count cells a more objective protocol has been used (Henderson *et al.*, 2001). Gr-1 is a cell surface, 21-25 kDa protein found on cells of the myeloid lineage (Fleming *et al.*, 1993). It can be used to distinguish neutrophils as these cells stain highly for Gr-1 whereas monocytes and macrophages are either negative or have very low staining for Gr-1 (Lagasse & Weissman, 1996). F4/80 is a 160 kDa glycoprotein found on the surface of murine macrophages and blood monocytes. It can be used to distinguish these cells from PMN as both peritoneal macrophages (Austyn & Gordon, 1981) and circulating blood monocytes (Nussenzweig *et al.*, 1981) stain positively for F4/80 whereas PMN are negative for this marker (Austyn & Gordon, 1981). As lymphocytes do not stain

positively for either marker this fact can be used to remove these cells from the analysis. A comparison of the data obtained by the two methods shows that this is a specific technique that can be used to accurately and reproducibly assess the levels of different myeloid cells (neutrophils and monocytic cells) in the peritoneal cavity of the mouse. It also has the added benefit of being able to measure the levels of other cell marker on these cells simultaneously.

In line with the data obtained by manual cell counting, zymosan induced time-dependent recruitment of neutrophils into the peritoneal cavity could be quantified. As ANX-A1 has been shown to be an inhibitory mediator of inflammation (see Introduction) mice with no ANX-A1 (ANX-A1$^{-/-}$) may be expected to have a greater inflammation compared to the ANX-A1$^{+/+}$. This might explain the increased levels of neutrophils found in the peritoneal cavity of ANX-A1$^{-/-}$ mice after 4 hr zymosan peritonitis. This would fit in with previous work from the department showing that neutralisation of endogenous ANX-A1 successfully reverted the anti-migratory effect of DEX in zymosan peritonitis (Getting *et al.*, 1997; Perretti *et al.*, 1996a; Perretti *et al.*, 1996b). Addition of exogenous ANX-A1 or Ac2-26 reduces the influx produced by zymosan (Getting *et al.*, 1997; Perretti *et al.*, 1993). These data predated the initial experiments performed with the ANX-A1$^{-/-}$ mice. Indeed, an increased level of neutrophil emigration (4 hr) after zymosan was observed in the ANX-A1$^{-/-}$ mice (Hannon *et al.*, 2002). The data produced in this thesis confirm these findings, however this is the first time that peritonitis has been analysed using a more objective flow cytometry protocol. Using the combined Gr-1 and F4/80 analysis the ANX-A1$^{-/-}$ mice show a significantly lower level of monocytic cells at the 4 hr time-point when compared the ANX-A1$^{+/+}$. Ajuebor *et al* and others noted the disappearance of

monocytic cells from the peritoneal lavage fluids at 2 hr in normal mice. It has been suggested that this could be a "consequence of a generalised activation and adhesion to the internal mucosa layers" (Ajuebor *et al.*, 1998a; Kolaczkowska *et al.*, 2001). The numbers of F4/80 positive cells returned to normal by the 24 hr time-point. This could be due to the activated cells in the cavity detaching from the internal mucosa to be freely available within the cavity rather than due to the influx of newly recruited monocytes. In the case of the ANX-A1$^{-/-}$ mice therefore, there could be a delay in cell detachment from the inside of the cavity and/or the cells could be more activated and therefore more firmly adherent. This idea would fit with previous data, for example, it has been shown that when exogenous ANX-A1 (native protein or peptide Ac2-26) is administered adherent cells detach in inflamed mouse mesenteric post-capillary venules (Gavins *et al.*, 2003; Lim *et al.*, 1998). So it is possible that when the ANX-A1 gene is absent, and no ANX-A1 protein is present, the detachment process is delayed or diminished leading to a reduced return of monocytic cells to the peritoneal cavity. Alternatively, or in conjunction with this hypothesis, is the possibility that the F4/80 positive cells could be more highly activated and more firmly adherent to the cavity wall, so that it takes longer for the cells to detach and to appear in the cavity.

Along these lines, macrophages have been shown to be "super-sensitive" to an inflammatory stimulus (Yona *et al.*, 2004). Although basal CD11b expression has been shown to be significantly reduced in the ANX-A1$^{-/-}$ mice compared to the ANX-A1$^{+/+}$ mice, cell activation by either fMLP or PAF augmented expression of CD11b on ANX-A1$^{-/-}$ cells to a higher degree than on the ANX-A1$^{+/+}$ cells (Hannon *et al.*, 2002). Data presented in this thesis reports on CD11b expression in cells that have migrated into the peritoneal cavity in response to an inflammatory stimulus. These cells are clearly in an

activated state as they rolled, adhered and eventually emigrated through post-capillary venules to reach the cavity. Therefore CD11b expression was examined to highlight any alterations in the molecules expression which could be responsible for the differences seen in cell recruitment into the peritoneal cavity. Neither neutrophils nor monocytic cells collected from the 4 hr zymosan-treated mice showed a significantly different CD11b expression between genotypes. Also, the process of cell migration itself is accompanied by CD11b up-regulation (Jutila *et al.*, 1989; Mori *et al.*, 2000) such that it could be difficult to demonstrate differences modulated by any mediator as each extravasated cell may fully display CD11b on the cell surface.

Cytokines released into the peritoneal cavity were measured in ANX-A1$^{-/-}$ and ANX-A1$^{+/+}$ mice before and after zymosan peritonitis. Although levels of TNF-α and KC were not found to be different between genotypes after 4 hr zymosan treatment this does not rule out the possibility that differences in cytokine levels between genotypes are, at least in part, responsible for differences in cell recruitment seen. Differences in cytokine levels may well be altered at time-points prior to 4 hr and this could cause a greater degree of cell recruitment in the ANX-A1$^{-/-}$ mice compared to the ANX-A1$^{+/+}$ mice. Indeed, an increased IL-1β level was described in response to 2 hr zymosan peritonitis in the ANX-A1$^{-/-}$ mice (Hannon *et al.*, 2002). This may be one of the reasons why cell emigration is increased in the ANX-A1$^{-/-}$ mice. Although this study would have benefited from examination of more time-points, this was not possible because of constraints on the numbers of ANX-A1$^{-/-}$ mice available. And the 4 hr time-point was chosen as this gave a reproducible and well-defined inflammatory response.

- *Less neutrophils and more monocytic cells are found in the peritoneal cavity of the male ANX-A1^{TG} mice after 4 hr zymosan peritonitis compared to the ANX-A1^{LM}.*

Using the same model of zymosan peritonitis in male ANX-A1^{TG} mice gave an almost opposite result to the ANX-A1$^{-/-}$ mice. These are the first investigations of innate immunity in these mice which were generated by Dr. N. Wells and which we were very fortunate to have access to for this thesis. However, it is clear that these mice will require further analysis and characterisation. In any case, a dramatic difference in the ANX-A1^{TG} mice was measured compared to the matched littermates (ANX-A1^{LM}), using the flow cytometry protocol introduced into the laboratory during this study.

At the 4 hr time-point of zymosan peritonitis, significantly lower numbers of Gr-1 positive cells (neutrophils) were found in the cavity of the ANX-A1^{TG} mice compared to the ANX-A1^{LM} mice. This marked effect was mirrored by the detection of significantly higher numbers of F4/80 positive cells. It therefore seems that the over expression of ANX-A1 is able to reduce the level of inflammation in response to zymosan. Over-expressing ANX-A1 therefore produces similar results to administration of exogenous ANX-A1 protein or peptide (Getting *et al.*, 1997; Perretti *et al.*, 1993). As no data has yet been published using these mice this is a completely novel finding which fits in very well with the previous literature in the field. In addition, the data obtained for the ANX-A1^{TG} mice are in line with the augmented response to zymosan quantified in the ANX-A1$^{-/-}$ mice.

Interestingly, female ANX-A1^{TG} mice did not show any reduction in the inflammatory response to zymosan compared to the ANX-A1^{LM} mice which is in contrast to the

results obtained with the male ANX-A1^{TG} mice. The female ANX-A1$^{-/-}$ mice respond to zymosan peritonitis with a strong leukopenia as a result of a dramatic reduction in circulating neutrophils (Hannon *et al.*, 2002). This response is not seen in male mice suggesting a link between the sex hormones and the ANX-A1 system. The data obtained with the female ANX-A1^{TG} mice also suggest that the sex hormones may contribute to the anti-inflammatory actions seen when over-expressing ANX-A1. Some other sex related differences have also been observed in this study, for examples, almost double the amount of TNF-α was measured in peritoneal fluids from female mice compared to the males. This is not unusual; for example, in mice with a model of liver injury induced by concanavlin-A greater plasma levels of TNF-α are found in female mice during the injury (Takamoto *et al.*, 2003). Macrophages from female mice with cartilage implants as a model of chronic inflammation release higher levels of IL-1β compared to males (Da Silva *et al.*, 1993). As many studies have shown that females mount a greater inflammatory response in a number of cell-mediated and humoral immune responses (e.g. Grossman, 1989) this greater response may be masking the protective effects likely due to the over-expression of ANX-A1.

- *Different degrees of ANX-A1 degradation are seen in individual mice*

ANX-A1 is proteolytically cleaved *in vitro* by elastase yielding a number of degradation products with Mw ranging from 18-33 kDa (Huang *et al.*, 1987). Human neutrophil elastase cleaves native 37 kDa ANX-A1 to a 34 kDa protein *in vitro*, and samples of human bronchoalveloar lavage (BAL) fluids containing a higher number of PMN have proportionally less native ANX-A1 (and more degraded ANX-A1) compared to samples with less PMN (Smith *et al.*, 1990). A similar finding was made

when examining ANX-A1 in BAL fluids from patients with interstitial lung diseases, those containing the degraded form of ANX-A1 were those containing a higher percentage of neutrophils (Tsao *et al.*, 1998). Western blotting data from this thesis have shown in some cases, cells of both genotypes, showed a double band for ANX-A1 that corresponded to intact ANX-A1 and degraded ANX-A1 whereas others only contained the lower band corresponding to the degraded form of ANX-A1. A few samples were assessed to see if a correlation exists between the levels of neutrophils found in the peritoneal cavity inflamed with zymosan and the mass of ANX-A1 as assessed by western blotting. Animals with less Gr-1 positive events (less neutrophils) exhibited more degraded ANX-A1 and less native ANX-A1 compared to animals with more neutrophils. This does not entirely fit with the human study where patients with abnormal lungs that contained more PMN had more of the degraded ANX-A1 (Smith *et al.*, 1990). However, both this study in mice and the previous work with humans have noted that the proportion of native to degraded ANX-A1 can vary a great deal between subjects (Smith *et al.*, 1990). It is now accepted in the literature that the source of exudate ANX-A1 is mainly the extravasated neutrophils such that higher numbers of tissue neutrophils are associated with higher ANX-A1 content (Oliani *et al.*, 2001). In addition, neutrophil-infiltrated tissues, such as the gut of rats with induced colitis, display active secretion of ANX-A1 (Vergnolle *et al.*, 1995). Thus, a scenario is emerging, in which endogenous ANX-A1 moderates neutrophil recruitment (see data with ANX-A1$^{-/-}$ and ANX-A1^{TG} mice in the zymosan peritonitis model), however, once the cells have emigrated there is active *de novo* ANX-A1 synthesis (Oliani *et al.*, 2001). The western blot data obtained show higher ANX-A1 degradation in conditions of higher neutrophil numbers. It is likely that a greater concentration of elastase or other serine proteases could be the cause of this.

In addition, it has been suggested that the degraded form of ANX-A1 is inactive as it is the N-terminal of the protein is cleaved (Smith *et al.*, 1990) and this part confers the anti-inflammatory properties of the protein. In BAL fluid from smokers the predominant form of ANX-A1 is the degraded isoform whereas the native protein was predominant in non-smokers (Vishwanatha *et al.*, 1998). BAL fluid from patients with cystic fibrosis also exhibited degradation of ANX-A1 whereas normal volunteers had very little of the degraded protein (Tsao *et al.*, 1998). As emigrated cells in rat mesentery have been shown to contain more of the degraded/clipped isoform of ANX-A1 compared to intact ANX-A1 (Oliani *et al.*, 2001) this may be a mechanism that down-regulates inflammation in normal situations. However, in certain disease states the degradation and therefore inactivation of ANX-A1 may be important in contributing to the inflammation that characterises them.

- *No difference was found in cell numbers in the peritoneal cavity of the ANX-A1$^{-/-}$ mouse after 4 h IL-1β peritonitis compared to the ANX-A1$^{+/+}$ animals.*

The IL-1β-induced peritonitis model has also been characterised in our department (Ajuebor *et al.*, 1998b). IL-1β injection (10 ng) into the peritoneal cavity causes a time-dependent accumulation of PMN. As in the zymosan-induced model, the maximal influx of PMN into the peritoneal cavity is between 1 and 4 hr post injection. Peak cell numbers are counted at 4 hr post injection and numbers remain high, even at 24 hr. In contrast to the zymosan model levels of monocytic cells are not seen to change over 24 hr (Ajuebor *et al.*, 1998b). The data obtained for this thesis does not follow the previous study however, in the ANX-A1$^{+/+}$ the numbers had returned to

basal by 24 hr. However, the profile of monocytic cells remained stable over 24 hr following the previous study. Differences could be due to a number of factors including the different species used for each study. Of most importance, and in contrast to the zymosan-peritonitis model, no differences were found between ANX-A1$^{-/-}$ and ANX-A1$^{+/+}$ mice with respect to the cell numbers found in the peritoneal cavity after 4 hr IL-1β peritonitis.

It is clear that zymosan and IL-1β are very different inflammatory stimuli. Zymosan can activate a very complex inflammatory response whereby a number of different pathways are activated leading to endothelial cell activation. IL-1β also initiates inflammation which is largely attributed to the direct activation of endothelial cells leading to induction of endothelial CAM such as E-selectin and ICAM-1 (Bevilacqua *et al.*, 1987; Dustin *et al.*, 1986; Osborn *et al.*, 1989). This means that many other pathways activated by zymosan may not be activated in the IL-1β model and although endothelial cells are activated and leukocytes recruited in both cases, the two models are different from each other. Figure 4.1 is a very simple schematic to show how zymosan and IL-1β could induce inflammation. As ANX-A1$^{-/-}$ and ANX-A1$^{+/+}$ mice do not respond differently to IL-1β-induced inflammation but respond with increased leukocyte emigration in zymosan-induced peritonitis this could suggest that one difference in the ANX-A1$^{-/-}$ mice is in a pathway other than the IL-1β route. For example, as mentioned previously IL-10, a cytokine with anti-inflammatory properties is released during zymosan-peritonitis (Ajuebor *et al.*, 1999). A recent *in vitro* study has demonstrated that hrANX-A1 can stimulate the release of IL-10 from a macrophage cell line primed with LPS (Ferlazzo *et al.*, 2003). If this pathway is down regulated in the ANX-A1$^{-/-}$ it could cause a higher degree of inflammation. Recent

work in the department showed that ANX-A1$^{-/-}$ macrophages are more susceptible to activation following stimulation with several stimuli; for instance, they produce more PGE_2 after LPS addition (Yona *et al.*, 2004). An inherent defect in the ANX-A1$^{-/-}$ macrophages (and maybe mast cells) could be responsible, in part, for the modulation exerted by endogenous ANX-A1 in the peritonitis response produced by zymosan. This step, involving resident cells, is likely by-passed by IL-1β, such that the difference seen when zymosan is used as a stimulus, was not seen when using IL-1β as a stimulus.

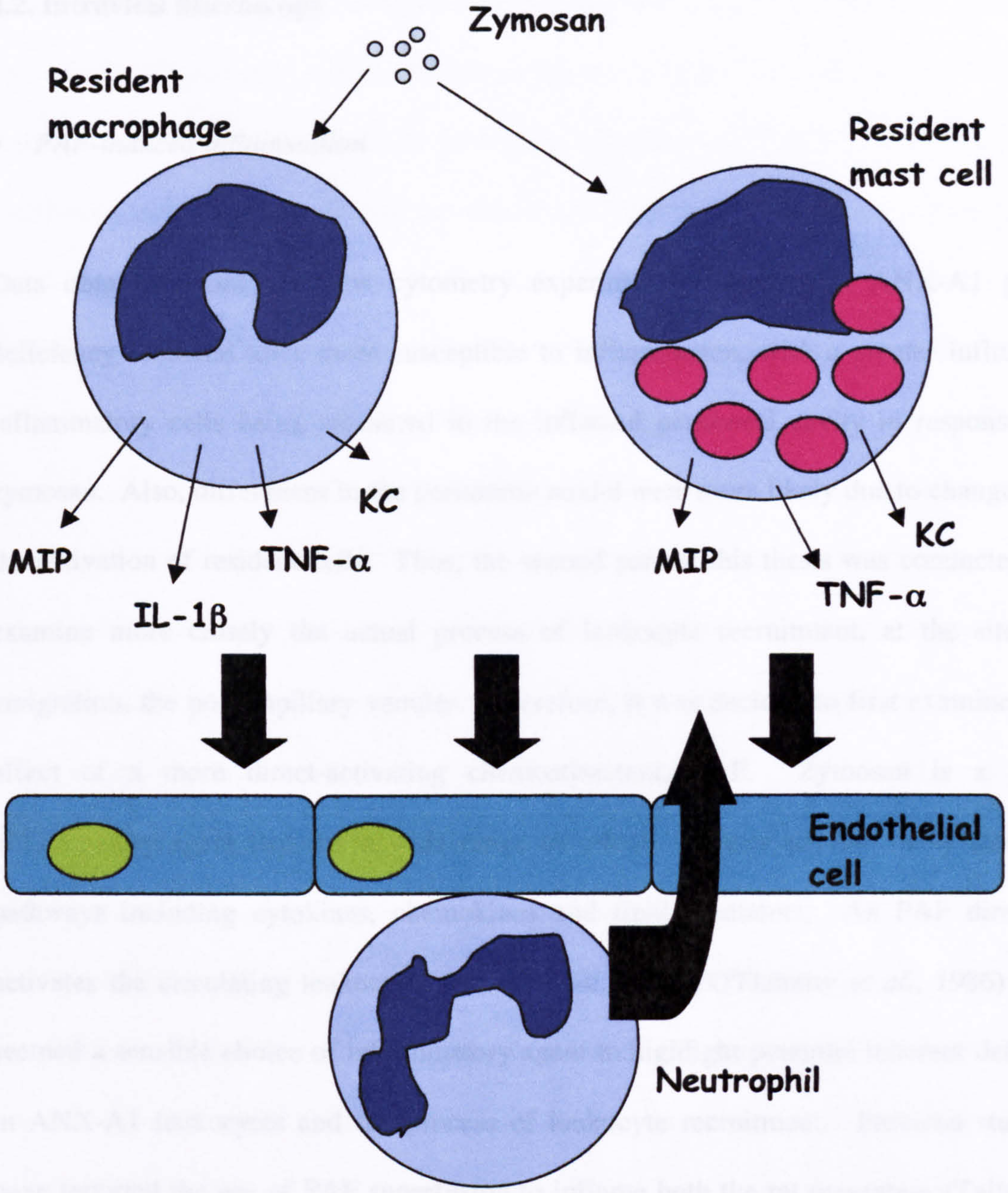

Figure 4.1. Schematic to show how zymosan and IL-1β can induce inflammation. Zymosan can activate resident leukocytes and tissue cells to produce pro-inflammatory cytokines including IL-1β. These activate endothelial cells leading to the eventual recruitment of leukocytes into the tissue.

4.2. Intravital Microscopy

- *PAF-induced inflammation*

Data obtained from the flow cytometry experiments showed that ANX-A1 gene deficiency rendered mice more susceptible to inflammation, with a greater influx of inflammatory cells being measured in the inflamed peritoneal cavity in response to zymosan. Also, differences in the peritonitis model were more likely due to changes in the activation of resident cells. Thus, the second part of this thesis was conducted to examine more closely the actual process of leukocyte recruitment, at the site of emigration, the post-capillary venules. Therefore, it was decided to first examine the effect of a more direct-activating chemoattractant, PAF. Zymosan is a pro-inflammatory agent that has a wide range of effects. It can activate many distinct pathways including cytokines, chemokines and lipid mediators. As PAF directly activates the circulating leukocytes (Kubes *et al.*, 1990; O'Flaherty *et al.*, 1986) this seemed a sensible choice of inflammatory agent to highlight potential inherent defects in ANX-A1 leukocytes and the process of leukocyte recruitment. Previous studies have reported the use of PAF superfusion to inflame both the rat mesentery (Tailor *et al.*, 1997; Zimmerman *et al.*, 1994) and the mouse cremaster muscle (Henninger *et al.*, 1997; Hickey *et al.*, 2000). In all of these studies, 100 nM PAF was made up in the superfusing buffer. Zimmerman and colleagues found that superfusion of the rat mesentery with PAF significantly reduced the rolling velocity of cells and significantly increased cell adhesion and emigration within 30 min superfusion (Zimmerman *et al.*, 1994). A study by Tailor and colleagues used the same strain of rat and also showed that PAF superfusion of the mesentery significantly increased cell adhesion and

emigration. However, even though leukocyte recruitment was examined over a longer time period (60 min compared to 30 min in the previous study), PAF had no effect on leukocyte rolling (velocity or flux of leukocytes) (Tailor *et al.*, 1997). A third study, by a different group, this time using the mouse cremaster muscle superfused with PAF, found that although PAF increased cell adhesion over 30 min the extent of emigration was not significantly altered (Henninger *et al.*, 1997). It is clear to see then, that before embarking on the study for this thesis, the effects of PAF superfusion would need to be carefully examined. Studies of the ANX-A1$^{+/+}$ mice showed that, in the case of the cremaster microcirculation, 100 nM PAF superfusion does indeed cause a significant inflammation over the 90 min time course examined. A time-dependent increase in cell adhesion and emigration is seen, with a reduction in leukocyte rolling velocity and cell flux. Examination of the ANX-A1$^{+/+}$ cremaster muscle under basal conditions shows that the preparation is stable over 90 min as none of the parameters indicative of inflammation (cell rolling, adhesion and emigration) are altered over the time course examined. So the model presented in this thesis was deemed suitable to use. Careful examination of the time-course of the cellular events promoted by PAF indicated that cell rolling, adhesion and emigration occurred in a time-related fashion. Indeed, the lowest WBC rolling velocity value was recorded at 30 min post start of PAF superfusion; cell adhesion was maximal at 45 to 60 min and emigration at 75 min. Since these phenomena are functionally related, this time-dependency further indicated that validity of this model.

- *Ac2-26 can abolish cell emigration in the PAF-inflamed cremaster muscle*

The action of the ANX-A1 mimetic, peptide Ac2-26 in the cremaster muscle preparation, had not previously been examined. The fact that it could significantly reduce emigration in response to PAF further reinforced the idea that this model was suitable to compare differences, if any, in leukocyte recruitment between the ANX-A1$^{-/-}$ and ANX-A1$^{+/+}$ mice. Both zymosan-induced (Lim *et al.*, 1998) and I/R-induced emigration (Gavins *et al.*, 2003) in the mouse mesentery is significantly reduced by intravenous administration of the peptide Ac2-26. Now this list can be extended to include inhibition by the peptide of PAF-induced cell emigration in the mouse cremaster muscle preparation. One difference between the models is the fact that in the mouse mesenteric preparations mentioned above the peptide was also shown to inhibit cell adhesion as well as reducing emigration. This finding was not mirrored in the cremaster preparation and the difference could be due to the difference in inflammatory stimulus and differences in the vascular beds. Interestingly, Mancuso and colleagues applied direct-acting stimuli onto the hamster cheek pouch preparation (fMLP and substance P) observing that peptide Ac2-26 displayed inhibitory effects selectively on the leukocyte emigration step (Mancuso *et al.*, 1995).

- *ANX-A1$^{-/-}$ mice exhibit a higher extent of cell emigration compared to ANX-A1$^{+/+}$ mice in response to 1 nM but not 100 nM PAF*

Data presented in this thesis show that although only minor differences were found between the ANX-A1$^{-/-}$ and the ANX-A1$^{+/+}$ cremaster microcirculation when inflamed using 100 nM PAF, bigger alterations were seen in the ANX-A1$^{-/-}$ mice when a milder

stimulus was used (1 nM PAF). In this case, cell emigration was found to be significantly higher in the ANX-A1$^{-/-}$ mice compared to the ANX-A1$^{+/+}$ mice. This is in line with unpublished work in this department, where cells from the ANX-A1$^{-/-}$ mice activated *ex-vivo* with 1 nM PAF were significantly more activated (with respect to CD11b expression) compared to the ANX-A1$^{+/+}$ cells, a difference which was not seen when using 100 nM PAF. In line with previous studies (Lim *et al.*, 1998; Mancuso *et al.*, 1995), it seems that it is the actual emigration stage of leukocyte recruitment that is affected by endogenous ANX-A1. In more general terms, these results indicate a tonic inhibitory role for endogenous ANX-A1 that can be unmasked by using moderate stimulation. This fact is unsurprising and in a way reinforces the modulatory nature of this mediator. When stronger stimuli are applied, then, its protective effect can be overcome. Similar findings were found by Yang *et al* who were able to highlight greater joint inflammation in the ANX-A1$^{-/-}$ mice when a low dose of methylated BSA was used (Yang *et al.*, 2004). Data presented in this thesis help to clarify this point further.

- *Alterations in the detachment phenomenon could be seen between ANX-A1$^{-/-}$ and ANX-A1$^{+/+}$ mice only prior to the start of inflammation*

The next step was to see if an alteration in detachment could be an explanation to as why more cells emigrate in these animals. One possible role of endogenous ANX-A1 may be to cause detachment as exogenous ANX-A1 has been shown to do this (Gavins *et al.*, 2003; Lim *et al.*, 1998; Mancuso *et al.*, 1995). If this is the case then the lack of ANX-A1 in the ANX-A1$^{-/-}$ mice could result less cell detachment and this could be a reason for the increased cell emigration found in these animals. In this context it

should be noted that the leukocyte detachment phenomenon occurs "spontaneously", i.e. without administration of ANX-A1. In fact, in the hamster cheek pouch microcirculation 20% of adherent cells were noted to detach spontaneously (Mancuso *et al.*, 1995). During neurogenic inflammation of the respiratory tract in the rat approximately half of the adherent neutrophils detached and re-entered the circulation within 4 hr of the inflammation (Umeno *et al.*, 1990). However, analysis of the detachment phenomenon proved to be complex and very time consuming. The number of adherent cells that detached rather than emigrated could be assessed and although a difference was seen between the genotypes with respect to the degree of detachment before the start of the inflammatory process this effect was lost during PAF-induced inflammation. The time taken for cells to detach was also not significantly different between the genotypes. So alterations in the detachment phenomenon *per se* do not seem responsible for differences seen between ANX-A1$^{+/+}$ and ANX-A1$^{-/-}$ mice in terms of low dose PAF–induced cell recruitment.

- *Zymosan-induced Inflammation*

As data obtained from the flow cytometry experiments demonstrated that ANX-A1$^{-/-}$ mice were more sensitive to inflammation in the zymosan peritonitis model it was decided to next study the effect of this stimulus in the cremaster muscle preparation. This stimulus has been used previously in intravital studies in both the mesentery (Lim *et al.*, 1998) and the cremaster muscle (Young *et al.*, 2004). As the response to zymosan had previously been characterised (Young *et al.*, 2004) the dose of zymosan (30 μg) and time-point (6 hr) were chosen for this study. A new technique was incorporated into the intravital procedure whereby the zymosan injected was

fluorescently labelled so that the emigrated cells could be examined for assessment of the degree of phagocytosis.

- *Leukocytes emigrate further in ANX-A1$^{-/-}$ mice compared to the ANX-A1$^{+/+}$. No difference in phagocytosis between genotypes is observed.*

A pilot study was carried out to study the effect of zymosan on both leukocyte emigration and phagocytosis. These parameters were quantified as per field of view and showed a significant increase in cell emigration in the ANX-A1$^{-/-}$ mice compared to the ANX-A1$^{+/+}$ animals. These data correlate well with the flow cytometry experiments showing that the ANX-A1$^{-/-}$ mice respond to zymosan with exaggerated leukocyte recruitment.

Recent data (Yona *et al.*, 2004) has shown that macrophages from ANX-A1$^{-/-}$ mice have a 'frustrated' phagocytosis whereby although they do phagocytose zymosan particles it takes them longer to do so. A reduction in phagocytosis was found in ANX-A1$^{-/-}$ macrophages although this was only seen with non-opsonised zymosan and not when opsonised zymosan was used (Yona *et al.*, 2004). So it was decided that the novel model of Young and colleagues would be ideal to measure phagocytosis *in vivo* and see if there were inherent differences between the ANX-A1$^{+/+}$ and the ANX-A1$^{-/-}$ animals with respect to neutrophil phagocytosis (Young *et al.*, 2004). However, the extent of phagocytosis of zymosan particles was not found to differ significantly between the ANX-A1$^{+/+}$ and the ANX-A1$^{-/-}$. These data may show that although ANX-A1 is involved in the macrophage phagocytosis process it is might not be involved in neutrophil phagocytosis. Alternatively the data obtained may substantiate the previous

study because in that study differences were not found between ANX-A1$^{-/-}$ and ANX-A1$^{+/+}$ macrophages with respect to opsonised zymosan phagocytosis (Yona *et al.*, 2004). It is likely that in the experimental conditions in this study, being injected zymosan would be opsonised thus cancelling the potential difference between the genotypes. It should also be noted that a 'frustrated' phagocytosis was reported in ANX-A1$^{-/-}$ macrophages and since zymosan was eventually phagocytosed it is also possible that the time-point used to determine neutrophil phagocytosis might have been too late to show differences in phagocytosis.

- *Cell flux, rolling, adhesion and emigration directly next to the vessel wall induced by zymosan are not significantly different between genotypes*

Since a different protocol was used for the cremaster muscle studies in Dr. S. Nourshargh's laboratory, it was deemed necessary to replicate the experimental model using a protocol similar to that applied for the PAF experiments. In this manner cell flux and rolling velocity, cell adhesion and cell emigration close to the vessel wall could be monitored. Local injection of zymosan was given into the scrotum and after 6 hr a significant inflammatory response was seen in the ANX-A1$^{+/+}$ mice with a significant increase in cell adhesion and emigration. No significant changes in response to zymosan treatment with respect to cell rolling velocity or cell flux were evident at this time-point which is in line with a previous study (Young *et al.*, 2004). This response was also seen in the ANX-A1$^{-/-}$ mice and no significant differences were found between the genotypes with respect to any of the parameters measured. This includes cell emigration which had been shown previously, in the pilot study, to be significantly higher in the ANX-A1$^{-/-}$ mice than the ANX-A1$^{+/+}$ mice. As in the first

study emigration was measured per field of view and not measured directly next to the vessel wall, the idea emerged that in the ANX-A1$^{-/-}$ mice there is an increased movement of emigrated cells further into the surrounding tissues. So using a method previously validated (Tailor *et al.*, 1997) cell emigration was assessed at different distances from the vessel under analysis. It was then observed that, in the ANX-A1$^{+/+}$ mice, the numbers of cells that had emigrated into the tissue decreased significantly the further from the vessel wall the measurement was made. In the ANX-A1$^{-/-}$ cells had emigrated further before the numbers decreased significantly from the initial emigration seen directly next to the vessel wall. Thus, ANX-A1$^{-/-}$ neutrophils likely have an increased movement into the sub-endothelial tissues/space.

Previous intravital studies along with data produced in this thesis have shown that administration of the ANX-A1 mimetic peptide, Ac2-26 has no effect on rolling velocity whilst still being able to reduce cell adhesion (although not in the cremaster) and emigration (Gavins *et al.*, 2003; Lim *et al.*, 1998). Emigration is altered in the ANX-A1$^{-/-}$ mice compared to the ANX-A1$^{+/+}$ with no difference in rolling and adhesion seen. As rolling is predominantly mediated by the selectin family of adhesion molecules the lack of effect of Ac2-26 on rolling suggests that ANX-A1 is unlikely to exert its anti-inflammatory activities by action on selectin expression and/or function. However, recent investigations have suggested another role for L-selectin, that is modulation of some of the inflammatory events downstream of rolling, i.e. emigration and extravascular locomotion (Hickey *et al.*, 2000). During PAF-induced inflammation of the mouse cremaster muscle, the absence of L-selectin (L-selectin$^{-/-}$ animals) reduces leukocyte emigration without effect on leukocyte rolling or adhesion. The leukocytes that did emigrate in the L-selectin$^{-/-}$ mice did not travel as far into the

extravascular tissue as wild type leukocytes, even though they were travelling at a similar velocity. This was the case for both non-directional locomotion (induced by PAF or KC superfusion) and also for directional chemotaxis (induced by controlled release of KC in the cremaster) (Hickey *et al.*, 2000). It seems, therefore, that L-selectin may also have a role in leukocyte emigration and extravascular locomotion.

It has been noted that GC can induce L-selectin shedding form peripheral blood neutrophils (Jilma *et al.*, 1997). It is possible that this may be one mechanism by which GC inhibit neutrophil recruitment *in vivo*. However, GC have not been shown to directly cause L-selectin shedding. DEX applied to human peripheral blood does not alter L-selectin expression whereas ANX-A1 does induce a dose-dependent decrease in L-selectin expression on blood neutrophils and monocytes (Strausbaugh & Rosen, 2001). Blocking L-selectin shedding (using a sheddase inhibitor) attenuates the ANX-A1 decrease in L-selectin expression (Strausbaugh & Rosen, 2001). So ANX-A1 may be a mediator for GC-induced L-selectin shedding *in vivo*, and this may be at least one of the mechanisms responsible for the regulation of the inflammatory response exerted by endogenous ANX-A1. To look more closely at the role of L-selectin shedding, the process can be blocked using inhibitors or by using mice with mutant versions of L-selectin. In a model of L-selectin dependent rolling in the cremaster intravital model (TNF-α stimulated E/P-selectin$^{-/-}$ mice), the blockade of L-selectin shedding was achieved using a hydroxamic acid derivative, KD-IX-73-4 (Hafezi-Moghadam *et al.*, 2001). The rolling velocity of leukocytes was reduced and cell adhesion and emigration increased. In addition to this, leukocytes were more activated. This group suggested that by blocking the continuous L-selectin shedding that occurs in vessels leads to less jerky leukocyte rolling which in turn allows cells to be in closer contact

with the endothelium and inflammatory signals so this leads to increased activation, adhesion and emigration (Hafezi-Moghadam *et al.*, 2001). Another study used gene-targeted mice which express modified L-selectin resistant to cleavage. These mice had increased numbers of neutrophils migrating into the peritoneal cavity in response to thioglycollate challenge and the response was prolonged, i.e. numbers of leukocytes in the cavity were still high after 24 hr (whereas in the wild type mice the numbers were decreasing) (Venturi *et al.*, 2003). These results indicate that L-selectin cleavage and shedding is not an absolute requirement for emigration but also that in the absence of L-selectin shedding the density on cells is increased or maintained and this facilitates the entry of neutrophil to the peritoneal cavity. The shedding of L-selectin may be a physiological process that regulates leukocyte recruitment such that it dampens down the inflammatory response. When exogenous ANX-A1 is administered it may cause or increase the degree of L-selectin shedding, however cells may not be committed to emigration and so they detach (Gavins *et al.*, 2003; Lim *et al.*, 1998) and in this way leukocyte recruitment could be reduced. The removal of the ANX-A1 gene in the ANX-A1$^{-/-}$ mice could mean that there is an absence or reduction in L-selectin shedding in response to inflammatory stimuli and this may be functionally linked to the greater degree of cell extravasation observed these animals.

Another related point is that L-selectin$^{-/-}$ mice have reduced emigration and reduced movement from the vessel wall into the extravascular tissues (Hickey *et al.*, 2000). If ANX-A1 is involved in patho-physiological L-selectin shedding, then the cells of the ANX-A1$^{-/-}$ mice would have a lower degree of L-selectin shedding so the emigrating leukocyte would have a greater density of L-selectin on their surface. In fact, higher levels of L-selectin have been reported on peripheral blood neutrophils and monocytes

taken from ANX-A1$^{-/-}$ mice (Hannon *et al.*, 2002). This could lead to an effect opposite to what is seen in the L-selectin$^{-/-}$ mice, i.e. there may be an increased movement of emigrated cells and so they move further from the vessel wall. This could begin to explain some of the results obtained in this thesis. Data obtained from zymosan-induced inflammation of the cremaster muscle showed no significant difference between the ANX-A1$^{+/+}$ and the ANX-A1$^{-/-}$ mice with respect to cell emigration when it was measured directly next to the vessel wall. However, when emigration further into the tissue was analysed a significantly higher number of emigrated cells were found in the ANX-A1$^{-/-}$ mice compared to the ANX-A1$^{+/+}$ mice. This may be due the higher L-selectin density on the surface of ANX-A1$^{-/-}$ cells (due to the fact that ANX-A1 is not present to induce/increase L-selectin shedding) causing the cells to emigrate further from the vessel wall. This may also explain why a greater difference was seen when inflammation was induced using 1 nM PAF but not with 100 nM PAF. The higher dose of PAF may induce more emigration than the lower dose but as cells from the ANX-A1$^{-/-}$ animals have higher L-selectin levels (as ANX-A1 not present to increase shedding) they may have emigrated further from the vessel. However, these differences may not be seen between genotypes when cell emigration was assessed immediately adjacent to the vessel wall. In the case of 1 nM PAF, as this was a milder stimulus the cells would take longer to emigrate, and at the time-points examined the cells were still close to the vessel and so a difference was found between genotypes. Figure 4.2. is a simple summary of these ideas. This scheme highlights the importance of the time frame during which the mice are examined. Differences obviously exist between the genotypes as has been shown with 1 nM PAF and zymosan but there may be certain times where greater differences between genotypes will be detected and other times where no differences will be found. Future assessment of

ANX-A1 inhibitory (anti-migratory) properties in genetically modified mice (mice deficient in L-selectin or with an uncleavable version of L-selectin) would be of great help to test this hypothesis.

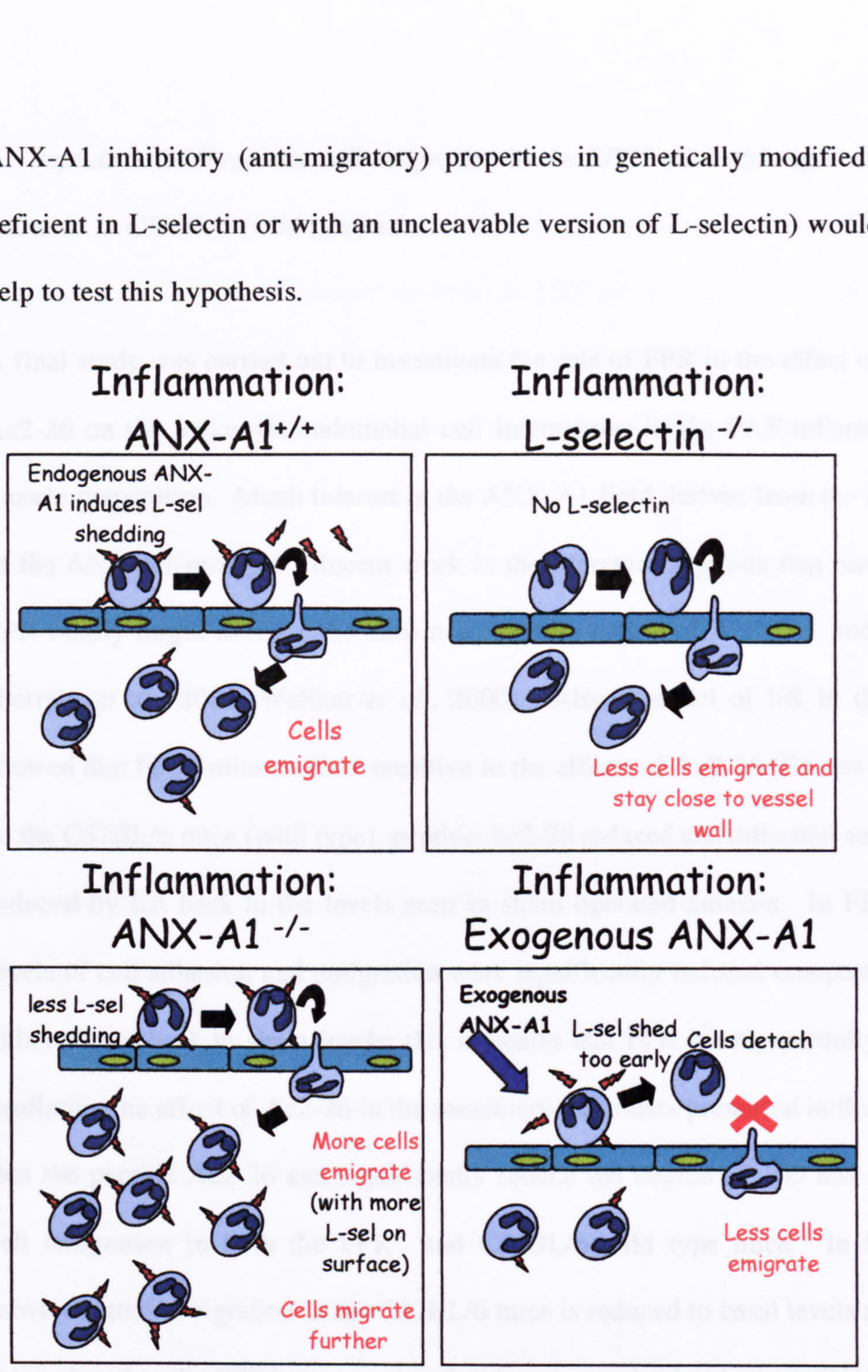

Figure 4.2. ANX-A1 and L-selectin shedding. Simple summary diagram to explain suggestion that ANX-A1-induced shedding of L-selectin could regulate leukocyte recruitment during inflammation.

- *Peptide Ac2-26 reduces cell emigration in the FPR$^{-/-}$ mice although not to the same extent as in C57BL/6 (wild type) mice*

A final study was carried out to investigate the role of FPR in the effect of the peptide Ac2-26 on the leukocyte-endothelial cell interactions in the PAF-inflamed cremaster muscle preparation. Much interest in the ANX-A1 field derives from the identification of the ANX-A1 receptor. Recent work in the literature suggests that members of the FPR family might mediate the anti-inflammatory action of ANX-A1 and its peptides (Perretti *et al.*, 2002; Walther *et al.*, 2000). Also a model of I/R in the mesentery showed that FPR$^{-/-}$ mice are less sensitive to the effects of Ac2-26 (Gavins *et al.*, 2003). In the C57BL/6 mice (wild type), peptide Ac2-26 reduced cell adhesion and emigration induced by I/R back to the levels seen in sham operated animals. In FPR$^{-/-}$ mice the levels of cell adhesion and emigration were significantly reduced compared to vehicle, although not back to sham levels; this indicates that FPR is only partially involved in mediating the effect of Ac2-26 in the mesentery. The data presented in this thesis show that the peptide Ac2-26 can significantly reduce the degree of 100 nM PAF-induced cell emigration in both the FPR$^{-/-}$ and C57BL/6 wild type mice. In line with the previous study emigration in the C57BL/6 mice is reduced to basal levels and, although it is reduced in the FPR$^{-/-}$ mice, emigration is not completely blocked. This supports the notion that FPR whilst important is not the sole receptor responsible for the anti-inflammatory actions of ANX-A1. In contrast to the previous study however, cell adhesion seems to be unaffected by the addition of exogenous Ac2-26 (even though a higher dose was used here). The effect of the peptide seems to be dependent either on the vascular bed examined or the inflammatory stimulus used. This conclusion is clearly in line with that observed for native ANX-A1. Another recent study that

illustrates this point well is the effect of peptide Ac2-26 in a model of heart I/R in the rat. I/R of the heart produces significant damage to the heart ventricle and this could be reduced by the administration of peptide Ac2-26 given after the reperfusion period. None of the doses of peptide tested managed completely to reverse the damage levels back to sham levels. To assess the potential role of FPR in the protective effects of Ac2-26, the FPR antagonist Boc2 was used. Boc2 significantly reversed the actions of Ac2-26 reinforcing the proposal that ANX-A1 peptides interact with FPR (La *et al.*, 2001). A similar finding is made in the mouse model (Gavins *et al.*, 2004), that is, Ac2-26 is protective in heart I/R and these effects are blocked by the FPR antagonist, Boc2. However, this study looked more in depth at the role of FPR by using mice deficient in this receptor ($FPR^{-/-}$ mice). The same protective effect of Ac2-26 was also seen in these mice indicating that the FPR is not the receptor responsible for the effects of ANX-A1 in the heart model. In the case of heart I/R different results are obtained to those from I/R of the mesentery where complete inhibition by peptide Ac2-26 is seen and a partial role for FPR can be found. This is another case of tissue specific actions of peptide Ac2-26, which may be linked to the receptor expression in different tissues.

4.3. Conclusion

In summary, this study has found;

Peritonitis induced by zymosan-, but not IL-1β-, in the ANX-A1$^{-/-}$ mice leads to higher levels of inflammatory cell recruitment, i.e. more inflammation, at the 4 hr time-point than in the ANX-A1$^{+/+}$ mice.

Male ANX-A1^{TG} mice show reduced cell recruitment, in response to 4 hr zymosan peritonitis. This is effectively the opposite result to that obtained in the ANX-A1$^{-/-}$ mice. This pattern is however not seen in female mice.

In the mouse cremaster muscle peptide Ac2-26 can effectively abolish cell emigration induced using 100 nM PAF superfusion with no effect on cell adhesion or rolling.

ANX-A1$^{-/-}$ mice have a significantly higher cell emigration in response to 1 nM PAF superfusion as measured by the intravital microscopy studies in the cremaster muscle with no differences being found in cell rolling or adhesion. Basal leukocyte recruitment and inflammation induced by a higher concentration of PAF (100 nM) are not significantly different between the ANX-A1$^{-/-}$ and ANX-A1$^{+/+}$ mice.

Local injection of zymosan causes a similar effect on cell rolling velocity, increase in cell adhesion and initial cell emigration in the cremaster muscle preparation in both genotypes however, in the ANX-A1$^{-/-}$ there is an increased movement of emigrated

cells from the blood vessel. No difference in phagocytosis by emigrated cells in ANX-A1$^{+/+}$ and ANX-A1$^{-/-}$ mice was seen.

Peptide Ac2-26 can reduce, but not abolish, cell emigration in the cremaster muscle of FPR$^{-/-}$ mice inflamed with 100 nM PAF suggesting FPR is not the sole receptor responsible for the anti-inflammatory actions of ANX-A1. The peptide does not affect cell rolling or adhesion in this model.

Data obtained in this thesis have helped to dissect out the role of endogenous ANX-A1 in inflammatory conditions and add considerably to the few data so far obtained in the newly generated ANX-A1$^{-/-}$ mice. It seems the effect of removal of the ANX-A1 gene is not as striking as may have been expected from the many previous studies using exogenous ANX-A1 and its peptido-mimetics. What has become clear is the role of endogenous ANX-A1 as a *modulator* of inflammation, although careful choice of time-points and inflammatory agents are needed to unmask this action.

Findings made in this study clearly need further investigation and this could form the basis of further PhD studies in the department. Important experiments would be to deduce further the actual mechanism by which ANX-A1 is modulating the inflammatory response. An example for future experiments could be the examination of the role of ANX-A1 in mice which are deficient in L-selectin to test further the hypothesis that ANX-A1 induced L-selectin shedding could be involved in the recruitment of leukocytes to the site of inflammation. Also future experiments could make more use of the newly developed ANX-A1^{TG} mice.

Importantly, during the completion of this PhD a number of new techniques have been introduced into our laboratory including the flow cytometry protocol as an accurate and objective method to analyse cell recruitment into the peritoneal cavity. More importantly perhaps is the introduction of the cremaster muscle preparation for intravital microscopy which mean that these experiments can now be carried out on older mice and for longer periods of time than were possible in the mesenteric preparation which was previously used.

Appendix

ADAMS, D.H. & LLOYD, A.R. (1997). Chemokines: leucocyte recruitment and activation cytokines. *Lancet*, **349**, 490-5.

AHLUWALIA, A. (1996). *The Biology of Annexin 1 in Annexins:Molecular Structure to Cellular Function.* Austin: R. G. Landes.

AJUEBOR, M.N., DAS, A.M., VIRAG, L., FLOWER, R.J., SZABO, C. & PERRETTI, M. (1999). Role of resident peritoneal macrophages and mast cells in chemokine production and neutrophil migration in acute inflammation: evidence for an inhibitory loop involving endogenous IL-10. *J Immunol*, **162**, 1685-91. frame.html.

AJUEBOR, M.N., FLOWER, R.J., HANNON, R., CHRISTIE, M., BOWERS, K., VERITY, A. & PERRETTI, M. (1998a). Endogenous monocyte chemoattractant protein-1 recruits monocytes in the zymosan peritonitis model. *J Leukoc Biol*, **63**, 108-16.

AJUEBOR, M.N., GIBBS, L., FLOWER, R.J., DAS, A.M. & PERRETTI, M. (1998b). Investigation of the functional role played by the chemokine monocyte chemoattractant protein-1 in interleukin-1-induced murine peritonitis. *Br J Pharmacol*, **125**, 319-26.

AJUEBOR, M.N., VIRAG, L., FLOWER, R.J., PERRETTI, M. & SZABO, C. (1998c). Role of inducible nitric oxide synthase in the regulation of neutrophil migration in zymosan-induced inflammation. *Immunology*, **95**, 625-30.

ALLCOCK, G.H., ALLEGRA, M., FLOWER, R.J. & PERRETTI, M. (2001). Neutrophil accumulation induced by bacterial lipopolysaccharide: effects of dexamethasone and annexin 1. *Clin Exp Immunol*, **123**, 62-7.

ANDO, Y., IMAMURA, S., HONG, Y.M., OWADA, M.K., KAKUNAGA, T. & KANNAGI, R. (1989). Enhancement of calcium sensitivity of lipocortin I in phospholipid binding induced by limited proteolysis and phosphorylation at the amino terminus as analyzed by phospholipid affinity column chromatography. *J Biol Chem*, **264**, 6948-55.

ARGENBRIGHT, L.W., LETTS, L.G. & ROTHLEIN, R. (1991). Monoclonal antibodies to the leukocyte membrane CD18 glycoprotein complex and to intercellular adhesion molecule-1 inhibit leukocyte-endothelial adhesion in rabbits. *J Leukoc Biol*, **49**, 253-7.

ARNAOUT, M.A. (1990). Structure and function of the leukocyte adhesion molecules CD11/CD18. *Blood*, **75**, 1037-50.

ASA, D., RAYCROFT, L., MA, L., AEED, P.A., KAYTES, P.S., ELHAMMER, A.P. & GENG, J.G. (1995). The P-selectin glycoprotein ligand functions as a common human leukocyte ligand for P- and E-selectins. *J Biol Chem*, **270**, 11662-70.

AUSTYN, J.M. & GORDON, S. (1981). F4/80, a monoclonal antibody directed specifically against the mouse macrophage. *Eur J Immunol*, **11**, 805-15.

BAEZ, S. (1973). An open cremaster muscle preparation for the study of blood vessels by in vivo microscopy. *Microvasc Res*, **5**, 384-94.

BAGGIOLINI, M., DEWALD, B. & MOSER, B. (1994). Interleukin-8 and related chemotactic cytokines--CXC and CC chemokines. *Adv Immunol*, **55**, 97-179.

BARNES, P.J. (1998). Anti-inflammatory actions of glucocorticoids: molecular mechanisms. *Clin Sci (Lond)*, **94**, 557-72.

BERG, J.M., TYMOCZKO, J.L. & STRYER, L. (2002). *Biochemistry*. New York: W.H. Freeman and Co.

BEVILACQUA, M.P., POBER, J.S., MENDRICK, D.L., COTRAN, R.S. & GIMBRONE, M.A., JR. (1987). Identification of an inducible endothelial-leukocyte adhesion molecule. *Proc Natl Acad Sci U S A*, **84**, 9238-42.

BOGEN, S., PAK, J., GARIFALLOU, M., DENG, X. & MULLER, W.A. (1994). Monoclonal antibody to murine PECAM-1 (CD31) blocks acute inflammation in vivo. *J Exp Med*, **179**, 1059-64.

BORREGAARD, N. & COWLAND, J.B. (1997). Granules of the human neutrophilic polymorphonuclear leukocyte. *Blood*, **89**, 3503-21.

BRADFORD, M.M. (1976). A rapid and sensitive method for the quantitation of microgram quantities of protein utilizing the principle of protein-dye binding. *Anal Biochem*, **72**, 248-54.

CAREY, F., FORDER, R., EDGE, M.D., GREENE, A.R., HORAN, M.A., STRIJBOS, P.J. & ROTHWELL, N.J. (1990). Lipocortin 1 fragment modifies pyrogenic actions of cytokines in rats. *Am J Physiol*, **259**, R266-9.

CHRISTMAS, P., CALLAWAY, J., FALLON, J., JONES, J. & HAIGLER, H.T. (1991). Selective secretion of annexin 1, a protein without a signal sequence, by the human prostate gland. *J Biol Chem*, **266**, 2499-507.

CIRINO, G., PEERS, S.H., FLOWER, R.J., BROWNING, J.L. & PEPINSKY, R.B. (1989a). Human recombinant lipocortin 1 has acute local anti-inflammatory properties in the rat paw edema test. *Proc Natl Acad Sci U S A*, **86**, 3428-32.

CIRINO, G., PEERS, S.H., WALLACE, J.L. & FLOWER, R.J. (1989b). A study of phospholipase A2-induced oedema in rat paw. *Eur J Pharmacol*, **166**, 505-10.

CUZZOCREA, S., TAILOR, A., ZINGARELLI, B., SALZMAN, A.L., FLOWER, R.J., SZABO, C. & PERRETTI, M. (1997). Lipocortin 1 protects against splanchnic artery occlusion and reperfusion injury by affecting neutrophil migration. *J Immunol*, **159**, 5089-97.

DA SILVA, J.A., PEERS, S.H., PERRETTI, M. & WILLOUGHBY, D.A. (1993). Sex steroids affect glucocorticoid response to chronic inflammation and to interleukin-1. *J Endocrinol*, **136**, 389-97.

DANGERFIELD, J., LARBI, K.Y., HUANG, M.T., DEWAR, A. & NOURSHARGH, S. (2002). PECAM-1 (CD31) homophilic interaction up-regulates alpha6beta1 on transmigrated neutrophils in vivo and plays a functional role in the ability of alpha6 integrins to mediate leukocyte migration through the perivascular basement membrane. *J Exp Med*, **196**, 1201-11.

DI ROSA, M., FLOWER, R.J., HIRATA, F., PARENTE, L. & RUSSO-MARIE, F. (1984). Anti-phospholipase proteins. *Prostaglandins*, **28**, 441-2.

DIAMOND, M.S., STAUNTON, D.E., MARLIN, S.D. & SPRINGER, T.A. (1991). Binding of the integrin Mac-1 (CD11b/CD18) to the third immunoglobulin-like domain of ICAM-1 (CD54) and its regulation by glycosylation. *Cell*, **65**, 961-71.

DUSTIN, M.L., ROTHLEIN, R., BHAN, A.K., DINARELLO, C.A. & SPRINGER, T.A. (1986). Induction by IL 1 and interferon-gamma: tissue distribution, biochemistry, and function of a natural adherence molecule (ICAM-1). *J Immunol*, **137**, 245-54.

ELICES, M.J., OSBORN, L., TAKADA, Y., CROUSE, C., LUHOWSKYJ, S., HEMLER, M.E. & LOBB, R.R. (1990). VCAM-1 on activated endothelium interacts with the leukocyte integrin VLA-4 at a site distinct from the VLA-4/fibronectin binding site. *Cell*, **60**, 577-84.

EUZGER, H.S., FLOWER, R.J., GOULDING, N.J. & PERRETTI, M. (1999). Differential modulation of annexin I binding sites on monocytes and neutrophils. *Mediators Inflamm*, **8**, 53-62.

FERLAZZO, V., D'AGOSTINO, P., MILANO, S., CARUSO, R., FEO, S., CILLARI, E. & PARENTE, L. (2003). Anti-inflammatory effects of annexin-1: stimulation of IL-10 release and inhibition of nitric oxide synthesis. *Int Immunopharmacol*, **3**, 1363-9.

FERREIRA, S.H., CUNHA, F.Q., LORENZETTI, B.B., MICHELIN, M.A., PERRETTI, M., FLOWER, R.J. & POOLE, S. (1997). Role of lipocortin-1 in the anti-hyperalgesic actions of dexamethasone. *Br J Pharmacol*, **121**, 883-8.

FLEMING, T.J., FLEMING, M.L. & MALEK, T.R. (1993). Selective expression of Ly-6G on myeloid lineage cells in mouse bone marrow. RB6-8C5 mAb to granulocyte-differentiation antigen (Gr-1) detects members of the Ly-6 family. *J Immunol*, **151**, 2399-408.

FLOWER, R.J. (1988). Eleventh Gaddum memorial lecture. Lipocortin and the mechanism of action of the glucocorticoids. *Br J Pharmacol*, **94**, 987-1015.

FLOWER, R.J. & BLACKWELL, G.J. (1979). Anti-inflammatory steroids induce biosynthesis of a phospholipase A2 inhibitor which prevents prostaglandin generation. *Nature*, **278**, 456-9.

FRANCIS, J.W., BALAZOVICH, K.J., SMOLEN, J.E., MARGOLIS, D.I. & BOXER, L.A. (1992). Human neutrophil annexin I promotes granule aggregation and modulates Ca(2+)-dependent membrane fusion. *J Clin Invest*, **90**, 537-44.

FRENETTE, P.S., DENIS, C.V., WEISS, L., JURK, K., SUBBARAO, S., KEHREL, B., HARTWIG, J.H., VESTWEBER, D. & WAGNER, D.D. (2000). P-Selectin glycoprotein ligand 1 (PSGL-1) is expressed on platelets and can mediate platelet-endothelial interactions in vivo. *J Exp Med*, **191**, 1413-22.

GAVINS, F.N., KAMAL, A.M., D'AMICO, M., OLIANI, S.M. & PERRETTI, M. (2004). Formyl-peptide receptor is not involved in the protection afforded by annexin 1 in murine acute myocardial infarct. *Faseb J*, **19**, 100-2.

GAVINS, F.N., YONA, S., KAMAL, A.M., FLOWER, R.J. & PERRETTI, M. (2003). Leukocyte anti-adhesive actions of annexin 1: ALXR and FPR related anti-inflammatory mechanisms. *Blood*, 4140-47.

GENG, J.G., BEVILACQUA, M.P., MOORE, K.L., MCINTYRE, T.M., PRESCOTT, S.M., KIM, J.M., BLISS, G.A., ZIMMERMAN, G.A. & MCEVER, R.P. (1990). Rapid neutrophil adhesion to activated endothelium mediated by GMP-140. *Nature*, **343**, 757-60.

GETTING, S.J., FLOWER, R.J. & PERRETTI, M. (1997). Inhibition of neutrophil and monocyte recruitment by endogenous and exogenous lipocortin 1. *Br J Pharmacol*, **120**, 1075-82.

GOULDING, N.J., GODOLPHIN, J.L., SHARLAND, P.R., PEERS, S.H., SAMPSON, M., MADDISON, P.J. & FLOWER, R.J. (1990). Anti-inflammatory lipocortin 1 production by peripheral blood leucocytes in response to hydrocortisone. *Lancet*, **335**, 1416-8.

GOULDING, N.J., PAN, L., WARDWELL, K., GUYRE, V.C. & GUYRE, P.M. (1996). Evidence for specific annexin I-binding proteins on human monocytes. *Biochem J*, **316 (Pt 2)**, 593-7.

GRANGER, D.N. & KUBES, P. (1994). The microcirculation and inflammation: modulation of leukocyte- endothelial cell adhesion. *J Leukoc Biol*, **55**, 662-75.

GROSSMAN, C. (1989). Possible underlying mechanisms of sexual dimorphism in the immune response, fact and hypothesis. *J Steroid Biochem*, **34**, 241-51.

HAFEZI-MOGHADAM, A., THOMAS, K.L., PROROCK, A.J., HUO, Y. & LEY, K. (2001). L-selectin shedding regulates leukocyte recruitment. *J Exp Med*, **193**, 863-72.

HANNON, R., CROXTALL, J.D., GETTING, S.J., ROVIEZZO, F., YONA, S., PAUL-CLARK, M.J., GAVINS, F.N., PERRETTI, M., MORRIS, J.F., BUCKINGHAM, J.C. & FLOWER, R.J. (2002). Aberrant inflammation and resistance to glucocorticoids in Annexin 1-/- Mouse. *Faseb J*, **17**, 253-5.

HARRICANE, M.C., CARON, E., PORTE, F. & LIAUTARD, J.P. (1996). Distribution of annexin I during non-pathogen or pathogen phagocytosis by confocal imaging and immunogold electron microscopy. *Cell Biol Int*, **20**, 193-203.

HATTORI, R., HAMILTON, K.K., FUGATE, R.D., MCEVER, R.P. & SIMS, P.J. (1989). Stimulated secretion of endothelial von Willebrand factor is accompanied by rapid redistribution to the cell surface of the intracellular granule membrane protein GMP-140. *J Biol Chem*, **264**, 7768-71.

HEMLER, M.E. (1990). VLA proteins in the integrin family: structures, functions, and their role on leukocytes. *Annu Rev Immunol*, **8**, 365-400.

HENDERSON, R.B., LIM, L.H., TESSIER, P.A., GAVINS, F.N., MATHIES, M., PERRETTI, M. & HOGG, N. (2001). The use of lymphocyte function-associated antigen (LFA)-1-deficient mice to determine the role of LFA-1, Mac-1, and alpha4 integrin in the inflammatory response of neutrophils. *J Exp Med*, **194**, 219-26.

HENNINGER, D.D., GERRITSEN, M.E. & GRANGER, D.N. (1997). Low-density lipoprotein receptor knockout mice exhibit exaggerated microvascular responses to inflammatory stimuli. *Circ Res*, **81**, 274-81.

HICKEY, M.J., FORSTER, M., MITCHELL, D., KAUR, J., DE CAIGNY, C. & KUBES, P. (2000). L-selectin facilitates emigration and extravascular locomotion of leukocytes during acute inflammatory responses in vivo. *J Immunol*, **165**, 7164-70.

HUANG, K.S., MCGRAY, P., MATTALIANO, R.J., BURNE, C., CHOW, E.P., SINCLAIR, L.K. & PEPINSKY, R.B. (1987). Purification and characterization of proteolytic fragments of lipocortin I that inhibit phospholipase A2. *J Biol Chem*, **262**, 7639-45.

HUBER, R., BERENDES, R., BURGER, A., SCHNEIDER, M., KARSHIKOV, A., LUECKE, H., ROMISCH, J. & PAQUES, E. (1992). Crystal and molecular structure of human annexin V after refinement. Implications for structure, membrane binding and ion channel formation of the annexin family of proteins. *J Mol Biol*, **223**, 683-704.

HWANG, S.B. (1988). Identification of a second putative receptor of platelet-activating factor from human polymorphonuclear leukocytes. *J Biol Chem*, **263**, 3225-33.

JILMA, B., VOLTMANN, J., ALBINNI, S., STOHLAWETZ, P., SCHWARZINGER, I., GLEITER, C.H., RAUCH, A., EICHLER, H.G. & WAGNER, O.F. (1997). Dexamethasone down-regulates the expression of L-selectin on the surface of neutrophils and lymphocytes in humans. *Clin Pharmacol Ther*, **62**, 562-8.

JOHNSTON, B. & BUTCHER, E.C. (2002). Chemokines in rapid leukocyte adhesion triggering and migration. *Semin Immunol*, **14**, 83-92.

JUTILA, M.A., ROTT, L., BERG, E.L. & BUTCHER, E.C. (1989). Function and regulation of the neutrophil MEL-14 antigen in vivo: comparison with LFA-1 and MAC-1. *J Immunol*, **143**, 3318-24.

KAHN, J., INGRAHAM, R.H., SHIRLEY, F., MIGAKI, G.I. & KISHIMOTO, T.K. (1994). Membrane proximal cleavage of L-selectin: identification of the cleavage site and a 6-kD transmembrane peptide fragment of L-selectin. *J Cell Biol*, **125**, 461-70.

KISHIMOTO, T.K., JUTILA, M.A., BERG, E.L. & BUTCHER, E.C. (1989). Neutrophil Mac-1 and MEL-14 adhesion proteins inversely regulated by chemotactic factors. *Science*, **245**, 1238-41.

KOLACZKOWSKA, E., SELJELID, R. & PLYTYCZ, B. (2001). Role of mast cells in zymosan-induced peritoneal inflammation in Balb/c and mast cell-deficient WBB6F1 mice. *J Leukoc Biol*, **69**, 33-42.

KONNO, S. & TSURUFUJI, S. (1983). Induction of zymosan-air-pouch inflammation in rats and its characterization with reference to the effects of anticomplementary and anti-inflammatory agents. *Br J Pharmacol*, **80**, 269-77.

KUBES, P. & KANWAR, S. (1994). Histamine induces leukocyte rolling in post-capillary venules. A P-selectin-mediated event. *J Immunol*, **152**, 3570-7.

KUBES, P., SUZUKI, M. & GRANGER, D.N. (1990). Modulation of PAF-induced leukocyte adherence and increased microvascular permeability. *Am J Physiol*, **259**, G859-64.

LA, M., D'AMICO, M., BANDIERA, S., DI FILIPPO, C., OLIANI, S.M., GAVINS, F.N., FLOWER, R.J. & PERRETTI, M. (2001). Annexin 1 peptides protect against experimental myocardial ischemia-reperfusion: analysis of their mechanism of action. *Faseb J*, **15**, 2247-56.

LAEMMLI, U.K., BEGUIN, F. & GUJER-KELLENBERGER, G. (1970). A factor preventing the major head protein of bacteriophage T4 from random aggregation. *J Mol Biol*, **47**, 69-85.

LAGASSE, E. & WEISSMAN, I.L. (1996). Flow cytometric identification of murine neutrophils and monocytes. *J Immunol Methods*, **197**, 139-50.

LEY, K., BULLARD, D.C., ARBONES, M.L., BOSSE, R., VESTWEBER, D., TEDDER, T.F. & BEAUDET, A.L. (1995). Sequential contribution of L- and P-selectin to leukocyte rolling in vivo. *J Exp Med*, **181**, 669-75.

LEY, K., GAEHTGENS, P., FENNIE, C., SINGER, M.S., LASKY, L.A. & ROSEN, S.D. (1991). Lectin-like cell adhesion molecule 1 mediates leukocyte rolling in mesenteric venules in vivo. *Blood*, **77**, 2553-5.

LEY, K. & TEDDER, T.F. (1995). Leukocyte interactions with vascular endothelium. New insights into selectin-mediated attachment and rolling. *J Immunol*, **155**, 525-8.

LIM, L.H., SOLITO, E., RUSSO-MARIE, F., FLOWER, R.J. & PERRETTI, M. (1998). Promoting detachment of neutrophils adherent to murine postcapillary venules to control inflammation: effect of lipocortin 1. *Proc Natl Acad Sci U S A*, **95**, 14535-9.

LIU, L., FISHER, A.B. & ZIMMERMAN, U.J. (1995). Regulation of annexin I by proteolysis in rat alveolar epithelial type II cells. *Biochem Mol Biol Int*, **36**, 373-81.

LUSTER, A.D. (1998). Chemokines--chemotactic cytokines that mediate inflammation. *N Engl J Med*, **338**, 436-45.

MAMDOUH, Z., CHEN, X., PIERINI, L.M., MAXFIELD, F.R. & MULLER, W.A. (2003). Targeted recycling of PECAM from endothelial surface-connected compartments during diapedesis. *Nature*, **421**, 748-53.

MANCUSO, F., FLOWER, R.J. & PERRETTI, M. (1995). Leukocyte transmigration, but not rolling or adhesion, is selectively inhibited by dexamethasone in the hamster post-capillary venule. Involvement of endogenous lipocortin 1. *J Immunol*, **155**, 377-86.

MARASCO, W.A., PHAN, S.H., KRUTZSCH, H., SHOWELL, H.J., FELTNER, D.E., NAIRN, R., BECKER, E.L. & WARD, P.A. (1984). Purification and identification of formyl-methionyl-leucyl-phenylalanine as the major peptide neutrophil chemotactic factor produced by Escherichia coli. *J Biol Chem*, **259**, 5430-9.

MARLIN, S.D. & SPRINGER, T.A. (1987). Purified intercellular adhesion molecule-1 (ICAM-1) is a ligand for lymphocyte function-associated antigen 1 (LFA-1). *Cell*, **51**, 813-9.

MCEVER, R.P. & CUMMINGS, R.D. (1997). Perspectives series: cell adhesion in vascular biology. Role of PSGL-1 binding to selectins in leukocyte recruitment. *J Clin Invest*, **100**, 485-91.

MOORE, K.L., PATEL, K.D., BRUEHL, R.E., LI, F., JOHNSON, D.A., LICHENSTEIN, H.S., CUMMINGS, R.D., BAINTON, D.F. & MCEVER, R.P. (1995). P-selectin glycoprotein ligand-1 mediates rolling of human neutrophils on P-selectin. *J Cell Biol*, **128**, 661-71.

MOORE, K.L., STULTS, N.L., DIAZ, S., SMITH, D.F., CUMMINGS, R.D., VARKI, A. & MCEVER, R.P. (1992). Identification of a specific glycoprotein ligand for P-selectin (CD62) on myeloid cells. *J Cell Biol*, **118**, 445-56.

MORAND, E.F., HUTCHINSON, P., HARGREAVES, A., GOULDING, N.J., BOYCE, N.W. & HOLDSWORTH, S.R. (1995). Detection of intracellular lipocortin 1 in human leukocyte subsets. *Clin Immunol Immunopathol*, **76**, 195-202.

MORI, T., MASUDA, M., TAKAHASHI, H. & HIOKI, K. (2000). Functional properties of circulating and transmigrated neutrophils in a rat peritonitis model. *Eur Surg Res*, **32**, 331-6.

MULLER, W.A. (2003). Leukocyte-endothelial-cell interactions in leukocyte transmigration and the inflammatory response. *Trends Immunol*, **24**, 327-34.

MULLER, W.A., WEIGL, S.A., DENG, X. & PHILLIPS, D.M. (1993). PECAM-1 is required for transendothelial migration of leukocytes. *J Exp Med*, **178**, 449-60.

NEVID, N. & HORSEMAN, N. (1996). *Annexin gene structure in Annexins:Molecular Structure to Cellular Function.* Austin: R. G. Landes.

NOBIS, U., PRIES, A.R., COKELET, G.R. & GAEHTGENS, P. (1985). Radial distribution of white cells during blood flow in small tubes. *Microvasc Res*, **29**, 295-304.

NOLTE, D., SCHMID, P., JAGER, U., BOTZLAR, A., ROESKEN, F., HECHT, R., UHL, E., MESSMER, K. & VESTWEBER, D. (1994). Leukocyte rolling in venules of striated muscle and skin is mediated by P-selectin, not by L-selectin. *Am J Physiol*, **267**, H1637-42.

NORMAN, K.E., MOORE, K.L., MCEVER, R.P. & LEY, K. (1995). Leukocyte rolling in vivo is mediated by P-selectin glycoprotein ligand-1. *Blood*, **86**, 4417-21.

NOURSHARGH, S., LARKIN, S.W., DAS, A. & WILLIAMS, T.J. (1995). Interleukin-1-induced leukocyte extravasation across rat mesenteric microvessels is mediated by platelet-activating factor. *Blood*, **85**, 2553-8.

NUSSENZWEIG, M.C., STEINMAN, R.M., UNKELESS, J.C., WITMER, M.D., GUTCHINOV, B. & COHN, Z.A. (1981). Studies of the cell surface of mouse dendritic cells and other leukocytes. *J Exp Med*, **154**, 168-87.

NUSSEY, S.S. & WHITEHEAD, S.A. (2001). *Endocrinology: An Integrated Approach.* Oxford: BIOS Scientific Publishers.

O'FLAHERTY, J.T., SURLES, J.R., REDMAN, J., JACOBSON, D., PIANTADOSI, C. & WYKLE, R.L. (1986). Binding and metabolism of platelet-activating factor by human neutrophils. *J Clin Invest*, **78**, 381-8.

OLIANI, S.M., PAUL-CLARK, M.J., CHRISTIAN, H.C., FLOWER, R.J. & PERRETTI, M. (2001). Neutrophil interaction with inflamed postcapillary venule endothelium alters annexin 1 expression. *Am J Pathol*, **158**, 603-15.

OLOFSSON, A.M., ARFORS, K.E., RAMEZANI, L., WOLITZKY, B.A., BUTCHER, E.C. & VON ANDRIAN, U.H. (1994). E-selectin mediates leukocyte rolling in interleukin-1-treated rabbit mesentery venules. *Blood*, **84**, 2749-58.

OSBORN, L., HESSION, C., TIZARD, R., VASSALLO, C., LUHOWSKYJ, S., CHI-ROSSO, G. & LOBB, R. (1989). Direct expression cloning of vascular cell adhesion

molecule 1, a cytokine-induced endothelial protein that binds to lymphocytes. *Cell*, **59**, 1203-11.

OSTERMANN, G., WEBER, K.S., ZERNECKE, A., SCHRODER, A. & WEBER, C. (2002). JAM-1 is a ligand of the beta(2) integrin LFA-1 involved in transendothelial migration of leukocytes. *Nat Immunol*, **3**, 151-8.

PANES, J., PERRY, M. & GRANGER, D.N. (1999). Leukocyte-endothelial cell adhesion: avenues for therapeutic intervention. *Br J Pharmacol*, **126**, 537-50.

PATEL, K.D., ZIMMERMAN, G.A., PRESCOTT, S.M., MCEVER, R.P. & MCINTYRE, T.M. (1991). Oxygen radicals induce human endothelial cells to express GMP-140 and bind neutrophils. *J Cell Biol*, **112**, 749-59.

PEERS, S.H., SMILLIE, F., ELDERFIELD, A.J. & FLOWER, R.J. (1993). Glucocorticoid- and non-glucocorticoid induction of lipocortins (annexins) 1 and 2 in rat peritoneal leucocytes in vivo. *Br J Pharmacol*, **108**, 66-72.

PEPINSKY, R.B., SINCLAIR, L.K., BROWNING, J.L., MATTALIANO, R.J., SMART, J.E., CHOW, E.P., FALBEL, T., RIBOLINI, A., GARWIN, J.L. & WALLNER, B.P. (1986). Purification and partial sequence analysis of a 37-kDa protein that inhibits phospholipase A2 activity from rat peritoneal exudates. *J Biol Chem*, **261**, 4239-46.

PERRETTI, M., AHLUWALIA, A., HARRIS, J.G., GOULDING, N.J. & FLOWER, R.J. (1993). Lipocortin-1 fragments inhibit neutrophil accumulation and neutrophil-dependent edema in the mouse. A qualitative comparison with an anti-CD11b monoclonal antibody. *J Immunol*, **151**, 4306-14.

PERRETTI, M., AHLUWALIA, A., HARRIS, J.G., HARRIS, H.J., WHELLER, S.K. & FLOWER, R.J. (1996a). Acute inflammatory response in the mouse: exacerbation by immunoneutralization of lipocortin 1. *Br J Pharmacol*, **117**, 1145-54.

PERRETTI, M., CHIANG, N., LA, M., FIERRO, I.M., MARULLO, S., GETTING, S.J., SOLITO, E. & SERHAN, C.N. (2002a). Endogenous lipid- and peptide-derived anti-inflammatory pathways generated with glucocorticoid and aspirin treatment activate the lipoxin A4 receptor. *Nat Med*, **8**, 1296-302.

PERRETTI, M., CHRISTIAN, H., WHELLER, S.K., AIELLO, I., MUGRIDGE, K.G., MORRIS, J.F., FLOWER, R.J. & GOULDING, N.J. (2000). Annexin I is stored within gelatinase granules of human neutrophil and mobilized on the cell surface upon adhesion but not phagocytosis. *Cell Biol Int*, **24**, 163-74.

PERRETTI, M., CROXTALL, J.D., WHELLER, S.K., GOULDING, N.J., HANNON, R. & FLOWER, R.J. (1996b). Mobilizing lipocortin 1 in adherent human leukocytes downregulates their transmigration. *Nat Med*, **2**, 1259-62.

PERRETTI, M. & FLOWER, R.J. (2004). Annexin 1 and the biology of the neutrophil. *J Leukoc Biol*, **76**, 25-9

PERRETTI, M. & FLOWER, R.J. (1993). Modulation of IL-1-induced neutrophil migration by dexamethasone and lipocortin 1. *J Immunol*, **150**, 992-9.

PERRETTI, M., GETTING, S.J., SOLITO, E., MURPHY, P.M. & GAO, J.L. (2001). Involvement of the receptor for formylated peptides in the in vivo anti-migratory actions of annexin 1 and its mimetics. *Am J Pathol*, **158**, 1969-73.

PERRETTI, M., INGEGNOLI, F., WHELLER, S.K., BLADES, M.C., SOLITO, E. & PITZALIS, C. (2002b). Annexin 1 modulates monocyte-endothelial cell interaction in vitro and cell migration in vivo in the human SCID mouse transplantation model. *J Immunol*, **169**, 2085-92.

PERRETTI, M., SOLITO, E. & PARENTE, L. (1992). Evidence that endogenous interleukin-1 is involved in leukocyte migration in acute experimental inflammation in rats and mice. *Agents Actions*, **35**, 71-8.

PIERETTI, S., DI GIANNUARIO, A., DE FELICE, M., PERRETTI, M. & CIRINO, G. (2004). Stimulus-dependent specificity for annexin 1 inhibition of the inflammatory nociceptive response: the involvement of the receptor for formylated peptides. *Pain*, **109**, 52-63.

PREECE, G., MURPHY, G. & AGER, A. (1996). Metalloproteinase-mediated regulation of L-selectin levels on leucocytes. *J Biol Chem*, **271**, 11634-40.

PREMACK, B.A. & SCHALL, T.J. (1996). Chemokine receptors: gateways to inflammation and infection. *Nat Med*, **2**, 1174-8.

RANG, H.R., DALE, M.M., RITTER, J.M. & MOORE, P.K. (2003). *Pharmacology*. London: Churchill Livingstone.

RAO, T.S., CURRIE, J.L., SHAFFER, A.F. & ISAKSON, P.C. (1994). In vivo characterization of zymosan-induced mouse peritoneal inflammation. *J Pharmacol Exp Ther*, **269**, 917-25.

RAYNAL, P. & POLLARD, H.B. (1994). Annexins: the problem of assessing the biological role for a gene family of multifunctional calcium- and phospholipid-binding proteins. *Biochim Biophys Acta*, **1197**, 63-93.

RELTON, J.K., STRIJBOS, P.J., O'SHAUGHNESSY, C.T., CAREY, F., FORDER, R.A., TILDERS, F.J. & ROTHWELL, N.J. (1991). Lipocortin-1 is an endogenous inhibitor of ischemic damage in the rat brain. *J Exp Med*, **174**, 305-10.

ROSEN, S.D. (1993). Cell surface lectins in the immune system. *Semin Immunol*, **5**, 237-47.

ROSENGARTH, A., GERKE, V. & LUECKE, H. (2001). X-ray structure of full-length annexin 1 and implications for membrane aggregation. *J Mol Biol*, **306**, 489-98.

ROVIEZZO, F., GETTING, S.J., PAUL-CLARK, M.J., YONA, S., GAVINS, F.N., PERRETTI, M., HANNON, R., CROXTALL, J.D., BUCKINGHAM, J.C. & FLOWER, R.J. (2002).

The annexin-1 knockout mouse: what it tells us about the inflammatory response. *J Physiol Pharmacol*, **53**, 541-53.

SCHENKEL, A.R., MAMDOUH, Z., CHEN, X., LIEBMAN, R.M. & MULLER, W.A. (2002). CD99 plays a major role in the migration of monocytes through endothelial junctions. *Nat Immunol*, **3**, 143-50.

SCHMID-SCHONBEIN, G.W., USAMI, S., SKALAK, R. & CHIEN, S. (1980). The interaction of leukocytes and erythrocytes in capillary and postcapillary vessels. *Microvasc Res*, **19**, 45-70.

SEEMANN, J., WEBER, K., OSBORN, M., PARTON, R.G. & GERKE, V. (1996). The association of annexin I with early endosomes is regulated by Ca2+ and requires an intact N-terminal domain. *Mol Biol Cell*, **7**, 1359-74.

SJOLIN, C., STENDAHL, O. & DAHLGREN, C. (1994). Calcium-induced translocation of annexins to subcellular organelles of human neutrophils. *Biochem J*, **300 (Pt 2)**, 325-30.

SMITH, P.D. & MOSS, S.E. (1994). Structural evolution of the annexin supergene family. *Trends Genet*, **10**, 241-6.

SMITH, S.F., TETLEY, T.D., GUZ, A. & FLOWER, R.J. (1990). Detection of lipocortin 1 in human lung lavage fluid: lipocortin degradation as a possible proteolytic mechanism in the control of inflammatory mediators and inflammation. *Environ Health Perspect*, **85**, 135-44.

SPERTINI, O., CORDEY, A.S., MONAI, N., GIUFFRE, L. & SCHAPIRA, M. (1996). P-selectin glycoprotein ligand 1 is a ligand for L-selectin on neutrophils, monocytes, and CD34+ hematopoietic progenitor cells. *J Cell Biol*, **135**, 523-31.

SPRINGER, T.A. (1994). Traffic signals for lymphocyte recirculation and leukocyte emigration: the multistep paradigm. *Cell*, **76**, 301-14.

STAUNTON, D.E., DUSTIN, M.L. & SPRINGER, T.A. (1989). Functional cloning of ICAM-2, a cell adhesion ligand for LFA-1 homologous to ICAM-1. *Nature*, **339**, 61-4.

STEEGMAIER, M., LEVINOVITZ, A., ISENMANN, S., BORGES, E., LENTER, M., KOCHER, H.P., KLEUSER, B. & VESTWEBER, D. (1995). The E-selectin-ligand ESL-1 is a variant of a receptor for fibroblast growth factor. *Nature*, **373**, 615-20.

STRAUSBAUGH, H.J. & ROSEN, S.D. (2001). A potential role for annexin 1 as a physiologic mediator of glucocorticoid-induced L-selectin shedding from myeloid cells. *J Immunol*, **166**, 6294-300.

SUBRAMANIAM, M., KOEDAM, J.A. & WAGNER, D.D. (1993). Divergent fates of P- and E-selectins after their expression on the plasma membrane. *Mol Biol Cell*, **4**, 791-801.

SUGAMA, Y., TIRUPPATHI, C., OFFAKIDEVI, K., ANDERSEN, T.T., FENTON, J.W., 2ND & MALIK, A.B. (1992). Thrombin-induced expression of endothelial P-selectin and intercellular adhesion molecule-1: a mechanism for stabilizing neutrophil adhesion. *J Cell Biol*, **119**, 935-44.

TAILOR, A., FLOWER, R.J. & PERRETTI, M. (1997). Dexamethasone inhibits leukocyte emigration in rat mesenteric post-capillary venules: an intravital microscopy study. *J Leukoc Biol*, **62**, 301-8.

TAKAMOTO, S., NAKAMURA, K., YONEDA, M. & MAKINO, I. (2003). Gender-related differences in concanavalin A-induced liver injury and cytokine production in mice. *Hepatol Res*, **27**, 221-229.

TEIXEIRA, M.M., DAS, A.M., MIOTLA, J.M., PERRETTI, M. & HELLEWELL, P.G. (1998). The role of lipocortin-1 in the inhibitory action of dexamethasone on eosinophil trafficking in cutaneous inflammatory reactions in the mouse. *Br J Pharmacol*, **123**, 538-44.

TEIXEIRA, M.M., WILLIAMS, T.J. & HELLEWELL, P.G. (1995). Mechanisms and pharmacological manipulation of eosinophil accumulation in vivo. *Trends Pharmacol Sci*, **16**, 418-23.

THOMPSON, R.D., NOBLE, K.E., LARBI, K.Y., DEWAR, A., DUNCAN, G.S., MAK, T.W. & NOURSHARGH, S. (2001). Platelet-endothelial cell adhesion molecule-1 (PECAM-1)-deficient mice demonstrate a transient and cytokine-specific role for PECAM-1 in leukocyte migration through the perivascular basement membrane. *Blood*, **97**, 1854-60.

TSAO, F.H., MEYER, K.C., CHEN, X., ROSENTHAL, N.S. & HU, J. (1998). Degradation of annexin I in bronchoalveolar lavage fluid from patients with cystic fibrosis. *Am J Respir Cell Mol Biol*, **18**, 120-8.

ULBRICH, H., ERIKSSON, E.E. & LINDBOM, L. (2003). Leukocyte and endothelial cell adhesion molecules as targets for therapeutic interventions in inflammatory disease. *Trends Pharmacol Sci*, **24**, 640-7.

UMENO, E., NADEL, J.A. & MCDONALD, D.M. (1990). Neurogenic inflammation of the rat trachea: fate of neutrophils that adhere to venules. *J Appl Physiol*, **69**, 2131-6.

VAN DER FLIER, A. & SONNENBERG, A. (2001). Function and interactions of integrins. *Cell Tissue Res*, **305**, 285-98.

VAPORCIYAN, A.A., DELISSER, H.M., YAN, H.C., MENDIGUREN, II, THOM, S.R., JONES, M.L., WARD, P.A. & ALBELDA, S.M. (1993). Involvement of platelet-endothelial cell adhesion molecule-1 in neutrophil recruitment in vivo. *Science*, **262**, 1580-2.

VENTURI, G.M., TU, L., KADONO, T., KHAN, A.I., FUJIMOTO, Y., OSHEL, P., BOCK, C.B., MILLER, A.S., ALBRECHT, R.M., KUBES, P., STEEBER, D.A. & TEDDER, T.F. (2003). Leukocyte migration is regulated by L-selectin endoproteolytic release. *Immunity*, **19**, 713-24.

VERGNOLLE, N., COMERA, C. & BUENO, L. (1995). Annexin 1 is overexpressed and specifically secreted during experimentally induced colitis in rats. *Eur J Biochem*, **232**, 603-10.

VERGNOLLE, N., PAGES, P., GUIMBAUD, R., CHAUSSADE, S., BUENO, L., ESCOURROU, J. & COMERA, C. (2004). Annexin 1 is secreted in situ during ulcerative colitis in humans. *Inflamm Bowel Dis*, **10**, 584-92.

VESTWEBER, D. & BLANKS, J.E. (1999). Mechanisms that regulate the function of the selectins and their ligands. *Physiol Rev*, **79**, 181-213.

VISHWANATH, B.S., FREY, F.J., BRADBURY, M., DALLMAN, M.F. & FREY, B.M. (1992). Adrenalectomy decreases lipocortin-I messenger ribonucleic acid and tissue protein content in rats. *Endocrinology*, **130**, 585-91.

VISHWANATHA, J.K., DAVIS, R.G., RUBINSTEIN, I. & FLOREANI, A. (1998). Annexin I degradation in bronchoalveolar lavage fluids from healthy smokers: a possible mechanism of inflammation. *Clin Cancer Res*, **4**, 2559-64.

VON ANDRIAN, U.H., CHAMBERS, J.D., MCEVOY, L.M., BARGATZE, R.F., ARFORS, K.E. & BUTCHER, E.C. (1991). Two-step model of leukocyte-endothelial cell interaction in inflammation: distinct roles for LECAM-1 and the leukocyte beta 2 integrins in vivo. *Proc Natl Acad Sci U S A*, **88**, 7538-42.

WALLNER, B.P., MATTALIANO, R.J., HESSION, C., CATE, R.L., TIZARD, R., SINCLAIR, L.K., FOELLER, C., CHOW, E.P., BROWING, J.L., RAMACHANDRAN, K.L. & ET AL. (1986). Cloning and expression of human lipocortin, a phospholipase A2 inhibitor with potential anti-inflammatory activity. *Nature*, **320**, 77-81.

WALTHER, A., RIEHEMANN, K. & GERKE, V. (2000). A novel ligand of the formyl peptide receptor: annexin I regulates neutrophil extravasation by interacting with the FPR. *Mol Cell*, **5**, 831-40.

WELLER, A., ISENMANN, S. & VESTWEBER, D. (1992). Cloning of the mouse endothelial selectins. Expression of both E- and P-selectin is inducible by tumor necrosis factor alpha. *J Biol Chem*, **267**, 15176-83.

WERR, J., XIE, X., HEDQVIST, P., RUOSLAHTI, E. & LINDBOM, L. (1998). beta1 integrins are critically involved in neutrophil locomotion in extravascular tissue In vivo. *J Exp Med*, **187**, 2091-6.

WILSON, R.W., BALLANTYNE, C.M., SMITH, C.W., MONTGOMERY, C., BRADLEY, A., O'BRIEN, W.E. & BEAUDET, A.L. (1993). Gene targeting yields a CD18-mutant mouse for study of inflammation. *J Immunol*, **151**, 1571-8.

YANG, Y., HUTCHINSON, P. & MORAND, E.F. (1999). Inhibitory effect of annexin I on synovial inflammation in rat adjuvant arthritis. *Arthritis Rheum*, **42**, 1538-44.

YANG, Y., LEECH, M., HUTCHINSON, P., HOLDSWORTH, S.R. & MORAND, E.F. (1997). Antiinflammatory effect of lipocortin 1 in experimental arthritis. *Inflammation*, **21**, 583-96.

YANG, Y.H., MORAND, E.F., GETTING, S.J., PAUL-CLARK, M., LIU, D.L., YONA, S., HANNON, R., BUCKINGHAM, J.C., PERRETTI, M. & FLOWER, R.J. (2004). Modulation of inflammation and response to dexamethasone by Annexin 1 in antigen-induced arthritis. *Arthritis Rheum*, **50**, 976-84.

YAO, V., MCCAULEY, R., COOPER, D., PLATELL, C. & HALL, J.C. (2004). Zymosan induces nitric oxide production by peritoneal mesothelial cells. *ANZ J Surg*, **74**, 266-9.

YONA, S., BUCKINGHAM, J.C., PERRETTI, M. & FLOWER, R.J. (2004). Stimulus-specific defect in the phagocytic pathways of annexin 1 null macrophages. *Br J Pharmacol*, **142**, 890-8.

YOUNG, R.E., THOMPSON, R.D., LARBI, K.Y., LA, M., ROBERTS, C.E., SHAPIRO, S.D., PERRETTI, M. & NOURSHARGH, S. (2004). Neutrophil elastase (NE)-deficient mice demonstrate a nonredundant role for NE in neutrophil migration, generation of proinflammatory mediators, and phagocytosis in response to zymosan particles in vivo. *J Immunol*, **172**, 4493-502.

YOUNG, R.E., THOMPSON, R.D. & NOURSHARGH, S. (2002). Divergent mechanisms of action of the inflammatory cytokines interleukin 1-beta and tumour necrosis factor-alpha in mouse cremasteric venules. *Br J Pharmacol*, **137**, 1237-46.

ZIMMERMAN, B.J., HOLT, J.W., PAULSON, J.C., ANDERSON, D.C., MIYASAKA, M., TAMATANI, T., TODD, R.F., 3RD, RUSCHE, J.R. & GRANGER, D.N. (1994). Molecular determinants of lipid mediator-induced leukocyte adherence and emigration in rat mesenteric venules. *Am J Physiol*, **266**, H847-53.

ZIMMERMAN, G.A., MCINTYRE, T.M., MEHRA, M. & PRESCOTT, S.M. (1990). Endothelial cell-associated platelet-activating factor: a novel mechanism for signaling intercellular adhesion. *J Cell Biol*, **110**, 529-40.

5.2. Publications arising from this thesis

Abstracts

Chatterjee, B.E., Flower, R.J. & Perretti, M. (2003). Alteration of the leukocyte endothelium interaction in the vascular bed of annexin 1 null mice
Journal of Leukocyte Biology Supplement 2003, pp. 34

Chatterjee, B.E., Flower, R.J. & Perretti, M. (2003). Altered leukocyte emigration in post-capillary venules of the cremaster microcirculation in annexin 1 knockout mice.
Proceedings of the British Pharmacological Society, 146P
http://www.pa2online.org/Vol1Issue4abst146P.html

Chatterjee, B.E., Yona, S.Y., Flower, R.J. & Perretti, M. (2003). Annexin 1 deficiency alters leukocyte extravasation in the mouse as determined by flow cytometry.
Journal of Vascular Research, **40**

Papers

Gavins, F.N. & Chatterjee, B.E. (2004). Intravital microscopy for the study of mouse microcirculation in anti-inflammatory drug research: focus on the mesentery and cremaster preparations.
J Pharmacol Toxicol Methods, **49**, pp 1-14

Chatterjee, B.E., Yona, S., Young, R.E., Nourshargh, S., Flower, R.J. & Perretti, M. (2004). Higher sensitivity of annexin 1 null neutrophils to *in vitro* activation and *in vivo* recruitment within the cremaster microcirculation.
Manuscript in process